Þekkingarnet
Þingeyinga

PROCEEDINGS OF THE NORTHQUAKE 2019 WORKSHOP

Husavik, North Iceland, 21-24 May 2019




October 2019

Október 2019

Útgefandi/Publisher: Þekkingarnet Þingeyinga / Husavik Academic Centre

Forsíðumyndir (frá vinstri)/Frontpage pictures (from left to right):

Vettvangsferð /Excursion. Mynd / Photo: Sigurjón Jónsson
Frá ráðstefnunni / From the workshop Mynd / Photo: Benedikt Halldórsson
Ráðstefnugestir //Participants in Northquake 2019. Mynd / Photo:Benedikt Halldórsson
Vettvangsferð / Excursion Mynd / Photo: Sigurjón Jónsson

Ábyrgð/Director:
Óli Halldórsson

Ritstjórn/Editors:
Sigurjón Jónsson, Benedikt Halldórsson, Kristín Jónsdóttir, Páll Einarsson,
Ragnar Stefánsson, Helena Eydís Ingólfsdóttir, Heiða Elín Aðalsteinsdóttir.

ISBN 978-9935-405-58-6

TABLE OF CONTENTS

INNGANGUR

Rúmlega 40 ár eru liðin frá síðasta stórskjálfta (stærð 6 til 7) á Norðurlandi og er það lengsta hlé á milli slíkra atburða á svæðinu í hartnær 200 ár. Frásagnir og gögn um stóra jarðskjálfta, t.d. nálægt Kópaskeri 1976, í mynni Skagafjarðar 1963 og við Dalvík 1934, gefa okkur hugmynd um hvers má vænta á næstu áratugum. Þessir stóru skjálftar og stöðug smáskjálftavirkni úti fyrir Norðurlandi á svæði sem oft er kallað Tjörnesbrotabeltið er áminning til vísindamanna og yfirvalda um að jarðskjálftavá á Norðurlandi er mikil og ámóta þeirri vá sem er á Suðurlandsundirlendinu.

Mikil uppbygging hefur átt sér stað á Norðurlandi á síðustu misserum og þá sérstaklega á Húsavík og nágrenni. Af helstu framkvæmdum má nefna Kísilmálmverksmiðju PCC á Bakka, jarðgöng í gegnum Húsavíkurhöfða og Þeistareykjavirkjun, ásamt uppbyggingu tengdri ferðaþjónustu, t.d. sjóböðin á Húsavíkurhöfða og hótelbyggingar. Í ljósi þessarar nýju uppbyggingar og til að efla viðbúnað er mikilvægt að fara reglulega yfir stöðu rannsókna á jarðskjálftum og jarðskjálftavá á svæðinu í viðleitni okkar til að skilja betur eðli og orsakir jarðskjálftavirkninnar og til að meta betur þá áhættu sem af stórskjálftum framtíðarinnar stafar.

Í maí 2019 var því boðað til þriðju ráðstefnunnar um jarðskjálfta á Norðurlandi. Markmið ráðstefnunnar var að fá yfirlit yfir nýjustu rannsóknir á jarðskjálftum á svæðinu, orsökum þeirra, eðli, áhrifum og ennfremur kynna hagnýtingu rannsóknarniðurstaðna. Meðal efnisþátta á ráðstefnunni voru jarðsaga, skjálftavirkni, plötuhreyfingar, jarðsprungur, sterkhreyfingar, yfirborðsáhrif, skriðuföll, jarðskjálftavá, og jarðváreftirlit. Sérstök áhersla var lögð á að samtúlka margvíslegar mælingar og athuganir fyrir betra og skilvirkara jarðváreftirlit. Í tengslum við ráðstefnuna var einnig sett á svið jarðskjálftaæfing og viðbragðsaðilar æfðu viðbrögð. Þessar viðbragðsáætlanir voru rýndar og niðurstöður kynntar á ráðstefnunni. Að auki var haldinn opinn fræðslufundur fyrir almenning þar sem efni frá ráðstefnunni var kynnt og vísindamenn og almannavarnaaðilar sátu fyrir svörum.

Ráðstefnan byggði á ráðstefnum sama efnis á Húsavík 2013 og 2016 og var með alþjóðlegu sniði sem fyrr þar sem vísindamenn frá mörgum löndum komu saman og kynntu niðurstöður rannsókna sinna frá Norðurlandi. Alls sóttu 47 manns ráðstefnuna í þetta skiptið, þeirra á meðal um 20 erlendir nemendur og vísindamenn frá 14 löndum. Fyrstu tveir dagarnir samanstóðu af margvíslegum 15 mínútna erindum þar sem fyrri daginn var fjallað um m.a. jarðskjálftavirkni og hrinur, sprungukortlagningu, skriðuföll og hugsanlegar flóðbylgjur. Seinni daginn var áherslan meira á sterkhreyfingar í jarðskjálftum, mat á jarðskjálftavá, jarðváreftirlit og samþættingu margvíslegra gagna til eftirlits. Þriðja daginn var byrjað á umræðum um efni ráðstefnunnar, fyrst um efni tengdu jarðskjálftavá og rannsóknum þar að lútandi og svo um margþætt jarðskjálfta- og jarðváreftirlit. Eftir umræðurnar var haldinn opinn fundur fyrir almenning, eins og nefnt var hér að ofan, þar sem efni ráðstefnunnar var kynnt í þremur fyrirlestrum áður en opnað var fyrir spurningar og umræður. Fyrir svörum voru Kristín Jónsdóttir, Benedikt Halldórsson, Páll Einarsson, Sigurjón Jónsson sem og Halla Bergþóra Björnssdóttir, lögreglustjóri á Norðurlandi Eystra. Ráðstefnunni lauk svo með skoðunarferð um Kelduhverfi og Tjörnes í fylgd Páls Einarssonar.

Undirbúningur og styrktaraðilar

Frumkvæði að ráðstefnunni kom frá sömu aðilum og fyrir ráðstefnurnar 2013 og 2016. Fræðilegur undirbúningur ráðstefnunnar var í höndum undirbúningsnefndar sem var svona skipuð:

- Sigurjón Jónsson, nefndarformaður, KAUST (sigurjon.jonsson@kaust.edu.sa)
- Kristín Jónsdóttir, Veðurstofa Íslands (kristin.jonsdottir@vedur.is)
- Páll Einarsson, Háskóli Íslands, (palli@hi.is)
- Benedikt Halldórsson, Háskóli Íslands og Veðurstofa Íslands (skykkur@hi.is)
- Ragnar Stefánsson, Háskólinn á Akureyri (raha@simnet.is)

Þekkingarnet Þingeyinga sá um skipulag og framkvæmd ráðstefnunnar í samstarfi við undirbúningnefndina. Fyrir hönd Þekkingarnetsins unnu Gréta Bergrún Jóhannsdóttir, Heiða Elín Aðalsteinsdóttir og Helena Eydís Ingólfsdóttir, ásamt Óla Halldórssyni forstöðumanni Þekkingarnetsins, að undirbúningi, kynningu og framkvæmd ráðstefnunnar sem og að frágangi þessa ráðstefnurits.

Eftirtaldir aðilar styrktu ráðstefnuhaldið:

Rannsóknamiðstöð í jarðskjálftaverkfræði við Háskóla Íslands, Háskólinn á Akureyri, Veðurstofa Íslands, King Abdullah University of Science and Technology (KAUST), Náttúruhamfaratrygging Íslands og Sparisjóður Suður-Þingeyinga.

Ráðstefnurit

Þetta ráðstefnurit samanstendur af ágripum og stuttum greinum um það efni sem fjallað var um í erindum á ráðstefnunni. Alls voru 31 erindi á ráðstefnunni þá tvö daga sem fyrirlestrahaldið stóð. Þriðja daginn voru líflegar umræður um efni ráðstefnunnar og eru punktar frá þeim umræðum ásamt ráðleggingum um frekari rannsóknir og aðgerðir í lok þessa ráðstefnurits.

Ef vitnað er til ágripa í þessu ráðstefnuriti má gera það eins og í dæmunum hér að neðan:

Bryndís Brandsdóttir, Jeffrey A. Karson, Gunnar B. Guðmundsson, Kristín Jónsdóttir, Robert S. Detrick, and Neal W. Driscoll, Tectonics of the Eyjafjarðaráll rift, abandoned southern segment of the Kolbeinsey ridge, North Iceland. Í ágripahefti Northquake 2019 ráðstefnunnar, Sigurjón Jónsson o.fl. (ritstj.). Þekkingarnet Þingeyinga, 16-17, 2019.

eða

Brandsdóttir, B., J.A. Karson, G.B. Guðmundsson, K. Jónsdóttir, R.S. Detrick and N.W. Driscoll, Tectonics of the Eyjafjarðaráll rift, abandoned southern segment of the Kolbeinsey ridge, North Iceland. In *Proceedings of the Northquake 2019 workshop* (ed. S. Jónsson et al.), Húsavík Academic Centre, 16-17, 2019.

INTRODUCTION

More than 40 years have passed since the last major earthquake (magnitude 6-7) struck in North Iceland, which is the longest period of quiescence in almost 200 years. First-hand accounts and data of the earthquakes near Kópasker village in 1976, in Skagafjörður in 1963 and near Dalvík in 1934 provide information about what we can expect in the coming decades. These past major earthquakes as well as the persistent seismic activity off the north coast of Iceland, in an area that is usually referred to as the Tjörnes Fracture Zone, show that the earthquake hazard in North Iceland is high and similar to the hazard in the South Iceland Seismic Zone.

Significant infrastructure build-up has taken place in North Iceland during the past several years. This includes the PCC silicon metal plant just north of Húsavík, a tunnel through Húsavík Cape, and the Theistareykir geothermal power plant. In light of these new infrastructure projects and to increase preparedness in North Iceland it is important to regularly review recent research results on earthquake activity in the region, the associated hazards and risks for the population and infrastructure, as well as to discuss possible ways to reduce risks and review response plans in case of a major event.

A workshop was therefore held in May 2019 on earthquake activity in North Iceland. The goal of the workshop was to review the status of knowledge and report new results in earthquake-related research in the area and to discuss possible use of these results for risk reduction. Workshop topics included earthquake geology, tectonics and geodesy, mapping of faults and fractures, current earthquake activity, strong-motion analysis, near-surface effects, earthquake monitoring, possible early warning, earthquake hazard and risk. In addition, plans and actions to decrease earthquake risk were discussed. Special emphasis was put on multi-variable data collection and measurements for improved earthquake monitoring. Response to hypothetical earthquake scenarios in the region was exercised prior to the workshop and a review of the results and existing response plans presented at the workshop. In addition, an open public meeting was held at the end of the workshop during which key results from the workshop were presented and scientists and response team personnel answered questions.

The workshop followed earlier workshops that were held in Húsavík in 2013 and 2016 and like before scientists from several different countries presented their research results focused on North Iceland. In total, 47 people participated in the workshop, of which almost 20 were overseas students and researchers from 14 different countries. The first two days consisted of 15-minute long presentations with earthquake activity and swarms, mapping of earthquake faults, landslides and possible tsunamis being the main topics during the first day. On the second day the main focus was on earthquake strong motion, seismic hazard assessments, seismicity monitoring and combination of different measurements for monitoring. The third day began with general discussions about the workshop topics, first on seismic hazard and related research and then on seismic monitoring. Following the discussion, the open public meeting, mentioned above, was held and then the workshop ended with a field excursion to Kelduhverfi and Tjörnes that was led by Páll Einarsson.

Preparation and support

The members of the scientific committee for the Northquake 2019 workshop were:

- Sigurjón Jónsson, KAUST (sigurjon.jonsson@kaust.edu.sa)
- Kristín Jónsdóttir, The Icelandic Met Office (kristin.jonsdottir@vedur.is)
- Páll Einarsson, University of Iceland, (palli@hi.is)
- Benedikt Halldórsson, Univ. of Iceland & the Icelandic Met Office (skykkur@hi.is)
- Ragnar Stefánsson, University of Akureyri (raha@simnet.is)

The Húsavík Academic Centre planned, advertised and ran the workshop together with the scientific committee, as well as preparing this workshop proceedings volume. On behalf of the Húsavík Academic Centre, Gréta Bergrún Jóhannsdóttir, Heiða Elín Aðalsteinsdóttir and Helena Eydís Ingólfsdóttir played the main roles in preparing the workshop, along with director Óli Halldórsson.

Finacial support for the workshop was provided by the Earthquake Engineering Research Centre of University of Iceland, University of Akureyri, The Icelandic Met. Office, King Abdullah University of Science and Technology (KAUST), the Natural Catastrophe Insurance of Iceland and Sparisjóður Suður-Þingeyinga.

Workshop Proceedings

This workshop proceedings volume consists of extended abstracts of the contributions presented at the Northquake 2019 workshop. A total of 31 contributions were presented during the first two days of the workshop. On the third day, general discussions took place and a summary of the discussion is at the end of the proceedings volume along with recommendations for immediate actions as well as for further research.

Citations to abstracts published in this proceedings volume should be as follows

Name of authors, contribution title. In *Proceedings of the Northquake 2019 workshop* (Ed. S. Jónsson et al.), Húsavík Academic Centre, pp-pp, 2019.

Example:

Brandsdóttir, B., J.A. Karson, G.B. Guðmundsson, K. Jónsdóttir, R.S. Detrick and N.W. Driscoll, Tectonics of the Eyjafjarðaráll rift, abandoned southern segment of the Kolbeinsey ridge, North Iceland. In *Proceedings of the Northquake 2019 workshop* (Ed. S. Jónsson et al.), Húsavík Academic Centre, 16-17, 2019.

WORKSHOP PROGRAM

Tuesday, 21 May, 2019	
21:00 – 22:30	**Registration and icebreaker**

Wednesday, 22 May, 2019	
09:00 – 10:00	**Registration and coffee**
10:00 – 10:20	**Introduction to the workshop**
10:20 – 12:00	**Tectonics, earthquake geology, fault mapping, tomography** **Session chairs:** Kristín Jónsdóttir and Halldór Geirsson
10:20 – 10:40	**Seismicity, faults, and bathymetry of the Tjörnes Fracture Zone** Páll Einarsson, Bryndís Brandsdóttir, Ásta Rut Hjartardóttir
10:40 – 11:00	Tectonics of the Eyjafjarðaráll rift, abandoned southern segment of the Kolbeinsey ridge, North Iceland Bryndís Brandsdóttir, Jeffrey A. Karson, Gunnar B. Guðmundsson, Kristín Jónsdóttir, Robert S. Detrick, Neal W. Driscoll
11:00 – 11:20	**Marine glacial features and faulting in the Eyjafjarðaráll basin, North Iceland** Bailey M. OConnell, Patricia Höfer, Bryndís Brandsdóttir
11:20 – 11:40	**Geomorphological evidence for post-glacial displacement on the Húsavík-Flatey fault, observed with drone images** Rémi Matrau, Sigurjón Jónsson, Daniele Trippanera, Yann Klinger
11:40 – 12:00	**Local earthquake tomography in North Iceland** Claudia Abril, Ari Tryggvason, Ólafur Gudmundsson, Rebekka Steffen
12:00 – 13:00	**Lunch**
13:00 – 15:00	**Kópasker activity, earthquake relocations, swarms, seasons** **Session chairs:** Bryndís Brandsdóttir and Ari Tryggvason
13:00 – 13:20	**Kópasker earthquake in 1976: About pre-activity, location and post-activity** Ragnar Stefánsson, Gunnar B. Guðmundsson
13:20 – 13:40	**The Kópasker seismic swarm in Spring 2019** Kristín Jónsdóttir, Gunnar B. Guðmundsson, Luigi Passarelli, Sigurjón Jónsson, the Monitoring team at IMO
13:40 – 14:00	**Earthquake relocation in the Tjörnes Fracture Zone** Claudia Abril, Ólafur Gudmundsson, Ari Tryggvason

14:00 – 14:20	**Seismicity and seismic swarms on the Húsavík-Flatey Fault and Grímsey Oblique Rift** Luigi Passarelli, Sigurjón Jónsson, Claudia Abril, Kristín Jónsdóttir, Gunnar B. Guðmundsson, Ólafur Guðmundsson, Eleonora Rivalta
14:20 – 14:40	**Do large earthquakes in North Iceland usually occur in Winter?** Sigurjón Jónsson
14:40 – 15:00	**Session wrap-up discussion**
15:00 – 15:20	**Coffee break**
15:20 – 17:00	**Landslides and tsunamis** **Session chairs:** Benedikt Halldórsson and Helga Rakel Guðrúnardóttir
15:20 – 15:40	**Spatial distribution of landslides and rock fall in connection with major earthquakes in Northern Iceland** Jón Kristinn Helgason, Halldór G. Pétursson, Sveinn Brynjólfsson
15:40 – 16:00	**Avalanche- and landslide monitoring at the Icelandic Met Office** Harpa Grímsdóttir, Sveinn Brynjólfsson
16:00 – 16:20	**Monitoring slope instabilities with Sentinel-1 satellite interferometry** Vincent Drouin, Freysteinn Sigmundsson
16:20 – 16:40	**Preliminary simulations for tsunami hazard in connection with a major earthquake on the HFF** Angel Ruiz-Angulo, Kristín Jónsdóttir, Ragnar H. Þrastarson, Benedikt Halldórsson, Harpa Grímsdóttir, Sigurjón Jónsson
16:40 – 17:00	**Session wrap-up discussion**

Thursday, 23 May, 2019	
09:00 – 10:40	**Earthquake strong motion and earthquake engineering** Session chairs: **Kristín Jónsdóttir and Bryndís Brandsdóttir**
09:00 – 09:20	**On the scaling of earthquake strong-motion in North Iceland** Benedikt Halldorsson, Tim Sonnemann, Milad Kowsari, Sahar Rahpeyma, Birgir Hrafnkelsson, Sigurjón Jónsson
09:20 – 09:40	**Sensitivity analysis of seismicity parameters and ground motion models used in PSHA to its input assumptions: A case study of Húsavík, North Iceland.** Milad Kowsari, Benedikt Halldorsson, N. Eftekhari, J.Þ. Snæbjörnsson, S. Jónsson
09:40 – 10:00	**Site effect estimation on two Icelandic strong-motion arrays using a Bayesian multi-level model for the spatial distribution of earthquake ground motion amplitudes** Sahar Rahpeyma, Benedikt Halldorsson, Birgir Hrafnkelsson, Sigurjón Jónsson
10:00 – 10:20	**Microseismic response characteristics of typical gravel fills in Iceland using HVSR and SSR techniques** Thomas J. Kennedy, Benedikt Halldorsson, Jónas Þ. Snæbjörnsson, Russel A. Green, Sahar Rahpeyma
10:20 – 10:40	**Concise map-based representation of the tectonics, geology, geomorphology and building stock of Húsavík, North Iceland** Peter Waltl, Benedikt Halldorsson, Halldór G. Pétursson, Markus Fiebig
10:40 – 11:00	**Coffee break**
11:00 – 12:40	**Earthquake sources, modeling and seismic hazard** **Session chairs:** Sigurjón Jónsson and Halldór Geirsson
11:00 – 11:20	**A moment tensor catalog based on surface waveform inversions for Iceland: Perspectives and opportunities for the Tjörnes Fracture Zone** Félix Rodríguez Cardozo, Vala Hjörleifsdóttir, Kristín Jónsdóttir, Halldór Geirsson, Nancy Trujillo Cartrillón, Arturo Iglesias, Sara Franco
11:20 – 11:40	**Earthquake source modeling and ground motion simulation in North Iceland** Tim Sonnemann, B. Halldorsson, B. Hrafnkelsson, S. Jónsson, J.Þ. Snæbjörnsson
11:40 – 12:00	**Towards physics-based probabilistic seismic hazard assessment in complex fault networks – the ChEESE project** Bo Li, Aniko Wirp, Alice-Agnes Gabriel, Michael Bader, Benedikt Halldorsson

12:00 – 12:20	**An overview of the North Anatolian fault zone and 3D crustal structure of Western Turkey by using full waveform tomography** Yeşim Çubuk-Sabuncu, Tuncay Taymaz, Andreas Fichtner
12:20 - 12:40	**Session wrap-up discussion**
12:40 – 13:40	**Lunch**
13:40 – 15:00	**Groundwater and deformation monitoring** **Session chairs:** Benedikt Halldórsson and Ari Tryggvason
13:40 – 14:00	**Update on groundwater monitoring at Húsavík and Hafralækur** Gabrielle Stockmann, Alasdair Skelton, Erik Sturkell, Ríkey Kjartansdóttir, Andri Stefánsson, Heike Siegmund, Hreinn Hjartarson
14:00 – 14:20	**Creating a monitoring network for studying hydrological changes in relation to earthquakes. Project status** Helga Rakel Guðrúnardóttir, Heiko Woith, Daniel Müller, Rémi Matrau
14:20 – 14:40	**An update of GPS measurements in North Iceland** Sigurjón Jónsson, Rémi Matrau, Renier Viltres, Benedikt Ófeigsson
14:40 – 15:00	**The potential use of seafloor geodesy in North Iceland** Halldór Geirsson, Vala Hjörleifsdóttir, Sigurjón Jónsson
15:00 – 15:20	**Coffee break**
15:20 – 17:00	**Multi-component monitoring, warning, planning, response** **Session chairs:** Helga Rakel Guðrúnardóttir og Páll Einarsson
15:20 – 15:40	**Pre-earthquake processes and warnings in the Tjörnes Fracture Zone** Ragnar Stefánsson, Gunnar B. Guðmundsson
15:40 – 16:00	**Seismic monitoring, earthquake modeling and ground motion simulation for early warning and hazard estimates in North Iceland** Benedikt Halldorsson
16:00 – 16:20	**Earthquake monitoring in N-Iceland and the Húsavík-Flatey fault earthquake exercise held in May 2019** Kristín Jónsdóttir, The IMO research and monitoring team, The National and Local Civil Protection response teams, The Road Authority response team, The Natural Catastrophe Insurance response team
16:20 – 16:40	**Monitoring – Planning – Action! What comes after research and monitoring?** Hjálmar Björgvinsson, Rögnvaldur Ólafsson

16:40 – 17:00	**Session wrap-up discussion**

21:00 - 23:00	**Geosea - geothermal sea baths**

Friday, 24 May, 2019	
09:00 – 11:30	**Discussion** **Session chairs:** Sigurjón Jónsson and Benedikt Halldórsson
09:00 – 09:10	**Introduction to discussion**
09:10 – 10:10	**Discussion**
10:10 – 10:30	**Coffee break**
10:30 – 11:30	**Discussion, cont.**
12:00 – 13:00	**Fræðslufundur fyrir almenning um jarðskjálfta á Norðurlandi** *An open information meeting for the general public (in Icelandic)*
13:30 – 17:00	**Excursion to Kelduhverfi, Ásbyrgi, and Tungulending** Páll Einarsson

WORKSHOP PARTICIPANTS

Name	Organization
Angel Ruiz-Angulo	Icelandic Meteorological Office
Ari Tryggvason	Uppsala University
Ásta Rut Hjartardóttir	Institute of Earth Sciences, University of Iceland
Bailey M. OConnell	Institute of Earth Sciences, University of Iceland
Benedikt Gunnar Ófeigsson	Icelandic Meteorological Office
Benedikt Halldórsson	University of Iceland / Icelandic Meteorological Office
Birgir Hrafnkelsson	University of Iceland
Björn Halldórsson	National Power Company of Iceland
Bo Li	LMU Munich
Bryndís Brandsdóttir	Institute of Earth Sciences, University of Iceland
Claudia Abril	Uppsala University
Daniele Trippanera	KAUST
Elísabet Pálmadóttir	Icelandic Meteorological Office
Elsa Dóra Vogler	The Icelandic Road and Coastal Administration
Erik Sturkell	University of Gothenburg
Eysteinn Tryggvason	Emeritus
Felix Rodríguez Cardozo	Icelandic Meteorological Office / UNAM Mexico
Flosi Þorgeirsson	
Gréta Bergrún Jóhannesdóttir	Húsavík Academic Centre
Hafdís Eygló Jónsdóttir	The Icelandic Road and Coastal Administration
Halldór Geirsson	Institute of Earth Sciences, University of Iceland
Harpa Grímsdóttir	The Icelandic Meteorological Office
Helga Rakel Guðrúnardóttir	
Hreiðar Hreiðarsson	The Police in Northeast Iceland
Ingibjörg Briem	Emeritus
Jón Hálfdánarson	Emeritus
Jón Örvar Bjarnason	Natural Catastrophe Insurance of Iceland
Kristín Elísa Guðmundsdóttir	Icelandic Meteorological Office
Kristín Jónsdóttir	Icelandic Meteorological Office
Kristján Jónasson	University of Iceland
Kristján Þór Magnússon	Norðurþing
Luigi Passarelli	KAUST

Milad Kowsari	University of Iceland
Páll Einarsson	Institute of Earth Sciences, University of Iceland (Emeritus)
Patricia Höfer	Institute of Earth Sciences, University of Iceland
Ragnar Stefánsson	University of Akureyri (Emeritus)
Rémi Matrau	KAUST
Revathy M. Parameswaran	University of Iceland
Rögnvaldur Ólafsson	National Commissioner of the Icelandic Police
Sahar Rahpeyma	University of Iceland
Sara Aniko Wirp	LMU Munich
Sigurjón Jónsson	KAUST
Sveinn Brynjólfsson	Icelandic Meteorological Office
Thomas J. Kennedy	Virgina Tech
Tim Sonnemann	University of Iceland / Icelandic Meteorological Office
Vincent Drouin	Institute of Earth Sciences, University of Iceland / National Land Survey of Iceland
Yesim Cubuk-Sabuncu	Icelandic Meteorological Office

NORTHQUAKE 2019 - The 3rd International Workshop on Earthquakes in North Iceland
Húsavík, North Iceland, 21-24 May 2019

SEISMICITY, FAULTS, AND BATHYMETRY OF THE TJÖRNES FRACTURE ZONE

Páll Einarsson, Bryndís Brandsdóttir, Ásta Rut Hjartardóttir

Institute of Earth Sciences, University of Iceland (palli@hi.is; bryndis@hi.is; astahj@hi.is)

The seismicity of North Iceland is mainly generated by the Tjörnes Fracture Zone, a transform zone that connects two divergent segments of the mid-Atlantic plate boundary (Fig. 1; *Einarsson*, 1991; 2008), i.e., the southern end of the submarine Kolbeinsey Ridge and the Northern Volcanic Zone of Iceland. This transform zone is comprised of a series of interconnecting, tectonic and volcano-tectonic zones, or branches, that together take up the transform motion. Understanding the characteristic activity of each branch, and how they interact, is essential for a meaningful estimate of seismic hazard and risk in this region. Most of this zone is off shore so tectonic interpretation relies on the quality of the bathymetric data available. We have assembled the best available bathymetric data and seismicity data for the last decades into a single map in order to delineate the main seismogenic structures (Fig. 1).

At its southern end the submarine Kolbeinsey Ridge (KR) bifurcates into the Eyjafjarðaráll Rift (ER) that continues southwards, and the Grímsey Oblique Rift (GOR) that extends to the SE. The Eyjafjarðaráll Rift is characterised by extensive normal faulting but no indications of Holocene volcanism can be found in the bathymetry. The Grímsey Oblique Rift, on the other hand, is composed of several active volcanic systems with N-S trending fissure swarms. Evidence for Holocene volcanism is abundant. At its SE end the GOR connects to the Krafla fissure swarm of the Northern Volcanic Zone (*Hjartardóttir et al.,* 2012). Large earthquakes along this branch are mostly caused by strike slip faulting, often on transverse faults (*Rögnvaldsson et al.,* 1998), by bookshelf-type kinematics similar to the fault configuration on the Reykjanes Peninsula Oblique Rift (*Björnsson et al*., 2018; *Einarsson et al.* 2018). The latest example of this type of faulting was provided by the earthquake swarm in early 2019 at the intersection with the Krafla fissure swarm (*Jónsdóttir et al.,* 2019).

The Húsavík-Flatey Zone (HFZ) is about 40 km south of and sub-parallel to the GOR. It is well defined by the distribution of seismicity from the southern end of the ER and can be traced on the ocean bottom to the coast in the Húsavík town (*Sæmundsson*, 1974). It then continues on land into the Northern Volcanic Zone, where it merges into the Theistareykir fissure swarm (e.g., *Tibaldi et al*., 2016; *Bonali et al.*, 2018). The HFZ consists of several splay faults that are parallel to the zone itself, sometimes arranged slightly en echelon. The type of faulting is strike-slip with a small component of normal faulting. The HFZ is divided into two main branches where it crosses the Skjálfandi Bay, separated by a 70 m high N-S aligned, normally magnetised hyaloclastic ridge. Several smaller WNW-trending faults are located sub-parallel with the main HFZ within the bay. The main faults have a vertical displacement of 0-15 m, increasing westwards. Four pull-apart basins occur along the fault zone, the largest at the intersection with Eyjafjarðaráll Rift, the southward continuation of the KR. The HFZ is seismically active with significant earthquakes sequences in 1867–1868, 1872 and 1884-1885, causing considerable structural damage at Húsavík and surrounding farms (*Thoroddsen*, 1905).

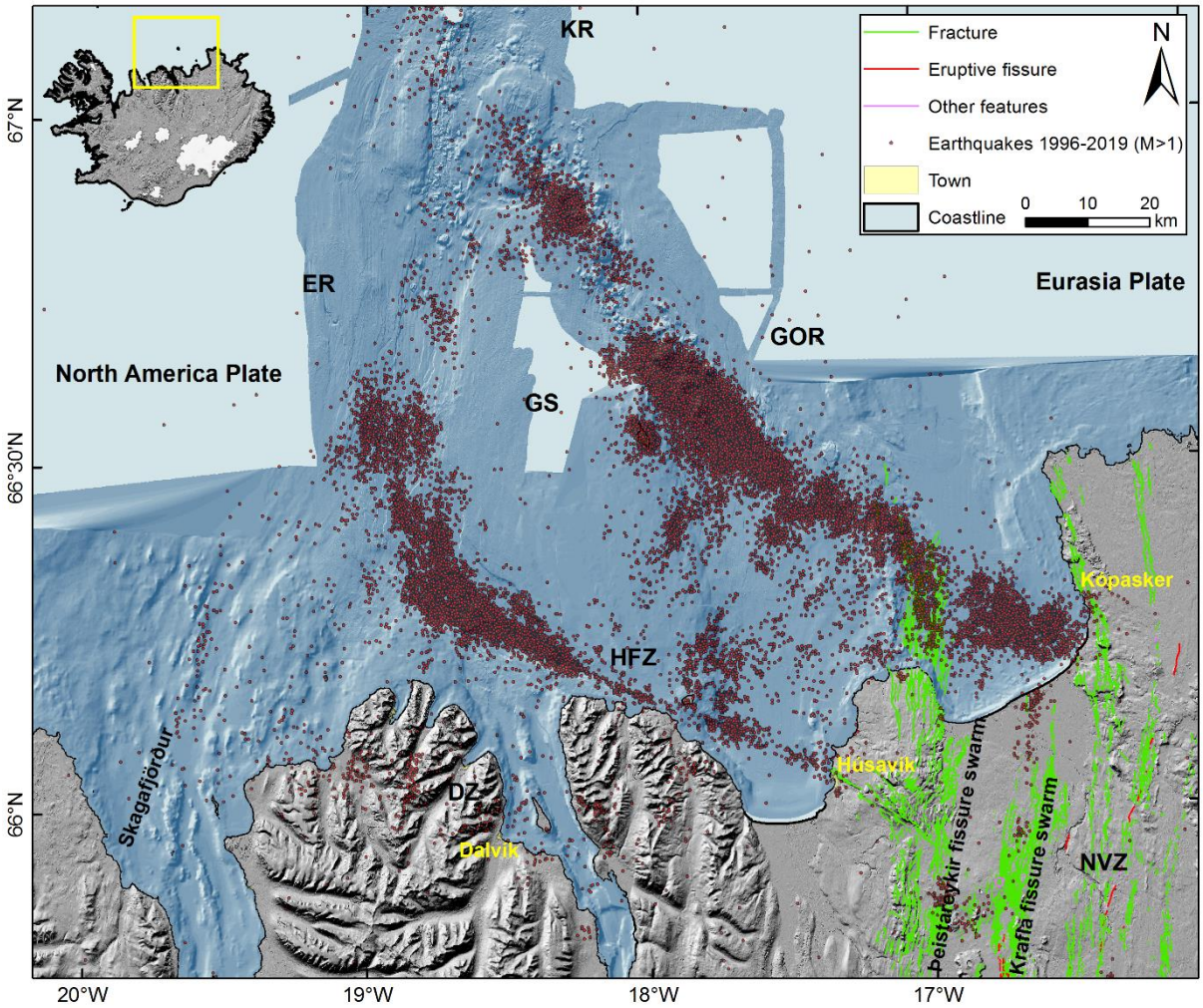

Fig. 1. Overview map of the topography and seismicity of the Tjörnes Fracture Zone. Epicenters of earthquakes larger than magnitude 1 for the period 1996 to 2019 are from the Icelandic Meteorological Office. Topographical data on land are from TanDEM-X digital elevation models. Bathymetric data off shore are a combination of multi-beam data (Magnúsdóttir et al., 2015) and single-beam data of the Icelandic Coast Guard, Hydrographic Department. Holocene fractures in green are from Hjartardóttir et al. (2015). KR, ER, GOR, GS, HFZ, DZ, and NVZ are the Kolbeinsey Ridge, Eyjafjarðaráll Rift, Grímsey Oblique Rift, Grímsey Shoal, Húsavík-Flatey Zone, Dalvík Zone, and Northern Volcanic Zone, respectively.

The crustal block demarcated by the GOR, ER, HFZ, and NVZ, in some way acts independently of the two major lithospheric plates, North America and Eurasia Plates. This Grímsey Block is too small to be a candidate for a microplate and is subjected to internal deformation. A prominent N-S trending zone of seismicity cuts it in two, connecting the GOR and the HFZ along the eastern edge of the Grímsey shoal. This zone consists of 3-4 NNE-striking faults. The sense of faulting is most likely left-lateral strike-slip.

There is indication of a third major shear zone about 30 km south of the HFZ, the enigmatic Dalvík Zone (DZ). Large historic earthquakes have occurred in this zone, most recently in 1963 and 1934 (*Einarsson*, 1976; *Halldórsson*, 2005; *Stefánsson et al*., 2008), but recent GPS measurements have failed to show significant movements along it (*Metzger et al*., 2013). Bookshelf-type tectonism has been suggested and is supported by the distribution of epicenters in the last decades. The epicentral zone of the 1963 Skagafjörður earthquake is off shore at the western end of the Dalvík Zone. It was a strike-slip event on a WNW- or NNE-striking fault (*Sykes*, 1967; *Stefánsson*, 1966). Epicenters of earthquakes in recent years define a faint seismic lineament with a NNE-trend, supporting the suggestion of Stefánsson (1966). The available single-channel reflection data reveal a topographic disturbance with the same trend in the area, here interpreted to be the source fault of the 1963 earthquake.

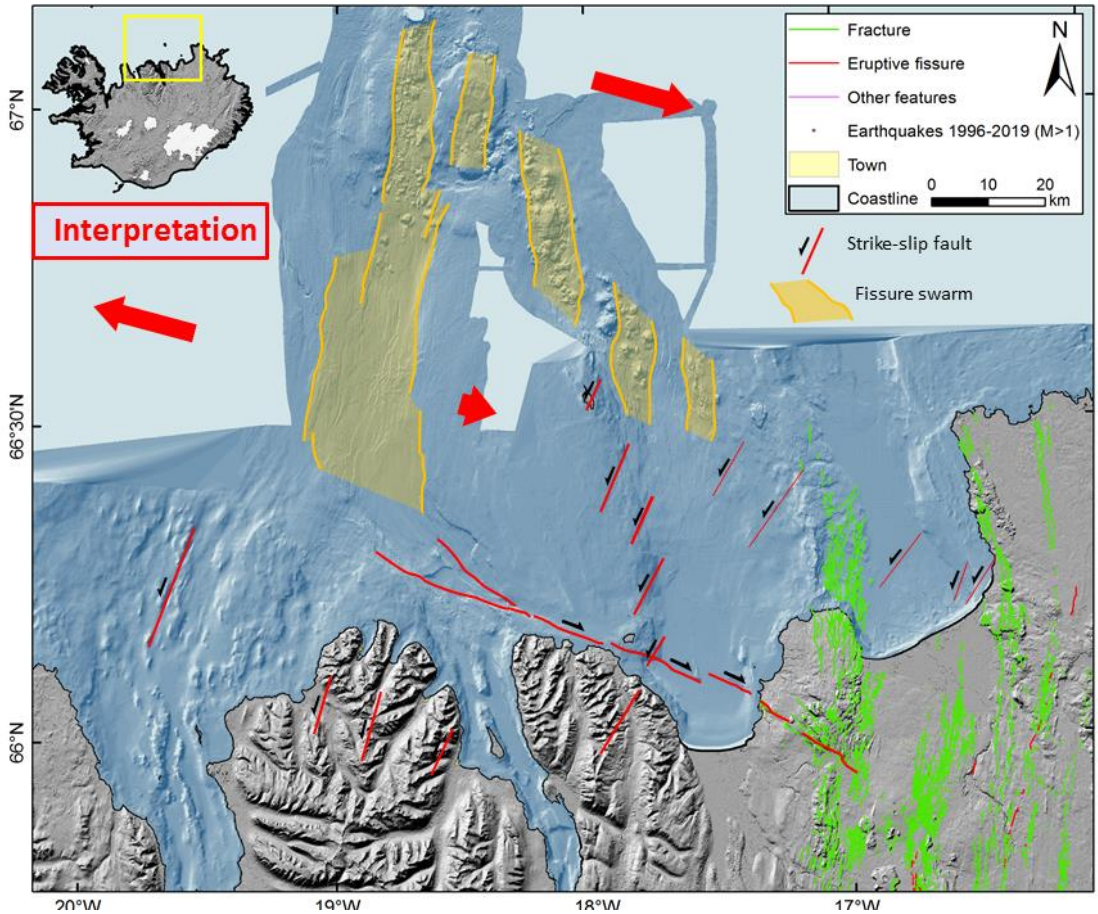

Fig. 2. Interpretation of seismogenic structures of the Tjörnes Fracture Zone, showing fissure swarms of the volcanic systems and strike-slip faults. Red arrows show the direction of the relative plate velocities. The arrow to the left shows the relative movement of the North America Plate with respect to a fixed Eurasia Plate. The two arrows to the right show the relative movement of the Grímsey Shoal and the Eurasia Plate, respectively, assuming a fixed North America Plate.

References

Björnsson, S., P. Einarsson, H. Tulinius, Á. R. Hjartardóttir. Seismicity of the Reykjanes Peninsula 1971-1976. *J. Volcanol. Geothermal Res.*, https://doi.org/10.1016/j.jvolgeores.2018.04.026, 2018.

Bonali, F.L., A. Tibaldi, P. Mariotto, E. Russo, Interplay between inherited rift faults and strike-slip structures: Insights from analogue models and field data from Iceland. Global and Planetary Change, 2018. https://doi.org/10.1016/j.gloplacha.2018.03.009

Einarsson, P. Relative location of earthquakes in the Tjörnes fracture zone, *Soc. Sci. Islandica, Greinar V*, 45-60, 1976.

Einarsson, P. Earthquakes and present-day tectonism in Iceland. *Tectonophysics*, **189,** 261-279, 1991.

Einarsson, P. Plate boundaries, rifts and transforms in Iceland. *Jökull*, **58,** 35-58, 2008.

Einarsson, P., Á. R. Hjartardóttir, P. Imsland, S. Hreinsdóttir. The structure of seismogenic strike-slip faults in the eastern part of the Reykjanes Peninsula oblique rift, SW Iceland. Journal of Volcanology and Geothermal Research, doi:10.1016/j.jvolgeores.2018.04.029, 2018.

Halldórsson, P. *Jarðskjálftavirkni á Norðurlandi* (Seismic activity in North Iceland, in Icelandic). Icelandic Meteorological Office, Report VÍ-ES-10, 41 pp., 2005.

Hjartardóttir, Á. R., P. Einarsson, E. Bramham, and T. J. Wright. The Krafla fissure swarm, Iceland, and its formation by rifting events. *Bulletin of Volcanology*, **74,** 2139-2153. doi 10.1007/s00445-012-0659-0. 2012.

Hjartardóttir, Á.R., Einarsson, P., Magnúsdóttir, S., Björnsdóttir, Þ. and Brandsdóttir, B. Fracture systems of the Northern Volcanic Rift Zone, Iceland – An onshore part of the Mid-Atlantic plate boundary. In: Wright, T. J., Ayele, A., Ferguson, D. J., Kidane, T. & Vye-Brown, C. (eds) Magmatic Rifting and Active Volcanism. Geological Society, London, Special Publications, 420, http://dx.doi.org/10.1144/SP420.1, 2015.

Jónsdóttir, K., G.B. Guðmundsson, L. Passarelli, S. Jónsson & monitoring team at IMO, The Kópasker seismic swarm in Spring 2019, In *Proceedings to the Northquake 2019 workshop* (this volume), 2019.

Magnúsdóttir, S., B. Brandsdóttir, N. Driscoll and R. Detrick. Postglacial tectonic activity within the Skjálfandadjúp Basin, Tjörnes Fracture Zone, offshore Northern Iceland, based on high resolution seismic stratigraphy. *Marine Geology* **367,** 159-170, doi:10.1016/j.margeo.2015.06.004, 2015.

Metzger, S., Jónsson, S., Danielsen, G., Hreinsdóttir, S., Jouanne, F., Giardini, D., & Villemin, T. Present kinematics of the Tjörnes Fracture Zone, North Iceland, from campaign and continuous GPS measurements. *Geophysical Journal International*, **192**, 441-455, 2013.

Rögnvaldsson, S. T., A. Gudmundsson, R. Slunga. Seismotectonic analysis of the Tjörnes Fracture Zone, an active transform fault in north Iceland. *J. Geophys. Res.* **103,** 30117-30129, 1998.

Saemundsson, K. Evolution of the axial rifting zone in Northern Iceland and the Tjörnes fracture zone. *Geol. Soc. Amer. Bull.*, **85**: 495-504, 1974.

Stefánsson, R., Methods of focal mechanism with application to two Atlantic earthquakes. *Tectonophysics*, **3**, 209-243, 1966.

Stefánsson, R., Gudmundsson, G. B., & Halldorsson, P. Tjörnes fracture zone. New and old seismic evidences for the link between the North Iceland rift zone and the Mid-Atlantic ridge. *Tectonophysics,* **447,** 117-126, doi:10.1016/j.tecto.2006.09.019. 2008.

Sykes, L. R. Mechanism of earthquakes and nature of faulting on the mid-oceanic ridges. *J. Geophys. Res.*, **72**, 2131-2153, 1967.

Thoroddsen, Þ. *Landskjálftar á Íslandi.* (Earthquakes in Iceland, in Icelandic). Hið Íslenska Bókmenntafélag, Kaupmannahöfn, 1905.

Tibaldi A., Bonali F.L., Einarsson P., Hjartardóttir Á.R., Pasquarè Mariotto F.A. Partitioning of Holocene kinematics and interaction between the Theistareykir Fissure Swarm and the Husavik-Flatey Fault, North Iceland. *J. Structural Geology*, doi:10.1016/j.jsg.2016.01.003, 2016.

NORTHQUAKE 2019 - The 3rd International Workshop on Earthquakes in North Iceland
Húsavík, North Iceland, 21-24 May 2019

TECTONICS OF THE EYJAFJARÐARÁLL RIFT, ABANDONED SOUTHERN SEGMENT OF THE KOLBEINSEY RIDGE, NORTH ICELAND

Bryndís Brandsdóttir[1], Jeffrey A. Karson[2], Gunnar B. Guðmundsson[3], Kristín Jónsdóttir[3], Robert S. Detrick[4], and Neal W. Driscoll[5]

[1]*Institute of Earth Sciences, Science Institute, University of Iceland (bryndis@hi.is)*
[2]*Department of Earth Sciences, Syracuse University, Syracus, New York, USA*
[3]*Icelandic Meteorological Office, Reykjavík, Iceland*
[4]*Incorporated Research Institutions for Seismology (IRIS), Washington DC, USA*
[5]*Scripps Institute of Oeanography, San Diego, California, USA*

The multi-branched plate boundary across Iceland is made up of divergent and oblique rifts, and transform zones, characterized by entwined extensional and transform tectonics. The Tjörnes Fracture Zone (TFZ) is a complex transform linking the northern rift zone (NVZ) on land with the offshore Kolbeinsey Ridge. The TFZ lacks a clear topographic expression typical of oceanic fracture zones. The transform zone is roughly 150 km long (E-W) by 50-75 km wide (N-S) with three N-S trending pull-apart basins bounded by a complex array of normal and oblique-slip faults. The offshore extension of the NVZ, the Grímsey Oblique Rift, is composed of several active volcanic systems with N-S trending fissure swarms, including the Skjálfandadjúp Basin (SB). The magma-starved southern extension of the KR, the ~80 km NS and 15-20 EW Eyjafjarðaráll Rift (ER), is made up of dominantly normal faults merging southwards with a system of right-lateral strike-slip faults with vertical displacement up to 15 m in the Húsavík Flatey Fault Zone (HFFZ). The northern ER is a 500-700 m deep asymmetric rift, framed by normal faults with 20-25 m vertical displacement, To the south, transform movement associated with the HFFZ has created a NW- striking pull-apart basin with frequent earthquake swarms. Details of the tectonic framework of the ER are documented in a compilation of data from aerial photos, satellite images, field mapping, multibeam bathymetry, high-resolution seismic reflection surveys (Chirp) and seismicity. The TFZ rift basins contain post-glacial sediments of variable thickness. Strata in the western ER and SB basins dip steeply E along the normal faults, towards the deepest part of the rift. The eastern side of the ER and SB basins differ considerably from the western side, with near-vertical faults. Correlation of Chirp reflection data and tephrochronology from a sediment core reveal major rifting episodes between 10-12.1 kyrs BP activating both the Eyjafjarðaráll and Skjálfandadjúp rift basins, followed by smaller-scale fault movements throughout Holocene. These vertical fault movements reflect elevated tectonic activity during early postglacial time coinciding with isostatic rebound and enhanced volcanism within Iceland.

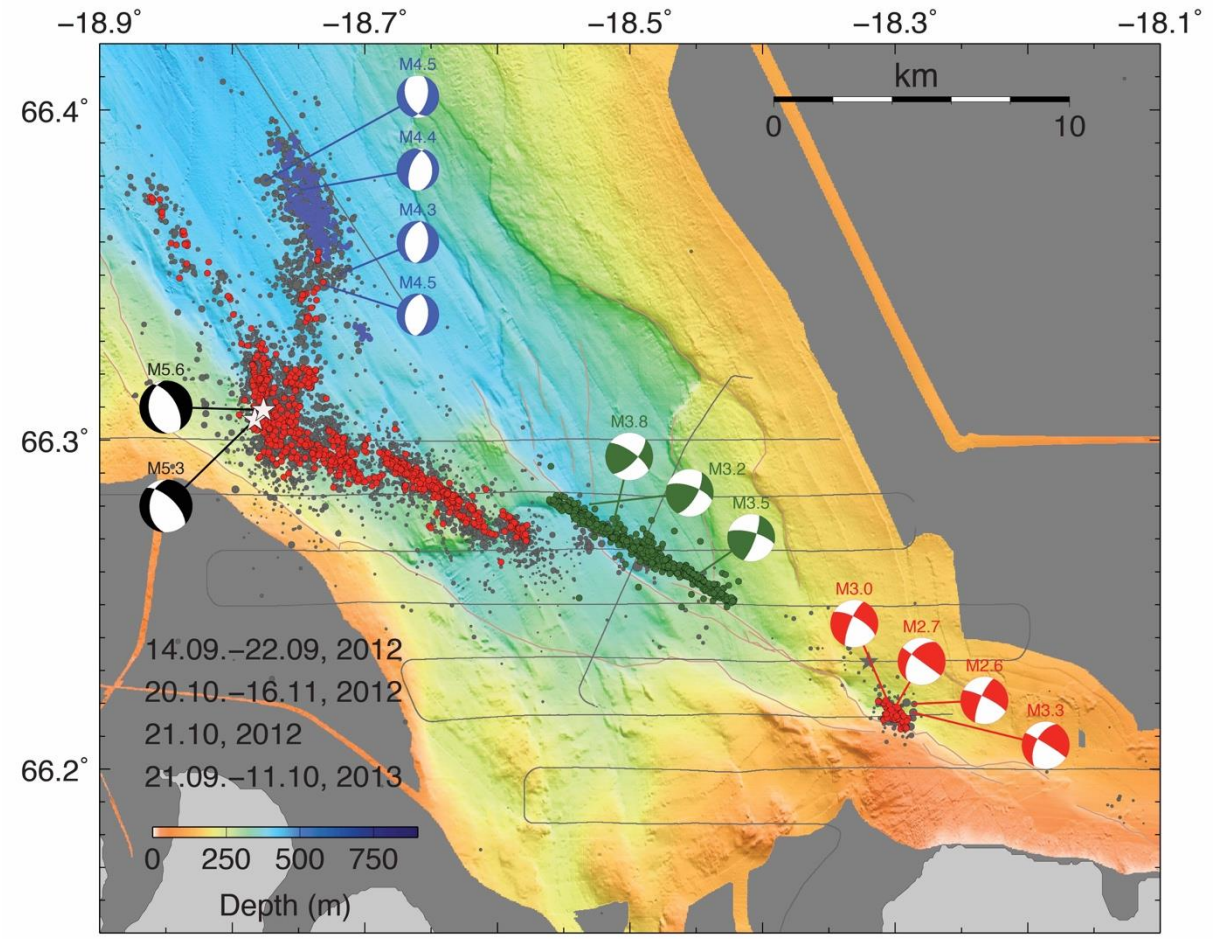

Figure 1. Bathymetry of the southern Eyjafjarðaráll rift. This complicated tectonic region is clearly represented by recent seismicity. Normal faulting events within the ER during a intense earthquake swarm in 2012 indicates active rifting within this region. The 2012 extension event is likely to have triggered strike-slip faulting along the westernmost Húsavík-Flatey fault system in 2012 and 2013. High-resolution Chirp reflection profiles are marked with grey lines.

NORTHQUAKE 2019 - The 3rd International Workshop on Earthquakes in North Iceland
Húsavík, North Iceland, 21-24 May 2019

MARINE GLACIAL FEATURES AND FAULTING IN THE EYJAFJARÐARÁLL BASIN, NORTH ICELAND

Bailey M OConnell, Patricia Höfer, Bryndís Brandsdóttir

Institute of Earth Sciences, University of Iceland (bmo11@hi.is, pah14@hi.is, bryndis@hi.is)

Multibeam bathymetric maps provide some answers to long-standing questions about the extent of the Iceland ice sheet during the last glacial maximum (LGM). Evidence of the retreat of individual ice streams associated with the N-Iceland ice sheet can be seen on the sea floor offshore North Iceland (Figure 1), represented by mega scale glacial lineations, elongated landforms formed typically in soft sediments, which reflect fast ice flow.

The Eyjafjarðaráll basin (EB) is a glacially eroded rift, ~80 km NS and 15-20 wide EW, narrowing southwards, towards Eyjafjörður. The southern EB merges with the Húsavík-Flatey Fault system whereas the northern EB forms a triple junction with the southern tip of the Kolbeinsey Ridge and Grímsey Oblique Rift. Recently collected multibeam bathymetric and Chirp shallow-reflection data show that the EB is made up of complex extensional (normal) and transform (strike-slip) faults draped by marginal and subglacial sedimentary features, such as moraines, megaflutes, eskers, mega scale glacial lineations (MSGLs), and unidentified complex till ridge features possibly representing a push moraine or lateral crevasse-squeeze ridges which have not been previously described in literature. These features reflect the past ice flow directions of two major ice streams or outlet glaciers, from Skagafjörður into Skagafjarðardjúp and northern EB, and from Eyjafjörður into southern EB. The MSGLs and megaflutes are orientated parallel to the direction of the major basins and the Kolbeinsey Ridge indicating that they were topographically constrained. Similar megaflutes are also present within Skjálfandadjúp, east of EB. The arcuate till ridges have a “V-shape” with an average width of 300-500 m and an average length ranging from 400-1500 m, opening towards the flow direction of the ice stream. Figure 2 shows an example of the till ridges cut with a lateral moraine running through them. The features occur in clusters where the glacier flow direction was altered. The average depth of the features is 320-450 meters b.s.l. Similar till ridges have not been identified elsewhere. The seafloor also bears ample scars made by icebergs from the Iceland ice sheet during Postglacial time. The faults present in the EB cut through the glacial features, indicating extensional activity within the EB after the deposition of the glacial features and throughout Holocene based on sedimentary structures and current seismicity.

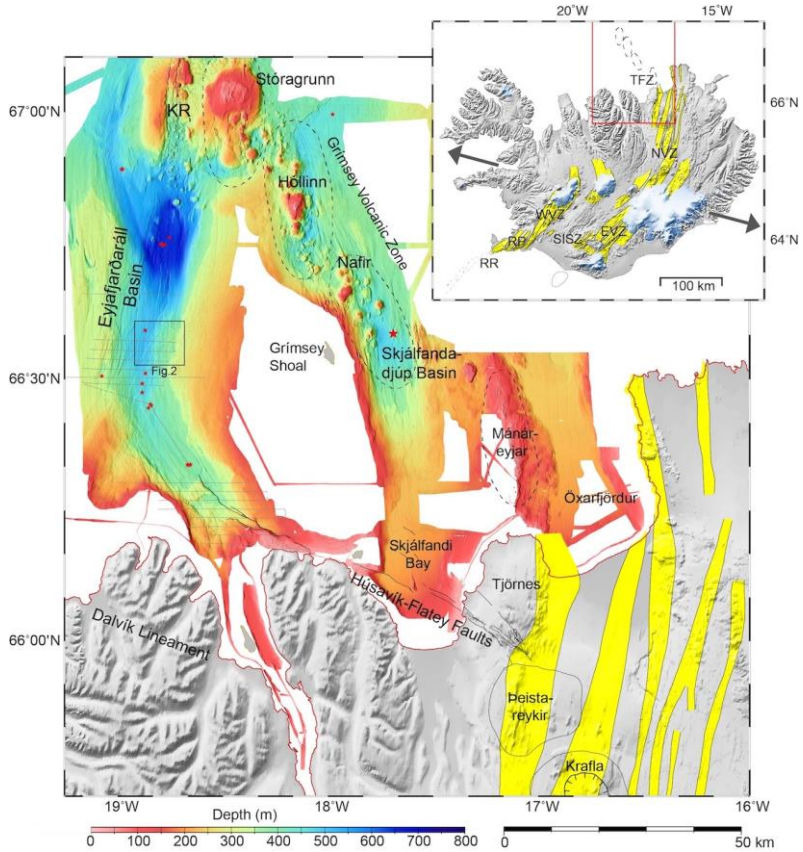

Figure 1. A bathymetric map of the study area, offshore N-Iceland. Location of Figure 2 is shown by a black box. Chirp survey lines are marked in light grey and sedimentary core sites by red stars.

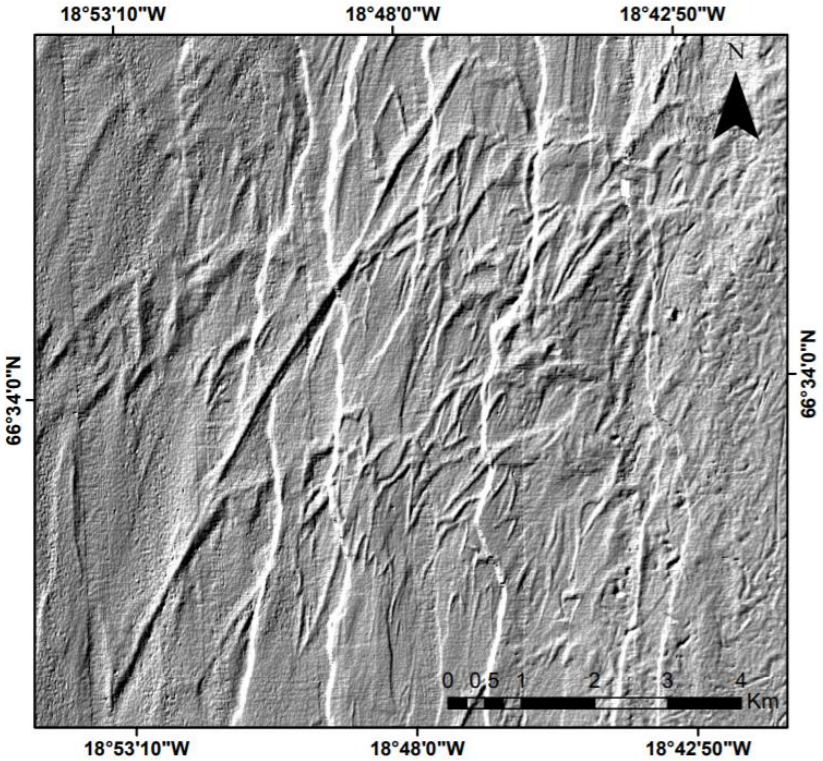

Figure 2. Bathymetric data showing a lateral moraine ridge running through a swarm of arcuate till ridges in Eyjafjarðaráll basin. Image created in ArcMap.

NORTHQUAKE 2019 - The 3rd International Workshop on Earthquakes in North Iceland
Húsavík, North Iceland, 21-24 May 2019

GEOMORPHOLOGICAL EVIDENCE FOR POST-GLACIAL DISPLACEMENT ON THE HÚSAVIK-FLATEY FAULT, OBSERVED WITH DRONE IMAGES

Rémi Matrau[1], Sigurjón Jónsson[1], Daniele Trippanera[1], and Yann Klinger[2]

[1]*King Abdullah University of Science and Technology (KAUST), Saudi Arabia (remi.matrau@kaust.edu.sa)*
[2]*Institut de Physique du Globe de Paris (IPGP), France*

Present-day deformation near the Húsavik-Flatey Fault (HFF), inferred from ~20 years of GPS data, indicates that 6 to 9 mm/yr of right-lateral strike-slip motion is focused on the fault (*Metzger and Jónsson*, 2014). However, little is known about whether this slip rate is representative for the HFF during the Holocene period. To address this topic, we study geomorphological and tectonic structures along the 20 km-long onshore segment of the HFF to assess the post-glacial displacement of the fault and understand the distribution of the deformation over the fault system.

We collected drone photos over four areas (labelled Area 1-4) along the onshore part of the HFF (Fig. 1) and used them to compute high resolution orthomosaic images (resolution down to 2.84 cm/px) and Digital Surface Models - DSMs (resolution down to 4.89 cm/px). The areas range from 0.07 to 0.68 km^2 in size and were covered with 200-2000 photos each. The orthomosaic images and DSMs were processed using the Agisoft PhotoScan © photogrammetry software. We placed and measured 5 to 10 Ground Control Points (GCP) in each area to correct the orthomosaic images and the DSMs for distortions. Using the orthomosaic images and the DSMs, we mapped geomorphological features that have been offset by faulting activity, in order to quantify the displacement along the fault. For each area, we mapped structures such as active and inactive drainage channels, alluvial fans, alluvial terraces, and glacial moraines (Fig. 2).

Area 1 is located at the northern edge of Húsavik town (Fig. 1) and consists of a sizable gully near a few horse stables. An alluvial fan is located at the outlet of the gully and it is offset by over 20 m (Fig. 2a). We also identified a clear, abandoned drainage channel to the southwest within Area 1 and we associate this channel to the currently active creek north of the fault trace, which yields an offset that is in the range of ~50 m (Fig. 2a and 2b).

The second area (Area 2) is located east of Botnsvatn Lake (Fig. 1) and is characterized by multiple sub-parallel fault strands and a pull-apart basin, called Krubbsskál, within which four paleoseismology trenches were excavated in 2014-15 (*Harrington et al*., 2016). The fault strand north of the basin displays three active drainage channels, consistently offset by roughly ~30 m (Fig 2d, 2e and 2f). Moreover, we identified an active stream channel, deeply incised, showing the largest offset we have measured so far on the HFF, of over 80 m (Fig. 2c).

Area 3 is located northwest of Höskuldsvatn Lake (Fig. 1) and is larger than the first two areas. Here we mapped a set of offset alluvial terraces showing clear right-lateral offsets, as well as a single-stream offset, where we measured a relatively small offset of <10 m.

Finally, the fourth area we studied (Area 4) is located near the eastern end of the HFF and stretches along south-facing slopes of a mountain, not far from the fault's junction with the Theistareykir fissure swarm (Fig. 1). In this area, we mapped several post-glacial features such as landslides and side moraines showing right-lateral offset.

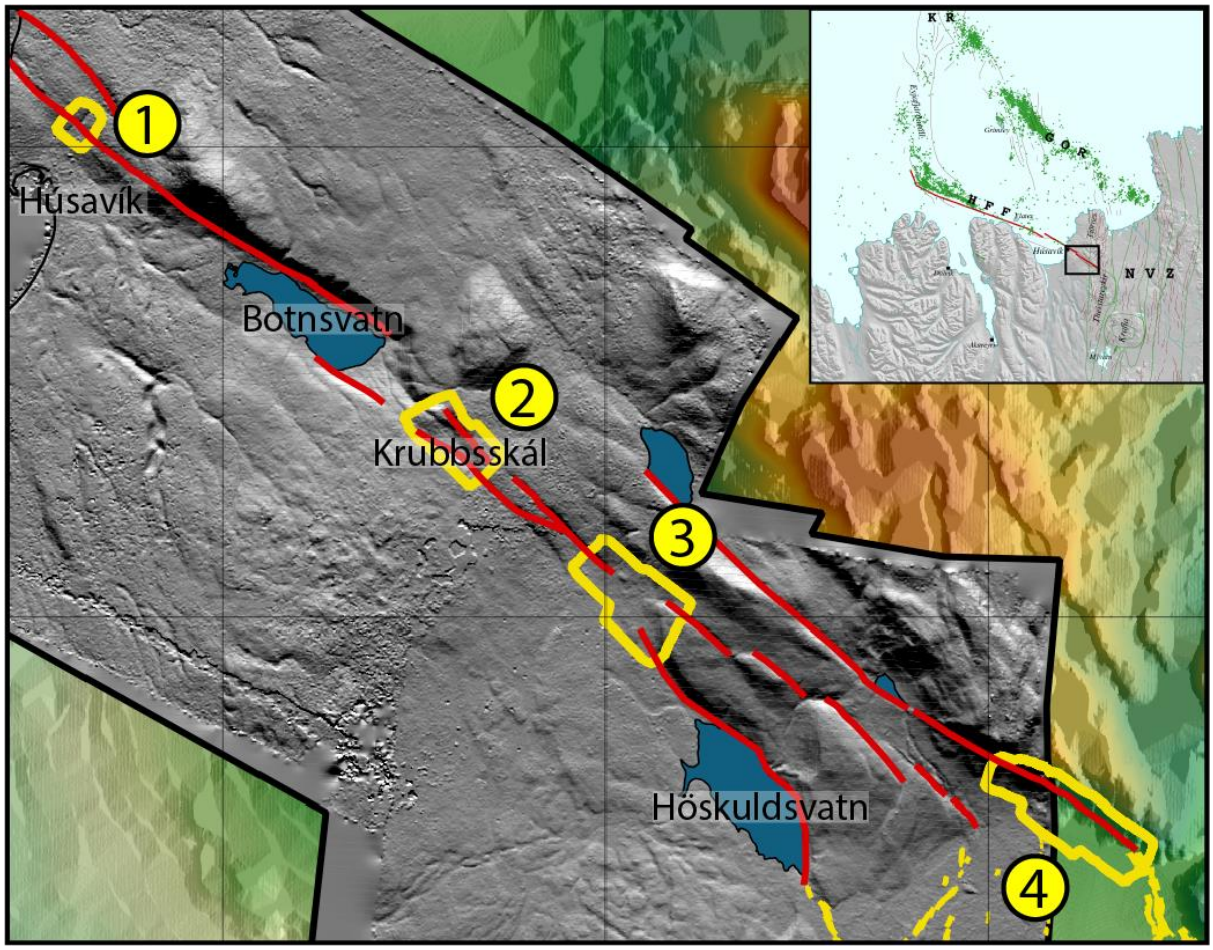

Figure 1. The on-land part of the Húsavik-Flatey Fault (HFF), southeast of Húsavík town, with red lines showing the main fault strands and yellow polygons outlining drone survey Areas 1-4. The inset shows the location of the main map in the Tjörnes Fracture Zone (black rectangle), with KR, GOR, and NVZ indicating the Kolbeinsey Ridge, the Grímsey Oblique Rift, and the Northern Volcanic Zone, respectively.

All the areas we surveyed show evidence of cumulative right-lateral offset in post-glacial landscapes as well as signs of vertical displacement. However, visible vertical displacements of several tens of meters, or even up to hundreds of meters in some places, appear to be older than Holocene. Traces of counter-slope fault scarps were also detected in Areas 3 and 4, indicating a sub-vertical fault, at least close to the surface.

During a 6 Myr period, from 7 Ma to 1 Ma, the HFF was the main transform structure in North Iceland (*Sæmundsson*, 2013), accommodating the 18 mm/yr transform motion between the Northern Volcanic Zone in North Iceland and the Kolbeinsey ridge north of Iceland. The slip rate of the HFF slowed down at about 1 Ma as the Northern Volcanic Zone propagated north into the present-day Öxarfjörður bay and the Grímsey Oblique Rift (GOR) became active (*Sæmundsson*, 2013). Since then, both the HFF and the GOR have accommodated the 18 mm/yr transform motion, but it has not been clear how it has been divided between the two transform structures. Present-day deformation observed by GPS suggests that less than half of the transform motion is focused on the HFF, as mentioned above, with the rest on the GOR (*Metzger and Jónsson*, 2014). One problem with the GPS-derived slip rate is that it is based on only ~20 years of data and the observations may be influenced by post-rifting transient deformation following the Krafla rifting episode 1975-84, which put the eastern half of the HFF into a long-lasting stress shadow (*Maccaferri et al.*, 2013). Quantifying Holocene offsets in post-glacial landscapes along the HFF may therefore help in revealing a more representative slip rate for the HFF.

The offsets determined from the drone data range from a few meters to almost 100 m, so it is clear that some of the drainage channel offsets are younger than the beginning of Holocene. However, if we take the beginning of Holocene at around 11.2 ka (*Ingólfsson et al., 2010*) and use our largest

measured offset in Area 2, it would yield a Holocene horizontal slip rate comparable to the GPS estimates, suggesting that the kinematics of the HFF has been roughly stable throughout the Holocene. However, this comparison is based on only one offset measurement and an inferred maximum age. More systematic offset measurements, as well as dating of the offset structures, are needed to better constrain the slip rate history of the HFF during the Holocene period.

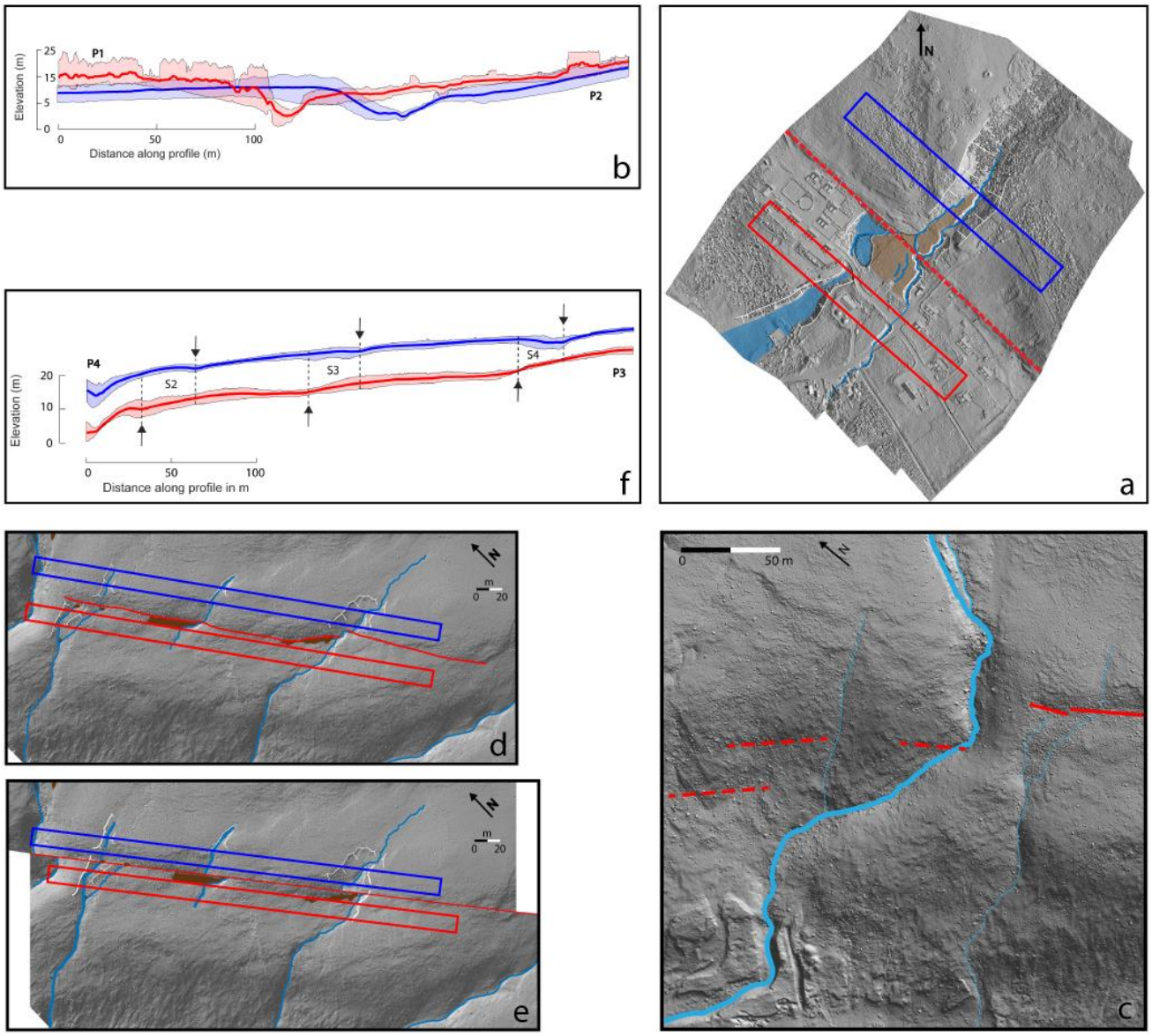

Figure 2. a) Shaded relief map of Area 1 showing a sizeable creek flowing from northeast to southwest, with the fault marked as red dashed line, an offset alluvial fan highlighted in brown, and an abandoned stream channel in blue. The red and blue rectangles indicate the red (downstream) and blue (upstream) fault-parallel topographical profiles in 2b. c) The largest drainage channel offset we have detected so far on the HFF, found in Area 2. d) Further drainage offsets in Area 2 with e) drainage reconstruction indicating consistency of the three parallel channels, where the red (downstream) and blue (upstream) rectangles indicate the fault-parallel upstream (blue) and downstream (red) topographic profiles shown in f), yielding a ~30 m offset.

References

Metzger, S. and S. Jónsson, Plate boundary deformation in North Iceland during 1992-2009 revealed by InSAR time-series analysis and GPS, *Tectonophysics* **634**, 127-138, 2014.

Ingólfsson, Ó., H. Norðdahl, and A. Schomacker, 4 deglaciation and holocene glacial history of Iceland, *Developments in Quaternary Sciences* **13**, 51-68, 2010.

Harrington, J., U. Avsar, Y. Klinger, S. Jónsson and E.R. Gudmundsottir, Fault trenching and geologic slip rates of the Húsavik-Flatey Fault, North Iceland, In *Proceedings to the 2nd workshop on Earthquakes in North Iceland*, 27-29, 2016.

Maccaferri, F., E. Rivalta, L. Passarelli, and S. Jónsson. The stress shadow induced by the 1975-1984 Krafla rifting episode, *J. Geophys. Res.* **118**, doi:10.1002/jgrb.50134, 2013.

Sæmundsson, K., Nature of the Húsavík Faults and Holocene movement on them, In *Proceedings to workshop on Earthquakes in North Iceland*, 30-33, 2013.

NORTHQUAKE 2019 - The 3rd International Workshop on Earthquakes in North Iceland
Húsavík, North Iceland, 21-24 May 2019

LOCAL EARTHQUAKE TOMOGRAPHY IN NORTH ICELAND

Claudia Abril[1], Ari Tryggvason[1], Olafur Gudmundsson[1], Rebekka Steffen[1]

[1]*Uppsala University, Sweden (claudia.abril@geo.uu.se, ari.tryggvason@geo.uu.se, olafur.gudmundsson@geo.uu.se, rebekka.steffen@lm.se)*

Local earthquake tomography has been carried out in the Tjörnes Fracture Zone (TFZ) using data of the North Iceland Experiment (NICE). The TFZ is a transform region that connects the Kolbeinsey Ridge with the Northern Volcanic Zone of Iceland in a mostly offshore area. The challenge to record seismic information in this area was the motivation for the NICE. Fourteen ocean-bottom seismometers and eleven on-land stations were installed in the project and operated simultaneously with the permanent Icelandic seismic network (SIL) during summer 2004 (see the distribution of the temporal network in Fig.1). 500 seismic events recorded during the experiment, including 16 explosions, were used to estimate P- and S-wave seismic velocities in the area. Crustal velocities are resolved over a broader area and wider depth range than in the tomographic results of *Riedel et al.* (2005). The velocity structure is illuminated approximately between 3 and 15 km depth near the main lineaments, Húsavík-Flatey Fault (HFF) and Grímsey Oblique Rift (GOR). This is also where resolution is the best (13 km in the horizontal and 3 km in depth).

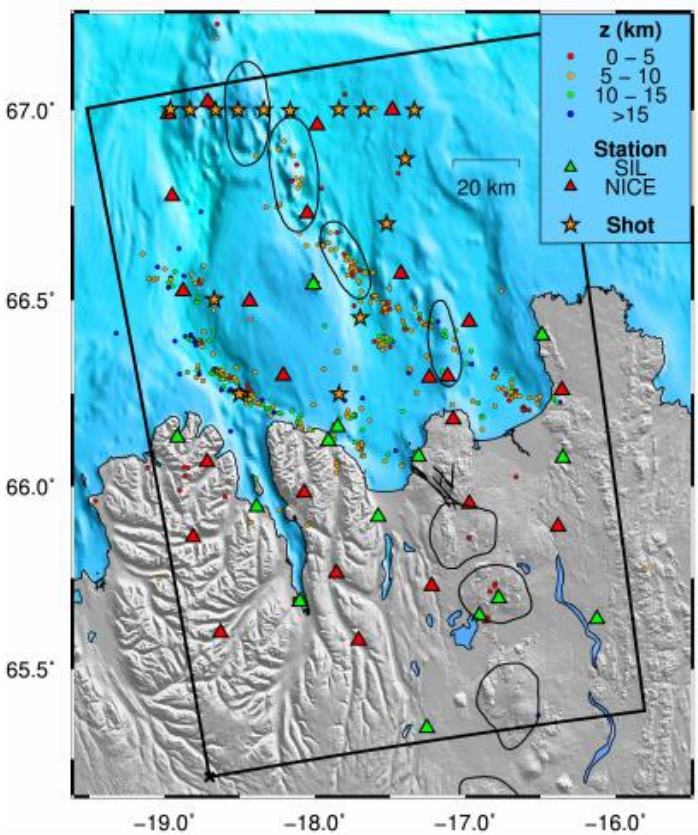

Figure 1. Distribution of seismic stations during the NICE experiment. Green triangles are the permanent SIL network stations. Red triangles are OBSs and additional on-land stations installed for the experiment. 484 earthquakes (coloured dots) together with the 16 shots (yellow stars) fired during the experiment were used in the LET. Earthquake locations are those estimated using the manual picking of P- and S-wave arrivals in SEISAN. The study area is enclosed by the black box.

Results of the local-earthquake tomography (LET) are shown in Fig. 2 that presents depth slices of the final velocity model for P- and S-waves and Vp/Vs ratio between depths of 3.25 and 8.5 km. Upper-crustal velocities (Vp and Vs) are found to be relatively low in the offshore region. In particular, low velocities are mapped along the Húsavík-Flatey Fault (HFF) (from x=10,y=150; to x=75,y=100). Low velocities are also mapped along the Grímsey Oblique Rift (GOR) (from x=50,y=175; to x=100,y=125) and in a zone connecting these two main lineaments north of Skjálfandi Bay (x=75,y=100). A region surrounding Grímsey Island appears as a fast anomaly. Furthermore, localized high-velocity anomalies are found beneath northern Tröllaskagi and Flateyjarskagi Peninsulas (x=10 and x=50,y=100), where bedrock dates from Upper and Middle Miocene (10-15 Ma). Regions of low Vp/Vs ratio are mapped at depth along the main lineaments.

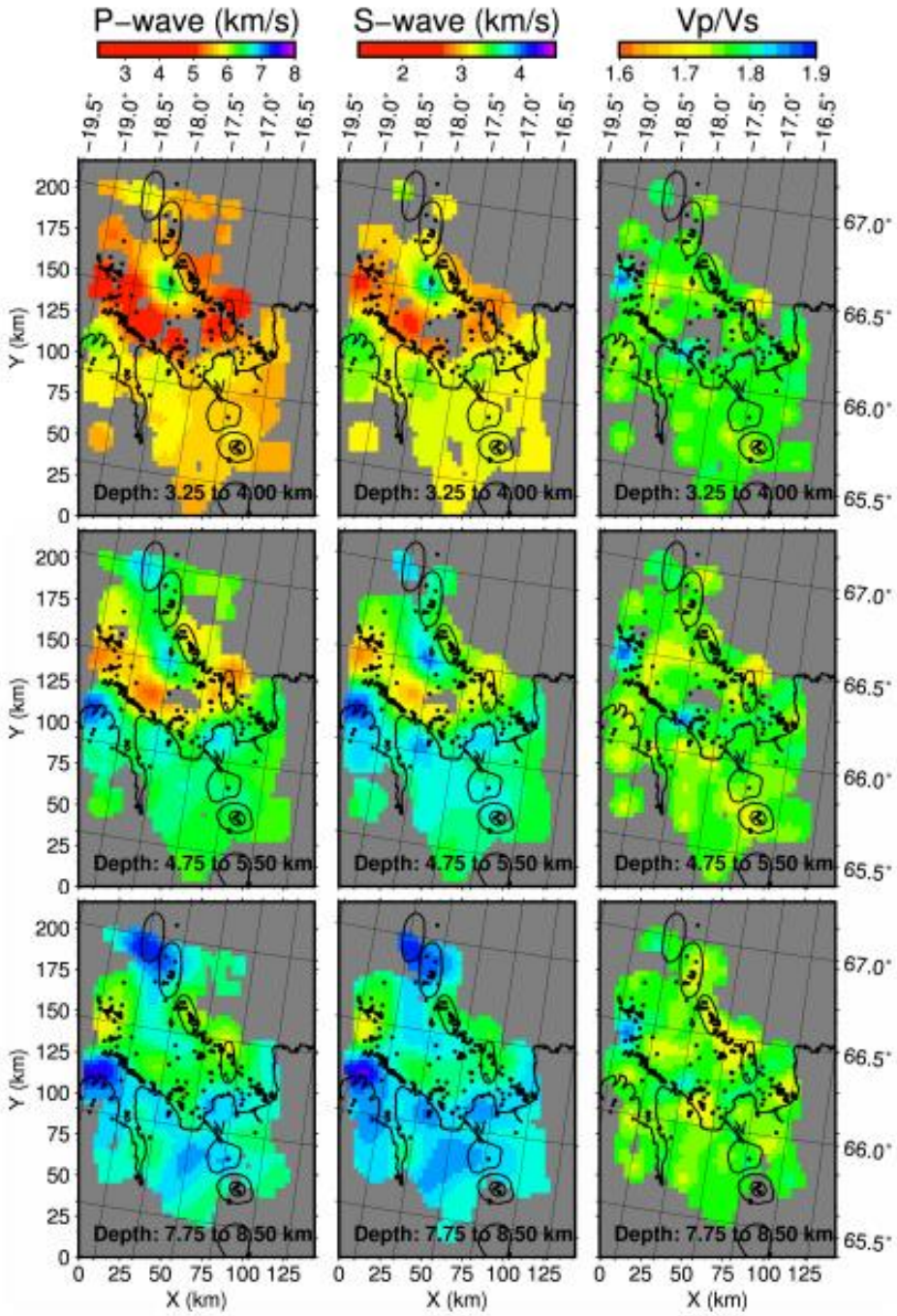

Figure 2. 3-D velocity model from the LET. The panels show map views of the model at different depth intervals. Vp and Vs velocity models are presented in the left and central panels, while the Vp/Vs ratio is shown in the right panels.

For comparison with the tomographic results, the Bouguer gravity anomaly was derived from the free-air gravity data of *Sandwell and Smith* (2009), smoothed with a 14 km wavelength filter. A Bouguer-plate and terrain correction was applied, using elevation data from *Smith and Sandwell* (1997). A regional NS trend was removed. The Bouguer anomaly is presented in Fig. 3, where we also outline the sedimentary thickness contours based on seismic reflection results reported by *Richter and Gunnarsson* (2010). A negative Bouguer anomaly lies parallel to and just north of the HFF. The sediments are also thickest along and north of the HFF, but the gravity anomaly is not strongest where the sediments appear thickest and the sediment anomaly is broader than the gravity anomaly. Other notable gravity anomalies of relevance to our tomographic results are a gravity high located at and westward of Grímsey Island, and a weak gravity low located north of TFZ (just north of 66.5ºN). Finally, positive gravity anomalies on northern Tröllaskagi and Flateyjarskagi Peninsulas are also comparable with the tomographic results.

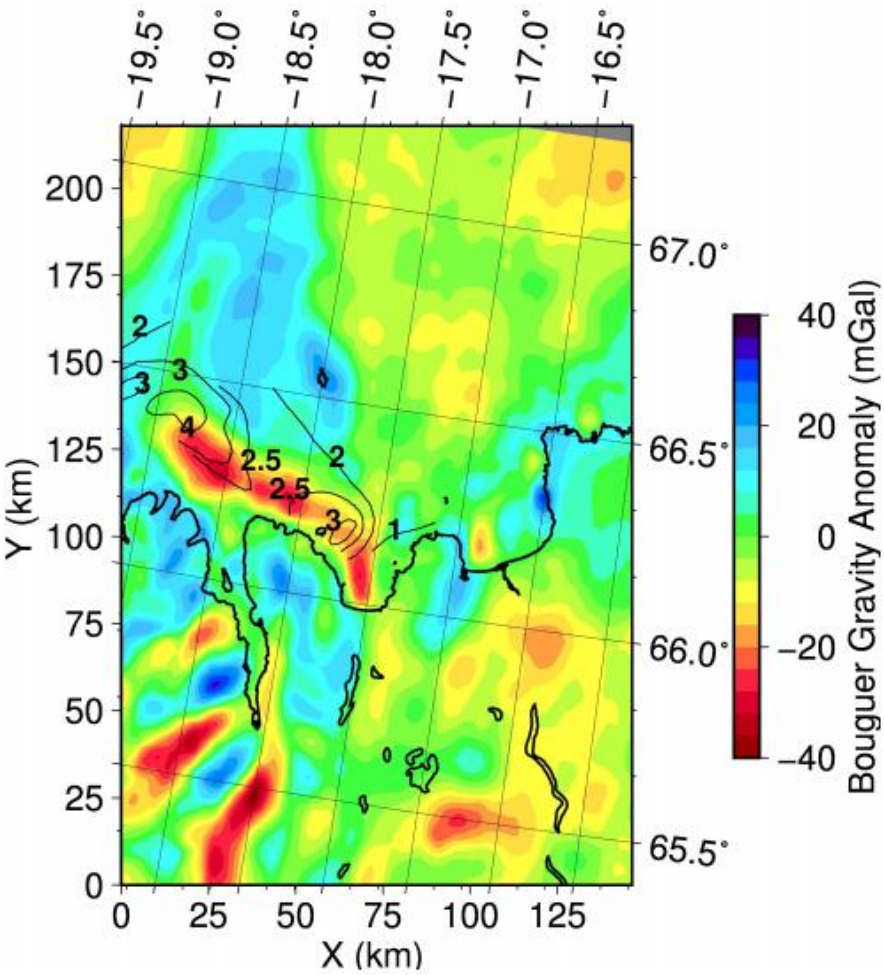

Figure 3. Bouguer gravity anomaly and contour lines of sediment thickness estimated by Gunnarsson (1998) (see also Richter and Gunnarsson (2010)). The map presents the detrended Bouguer anomaly removing the best fitting, northward, linear trend.

The low-velocity anomaly located offshore, north of the HFF, coincides with a Bouguer gravity low, although the gravity anomaly is considerably narrower. Thick (up to 4 km) Quaternary sediments are found in the same general area. However, velocities remain low at greater depth as a part of a larger region in between and including the GOR. This area corresponds to the extended gravity low, northeast of TFZ. Low velocities at depth along the HFF cannot be explained as a smearing of the low velocities of the overlying sediments to depth and are interpreted as due to fracturing associated with the transform motion extending into the middle crust (e.g. *Avendonk et al.*, 2001). Serpentinization can be excluded as the resolved volume is well within the crust (e.g. *Gudmundsson*, 2003). Low velocities along the

volcanic northwestern part of the GOR may relate to anomalous temperatures in the upper crust, e.g., due to intrusions, or fracturing of the crust. Fast upper-crustal velocities (also corresponding to positive gravity anomalies) located beneath and west of Grímsey Island and northern Tröllaskagi and Flateyjarskagi Peninsulas, are proposed to be either Tertiary formations associated with relic volcanoes (concentrations of crystalline intrusives and cumulates) (e.g., *Brandsdottir et al*., 1997; *Jeddi et al.*, 2017), or blocks of older crust (15-30 Ma) hidden beneath younger flood basalts (*Foulger*, 2006). Low Vp/Vs anomalies, found along the HFF and the GOR at a depth of 5-10 km, are interpreted as due to compressible, supercritical fluids (e.g. *Tryggvason et al*., 2002).

References

Avendonk, H., A. Harding and J. Orcutt. Contrast in crustal structure across the Clipperton transform fault from traveltime tomography, *J. Geophys. Res.* **106(B11)**, 10961-10981, 2001.

Brandsdottir, B., W. Menke, P. Einarsson and R. White. Färoe-Iceland Ridge Experiment 2: Crustal structure of the Krafla central volcano, *J. Geophys. Res.* **102(B4)**, 7867-7886, 1997.

Foulger, G. Older crust underlies Iceland, *Geophys. J. Int.* **165**, 672-676, 2006.

Gudmundsson, O. The dense root of the Icelandic crust, *Earth Planet. Sci. Lett.* **206**, 427-440, 2003.

Gunnarsson, K., Sedimentary basins of the N-Iceland shelf, *Report* **OS-98014**, 1998.

Jeddi, Z., O. Gudmundsson and A. Tryggvason. Ambient-noise tomography of Katla volcano, south Iceland, *J. Volcanol. Geoth. Res.* **347**, 264-277, 2017.

Richter, B. and K. Gunnarsson, Overview of hydrocarbon related research in Tjörnes, Re*port Project No.* **503402**, 2010.

Riedel, C., A. Tryggvason, T. Dahm, R. Stefanson, R. Bodvarson and G. Gudmundsson, The seismic velocity structure north of Iceland from joint inversion of local earthquake data, *J. Seis.*, **9**, 383–404, 2005.

Sandwell, D.T. and W.H.F. Smith, Global marine gravity from retracked Geosat and ERS-1 altimetry: Ridge Segmentation versus spreading rate, *J. Geophys. Res.*, **114(B01)**,411, 2009.

Smith, W.H.F. and D.T. Sandwell, Global sea-floor topography from satellite altimetry and ship depth soundings, *Science*, **277**, 1957–1962, 1997.

Tryggvason, A., S. Rögnvaldsson and O. Flóvenz, Three-dimensional imaging of the P- and S-wave velocity structure and earthquake locations beneath Southwest Iceland, *Geophys. J. Int.* **151**, 848-866, 2002.

NORTHQUAKE 2019 - The 3rd International Workshop on Earthquakes in North Iceland
Húsavík, North Iceland, 21-24 May 2019

KÓPASKER EARTHQUAKE IN 1976
ABOUT PRE-ACTIVITY, LOCATION AND POST-ACTIVITY

Ragnar Stefánsson[1] and Gunnar B. Guðmundsson[2]

[1] *University of Akureyri, Iceland (raha@simnet.is)*
[2] *Icelandic Meteorological Office (gg@vedur.is)*

The Kópasker earthquake occurred in the eastern part of the Tjörnes fracture zone, offshore North Iceland, on 13 January 1976. The mainshock epicenter was only about 8 km southwest of Kópasker village, causing considerable damage there, and the magnitude was 6.0 (Mb) – 6.4 (Ms). The earthquake was preceded by a rifting event in the Krafla fissure swarm of the northern rift zone of Iceland, which started 24 days earlier. Coseismic E-W opening was observed on the S-N trending rim of the fissure swarm going through Kópasker, most clearly seen in the area from 4-5 km south of Kópasker and passing the village, but fading away to the north of it.

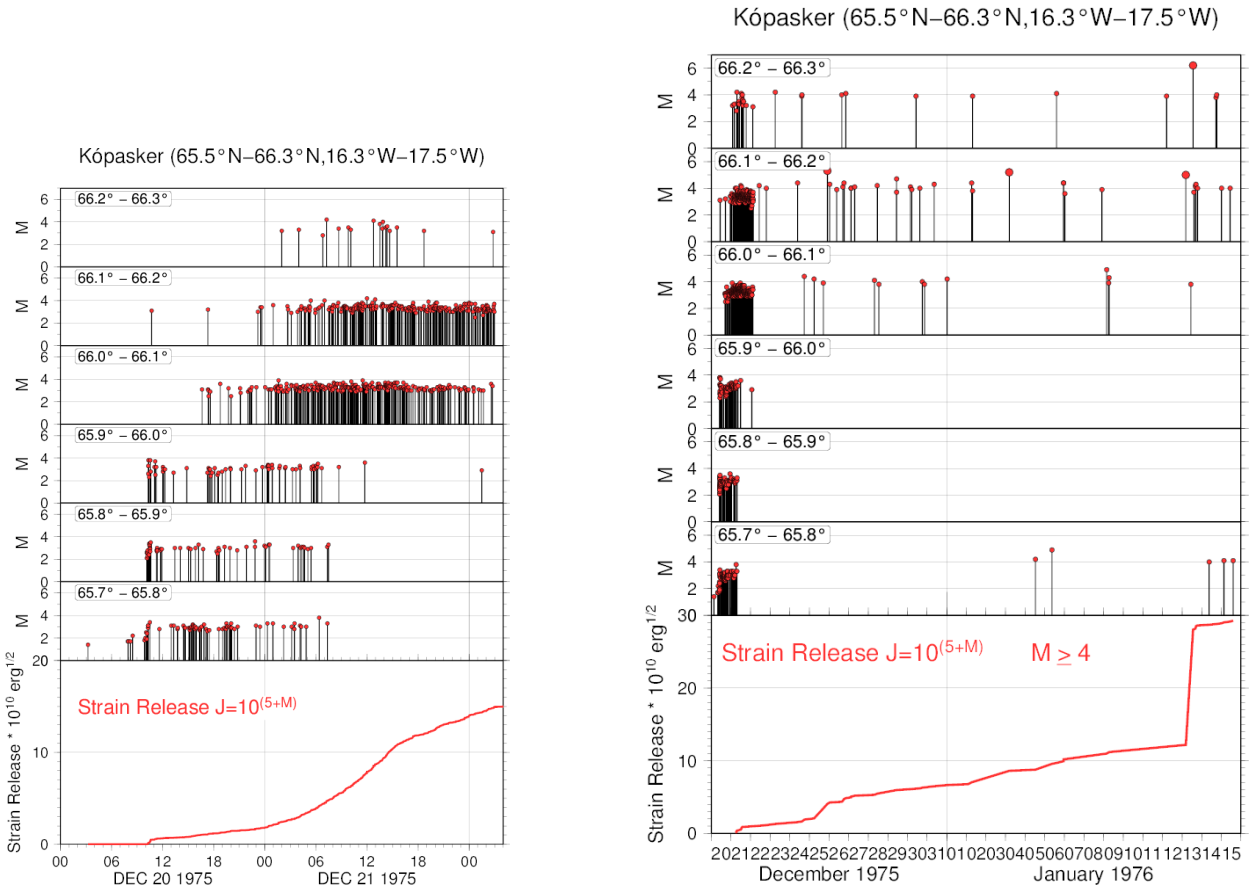

Figure 1. The left image shows monitored earthquake magnitudes (completeness M3) with time during the first two days of the Krafla rifting episode. The bottom M-row covers the Krafla Caldera to the south, and then the activity is shown in 11 km parts of the rift towards the northernmost part at 66.2°N-66.3°N where the Kópasker earthquake eventually occurred 23 days later. The right image contains M4 or larger earthquakes only, except for the first two days, from 20 December 1975 to 15 January 1976. This is based on IMO evaluations which did not reach below M4 for this sequence (Stefánsson et al., 2016).

The Krafla rifting episode.

Rifting started on 20 December 1975 at 10:17 am by an intensive seismic swarm at the Krafla caldera, coinciding with a minor eruption there, in the Leirhnjúkur crater. Within only one day, rifting initiated along the Krafla fissure swarm, from the Krafla caldera and 50 km to the north, towards the junction with the NW striking Grímsey rift in Öxarfjörður (Figures 1 and 2). After some slow-down, the activity took a definite NE turn towards the eventual epicenter of the Kópasker earthquake (Figure 2). The largest earthquakes of this rifting event, during the 23 days before the Kópasker earthquake, took place where the activity turned to the northeast from the northern part of the Krafla fissure swarm reaching magnitude 5 (Figures 1 and 2).

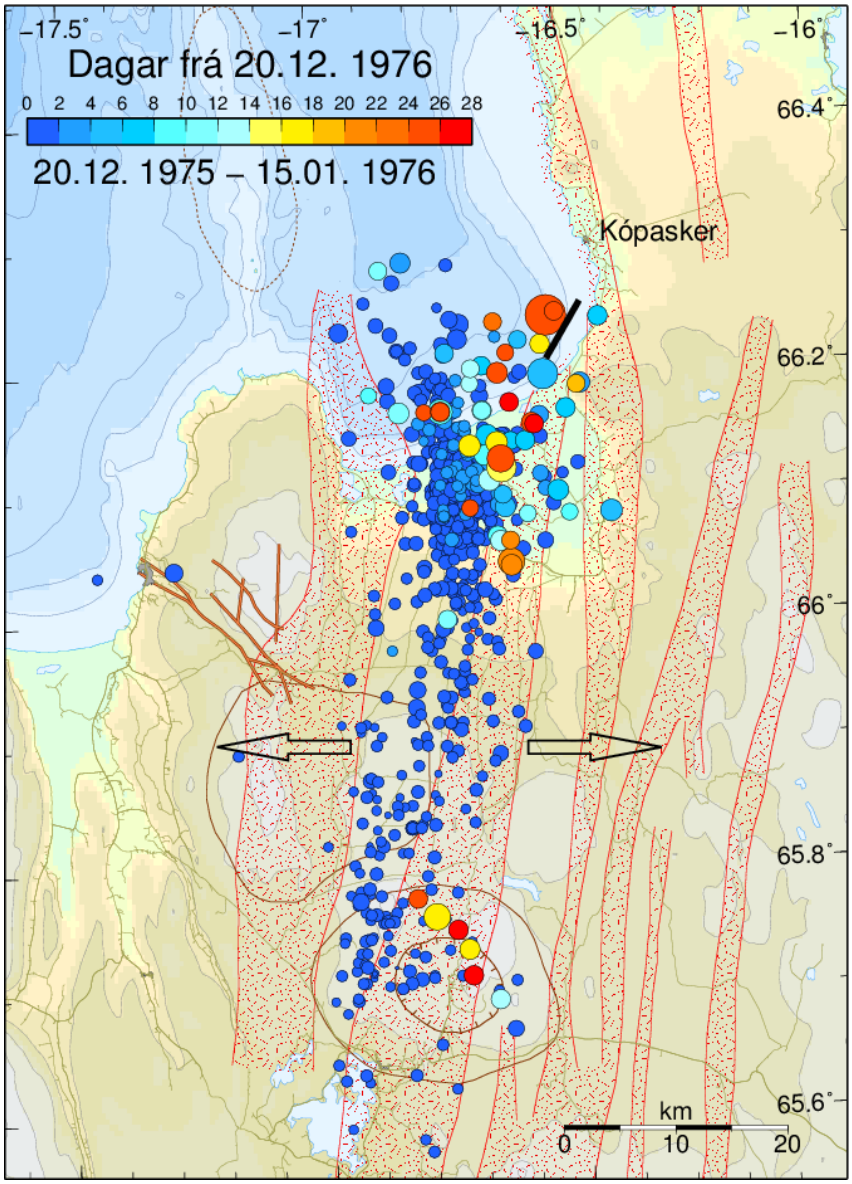

Figure 2. The first part of the Krafla rifting episode was expressed as a northward migration of earthquake epicenters from 20 December 1975 – 15 January 1976. The dark blue colored dots indicate the rifting started in the western part of the Krafla Caldera moving in less than 24 hours to the Öxarfjörður bay, and slowly swaying off towards northwest in the direction of the Grímsey rift. Already on the second day of the rifting event the rifting started to follow a more easterly path, on the Krafla rim and towards northeast, in direction towards Kópasker. The Kópasker earthquake on 13 January is the big red dot 8 km to the SW of Kópasker. The thick, black NE-striking line segment SW of Kópasker is the fault line of the earthquake as suggested by Stefánsson et al (2008). The dots having fresher red colors are aftershocks within a few km southwest of the mainshock and also at 50 km distance in the Krafla Caldera.

The total E-W widening of the Krafla fissure at 66.1°N, i.e. 15 km south of the epicenter of the Kópasker earthquake, during the 2-3 weeks before it, was of the order of two meters (*Sigurðsson*, 1980). The rifting shear stress loaded the focal area of the Kópasker earthquake of 13 January, and the moment released in the magnitude 6.2 strike-slip earthquake was largely built up by the preceding rifting activity (*Stefánsson et al.*, 1979). However, several days of relatively low seismic activity in the epicentral area preceded the mainshock, as seen in Figure 1, until a magnitude 5 earthquake occurred 10 km SSW of the eventual epicenter, just 9 hours before it.

So, although the 1976 earthquake can be considered as a part of a rift-transform process in the long term, it appears as a single tectonic earthquake in the short term, i.e. in the focal area. About 4-5 days of quiescence in the focal area was followed by a half to one day, just before the earthquake, of apparent asperity nucleation, although of course we can only speculate about this course of events as the seismic detection limit was close to magnitude 3.5-4 at that time.

The location and mechanism of the Kópasker earthquake

The epicenter location of the Icelandic Meteorological Office (IMO) is 66.241°N, 16.53°W, with an error limit of 3 km or so. The epicenter location by Stefánsson et al. (2008), determined from post-activity microearthquakes and the IMO location, is 66.23°N, 16.5°W. The magnitude from the different world network sources is typically 6.0 Mb and 6.4 Ms, and the MW (GCMT) is 6.3.

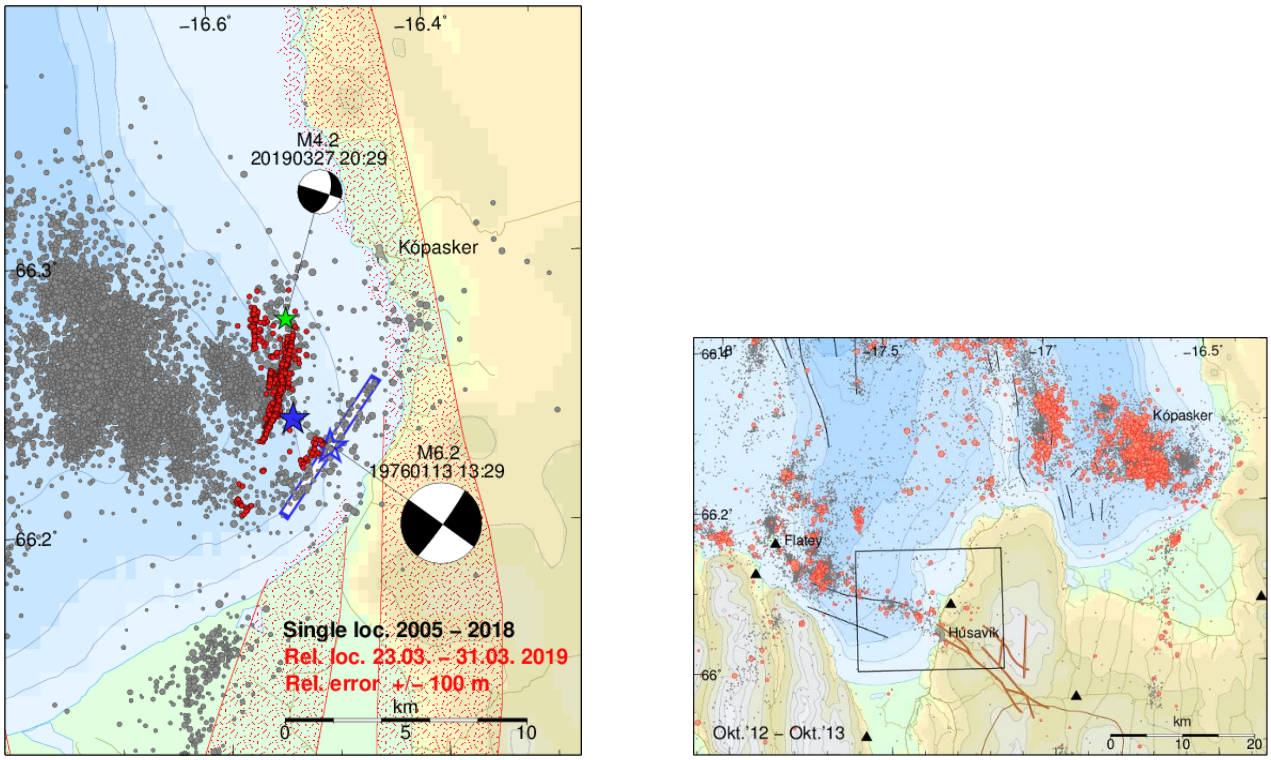

Figure 3. Left shows black dots as epicenters of earthquakes based on conventional routine single earthquake location procedure of the Icelandic Met. Office during the years 2005-2018. The 7-km-long rectangular blue box encloses a line of microearthquake activity, indicating post-activity of an earthquake of magnitude around 6 defining a fault striking 36°NE, suggested to express the left-lateral strike-slip fault of the 1976 Kópasker earthquake. The open star on the fault line is its epicenter as suggested in the paper by Stefánsson et al 2008. The blue star denotes the epicenter of the earthquake as determined by the local Icelandic seismic stations. The "beachball" shows fault plane solution by Einarsson et al. (1979) on basis of signs of first P waves. The red dots show the epicenters of an intensive swarm of earthquakes in March 2019 defined by the relative location method of Slunga et al. (1995). The green star is the largest earthquake in this swarm of magnitude 4.2. The right image shows earthquakes (red dots) recorded in the region during one year, Oct. 2014 - Oct. 2015, which also nicely indicate the NE-striking fault line south of Kópasker village.

Table 1, World networks epicenter locations

NEIC (USGS)	66.1570,	-16.5820	160 st
EHB	66.22,	-16.59	317 st
ISC	66.2708,	-16.8636	395 st.
CSEM/EMSC	66.35,	-16.36	
GCMT	66.33	-16.29 (centroid) 13 stations.	

Surface effects and mechanism

The surface effects of the earthquake were observed on a snowy surface within a day of the earthquake (*Stefánsson*, 1976) and in the summer of 1976 (*Pétursson*, 1997).

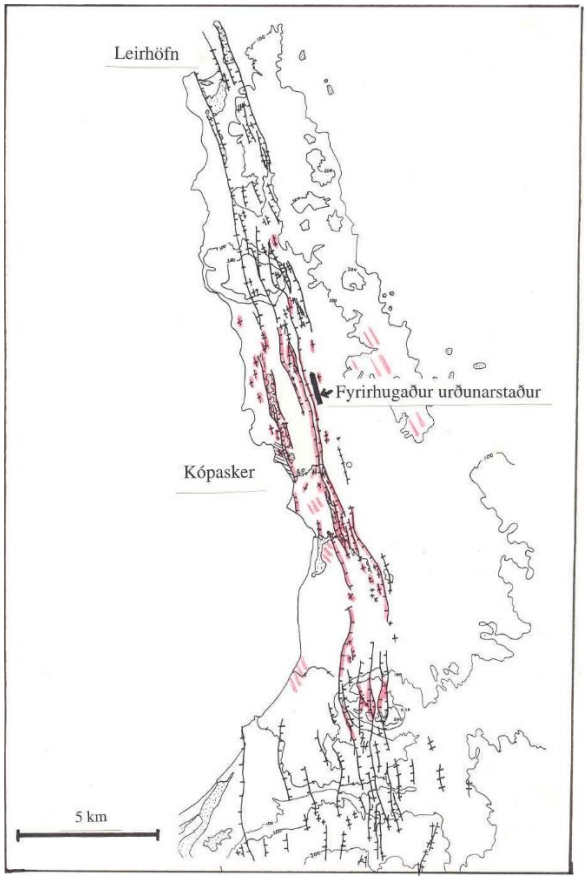

Figure 4. Map of the N-S striking fissure swarm east of Öxarfjörður bay that runs through Kópasker village. The fissure swarm is a part of the North Iceland rift zone and located east of the Krafla fissure swarm (see also Figure 2). The red color shows faults and fractures where recent movement was detected during observations in the summer of 1976. This figure is from a geological report for the planning of a site for garbage disposal for the region (Pétursson, 1997).

In personal communication, Halldór Pétursson, the author of the map in Figure 4, stated that from his observations it was difficult to estimate the amount of fissure opening. However, it was obvious that most of the fresh rifting was within 4 km south of Kópasker village and passed the village and faded out to the north of it (Figure 4). The most intensive evidence of rifting and cracking that he observed was found between Presthólar and further west at Klapparós at the sea-side, 4 km to the south of Kópasker. This agrees with Stefánsson's (1976) observations made on 14-15 January, just after the earthquake, of 30 cm open fresh cracks at Presthólar basically on NS lines, but there also to the west of the main NS rim. He concluded that the main EW opening was around 20-30 cm along the NS rim towards Kópasker. To the south of Presthólar the fissure opening was clearly smaller and disappearing towards the south. Vertical displacements were observed with net slip down to the west, although there were exceptions to this. Some opening was also observed to around 2 km north of Kópasker, along a road, which could not be followed farther north because of snow.

The conditions for observing and quantifying fracture movements were difficult because it had snowed just after the earthquake occurred. Although the fresh snow was underlain by an older hardened snow cover, exhibiting the fresh cracks directly, only locations with significant fissure opening could be detected, i.e., where snow had fallen down into the fresh cracks. According to local inhabitants who joined the initial inspection of the fresh cracks and rifted rim, the cracks formed at the time of the earthquake.

Soon after the initial inspection, I asked a local person in Kópasker (Rafn Ingimundarson), to study better the main road and its surroundings north of Kópasker towards Snartastaðanúpur mountain, 5 km north of Kópasker having heard from people telling about fresh cracks there. He inspected this area on 28 January, after it had rained on 17 January and then later cooled down again with sub-zero temperatures. He found cracks in the newly frozen snow surface all the way towards the mountain, reporting the largest opening of the order of 20 cm at an elevation of 100 m on the mountain slope. A more detailed description of the early observations of the fracture movement evidence after the earthquake can be found in Stefánsson (1976).

The general conclusions of the surface observations are the following: Immediate E-W opening of fractures, related to the earthquake, perpendicular to the north-south striking fissure swarm was 10-30 cm, with the largest values around 4 km south of Kópasker, but well observable to at least 2 km to the north of Kópasker. Vertical displacements were also detected, indicating net throw down to the west, although this was less definite than the opening. In addition, it seems that fracture movement continued in the northern part for at least 5 days after the earthquake.

Based on these field observations, it was therefore Stefánsson's (1976) early conclusion that the earthquake was a normal-faulting event on a plane striking due north along the coast and, based on the first epicenter determination, that the fault plane was dipping to the west.

A fault plane solution based on the signs of first motions of P waves (*Einarsson et al.*, 1979) revealed that the earthquake was a strike-slip event on nearly vertical nodal planes, indicating fault planes striking either 38°NE with left-lateral slip or 51°NW, with right-lateral slip. Bungum (1978) obtained a similar solution, also from signs of first motions. In Figure 2, following Stefánsson (2008), a fault plane with left-lateral strike slip is suggested. This was based on the Einarsson's fault-plane solution, assuming that the nodal plane striking N38°E was the fault plane, but also on the results by Rögnvaldsson et al. (1998), who found clear preference for NS left-lateral strike slip faulting in the area, and by picking as a fault plane a nearby fault line illuminated by microearthquakes with a similar strike as one of the two nodal planes found by Einarsson et al. (1979). This fault line has shown continued earthquake activity, as can e.g., be seen in microearthquake data covering 2005-2018 (Figure 3), indicating a strike of N36°E, i.e. within error limits the same as the fault plane solution.

Conclusions

The earthquake was triggered and to a significant level its moment was built up by the rifting event leading to it. So, its source process occurred under heterogenous stress conditions, created by the fast rifting, on one hand, and by the long-term stress build up in the region, on the other hand. Geological slip data (*Angelier et al.*, 2004) reveal for the Tjörnes fracture zone great variations in stress conditions in time and space leading up to the earthquake slips. In the Kópasker earthquake such variability occurred during its release.

The great variations of the routine epicenter determination of the world networks are to a large extent caused by complicated source processes, reflected in picking of different onset times at different stations. This is to a large extent because of the complicated source process, both concerning the frequency of the transmitted waves, with high frequencies suffering more absorption with distance than lower frequencies, but as it seems, also by a double earthquake feature of the release.

The mainshock epicenter inferred from the Icelandic stations expresses the location where the earthquake nucleation started (8 km SW of Kópasker), as a direct continuation of the rifting process, but after some delay. The earthquake rupture proceeded along a NE-striking left-lateral 8-km-long vertical

fault approaching the coast near Klapparós, a place about 4 km south of Kópasker. This was probably a typical fast release process with a rupture velocity lower than but close to the S-wave velocity. If we assume a plausible rupture velocity of 3 km/sec, the rupture of the fault towards a point 4 km south of Kópasker would have taken only 3 seconds. The left-lateral slip on the fault added to the E-W tension across the NS-striking Kópasker fissures and likely triggered a lower velocity normal fault rifting process, which possibly started 4 km south of Kópasker, near Klapparós, and proceeded 5-10 km northward along the coast.

Such a complicated source process can explain both the variability in the epicenter determinations as well as the significant difference between Mb and Ms magnitudes. The Ms is much more depending on low frequencies in the seismic wave spectrum than the Mb. Also, it was the impression of and noted by the readers of the seismograms of the Kópasker earthquake that a large part of its seismic energy release was of relatively low frequency (*Stefánsson*, 1976). This should be investigated further by studying available waveforms from broad-band seismometers worldwide.

Although the March 2019 swarm of earthquakes southwest of Kópasker occurred close to the epicenter of the 1976 Kópasker earthquake it was released on another fault with a different fault direction. These two processes occur in very different stress regimes as the stress which induced the Kópasker earthquake was strongly motivated by the Krafla rifting episode.

References

Angelier, J., R. Slunga, F. Bergerat, R. Stefansson, C. Homberg, Perturbation of stress and oceanic rift extension across transform faults shown by earthquake focal mechanisms in Iceland. *Earth Planet. Sci. Lett.*, **219**, 171–284, 2004.

Bungum, H., Reanalyzation of three focal-mechanism solutions for earthquakes from Jan Mayen, Iceland and Svaibard. *Tectonophysics*, **51**, T15-T16, 1978

Einarsson, P., Seismicity and earthquake focal mechanisms along the mid-Atlantic plate boundary between Iceland and the Azores. *Tectonophysics*, **55**, 127–153, 1979.

Pétursson, H., *Jarðfræðikönnun vegan sorpurðunar við Kópasker*. Report: Unnið fyrir Öxarfjarðarhrepp, NÍ-97008, Akureyri, 1997.

Rögnvaldsson, S.T., A. Gudmundsson, R. Slunga, Seismotectonic analysis of the Tjörnes Fracture Zone, an active transform fault in north Iceland. *J. Geophys. Res.*, **103**, 30117–30129, 1998.

Sigurdsson, O., Surface deformation of the Krafla fissure swarm in two rifting events, *J. Geophys.*, **47**, 154-159, 1980.

Slunga, R., S.Th. Rögnvaldsson, and R. Bödvarsson. Absolute and relative locations of similar events with application to microearthquakes in southern Iceland. *Geophys. J. Int.*, **123**, 409–419, 1995.

Stefánsson, R., Jarðskjálfti við Kópasker. *Skjálftabréf*, nr. **7**, 6-12, 1976.

Stefánsson, R, I.S. Sacks & A.T. Linde, Stress field changes during a tectonic episode in northern Iceland. *Carnegie Institution of Washington – Year Book*, **78**, 320-325, 1979.

Stefánsson R., G.B. Gudmundsson and P. Halldorsson, Tjörnes fracture zone. New and old seismic evidences for the link between the North Iceland rift zone and the Mid-Atlantic ridge. *Tectonophysics*, **447**, 117–126, 2008.

Stefánsson, R., G. B. Guðmundsson, and Th. Skaftadóttir, Pre-earthquake activity in North-Iceland. In *Proceedings to the 2nd workshop on earthquakes in North Iceland*, Húsavík, North Iceland, 31 May - 3 June 2016, 2016.

NORTHQUAKE 2019 - The 3rd International Workshop on Earthquakes in North Iceland
Húsavík, North Iceland, 21-24 May 2019

THE KÓPASKER SEISMIC SWARM IN SPRING 2019

Kristín Jónsdóttir[1], Gunnar B. Guðmundsson[1], Luigi Passarelli[2], Sigurjón Jónsson[2], and the Monitoring Team at the IMO[1]

[1]*Icelandic Meteorological Office (kristinj@vedur.is)*
[2]*King Abdullah University of Science and Technology (KAUST), Saudi Arabia (sigurjon.jonsson@kaust.edu.sa)*

The Tjörnes fracture zone (TFZ) is a seismically active zone with on average 4000 earthquakes detected annually since 1993 by the regional seismic network operated by the Icelandic Meteorological Office. Although most of the seismicity occurs offshore and with only one seismic station on an island (Grímsey) north of Iceland, the seismic network does an impressive job of detecting small earthquakes (down to magnitude -0.5) and locating their epicentre. The fracture zone, essentially a transform between the northern volcanic zone of Iceland and the Mid-Atlantic Ridge north of Iceland, has three major segments; the Grímsey Oblique Rift (GOR) farthest to the North, the Húsavík-Flatey Fault (HFF) in the middle and the Dalvík Lineament (DL) farthest to the south. The IMO's seismic catalogue clearly draws up the most active segments of the TFZ, the GOR and the HFF, each extending laterally roughly 100 km. (see Fig.1).

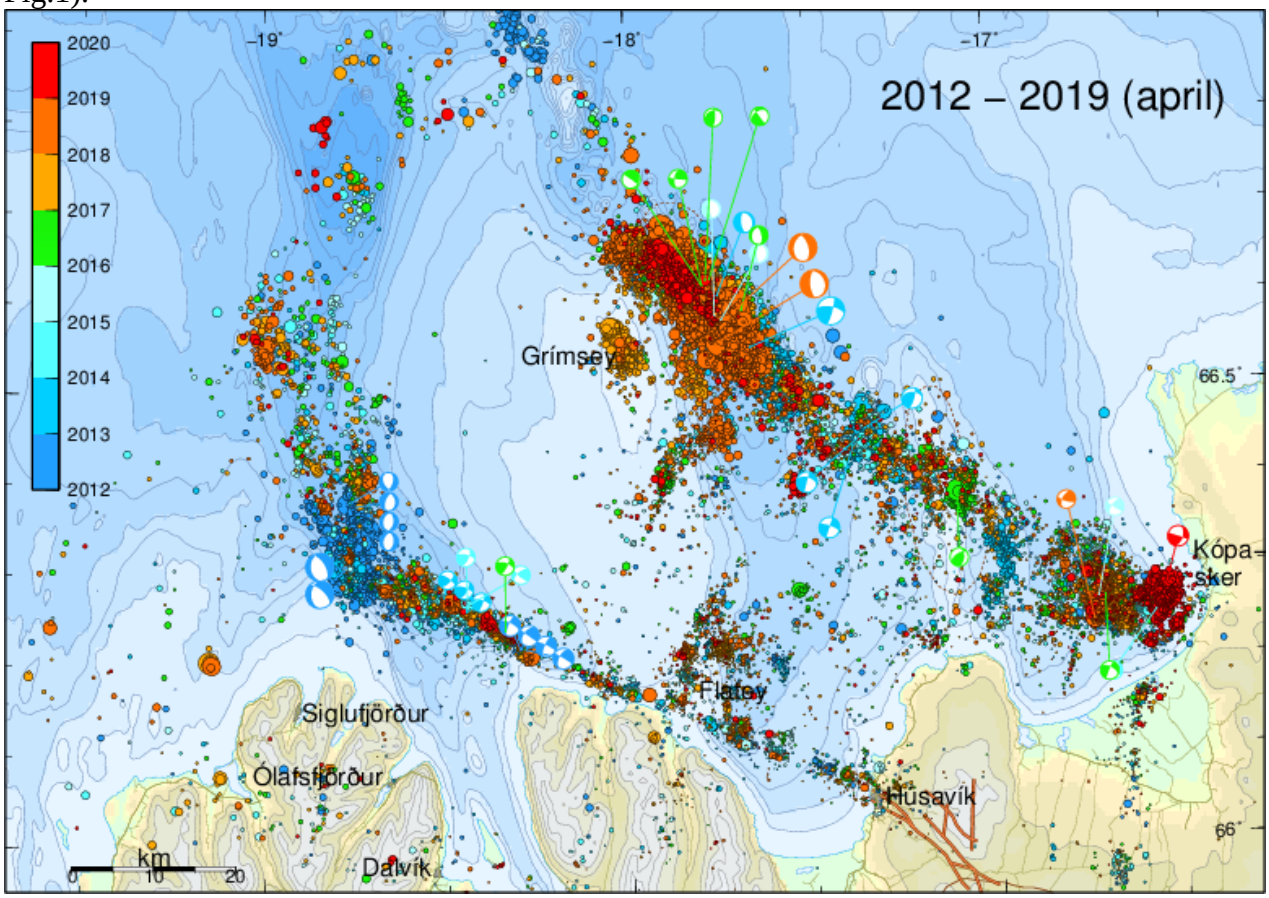

Figure 1. Map showing the main seismicity of the TFZ recorded by the regional seismic network of IMO between 2012-2019 (until April). The seismicity marks the two main segments of the TFZ clearly, the GOR farthest to the north and the HFF extending from Húsavík to the Eyjafjarðaráll graben.

The seismicity has different characteristics on these segments. The GOR is the most active where roughly 60% of the earthquakes occur, 38% of the earthquakes occur on the HFF and only about 2% occur on the DL. However, the largest earthquakes occur on the HFF where the accumulated seismic moment release is an order of magnitude higher than that for the GOR and three orders of magnitude higher than that for the DL. There are other interesting differences. The seismicity on the GOR often occurs on north-south faults (left-lateral strike slip) clearly seen with relative locations methods, and thus the seismic zone for GOR is wider in map-view. In addition, there are several known central volcanoes aligned along the GOR. Looking at the temporal behaviour of the seismicity, the GOR has high levels of background seismicity and every few years seismic swarms occur, however most often without a clear mainshock followed by an aftershock sequence. Taken all into account, the oblique rifting is likely to cause both tectonic and volcanic seismicity which shows up as a catalogue of many but similarly-sized earthquakes, in other words a catalogue with a higher b-value than the neighbouring HFF.

In late March 2019, one of this seismic swarms took place on GOR, mostly on a single NNE-SSW striking fault near Kópasker. Relative earthquake locations (Quakelook program) draw the fault up nicely and in addition a few shorter faults with similar strike of N15°E (see Fig. 2).

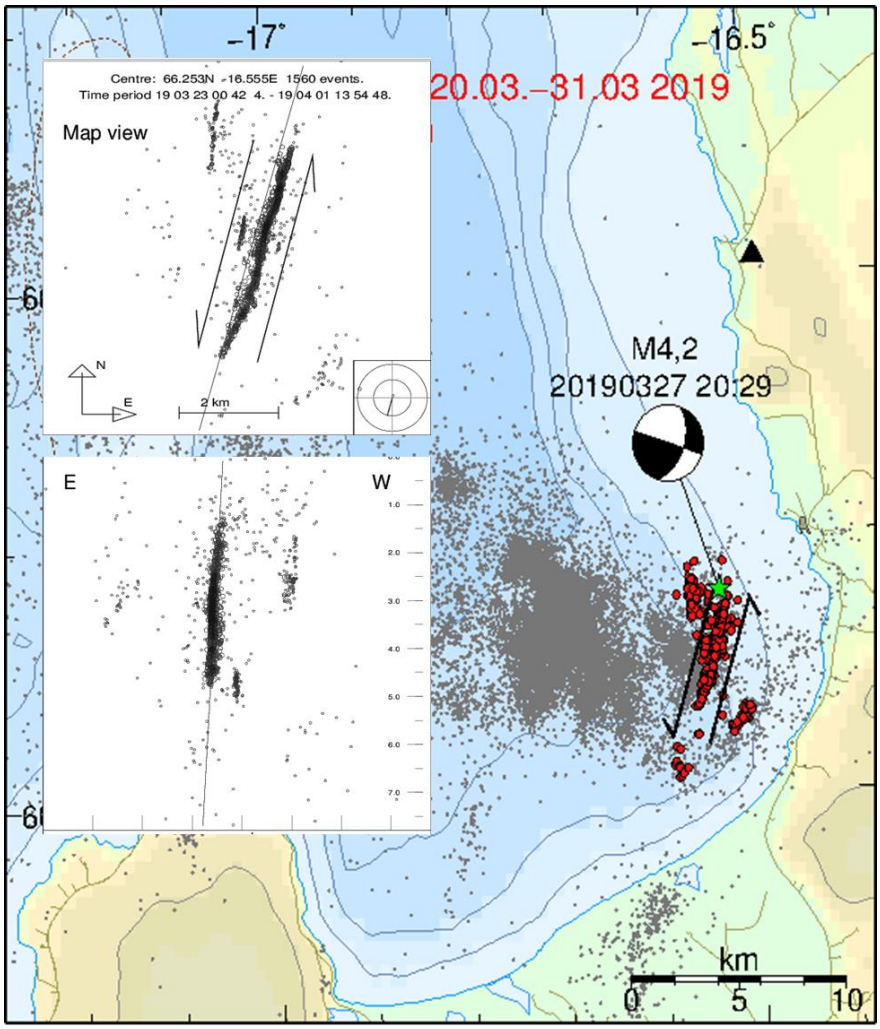

Figure 2. Map of Öxarfjörður showing in red, relative locations of the earthquake swarm that took place 20-31 March, 2019. The largest earthquake in the swarm (M4.2) and its focal mechanism indicates left-lateral strike-slip motion. The two included figures show results from 1516 relative located earthquakes between 19 March and 19 April. Included figure above; map view. Included figure below; depth section (seen from the northern end of the fault) shows the almost vertical fault. Relative locations show shallow hypocenters at 1-5 km depth.

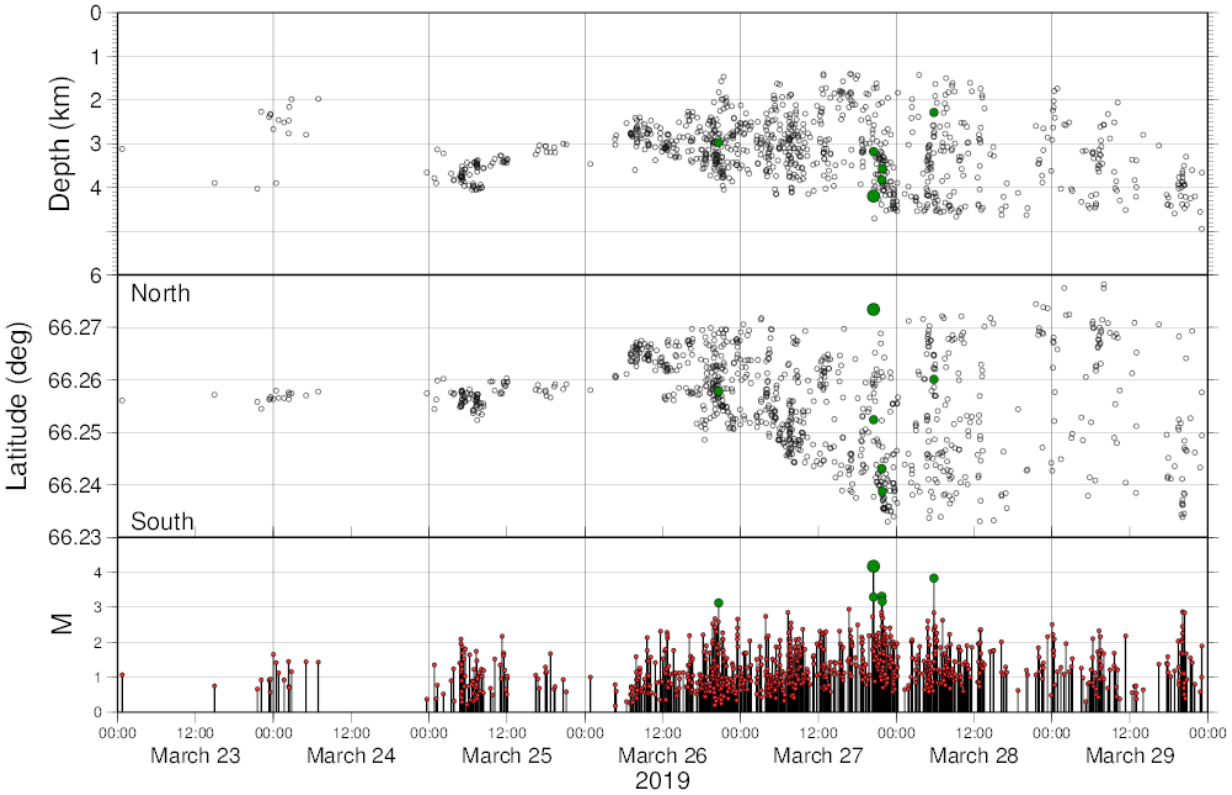

Figure 3. Graph that shows the temporal evolution of the first and most active days of the swarm (relatively located earthquakes).

Figure 3 shows the temporal evolution for the first days of the swarm. The depth evolution from 25 March shows upwards migration from 4 to 3 km depth and from the morning of 26 March the earthquakes migrate slowly slightly upwards but mostly downwards by some 2 km for about 48 hours. The epicentral trend shows how the seismicity starts at the middle of the fault, jumps a little to the north on 26 March and migrates in two days to the southern end of the fault over 7 km. When that point is reached, the largest earthquake in the swarm takes place M4.2, however in the very northern end of the fault. The focal mechanism of this largest event shows a left-lateral strike-slip as do the smaller earthquakes. The impulse plot of the magnitudes at the bottom clearly shows the swarm like behaviour of the seismicity and the lack of mainshock-aftershock behaviour. A b-value plot of the 2300 earthquakes that were recorded during the swarm reveal a value of 1.2, which is typical for volcanic seismicity.

The question rises if the swarm is linked to tectonic or volcanic processes? Interestingly, following the same strike as our swarm-fault, we can track epicentres of small earthquakes, that occurred before the swarm, further south and all the way into the Krafla fissure swarm. Only some 5-7 km south of the swarm fault there is a known geothermal area at Skógalón and some 7 km further south, the Bakkahlaup geothermal area (*Georgsson and Karlsdóttir, 2007*). Possibly supercritical fluids might have migrated along the fault. Supercritical fluids are thought to exist between 2-4 km depth close to the Krafla caldera, a depth that is quite comparable with the earthquake depths (relative locations) in the swarm (*Elders and Fridleifsson, 2010*).

Without other measurements, e.g. of the deformation in the near vicinity of the active fault it may be difficult to answer this question, as it is not clear if any opening was associated with the seismic swarm.

References

Elders, W. & G.Ó. Friðleifsson, The Science Program of the Iceland Deep Drilling Project (IDDP): a study of supercritical geothermal resources. In *Proceedings World Geothermal Congress*, Bali, Indonesia, paper 3903, 2010.

Georgsson, L.S. and R. Karlsdóttir, Resistivity methods - DC and TEM with examples and comparison from the Reykjanes peninsula and Öxarfjörður, Iceland, In: *Short course II on surface exploration for geothermal resources*, UNU-GTB and KenGen, Lake Naivasha, Kenya, 2007.

NORTHQUAKE 2019 - The 3rd International Workshop on Earthquakes in North Iceland
Húsavík, North Iceland, 21-24 May 2019

EARTHQUAKE RELOCATION IN THE TJÖRNES FRACTURE ZONE

Claudia Abril, Olafur Gudmundsson, Ari Tryggvason

Uppsala University, Sweden (claudia.abril@geo.uu.se, olafur.gudmundsson@geo.uu.se, ari.tryggvason@geo.uu.se)

Earthquake relocations have been carried out in the Tjörnes Fracture Zone (TFZ). Earthquake location in the area is challenging because of large azimuthal gaps (*Hensch et al.,* 2013) and large epicentral distances, consequences of the difficulty to install permanent seismic station in the offshore areas of the TFZ. Two methodologies have been used to relocate the seismicity recorded by the permanent Icelandic network (SIL) from 1993-2017: 1) We estimated empirical travel-time functions for stations of the SIL network and use those for earthquake relocation with a grid-search algorithm; 2) We estimated crustal velocities for P- and S-waves in North Iceland by tomography, and used the estimated three-dimensional (3D) velocity model to relocate the earthquakes. More 80.000 events have been relocated.

Empirical travel-time functions (ETTs) were estimated following the methodology in *Abril et al.* (2018). For each station in the SIL network, 3D functions were estimated to correct the predicted travel times by a one-dimensional velocity model. Residuals of the SIL catalog were assumed to have a structural component (caused by crustal heterogeneities that are not described by the one-dimensional velocity model), and a random-noise component (e.g., because of errors in arrival-time estimation and errors in estimated earthquake locations in the SIL catalog). A large-scale structural component (>10 km) was estimated by interpolation of the mapped residuals. From the remaining residuals, a small-scale structural component (<10 km) and noise were statistically separated based on spatial coherence (or not) in variograms (Kriging). The total structural component corresponds to the empirical travel-time functions. The estimated noise component corresponds to the uncertainty of those travel times. Empirical travel times and their uncertainties were used by a nested grid-search algorithm to relocate earthquakes.

Local-earthquake tomography was carried out using data of the North Iceland Experiment - NICE (*Abril et al.,* 2019). For the NICE project, a sub-network of 14 Ocean-bottom seismometers and 11 on-land stations were installed to extend the SIL network in the area and increase its coverage to offshore areas. 500 seismic events, including 16 explosions, were used to estimate 3D velocity models for P- and S-waves. For the local-earthquake tomography, we used the methodology described by *Tryggvason et al.* (2002). SIL catalog earthquakes in the area were then relocated using the estimated velocities.

We compare the epicenter distribution of the original SIL locations and the relocated seismicity in Fig. 1. The overall distribution is not much affected by relocation. However, both relocation strategies focus the seismicity on detailed tectonic features of the Tjörnes Fracture Zone. For example, seismicity in between the Grímsey Oblique Rift (GOR) and the Húsavík-Flatey Fault (HFF) is clearly concentrated along transverse lineaments that partly outline a concentrated deformation zone between Grímsey and Flatey (the Grímsey-Flatey Zone (GFZ)). This focusing effect is less visible in the sparser seismicity south of the HFF. Nevertheless, some transverse lineaments are clarified along the strike of the Dalvík Lineament.

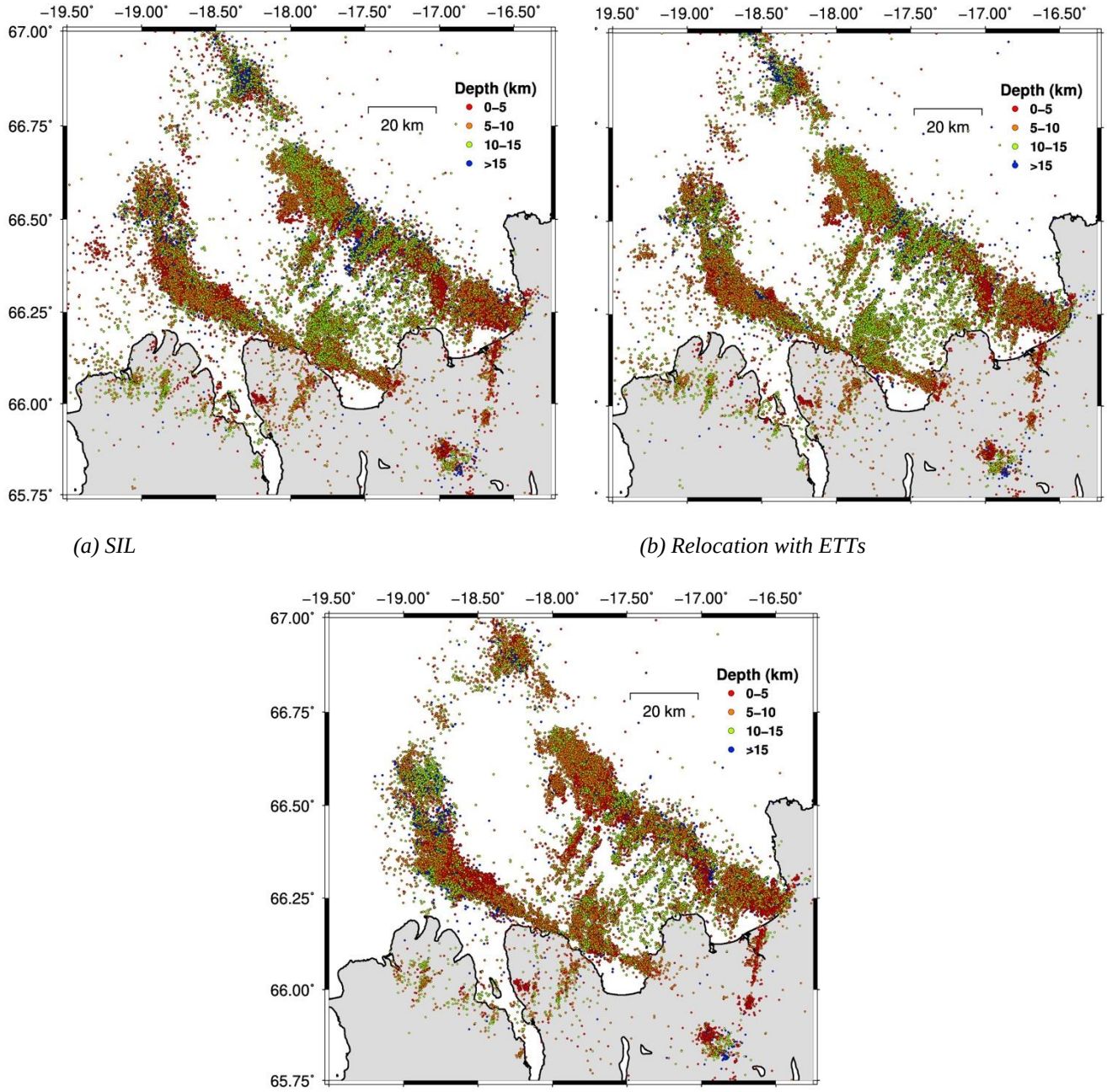

(a) SIL

(b) Relocation with ETTs

(c) Relocation using 3D velocity model

Figure 1. Seismicity in the TFZ from 1993-2017 (a) according to the SIL catalogue, (b) relocated using ETTs, and (c) relocated using the 3-D velocity model obtained by the LET. Colour code indicates depth of earthquakes.

The depth of events is colour coded in Fig. 1. In general, both relocation strategies have reduced the depth of the seismicity in the area, particularly the relocation in the 3D velocity models. The relocated seismicity is clearly shallower along the GOR. It is also shallower along the transverse lineaments inside the Tjörnes Microplate south of Grímsey Island. Also, the depth distribution of epicenters is more coherent after relocation. A group of earthquakes located at a depth >15 km appears in the southern Eyjafjarðaráll Basin after relocation using the 3D velocity model. The band of relatively deep seismicity discussed by *Riedel et al.* (2006) extending between Grímsey and Flatey Islands is not so deep in our relocations. Events are clearly concentrated in this band of seismicity, but depth estimates are clearly reduced by our relocations (see e.g. relocated events along the HFF in Fig. 2(b) at 60-70 km). A characteristic of seismicity before and after relocation is the sparse seismicity located in the Grímsey Shoal, where only few earthquakes have been recorded by the SIL network.

We compare the depth distributions of the SIL catalogue locations and the relocated seismicity in cross sections along the HFF and the GOR in Fig. 2. In general, the relocated seismicity is more concentrated along vertical lineations. We note, that these lineations tend to dip steeply westward in the western part of both cross sections, while they are more vertical in the east.

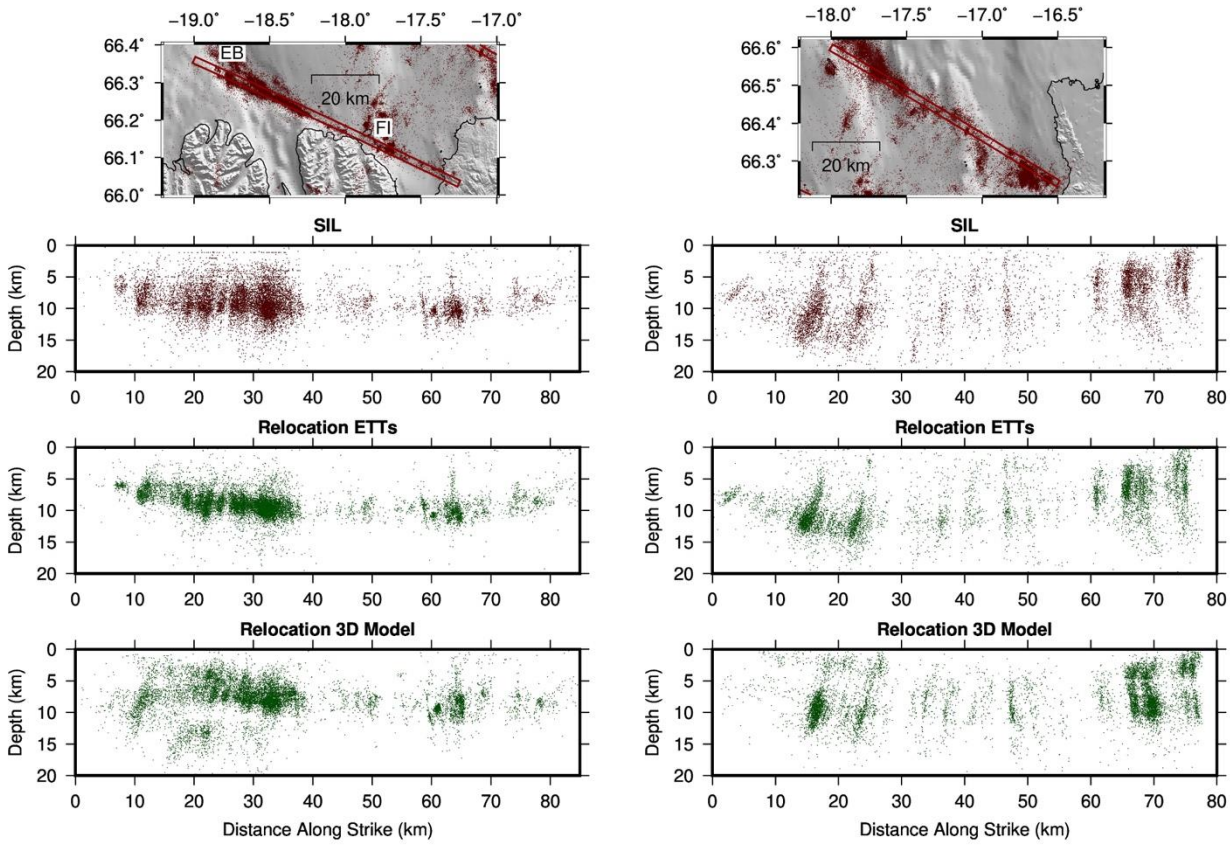

(a) Húsavík-Flatey Fault *(b) Grímsey Oblique Rift*

Figure 2. Cross sections of seismicity along the HFF (left panels) and the GOR (right panels). Upper panels present map views of the corridors where the cross sections are traced (red boxes), and the earthquake locations of the SIL catalogue. Lower panels show cross sections of the locations in the SIL catalog (top), the relocated seismicity using ETTs (middle), and the relocated seismicity using the 3D velocity model estimated by local-earthquake tomography (bottom).

The effect of relocations using the ETTs strategy is to concentrate locations in depth between 4 and 12 km in the HFF. Relocations using the tomographic model redistribute the seismicity in depth at the western end of the HFF, where a bimodal distribution of hypocenters is concentrated mainly above 10 km depth, but a group of earthquakes is relocated around 15 km depth. This deeper seismicity corresponds to the group of earthquakes located in the southern Eyjafjarðaráll Basin that we mentioned earlier. Seismicity along the GOR is concentrated between 5 and 15 km depth to the west, and above 10 km depth to the east after relocation with ETTs. Relocations in the tomographic model along the GOR concentrate the seismicity in the upper 15 km. Here a bimodal distribution in depth of the seismic is also evident at the eastern end of the corridor. This bimodality in the depth distribution has been analyzed in terms of depth uncertainties of locations. Much of the deep seismicity has a substantial depth uncertainty, but not all. For example, the separation in depth of the two concentrations of relocated seismicity to the west of the HFF is about 5 km. This exceeds the largest uncertainty estimates by a factor of about three. However, the uncertainty estimates include only a random component of error, not potential systematic bias due to, e.g., an erroneous velocity model. We note that the relocations are done using only observations from stations inside the TFZ model region. In the peripheral areas, the relocations may be constrained by fewer observations than in the SIL catalog. We have tested this bimodality in the depth distribution of the relocated events by relocating in different tomographic models obtained from different starting models and the feature persists.

The seismicity of the TFZ outlines complex and distributed deformation. It is known from GPS measurements that the HFF accommodates only about 40% of the transform motion between the Eurasian and American plates in the area (over a short time span) (*Metzger et al.*, 2011). Some of the remaining motion is certainly taken up by the GOR, but apparently the Tjörnes Microplate (TM), bounded by these two main lineaments and the rifts to the east and west, also undergoes internal deformation. The American plate to the west of the area may undergo internal deformation as evidenced by the Málmey M=7 earthquake in 1963 (*Stefansson et al.*, 2008). The concentrated seismicity along transverse lineaments in between Grímsey and Flatey (GFZ) suggests that internal deformation of the TM is concentrated there, leaving the Grímsey Shoal intact. We note that both of the main lineaments bounding the TM change character close to Grímsey (GOR) and Flatey (HFF). To the NW of Grímsey the GOR is an oblique rift, between Grímsey and Kópasker the GOR is dominated by bookshelf tectonics and should perhaps be referred to as the Grímsey Lineament (GL). To the SE of Flatey the HFF remains a concentrated shear zone while it branches and broadens to the NW. Perhaps this complexity reflects the evolution of the Tjörnes Microplate or the general complexity of crustal accretion in Iceland due to repeated ridge jumps and old hidden crustal blocks with inherited variation of strength in the crust.

References

Abril, C., O. Gudmundsson and SIL monitoring group, Relocating earthquakes with empirical traveltimes, *Geophys. J. Int*., **214(3)**, 2098-2114, 2018.

Abril, C., A. Tryggvason, O. Gudmundsson, R. Steffen, NICE people, Local earthquake tomography in North Iceland, manuscript to be submitted to *J. Geophys. Res.*, 2019.

Hensch, M., G. Guðmundsson and SIL monitoring group, Offshore seismicity with large azimuthal gap, *Proceedings of the Workshop on Earthquakes in North Iceland*, 2013.

Metzger, S., S. Jónsson and H. Geirsson, Locking depth and slip-rate of the Húsavík-Flatey Fault, North Iceland, derived from continuous GPS data 2006-2010, *Geophys. J. Int.*, **187**, 564-576, 2011.

Riedel, C., A. Tryggvason, B. Brandsdóttir, T. Dahm, R. Stéfansson, M. Hensch, R. Bödvarsson, K. Vogfjord, S. Jakobsdóttir, T. Eken, R. Herber, J. Holmjarn, M. Schnese, M. Thölen, B. Hofmann, B. Sigurdsson and S. Winter, First results from the North Iceland Experiment, *Mar. Geophys. Res.*, **27**, 267-281, 2006.

Stefansson, R., G. Gudmundsson and P. Halldorsson, Tjörnes Fracture Zone. New and old seismic evidences for the link between the North Iceland Rift Zone and the Mid-Atlantic Ridge, *Tectonophys.*, **447**, 117-126, 2008.

Tryggvason, A., S. Rögnvaldsson and Ó. Flóvenz, Three-dimensional imaging of the P- and S-wave velocity structure and earthquake locations beneath Southwest Iceland, *Geophys. J. Int*., **151**, 848-866, 2002.

NORTHQUAKE 2019 - The 3rd International Workshop on Earthquakes in North Iceland
Húsavík, North Iceland, 21-24 May 2019

SEISMICITY AND SEISMIC SWARMS ON THE HÚSAVÍK-FLATEY FAULT AND GRÍMSEY OBLIQUE RIFT

Luigi Passarelli[1], Sigurjón Jónsson[1], Claudia Abril[2], Kristín Jónsdóttir[3], Gunnar B. Guðmundsson[3], Ólafur Gudmundsson[2], and Eleonora Rivalta[4]

[1]*King Abdullah University of Science and Technology (KAUST), Saudi Arabia (luigi.passarelli@kaust.edu.sa)*
[2]*Department of Earth Sciences, Uppsala University, Sweden*
[3]*Icelandic Meteorological Office, Reykjavik, Iceland*
[4]*GFZ German Research Centre for Geosciences, Potsdam, Germany*

The Tjörnes Fracture Zone (TFZ) is a transform zone in North Iceland consisting primarily of two large structures, the Húsavík-Flatey Fault (HFF) and the Grímsey Oblique Rift (GOR). The HFF is a ~100 km long transform fault with right-lateral motion and an average strike of N120°E (*Rögnvaldsson et al.*, 1998; *Passarelli et al.*, 2018, Fig.1). The instrumental seismicity recorded along the HFF since 1995 by the Icelandic Met Office shows an uneven spatial distribution with the western third of the fault much more active than further east (Fig. 1). The low seismicity rate on the eastern part of the fault is due to stress-shadowing caused by the Krafla rifting episode in 1975-1984 (*Maccaferri et al.*, 2013). The GOR is further north than the HFF (Fig. 1) and overall its seismicity follows a N128°E trend. The apparent en-echelon segmentation of the GOR is typical of magma assisted oblique rifts where bookshelf fault distribution accommodates the tectonic strain by both normal and strike-slip motion (*Rögnvaldsson et al.*, 1998). The seismic activity illuminates four main regions within the GOR where earthquakes cluster approximately along North-South trends interspaced by aseismic zones (Fig. 1). Both the HFF and GOR have hosted large earthquakes in the past centuries with the last large magnitude earthquake (M_w=6.3) on 13 Jan. 1976 within the easternmost part of the GOR, close to the village of Kópasker, see Fig. 1 (*Passarelli et al.*, 2013). Here we study the main characteristics of the present-day seismicity along these two tectonic lineaments, in particular its spatio-temporal and source properties, to infer about the mechanisms of accumulation and release of tectonic strain in the area.

Our analysis of the seismic activity along the HFF and the GOR is mainly based on the relocated catalogs of seismicity along the HFF published in *Passarelli et al.* (2018) for 1995-2015 and a newly published relocated catalog by *Abril et al.*, (2018, 2019) for 1995-2017. Temporal gaps in the latter catalog and the most recent activity (2018-2019) have been filled with the SIL earthquake catalog of the Icelandic Met Office. The almost 25 years of seismicity consists of small to moderate magnitude events (M_l<5.5) with ~10500 and ~30500 events pertaining to the HFF and the GOR, respectively, and above magnitude M_l=1. The background seismicity rate calculated on a declustered catalog is two times higher on the GOR (~3 events/day) than for the HFF (~1.5 events/day). This is likely in part due to the eastern portion of the HFF being in a stress shadow (*Maccaferri et al.*, 2013) and then GPS results indicate that only about 1/3 of the relative motion in the TFZ is focused on the HFF, while the rest is on the GOR (*Metzger and Jónsson*, 2014). Aftershock productivity for both lineaments is similar to continental tectonic zones, e.g., like in Southern California (*Passarelli et al.*, 2018), and there is also a pronounced foreshock productivity that is comparable to what has been found on other ridge-transform fault systems (*McGuire et al.*, 2007). High foreshock activity is usually linked to seismicity driven by aseismic transients rather than isolated mainshock-aftershock sequences (*McGuire et al.*, 2007).
Our previous analysis of the seismicity along the HFF identified 6 major seismic swarms along a ~30 km long segment on the westernmost part of the HHF and the Eyjafjaráll Rift with a return period of ~4-5 years since 1995 (*Passarelli et al.*, 2018). The swarms represent 56% of all earthquakes and 99% of the total seismic moment released along the HFF during 1995-2015. The swarm activity shows

"spatial complementarity" on the activated fault segments, i.e., each new swarm occurred on a part of a fault segment that had not been occupied by previous swarms. In addition, all the swarms started with low magnitude events in a small localized fault patch and in a few days moved out activating a larger portion of the fault with increasing event magnitudes. The earthquake hypocenters were found to migrate at a constant velocity or with accelerating rates of the order of ~km/d, but the effective stress-drops associated with each swarm appears to be relatively low (~1-100kPa). The spatial complementarity, fast migration speed and low stress drops suggest that these swarms were accompanied by transient aseismic strain release that efficiently released the tectonic strain accumulated over 20 years on the western HFF (*Passarelli et al.*, 2018). However, no evidence has yet been found in GPS measurements for such strain release in the swarms, prompting an installation of a new continuous GPS station close to the activity (*Jónsson et al.*, 2019).

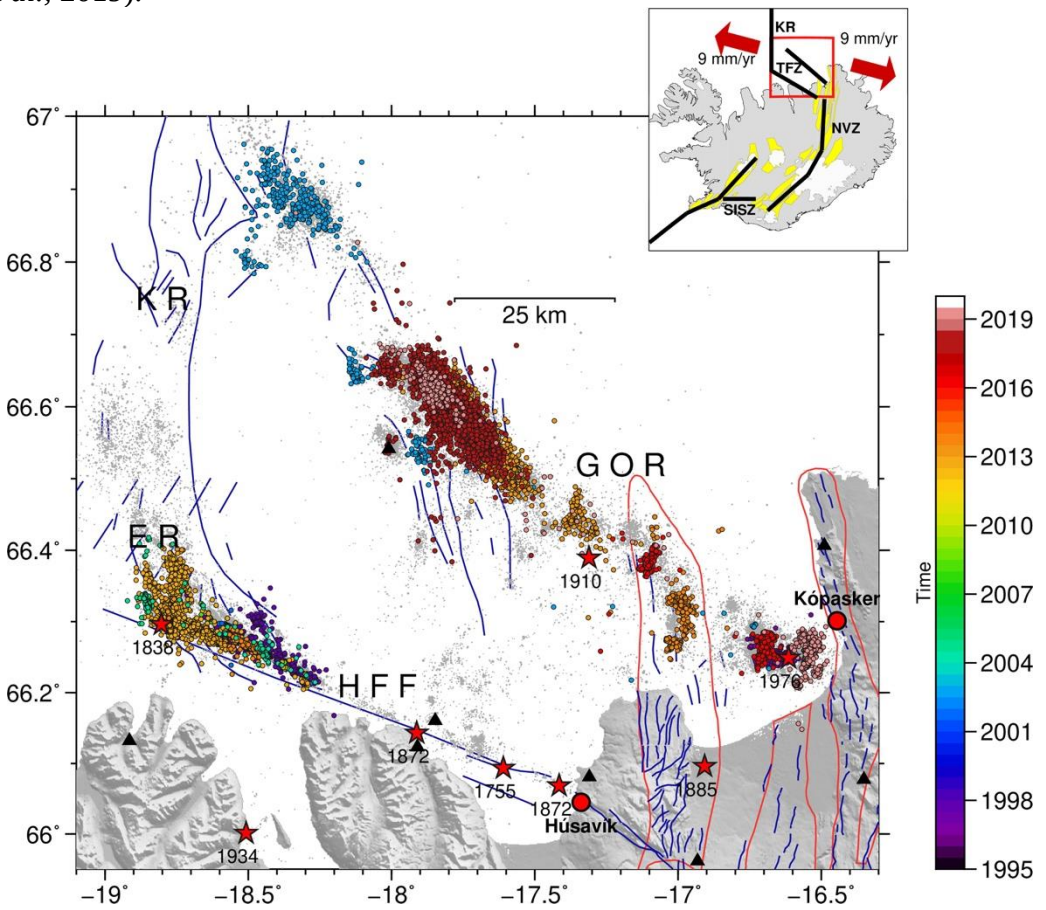

Figure 1. *Earthquake and swarm locations in the Tjörnes Fracture Zone (TFZ) along the Húsavík–Flatey Fault (HFF) and the Grímsey Oblique Rift (GOR). Larger circles are identified seismic swarm events, color-coded by time, while other earthquake locations are shown as small gray dots in the background. Red stars are approximate locations of historical M>6 earthquakes, black triangles are seismic stations, blue thin lines are faults and fractures, and red lines outline fissure swarms and volcanic systems. KR - Kolbeinsey Ridge, ER – Eyjafjarðaráll Rift, SISZ - South Iceland Seismic Zone, NVZ - Northern Volcanic Zone.*

On the GOR we identified 7 periods with very high seismicity rate with respect to the background activity using a similar approach as in *Passarelli et al.* (2018). The high seismicity rate windows correspond to seismic swarm activity lasting from a few to several weeks and occurring in ~N-S trending streaks (Fig. 1). In particular, we identified swarms in 1996 and 2002, and then, after a hiatus of 11 years, five more swarms in March-May and October 2013, January 2016, January-March 2018 and March-April 2019. The identified swarm activity represents 25% of all earthquakes (M_l>1) and 77% of the total seismic moment released along the GOR since 1995. In all the identified periods, except for the one in 1996, the swarms activate more than one fault segment within a time span of a few days to weeks (Fig. 1).

The GOR swarms occurring east of longitude 17.5°W show NNE-SSW or ~N-S trends (Fig. 1), in agreement with the fault plane orientations proposed by *Rögnvaldsson et al.,* (1998). The major swarm activity encompassing the segment between 18°W and 17.4°W, on the other hand, exhibits a NNW-SSE trend with activation of both normal and strike-slip faulting (*Hensch et al.,* 2016). Swarms in this area occurred both in 2013 and 2018 and are by far the most energetic with cumulative seismic moments of 1.4×10^{17} Nm and 1.1×10^{17} Nm, respectively. The area was activated once again by a small-magnitude swarm in March-April 2019. Almost coincident with the latter activity, a swarm of M_l<4.2 events struck the area offshore Kópasker village, near the location of the M_w6.3 earthquake in 1976 (*Jónsdóttir et al.,* 2019; *Stefánsson and Guðmundsson,* 2019). The cumulative seismic moment of all other swarms identified in the GOR is about two orders of magnitude lower than the moment of the 2013 and 2018 swarms. By looking at individual seismic sequences, the GOR swarms show spatio-temporal migration patterns that share similarities with the HFF swarms. The swarm activity starts locally in a small area and then gradually expands to a larger region at rates of ~km/d.

In conclusion, the seismic activity along the HFF and the GOR is dominated by swarm-like seismicity of small to moderate-magnitude events. The swarm activity along the GOR shows a period of quiescence between 2002 and 2013 and most of the seismic moment was released by the 2013 and 2018 swarms. On the contrary, the western half of HFF has had swarms every 4-5 years. The initial localized clustering of small swarm earthquakes and their fast spatial migration at speeds approaching km/d seem to be more indicative of fluid-triggered aseismic slip rather than earthquakes triggered by high pore-pressure diffusion (*Bhattacharya and Viesca,* 2019). The quasi-simultaneous activation of swarms on distant fault strands within days to weeks may point to large-scale response of pressurized crustal fluids to shaking-induced small strain changes (*Skelton et al.,* 2019). For the westernmost segment of the HFF, we have suggested that the swarm activity may be accompanied by aseismic slow slip transients or creep (although this has yet to be confirmed by GPS observations), releasing some of the accumulated tectonic strain over the past 20 years. However, whether this mechanism is also present on the en-echelon fault system of the GOR is unclear and requires further investigation.

References

Abril, C., Ó. Gudmundsson, & SIL seismological group, Relocating earthquakes with empirical traveltimes. *Geophysical Journal International*, **214(3)**, 2098-2114, 2018.

Abril, C., Ó. Gudmundsson & A. Tryggvason, Earthquake relocation in the Tjörnes Fracture Zone. In: *Proceedings to the Northquake 2019 workshop*, Húsavík Academic Centre, 2019 (this issue).

Bhattacharya, P., & R.C. Viesca, Fluid-induced aseismic fault slip outpaces pore-fluid migration. *Science* **364**, 464-468, 2019.

Hensch, M., G.B. Guðmundsson, K. Jónsdóttir and the SIL monitoring group, Seismic activity in North Iceland since 2011 with a special focus on the past three years. In: *Proceedings to the 2nd workshop on earthquakes in North Iceland*, Húsavík Academic Centre, 35-37, 2016.

Jónsdóttir, K., G.B. Guðmundsson, L. Passarelli, S. Jónsson & the monitoring team at the IMO, The Kópasker seismic swarm in Spring 2019. In: *Proceedings to the Northquake 2019 workshop*, Húsavík Academic Centre, 2019 (this issue).

Jónsson, S, R. Matrau, R. Viltres, B. Ófeigssion, An update of GPS measurements in North Iceland. In: *Proceedings to the Northquake 2019 work*shop, Húsavík Academic Centre, 2019 (this issue).

Maccaferri, F., E. Rivalta, L. Passarelli & S. Jónsson, The stress shadow induced by the 1975–1984 Krafla rifting episode. *J. Geophys. Res.* **118**, 1109–1121, 2013.

McGuire, J.J., M.S. Boettcher & T.H. Jordan, Foreshock sequences and short-term earthquake predictability on East Pacific Rise transform faults. *Nature* **434**, 457–461, 2007.

Metzger, S. & S. Jónsson, Plate boundary deformation in North Iceland during 1992-2009 revealed by InSAR time-series analysis and GPS, *Tectonophysics* **634**, 127-138, 2014.

Passarelli, L., F. Maccaferri, E. Rivalta, T. Dahm & E.A. Boku, A probabilistic approach for the classification of earthquakes as 'triggered' or 'not triggered'. *Journal of Seismology* **17**, 165-187, 2013.

Passarelli, L., E. Rivalta, S. Jónsson, M. Hensch, S. Metzger & S.S. Jakobsdóttir, Scaling and spatial complementarity of tectonic earthquake swarms, *Earth Planet. Sci. Lett.* **482**, 62–70, 2018.

Rögnvaldsson, S.T., A. Gudmundsson & R. Slunga, Seismotectonic analysis of the Tjörnes Fracture Zone, an active transform fault in north Iceland. *J. Geophys. Res*. **103**, 30117–30129, 1998.

Skelton, A. et al., Hydrochemical changes before and after earthquakes based on long-term measurements of multiple parameters at two sites in northern Iceland - a review. *J. Geophys. Res.* **124**, 2702-2720, 2019.
Stefánsson, R. & G.B. Guðmundsson, Kópasker earthquake in 1976: About pre-activity, location and post-activity. In: *Proceedings to the Northquake 2019 workshop*, Húsavík Academic Centre, 2019 (this issue).

NORTHQUAKE 2019 - The 3rd International Workshop on Earthquakes in North Iceland
Húsavík, North Iceland, 21-24 May 2019

DO LARGE EARTHQUAKES IN NORTH ICELAND USUALLY OCCUR IN WINTER?

Sigurjón Jónsson[1]

[1]*King Abdullah University of Science and Technology (KAUST), Saudi Arabia (sigurjon.jonsson@kaust.edu.sa)*

Sudden changes in earthquake rate have been studied since the early days of seismology and have usually been related to mainshock stress changes, volcanic intrusions, or other major geologic processes. Subtle earthquake rate changes have also caught the interest of researchers and many explanations have been put forward. One category of these studies has focused on seasonal variations in earthquake rate, indicating that some seasonal processes or meteorological phenomena is influencing the timing of earthquakes. For example, snow unloading was proposed as the explanation for more frequent summer occurrence of large crustal earthquakes in Japan (*Heki,* 2003), while seasonal earthquake activity in the Himalayas and in California has been correlated to hydrological load variations (e.g., *Bettinelli et al.*, 2008; *Johnson et al.,* 2017). In South Iceland, large historical earthquakes show a clear tendency for Spring and early Summer occurrence. This seasonal activity is being investigated and mechanisms like snow-load variations, groundwater pressure changes, and upward migration of high-pressure fluids are being studied (*Jónsson et al.,* 2018). Here we study whether large earthquakes in North Iceland also show a seasonal tendency in occurrence.

Less is known about the historical earthquakes in North Iceland than in South Iceland due to their location mostly offshore and due to less complete historical accounts. Ómar Þorgeirsson compiled a report of historical earthquakes in North Iceland from the earliest known earthquake in 1260 and until 1900 using information from annals, journals and previous publications (*Thorgeirsson,* 2013). Very few reliable accounts exist for the earlier centuries and the report probably contains almost all available information from before 1700. More documents exist from after 1700 and further information could be collected about the effects of the large earthquakes since then, such as of the earthquakes that occurred in 1755, 1838 and 1872.

While many North Iceland earthquakes are mentioned in historical documents, their locations and sizes are not well constrained for the same reasons as above, i.e. that they mostly occurred offshore and the historical accounts are limited. Table 1 lists notable historical earthquakes in North Iceland and later significant earthquakes that were instrumentally recorded. The information mostly comes from the abovementioned report by Ómar Þorgeirsson and from Ambraseys and Sigbjörnsson (2000), who revised locations and magnitudes for events that occurred during the 20th century.

In addition to past events, results of GPS measurements (*Metzger et al.,* 2011; 2013) can be used to assess the level of seismic activity in North Iceland. These results indicate that about 1/3 of the relative plate motion in the Tjörnes Fracture Zone (TFZ) in North Iceland is taken up by the Húsavík-Flatey Fault (HFF) while the rest is likely concentrated on the Grímsey Oblique Rift (GOR). If all the relative motion is taken up by the roughly 100 km long HFF and GOR lineaments and the locking depth is that about 6-10 km (*Metzger and Jónsson,* 2014), then one can expect a moment accumulation rate of 3.2-5.4×10^{19} Nm per century, which is equivalent to a single magnitude 7.0-7.1 earthquake. Adding up the

moment indicated by surface wave magnitudes M_s listed in Table 1 for the 20th century is 1.0×10^{20} Nm, i.e. similar to a single magnitude 7.3 event, which is significantly larger than what is suggested by GPS. This difference is due the M_s=7.19 size of the 1910 earthquake, which might have been overestimated by Ambraseys and Sigbjörnsson (2000). When the moment indicated by the other magnitudes (listed M and M_w in Table 1) is added for the 20th century, then it corresponds to a smaller M_w=7.1-7.2 earthquake, which corresponds better to the GPS moment accumulation rate. Indeed, when all events during the past 300 years with a listed magnitude are added, then the moment per century is somewhat lower or roughly corresponding to a single magnitude 7 event, which is in accord to the GPS results. While this exercise appears to match the GPS estimates, the event occurrence can be highly non-uniform in time and influenced by major events, such as the Krafla rifting episode, which put large part of the HFF into a stress shadow (*Maccaferri et al.*, 2013).

To test seasonal occurrence of large earthquakes in South Iceland, instrumentally recorded earthquakes of magnitude 6 and above were included and earlier earthquakes that caused reported damage (*Jónsson et al.*, 2018). In the TFZ, this is more difficult, as some large earthquakes occurred far offshore and did not cause any damage. Therefore, here I use a magnitude threshold of 5.5 and include events from previous centuries that appear more significant in the historical accounts. This results in 22 selected events for the TFZ, indicated in bold font in Table 1 (first column). Similar to South Iceland, I exclude events occurring within 5 years of a major event, based on the possible influence of postseismic processes (*Jónsson et al.*, 2003; *Jónsson*, 2008; *Decriem et al.*, 2012).

The majority of the selected 22 earthquakes did occur during winter months with only three events in May-August, as shown in the histogram in Fig. 1. To test the significance of this apparent winter occurrence of events a Schuster's random-walk phase diagram was generated, showing that the events almost reach the 95% confidence level and indicate a tendency for December-January event occurrence (Fig. 1). The confidence levels are generated using multiple random sequences of 22 events and the 95% level means that only 5% of the random sequences extended as far as the one produced by the TFZ earthquakes. In other words, it is only a bit over 5% chance that the TFZ sequence is due to random occurrence, suggesting that there is some seasonal process influencing the timing of the earthquake leading to the winter occurrence.

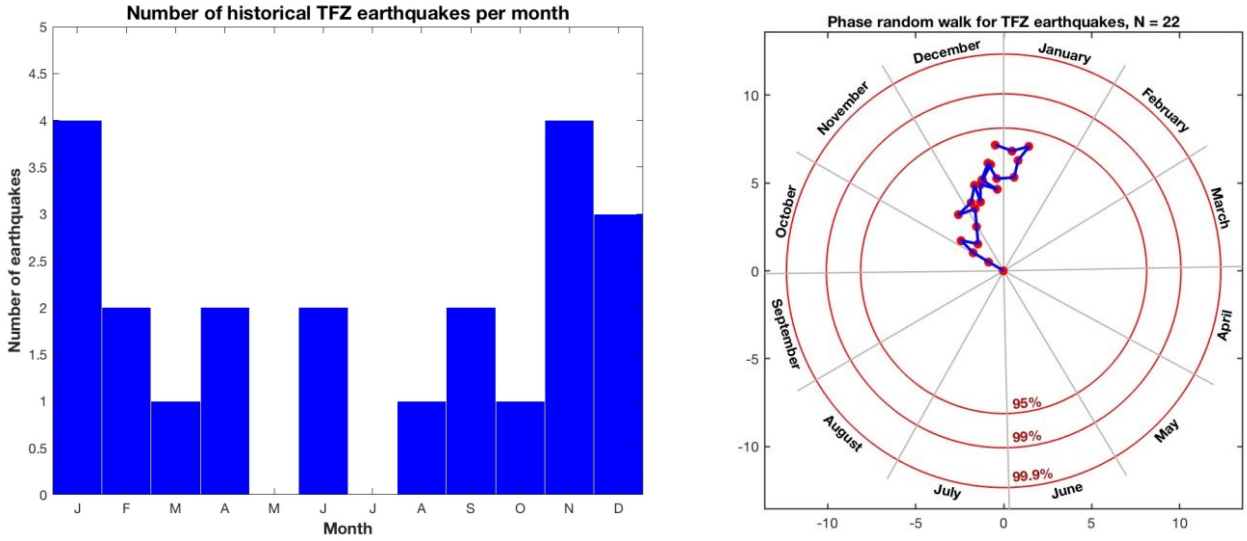

Figure 1. A histogram showing during which months significant earthquakes in North Iceland (Table 1) have occurred and a phase random walk diagram further demonstrating the preferential winter occurrence of events.

Table 1. Information about earthquakes in North Iceland from Thorgeirsson (2011) in black, Ambraseys and Sigbjörnsson (2000) in green, Stefánsson et al. (2008) in red, IMO online list in blue and Global CMT in purple. Dates in gray are uncertain and dates in italic font indicate events occurring within 4-5 years of a major event (indicated by bold font). Earthquakes selected for the seasonal statistics are highlighted with dates in bold font, see Fig. 1.

Date	Time	Lat.	Long.	M_S	M_b	M	M_w	Comments
1260		*Central TFZ*						*"A great earthquake in Flatey"*
1577-11-1	*Evening*	*West TFZ*						*Shaking for "half an hour"*
1584		*West TFZ*						*Damage at Hólar, repairs in many places*
1618-11-1		*East TFZ*						*EQs in Fall to Christmas, houses collapsed*
1624-11-15		*West TFZ*						*EQs in November, likely damage at Hólar*
1643-12-25		-						*Probably in South Iceland*
1645		*West TFZ*						*Large earthquakes reported, date not clear*
1658-4-13		*West TFZ*						*"A very large earthquake" reported*
1661-7-1		-						*EQs in summer, probably in South Iceland*
1664-12-26		*West TFZ*						*Limited information about damage*
1668-2-1		-						*EQs in winter 1668, not clear if in N-Iceland*
1681-12-26	*Afternoon*	*West TFZ*						*Limited info on damage, maybe not large*
1724-29, 1746		*Krafla*						*Earthquakes related to rifting at Krafla*
1755-9-11	~09:00	66.13	-17.76			7		*Major earthquakes affecting most of the TFZ*
1784-2-15	~11:00	*Central TFZ*						*"Very sharp quake", no damage reported*
1802-1-12		-						*No house collapse reported*
1826-6-25		-						*Late in June, no damage, hardly significant*
1837-10-15		-						*In October, no damage, not significant*
1838-6-12	~02:00	66.12	-18.82			6.5		*Major earthquake near Siglufjörður*
1847-4-15		*Grímsey*						*In April and May, not so significant*
1855-3-12	~09:00	*East TFZ*						*Morning, earthquakes felt, but not strong*
1867-12-31	~04:30	*East TFZ*						*Rifting related, damage, ground cracks*
1872-4-18	~10:00	66.08	-17.45			6.5		*Major earthquake in Húsavík*
1872-4-18	~11:00	66.18	-18.04			6.5		*Major earthquake near Flatey*
1875-1-2		*Central-East*						*Before Christmas and into January*
1876-12-31		*Central-East*						*End of year and early 1877, related to Askja*
1880-10-20		*East TFZ*						*Several quakes reported, no damage*
1882-10-29	13:54	*East TFZ*						*Swarm reported, no damage*
1884-11-2	07:30	*East TFZ*						*Damage reported in Húsavík*
1885-1-25	10:50	66.12	-16.88			6.3		*Large earthquake in Kelduhverfi*
1892-3-9		*Grímsey*						*Not a very significant swarm*
1893-4-12	20:00	*East TFZ*						*Objects fell down from shelves, but not large*
1896-3-2	00:00	*Central-West*						*Not significant*
1897-4-30		*West TFZ*						*Not significant*
1899-1-29	11:12	66.30	-19.90	5.77				*Objects from shelves fell down, felt all over*
1904-8-2	10:12	66.30	-18.70	5.59				
1905-11-15	06:50	66.20	-18.00	5.49		5.1		*Too small*
1906-3-19	07:57	68.70	-17.00	6.62	6.7	5.9		*Too far north*
1908-12-26	07:04	66.20	-18.00	5.03		4.6		*Too small*
1910-1-22	07:50	66.50	-17.50	7.19	7.1	7.0 / 7.1		*Grímsey EQ, another loc.: [66.35, -17.94]*
1913-5-19	15:45	66.30	-18.80	5.63	6.3	5.5		
1913-7-26	20:51	67.00	-18.00	5.69	6.0	5.6		
1921-8-23	20:17	67.00	-18.00	6.39	6.3	6.3		*North of Grímsey, too far north*
1927-4-29	11:19	66.30	-19.50	5.07		4.8 / 5.5		*Too small*
1934-6-2	13:42	65.95	-18.50	6.17	6.2	6.1 / 6.2		*Dalvík EQ, alternative loc.: [66, -18.44]*
1934-7-5	07:45	65.95	-18.50			5.6		
1936-10-22	23:49	66.80	-17.40	5.32		5.3 / 5.8		
1936-10-23	00:00	66.80	-17.40	5.40		5.4 / 5.8		
1963-3-28	00:16	66.37	-19.69	6.85	6.7	6.8 / 7		*The Skagafjörður earthquake, M=6.9 in NEIC, Alternative location: [66.23, -19.6]*
1963-10-15	09:59	67.20	-18.40	5.71	5.2	5.6		
1969-5-5	21:47	66.90	-18.28	5.09	5.2			*Too small*
1976-1-13	13.29	66.28	-16.57	6.33	5.9		6.3	*Kópasker EQ, another loc. [66.23, -16.5]*
1994-2-8	03:27	66.47	-19.25	5.46	5.2		5.5	*NNW of Siglufjörður*
2002-9-16	18:48	66.9	-18.67	5.5	5.7		5.8	*Northwest of Grímsey*
2012-10-21	01:25	66.42	-18.74	5.4	5.6		5.6	*Western HFF*
2013-4-2	00:59	66.62	-17.59	5.3	5.3		5.3	*Too small, activity southeast of Grímsey*
2019-3-27	20:29	66.27	-16.53			4.2		*Too small, activity west of Kópasker*

While the seasonal occurrence of the TFZ earthquakes may appear strong, it is much less significant than found for earthquakes in South Iceland (*Jónsson et al.*, 2018). Also, there has been a lot of discussion lately about the use of "p-values" and their usefulness. p-values are used check whether a null hypothesis can be rejected. In our case, the null hypothesis is that the earthquake occurrence in North Iceland is random. With a p-value near 0.05, the result may appear to be significant, i.e. that the hypothesis of random earthquake occurrence can be rejected. However, statisticians have been criticizing the use of p-values to test statistical significance (e.g., *Halsley et al.*, 2015) and have argued to omit it completely or use a much more stringent threshold of 0.005 (*Benjamin et al*., 2018). Therefore, while the TFZ earthquakes show tendency for winter occurrence, it does not prove that some seasonal processes are affecting the timing.

In addition to what has been discussed above, some of the large TFZ earthquakes appear to have been triggered by rifting activity in the Northern Volcanic Zone. For example, the 1976 Kópasker earthquake was triggered by the first and the largest intrusion of the Krafla rifting episode (*Passarelli et al.*, 2013) and the large earthquake of 1867 was likely related to rifting activity in the Þeistareykir fissure swarm. Therefore, while these events appear to have been triggered by external forcing, that forcing was seemingly unrelated to seasonal processes.

References

Ambraseys, N.N., & R. Sigbjörnsson. *Re-appraisal of the seismicity of Iceland*, Polytechnica – Engineering Seismology, **3**, 183 pp, 2000.

Bettinelli, J.-P. Avouac, M. Flouzat, L. Bollinger, G. Ramillien, S. Rajaure & S. Sapkota, Seasonal variations of seismi-city and geodetic strain in the Himalaya induced by surface hydrology, *Earth Planet. Sci. Lett.* **266**, 332-344, 2008.

Benjamin, D.J., et al., Redefine statistical significance, *Nature Human Behavior*, **2**, 6-10, 2018.

Decriem, J. & T. Árnadóttir, Transient crustal deformation in the south Iceland seismic zone observed by GPS and InSAR during 2000-2008. *Tectonophysics*, **581**, 6-18, 2012.

Halsey, L.G., D. Curran-Everett, S.L. Vowler & G.B. Drummond, The fickle P value generates irreproducible results, *Nature Methods*, **12**, 179-185, 2015.

Heki, K., Snow load and seasonal variation of earthquake occurrence in Japan, *Earth and Planetary Science Letters* **207**, 159-164, 2003.

IMO – The Icelandic Meteorological Office: *Large earthquakes (>4) during the time period 1706-1990* (an online earthquake list, in Icelandic). http://hraun.vedur.is/ja/ymislegt/storskjalf.html

Johnson, C.W., Y. Fu & R. Bürgmann, Seasonal water storage, stress modulation, and California seismicity, *Science* **356**, 1161-1164, 2017.

Jónsson, S., P. Segall, R. Pedersen & G. Björnsson, Post-earthquake ground movements correlated to pore-pressure transients, *Nature*, **424**, 179-183, 2003.

Jónsson, S., Importance of post-seismic viscous relaxation in southern Iceland, *Nature Geoscience*, **1**, 136-139, 2008.

Jónsson, S., V. Drouin, Y. Aoki & B. Ófeigsson. What causes seasonal earthquakes in South Iceland? Abstract G43A-06, AGU Fall Meeting, Washington D.C., 10-14 December, 2018.

Maccaferri, F., E. Rivalta, L. Passarelli & S. Jónsson. The stress shadow induced by the 1975-1984 Krafla rifting episode, *J. Geophys. Res.* **118**, doi:10.1002/jgrb.50134, 2013.

Metzger, S., S. Jónsson & H. Geirsson, Locking depth and slip-rate of the Húsavík Flatey fault, North Iceland, derived from continuous GPS data 2006-2010, *Geophys. J. Int.*, **187**, 564-576, 2011.

Metzger, S., S. Jónsson, G. Danielsen, S. Hreinsdóttir, F. Jouanne, G. Giardini & T. Villemin, Present kinematics of the Tjörnes Fracture Zone, North Iceland, from campaign and continuous GPS measurements, *Geophysical Journal International* **192**, 441-455, 2013.

Metzger, S. & S. Jónsson, Plate boundary deformation in North Iceland during 1992-2009 revealed by InSAR time-series analysis and GPS, *Tectonophysics* **634**, 127-138, 2014.

Passarelli, L., F. Maccaferri, E. Rivalta, T. Dahm & E.A. Boku, A probalistic approach for the classification of earthquakes as 'triggered' or 'not triggered', *Journal of Seismology*, **17**, 165-187, 2013.

Stefánsson R., G.B. Gudmundsson & P. Halldórsson, Tjörnes Fracture Zone. New and old seismic evidences for the link between the North Iceland rift zone and the Mid-Atlantic ridge, *Tectonophysics* **447**, 117-126, 2008.

Thorgeirsson, Ó., *Historical earthquakes in North Iceland* (in Icelandic), Húsavík Academic Centre report, 54pp, 2011.

NORTHQUAKE 2019 - The 3rd International Workshop on Earthquakes in North Iceland
Húsavík, North Iceland, 21-24 May 2019

SPATIAL DISTRIBUTION OF LANDSLIDES AND ROCK FALL IN CONNECTION WITH MAJOR EARTHQUAKES IN NORTHERN ICELAND

Jón Kristinn Helgason[1], Halldór G. Pétursson[2], and Sveinn Brynjólfsson[1]

[1] *Icelandic Meteorological Office, Bústaðarvegur 7-9, 108 Reykjavík.*
[2] *Icelandic Institute of Natural History, Borgum við Norðurslóð, 600 Akureyri*

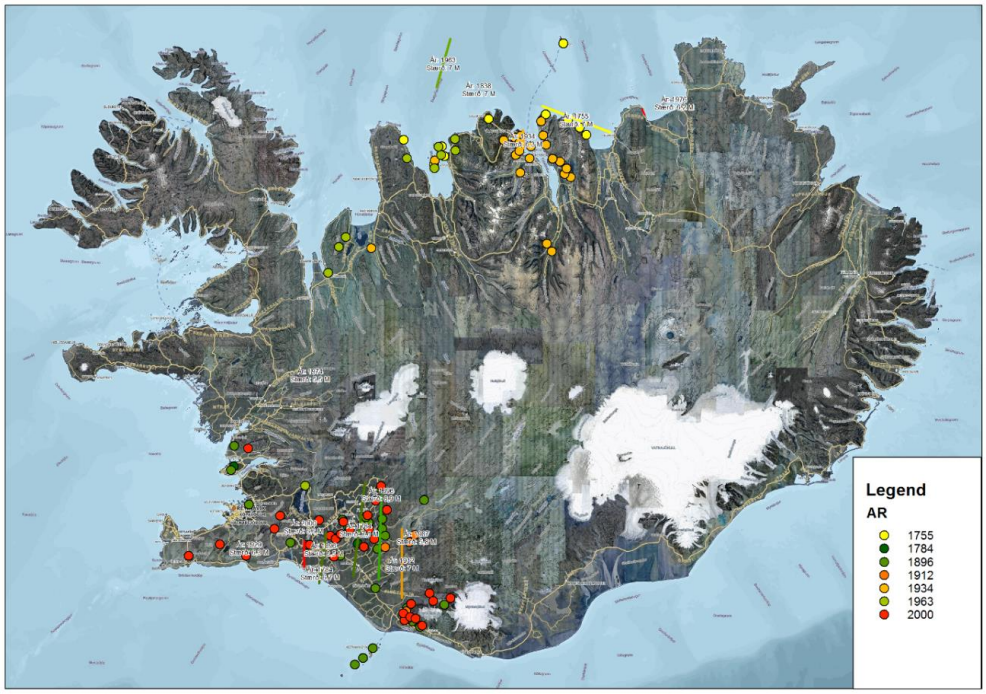

High magnitude earthquakes in many seismically active areas are known to have caused catastrophic landslides and rock fall with wide spatial distribution. Earthquakes generally trigger superficial ground movements and can therefore trigger slope failures. Rock fall is the most common type of slope failure but disrupted soil slides, debris flows and mudflows are also common. High magnitude earthquakes can trigger larger slope failures such as rock slides and rock avalanches and they are also known to have reactivated dormant landslides. It is widely considered that slope failures are triggered by earthquakes of moderate to high magnitude (>M5), however localized effect can occur during smaller earthquakes.

Earthquakes of magnitude 6 or higher are not very common in Iceland, but when they occur they have triggered a wide distribution of landslides and rock fall near the Tjörnes fracture zone (TFZ) and the South Iceland seismic zone (SISZ). Historical data of slope failure triggered by earthquakes in the TFZ can be traced back to 1755. The data, which are rather sparse, suggest that the areas most affected by high-magnitude earthquakes in the TFZ are the northernmost parts of Tröllaskagi and Flateyjarskagi peninsulas.

References

Turner, A.K., and R.L. Shuster, *Landslides, investigation and mitigation*, special report 247. Transportation research board, 1996.

NORTHQUAKE 2019 - The 3rd International Workshop on Earthquakes in North Iceland
Húsavík, North Iceland, 21-24 May 2019

AVALANCHE AND LANDSLIDE MONITORING AT THE ICELANDIC MET OFFICE

Harpa Grímsdóttir and Sveinn Brynjólfsson

Icelandic Meteorological Office (harpa@vedur.is, sveinnbr@vedur.is)

Snow avalanches is the type of natural hazard that has caused the greatest number of fatalities in Iceland and landslides are number two on the list. This is if storms at sea and land are not accounted for. Volcanic eruptions, earthquakes and floods have been by far less lethal, however, they have caused extensive economic damages.

Fatal accidents due to natural disasters in Iceland 1901–2018

Accident cause	Fatalities
Accidents at sea	Thousands
Storms on land	Hundreds
Snow avalanches	170
Landslides	40
Vulcanic eruptions, earthquakes and floods	<5

In 1995 two catastrophic avalanche accidents claimed 34 lives in the villages of Súðavík and Flateyri. The year 1995 became the turning point for avalanche and landslide work in Iceland. The government decided to put money into research, hazard mapping and mitigation. Since then hazard maps have been made for towns and villages based on criteria and methods developed after 1995. Defence structures have been designed and built in many areas where the risk is unacceptable. The monitoring system for avalanches and landslides was also reorganized.

A group of seven specialists form an avalanche- and landslide monitoring team at the Icelandic Met Office. The specialists work in Ísafjörður, Reykjavík and Akureyri. Furthermore, IMO has 19 snow observers around the country in towns and villages where the avalanche and landslide danger is considerable. The most important role of the monitoring team is to monitor avalanche hazard in towns and villages and order evacuations during periods of high risk. In recent years, however, the role has expanded and avalanche forecasting for the road administration as well as publication of public avalanche bulletins are examples of tasks that have been added since 2012. Monitoring landslide risk has also become increasingly important. Big landslides have been prominent during recent years, and it is possible that landslide risk in Iceland will increase with global warming. Also, tourism in Iceland has expanded rapidly which means that the likelihood of people being present in areas when rockfall or landslides occur is higher than before.

Earthquakes can trigger both landslides and snow avalanches. During periods of increased risk for high magnitude earthquakes, public warnings of rockfall, landslides and avalanches may be issued. Historical earthquakes in the North are known to have caused landslides in a widespread area, and in some cases snow avalanches as well. Especially Tröllaskagi and parts of Flateyjarskagi have infrastructure that is exposed to avalanches and landslides. A big part of the most exposed urban areas has been protected with permanent defence structures, however many road stretches are exposed as well as ski areas and other infrastructure, and there are still quite a few buildings and houses in hazard zones.

NORTHQUAKE 2019 - The 3rd International Workshop on Earthquakes in North Iceland
Húsavík, North Iceland, 21-24 May 2019

MONITORING SLOPE INSTABILITIES WITH SENTINEL-1 SATELLITE INTERFEROMETRY

Vincent Drouin[1,2] and Freysteinn Sigmundsson[1]

[1]*Nordic Volcanological Center, Institute of Earth Sciences, University of Iceland (vd@hi.is, fs@hi.is)*
[2]*National Land Survey of Iceland (vincent@lmi.is)*

Iceland is deforming under the influence of many processes, from wide-scale plate spreading and glacial isostatic adjustments (GIA) to local volcanic and geothermal processes. Ground movements can be observed and measured using geodetic techniques, usually GPS and SAR satellite interferometry (InSAR). In fall 2014, a new SAR satellite (Sentinel-1A) was launched by ESA: it continuously acquires images around the world, revisiting the same area every 12 days. The addition of a second satellite (Sentinel-1B) in early 2017 reduced the revisit time to 6 days. This is an unprecedented amount of data provided free of charge to monitor deformation around the world. In Iceland, this data has been used to obtain a deformation map covering the entire country at a 50 m resolution from summer 2015 to summer 2018 (*Drouin & Sigmundsson*, 2019). It clearly shows plate spreading, GIA, volcanoes and geothermal processes, and slope instabilities (Fig. 1).

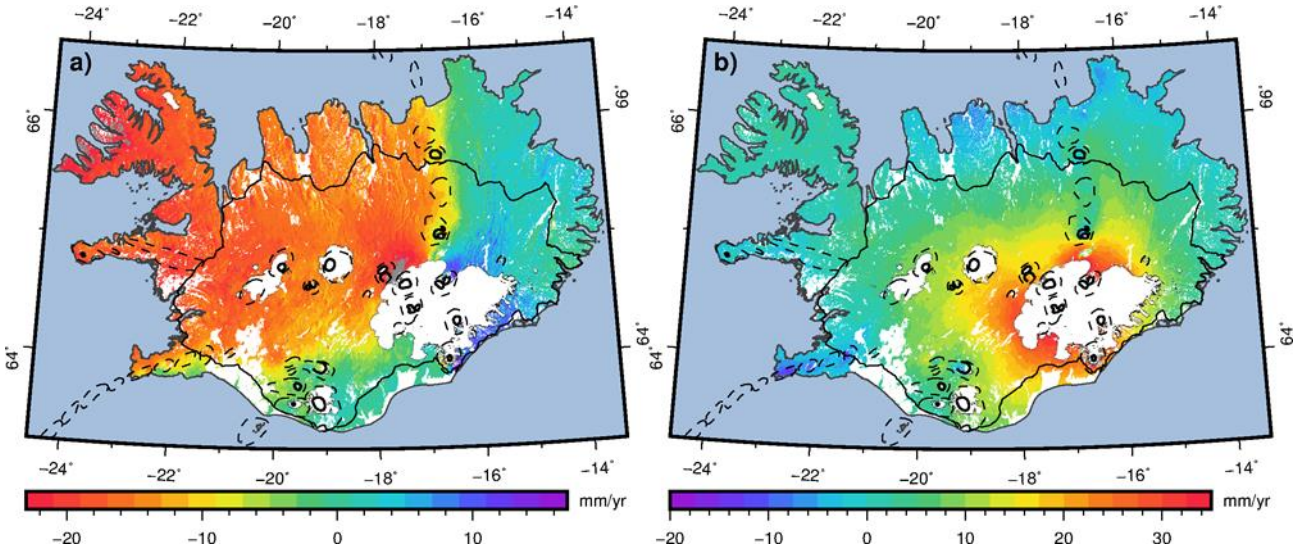

Figure 1. (Left) Near-East and (Right) near-Up velocity fields derived from the decomposition of LOS velocities from six InSAR tracks.

Slope instabilities in Iceland have previously been studied using InSAR (*Jónsson*, 2009) but were limited by the availability of SAR data. On our new country-wide deformation map, slope instabilities can be observed in many places but mostly in North and in East Iceland (e.g., Fig. 2). They appear to be located on partially collapsed slopes. The ability to detect movements and rate of deformation on these slopes is of prime importance, as shown by the July 2018 Hítardalur landslide which collapsed on such a slope. Some of the slopes which are currently moving present a greater hazard than Hítardalur due to their proximity to main roads, farms, or water bodies (tsunami risk). InSAR analysis of the deformation on the Hítardalur slope in the summers preceding the July 2018 collapse show that it was moving at about 1-2 cm/month in 2015 and in 2016, about 10 cm/month in 2017, and too fast in June 2018 for the

deformation to be measured (unpublished work). Acceleration of the slope deformation before collapsing is a common behavior in landslides (*Bozzano et al.*, 2014).

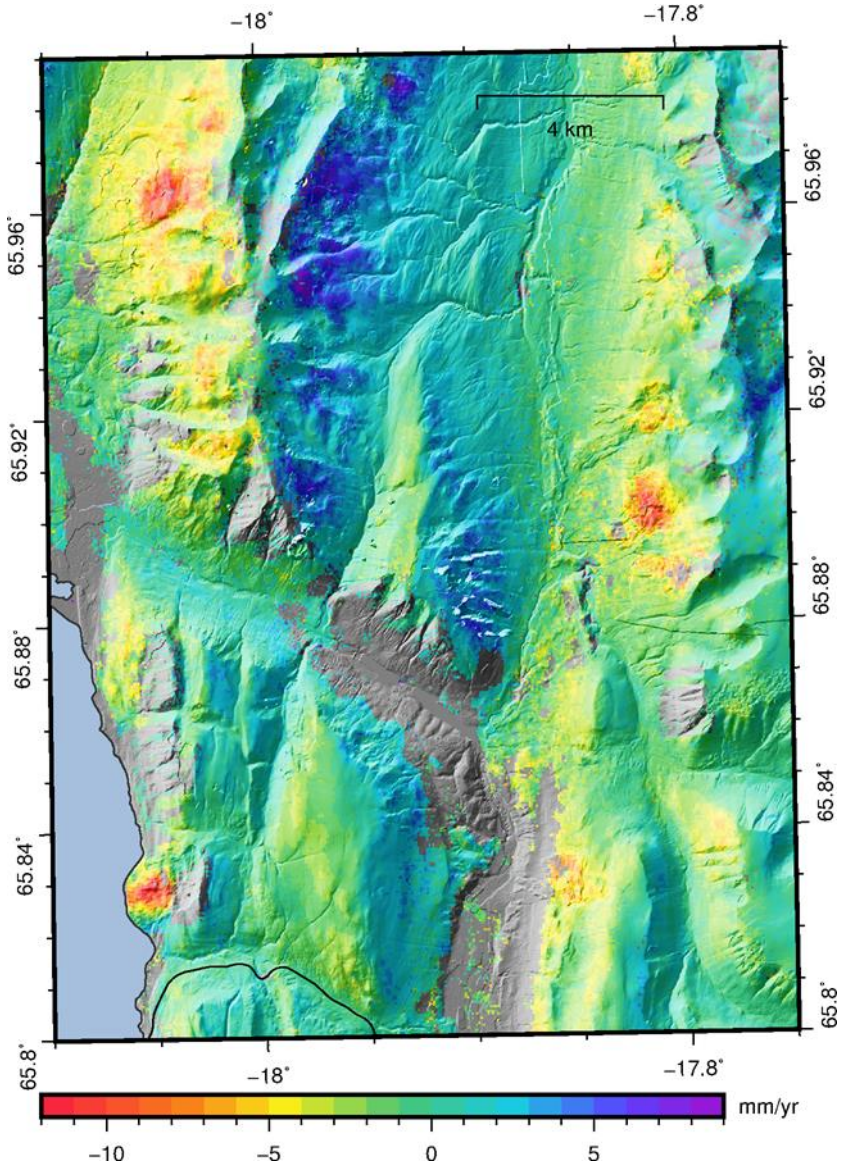

Figure 2. 2015-2018 average East velocities around Flateyjardalsheiði. The large red areas show slope instabilities: they are going about 10 mm/yr west, which is 5 to 10 mm/yr more west than the other west-facing slopes.

The images used to generate the country wide deformation fields were resampled and analyzed at about 50 x 100 m resolution to increase the signal to noise ratio and keep calculation time reasonable. However, because of filtering during the processing and temporal decorrelation, some slope instabilities were smoothed out and did not appeared in the final deformation fields. We therefore decided to use the permanent scatter (PS) technique on specific landslides to ensure we get the most information out of the original data and don't miss any signal. PS processing is done at full resolution (~2.3 m in range and ~14.1 m in azimuth) and therefore only applied to the landslide and its immediate surroundings. Figure 3 shows the example of the Almenningar landslides which is known to move several centimeters to tenths of centimeters per year according to fields measurements. The country-wide grid shows no significant deformation over the landslide area while the PS grid shows clearly the outline of the moving slope. The main reason for the difference that the country-wide grid shows the average deformation over 2015-2018 while the PS grid covers only summer 2018. And, as the slope is moving very fast, there is

signal loss from one summer to the next.

The PS processing was also tested on the Víknafjöll mountain range, located on the west side of Skjálfandi bay and facing the town of Húsavík. Landslides happening on these slopes would likely fall in the sea and could therefore generate tsunamis. Preliminary results of summer 2018 displacements show two potential locations for such landslides: Skálavík and Brúnkollur.

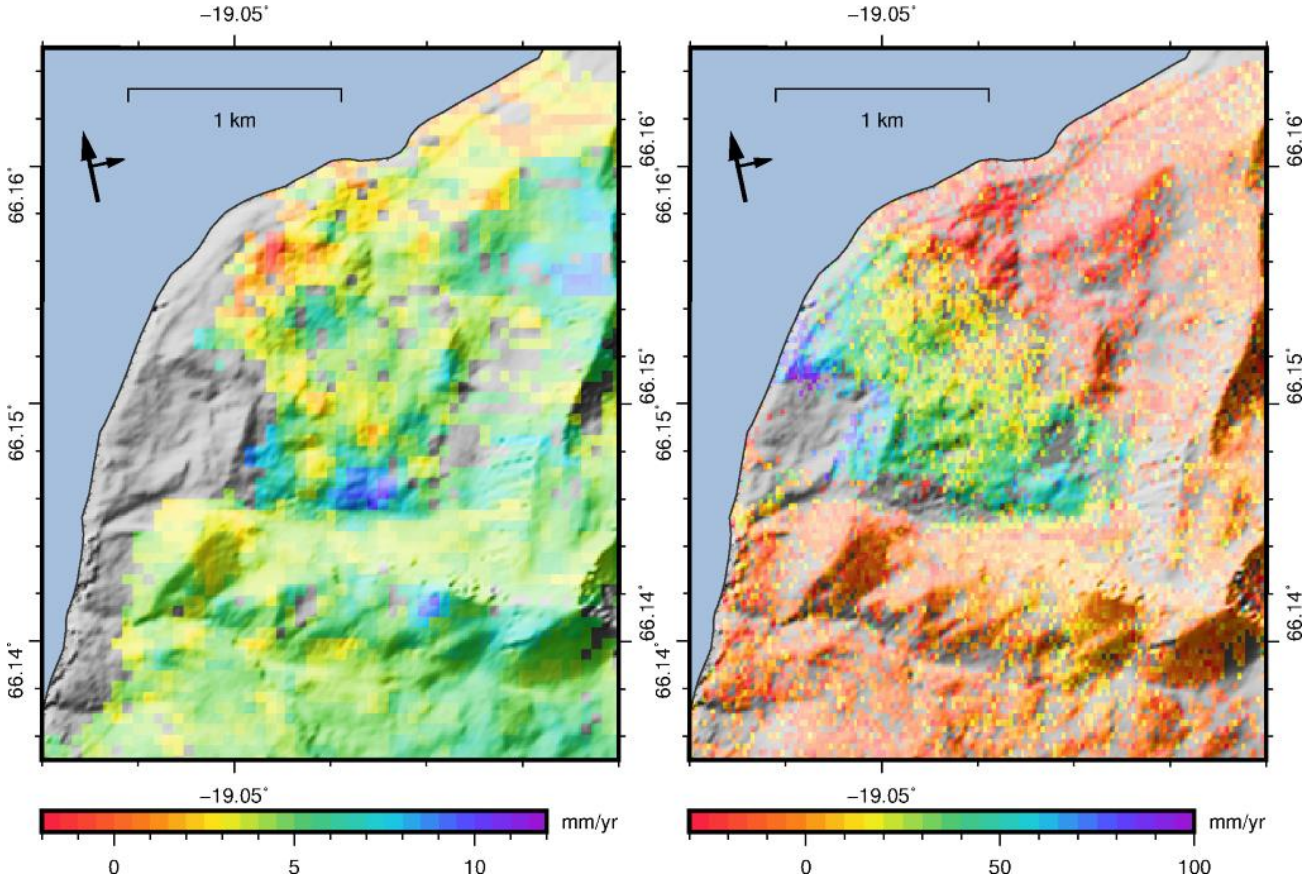

Figure 3. Comparison of line-of-sight deformation for Sentinel-1 track T118: country-wide velocities for 2015-2018 (left) and PS velocities for summer 2018 (right). Note the difference in resolution and temporal coverage.

The Sentinel-1 Copernicus mission is providing a very valuable dataset for landslides monitoring in Iceland. We can determine which slopes present the greatest risk, their current deformation rate, and monitor them to detect potential acceleration leading to collapse. High risk slopes can then be examined by a ground team and monitored with other techniques (e.g., GPS, extensometers) as is the case for Svínafellsheiði. Future work is needed to determine which processing approach is the best to monitor slope instabilities and the time period used to estimate velocities must be chosen with care to avoid signal loss.

References

Bozzano, F., I. Cipriani, P. Mazzanti & A. Prestininzi, A field experiment for calibrating landslide time-of-failure prediction functions. *International Journal of Rock Mechanics and Mining Sciences*, **67**, 69-77, 2014. https://doi.org/10.1016/j.ijrmms.2013.12.006

Drouin, V. & F. Sigmundsson, Country-wide observation of plate spreading and glacial isostatic adjustments in Iceland inferred by Sentinel-1 radar interferometry, 2015-2018. *Geophysical Research Letters*, **46**, 8046-8055, 2019.

Jónsson, S., Slope creep in East Iceland observed by satellite radar interferometry. *Jökull*, **59**, 89-102, 2009.

NORTHQUAKE 2019 - The 3rd International Workshop on Earthquakes in North Iceland
Húsavík, North Iceland, 21-24 May 2019

PRELIMINARY SIMULATIONS FOR TSUNAMI HAZARD IN CONNECTION WITH A MAJOR EARTHQUAKE ON THE HÚSAVÍK-FLATEY FAULT

Angel Ruiz-Angulo[1], Kristín Jónsdóttir[1], Ragnar H. Þrastarson[1], Benedikt Halldórsson[1,2], Vincent Drouin[3], Harpa Grímsdóttir[1], and Sigurjón Jónsson[4]

[1]*Icelandic Meteorological Office (angel@vedur.is)*
[2]*Earthquake Engineering Research Centre, University of Iceland*
[3]*Institute of Earth Sciences, University of Iceland and National Land Survey of Iceland*
[4]*King Abdullah University of Science and Technology (KAUST), Saudi Arabia*

In recent years, many tsunamis have surprised the scientific community with several unfortunate examples, which have led to changes in both forecast and prevention implementations (*Cienfuegos et al.*, 2018). Among key problems are underestimations of the size and inaccurate timing of pending tsunamis. For example, the tsunami generated by the magnitude 9.0 Tohoku (Japan) earthquake in 2011 surpassed tsunami barriers in the region of Sendai by several meters. In the town of Onagawa, the local morphology of the area resulted in constructive resonance effects that led to remarkable wave heights as high as 16 m with 75% of the town's buildings destroyed (*Mori et al.*, 2011; *Adriano et al.*, 2016). While the Tohoku earthquake was a major subduction zone event and expected to generate a large tsunami, some smaller events have caused surprisingly large tsunamis, e.g., the magnitude 7.5 Palu earthquake of 2018. The mechanism of this earthquake was primarily strike-slip, so a significant tsunami was not expected. Still, just 3 minutes after the earthquake occurred, a considerable tsunami hit the city of Palu. The tsunami wave height was 4-7 m while its forecasted height was only 1.5 meters (*Carvajal et al.*, 2019; JRC Emergency Report, 2018). The current hypotheses for explaining the Palu tsunami include complex morphology/bathymetric effects or submarine landslide movement, or perhaps both at the same time (*Pakoksung et al.*, 2019).

While major earthquakes in North Iceland are primarily strike-slip events and large tsunamis thus not expected, several historical accounts exist of tsunamis in past earthquakes. For example, a tsunami wave triggered by the 1755 earthquake appears to have overturned two boats near the harbor in Húsavík and killed several people (*Thorgeirsson*, 2013). There are also many reports of rockfalls and landslides in this event and in the 1838 earthquake along the coastline and on islands in the area (Grímsey, Drangey and Málmey). In addition, an account from Flatey island of the 1872 earthquake states that the ocean first retreated and then came back as a large wave (*Thorgeirsson*, 2013), a clear indication that the island was hit by a tsunami.

It is not clear what caused the tsunamis reported upon in historical accounts. The Húsavík-Flatey Fault (HFF) is not a pure strike-slip fault everywhere, i.e. its strike changes near its western and eastern ends, leading to significant normal faulting movement both in the Eyjafjarðaráll basin in the west and near Húsavík in the east. Large earthquakes on these segments of the fault would likely be oblique with a combination of strike-slip and normal faulting and could thus trigger tsunamis. Also, the topography along the fault is variable, e.g. on the western side of the Skjálfandi Bay, across from Húsavík, where the fault extends from the deep bay into a shallow saddle between the mainland and Flatey Island

(*Magnúsdóttir et al.*, 2015). Large lateral strike-slip movement on this part of the fault might cause significant displacement of seawater and possibly trigger a tsunami. In addition, rockfalls, landslides, and snow avalanches that advance beyond the coastline and into the sea could also cause tsunamis that locally might cause large wave heights. Finally, submarine landslide movement could also be responsible for generating tsunamis in the area, although submarine slumps have yet to be identified and mapped.

In our presented work here we propagate a tsunami induced by a simple uniform slip earthquake scenario on the HFF, which could represent a previous event or a possible future earthquake. GPS measurements in North Iceland indicate that the moment accumulated on the HFF since the last large earthquake on the HFF in 1872, corresponds to a single 6.8-7.0 earthquake (*Metzger and Jónsson,* 2014). The estimated size of the largest earthquakes that have occurred in North Iceland during the past 300 years is about 7 (*Stefánsson et al.,* 2008), although rare events rupturing the entire 100-km-long HFF might be somewhat larger. We therefore use a possible scenario earthquake of size 7.0 for the domain shown in Fig. 1.

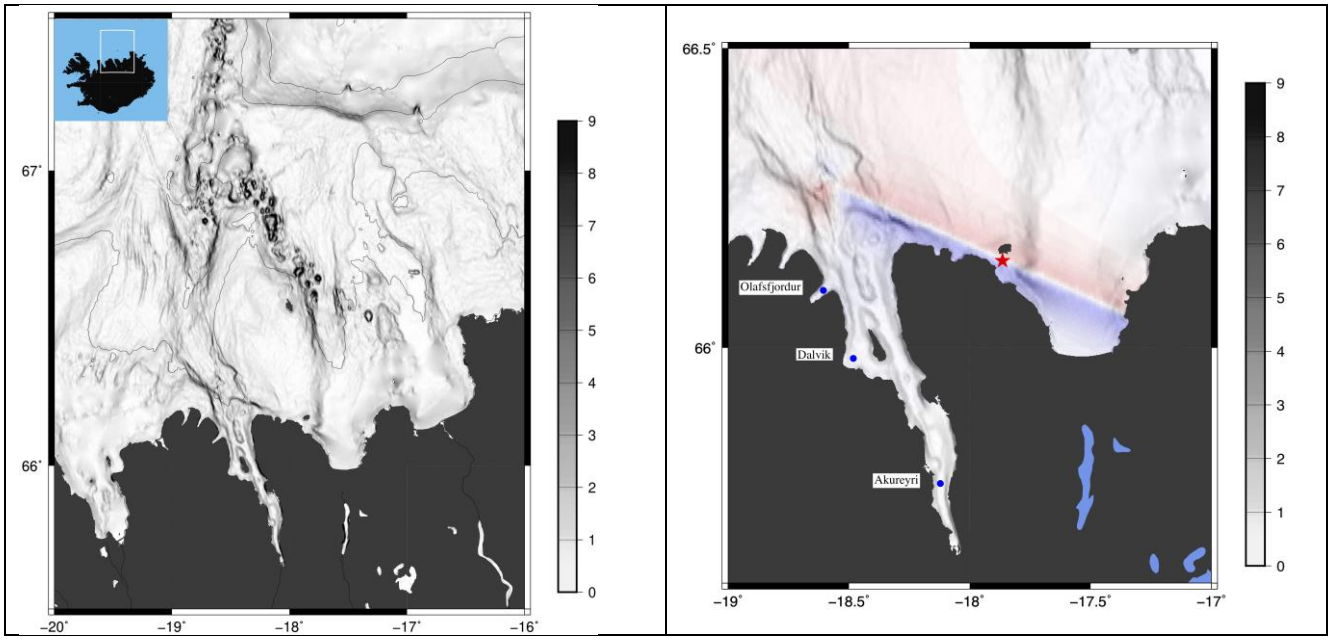

Figure 1. Left: Bathymetry slope in degrees for the HFF tsunami simulation area north of Iceland (saturated at 9□), highlighting the complexity of topographic features within the computational domain. Right: Detailed view for the central part of the area showing the hypocenter and the slip distribution for this scenario including the virtual tide gauges (shown as blue circles) near Akureyri, Dalvík, and Ólafsfjörður.

We converted a uniform fault-slip event of magnitude 7.0 on the HFF into a surface water perturbation following the simple Okada method and propagated the resulting waves using the numerical model GeoClaw (*LeVeque et al.,* 2011). Figure 2 shows snapshots of the resulting small-tsunami wave heights in this simple and preliminary scenario, wave heights that could change significantly if a more realistic non-uniform earthquake fault-slip distribution was used or advective contributions due to complex bathymetry were taken into account (*Melgar and Bock,* 2013). However, despite its simplicity, the tsunami model shows waves that travel around the north-pointing peninsulas and into the different fjords, including all the way to Akureyri. These trapped waves and focusing of energy could lead to unexpected wave heights in a real event (*Melgar and Ruiz-Angulo,* 2018).

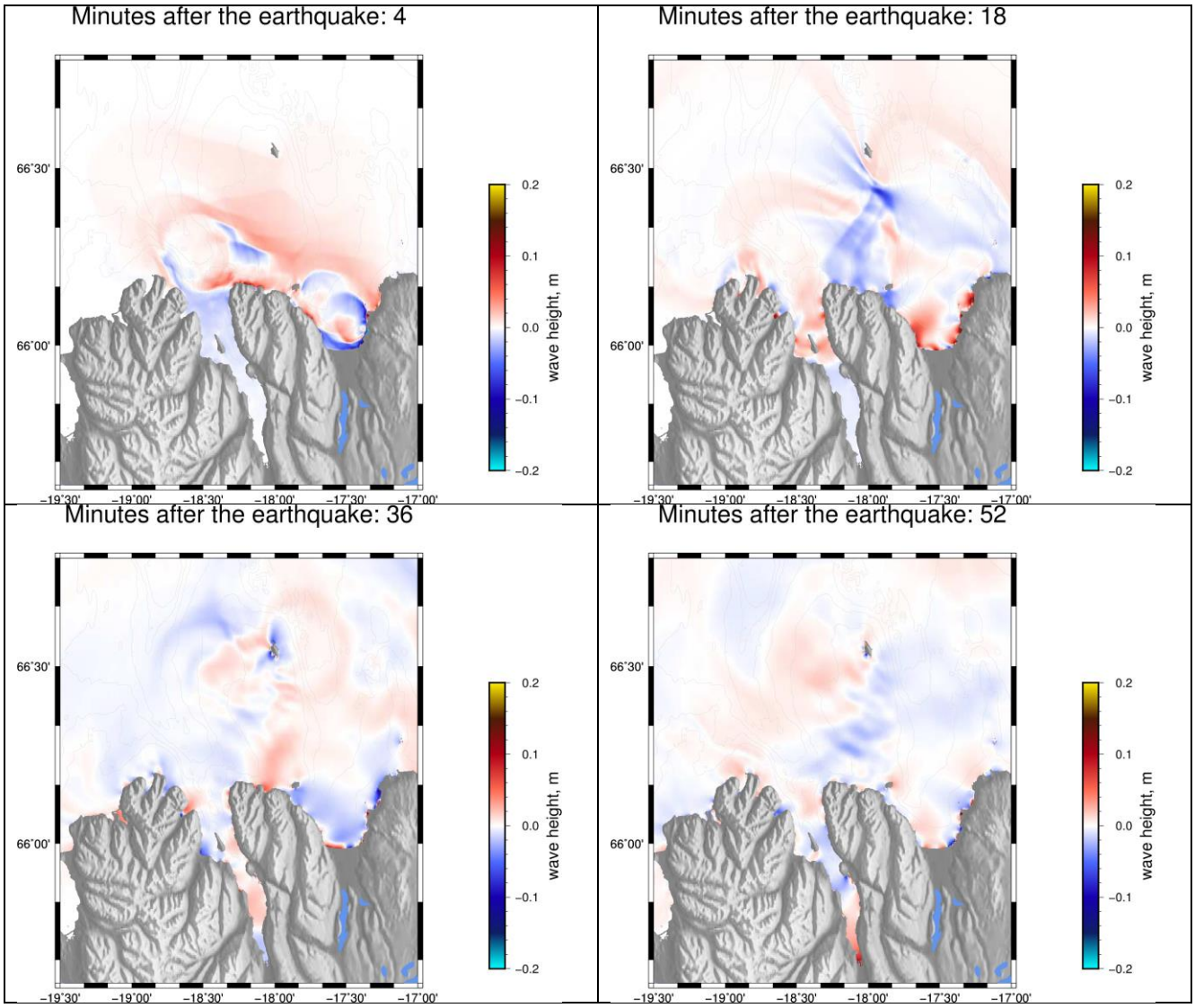

Figure 2. Preliminary results showing snapshots for the estimated tsunami wave height (in meters) 4, 18, 36 and 52 minutes after the occurrence of the scenario M_w7.0 strike-slip earthquake on the Húsavík-Flatey Fault. These results show the tsunami reaching the coastline near Húsavík within 4 minutes.

We also performed an exercise that includes a large underwater landslide (500 □10^6 m^3) occurring simultaneously to the magnitude 7.0 scenario above. The resulting tsunami wave height in Figure 3 shows that the submarine landslide perturbation dominates this simulation. This shows that submarine landslides could pose significant tsunami hazard and stresses the need for mapping past landslides on the seafloor.

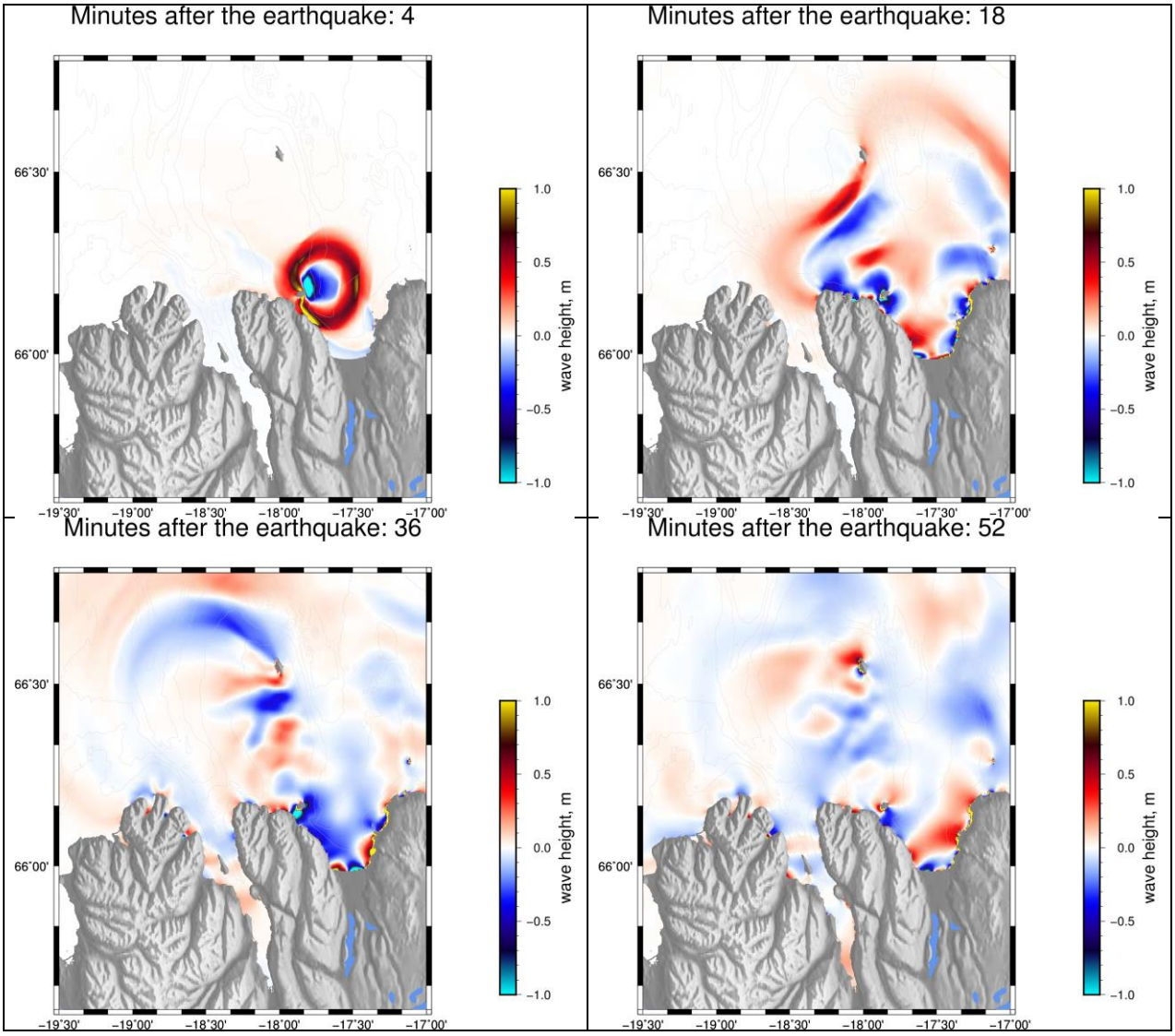

Figure 3. Preliminary results showing snapshots for the estimated tsunami wave height (in meters) 4, 18, 36 and 52 minutes after the occurrence of the scenario M_w7.0 strike-slip earthquake (same as in Fig. 2) with a hypothetical large submarine landslide southeast of Flatey Island, resulting in significantly larger wave heights.

For the two scenarios above, i.e., the earthquake-only and the combined earthquake and submarine landslide scenarios, we extracted the evolution of the wave heights at three locations shown in Figure 1: Akureyri, Dalvík, and Ólafsfjörður. Figure 4 shows the tsunami wave-height timeseries at these locations. The waveforms are quite different from one location to another showing the highest frequency response in Ólafsfjörður and the lowest for Akureyri. This demonstrates the importance of taking the local morphology and coastline structure into account, as the response in populated areas is complex and varies strongly between events and locations. Despite the large difference between the two scenarios presented here, however, the frequency response at each location is rather similar, with higher frequency waves predicted at Ólafsfjörður and Dalvík, but lower frequency swells in Akureyri (Fig. 4).

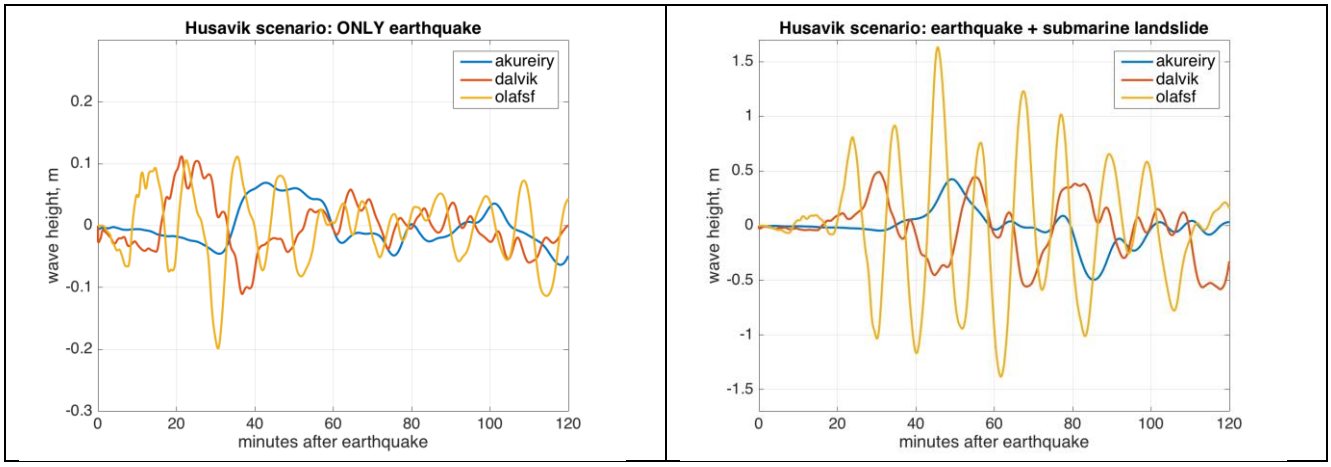

Figure 4. Synthetic tide-gauge signals for Akureyri, Dalvík, and Ólafsfjörður (locations shown in Fig. 1) for the two tsunami simulation scenarios presented in Figs. 2 and 3. The largest total amplitude (crest to valley) for the first case is only about 30 cm, while for the combined simulation it is about 2.5 m.

In addition to the two scenarios presented above, we added a third scenario to study possible tsunami effects of a small near-shore sudden landslide movement at a location that appears to be unstable, according to InSAR measurements (*Drouin and Sigmundsson*, 2019). The location of this landslide is in Skálavík, directly across the Skjálfandi Bay from Húsavík. We estimate the total volume of the landslide ~8.35□10^6 m^3 from the size of the area that appears unstable in the InSAR data. The perturbation is modeled as a simple gaussian function, emulating an abrupt landslide movement into the bay. The resulting tsunami wave heights are in Figure 5 showing that the first wave arrives in Húsavík about 15 minutes after the perturbation and that it is only of small magnitude.

The aim of these preliminary exercises is to assess the wave heights of possible tsunami in Húsavík due to a large earthquake. The results show that the waves exhibit a rather complex behavior as they propagate around the north-pointing peninsulas of North Iceland. They are quite different for each fjord and future work could lead to identification of hotspots prone to enhanced wave heights. The results presented here are preliminary and should by no means be used for official hazard assessments or warnings. However, they indicate that it is important to study tsunamis in North Iceland further, look at more scenarios for obtaining an ensemble of possible tsunami heights, study submarine slumps and unstable coastal slopes, and combine all the new information such that it could be used for future hazard maps.

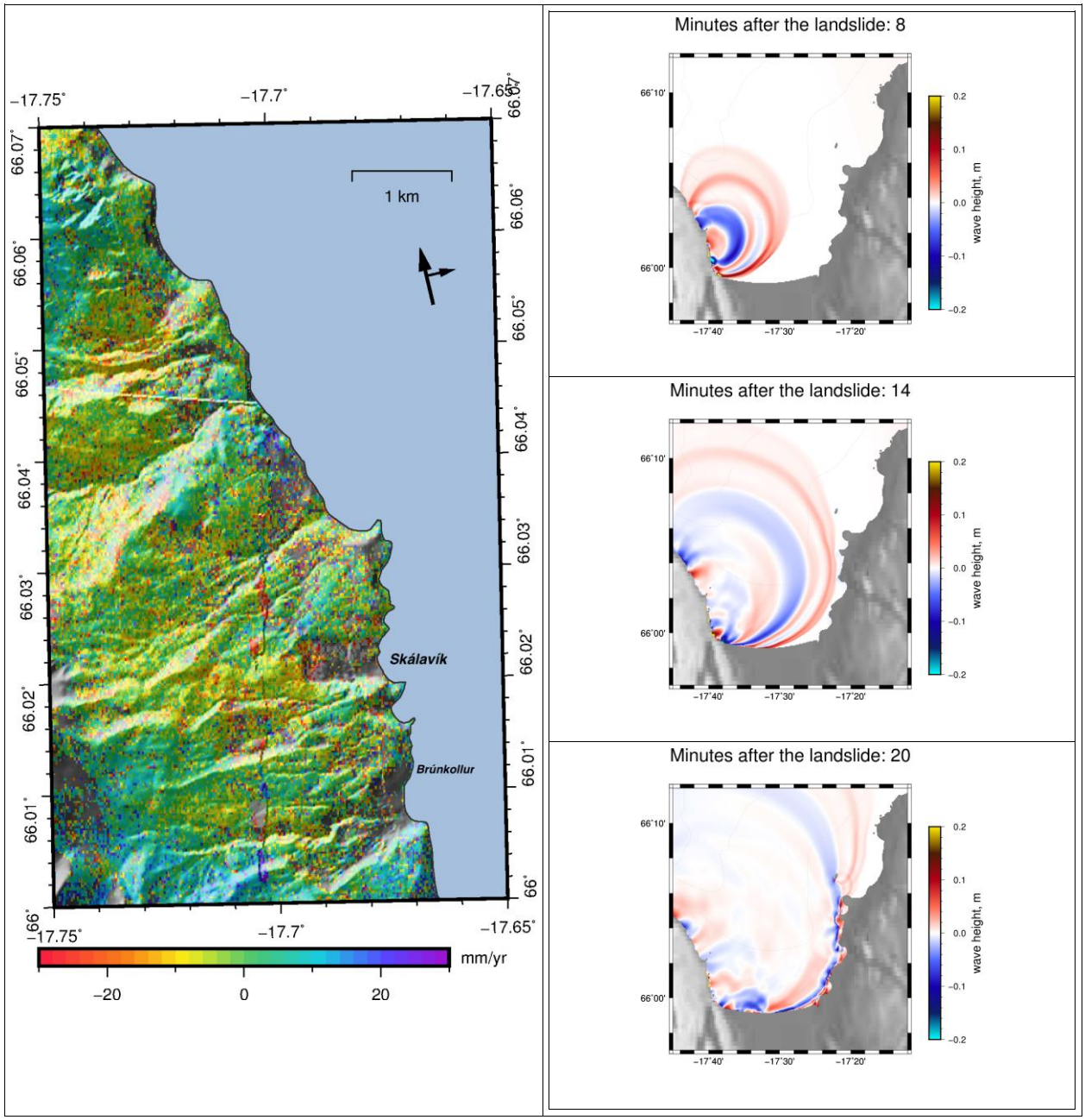

Figure 5. Left: InSAR image of Náttfaravíkur slopes, directly across the Skjálfandi bay from Húsavík, showing interferometric decorrelation in Skálavík and near Brúnkollur, likely due to too much landslide creep. Right: Three snapshots (at 8, 14, and 20 minutes) of the resulting simulated tsunami wave heights, with he waves arriving in Húsavík at about 15 minutes after the initiation of the tsunami by the landslide.

Acknowledgements

This project was partially supported by the project Æfingar v. náttúruvár.

References

Adriano, B., S. Hayashi, H. Gokon, E. Mas & S. Koshimura, Understanding the extreme tsunami inundation in Onagawa town by the 2011 Tohoku earthquake, its effects in urban structures and coastal facilities. *Coastal Eng. Journal*, **58**, 1640013-1 – 1640013-19, 2016.

Carvajal, M., C. Araya-Cornejo, I. Sepúlveda, D. Melnick & J.S. Haase, Nearly Instantaneous Tsunamis Following the Mw 7.5 2018 Palu Earthquake. *Geophys. Res. Lett.*, **46**, 5117-5126, 2019.

Cienfuegos, R., P. A. Catalán, A. Urrutia, R. Benavente, R. Aránguiz & G. González, What can we do to forecast tsunami hazards in the nearfield given large epistemic uncertainty in rapid seismic source inversions? *Geophys. Res. Lett.*, **45**, 4944-4955, 2018.

Drouin, V. & F. Sigmundsson, Monitoring slope instabilities with Sentinel-1 satellite interferometry, In *Proceedings to the Northquake 2019 workshop*, 2019.

JRC Emergency Reporting - Activation #021 - 28 Sep 2018. European Commission, Joint Research Centre.

LeVeque, R. J., D. L. George & M. J. Berger, Tsunami modelling with adaptively refined finite volume methods. *Acta Numerica*, **20**, 211–289, 2011.

Magnúsdóttir, S., B. Brandsdóttir, N. Driscoll & R. Detrick, Postglacial tectonic activity within the Skjálfandadjúp basin, Tjörnes Fracture Zone, offshore Northern Iceland, based on high resolution seismic stratigraphy, *Marine Geology*, **367**, 159-170, 2015.

Melgar, D. & Y. Bock, Near-field tsunami models with rapid earthquake source inversions from land-and ocean-based observations: The potential for forecast and warning, *J. Geophys. Res.*, **118**, 5939–5955, 2013.

Melgar, D. & A. Ruiz-Angulo, Long-lived tsunami edge waves and shelf resonance from the M8.2 Tehuantepec earthquake. *Geophys. Res. Lett.*, **45(12)**, 414– 421, 2018.

Metzger, S. & S. Jónsson, Plate boundary deformation in North Iceland during 1992-2009 revealed by InSAR time-series analysis and GPS, *Tectonophysics* **634**, 127-138, 2014.

Mori, N., T. Takahashi, T. Yasuda & H. Yanagisawa, Survey of 2011 Tohoku earthquake tsunami inundation and run-up, *Geophys. Res. Lett.*, **38**, 2011.

Stefánsson R., G.B. Gudmundsson & P. Halldórsson, Tjörnes fracture zone. New and old seismic evidences for the link between the North Iceland rift zone and the Mid-Atlantic ridge, *Tectonophysics* **447**, 117-126, 2008.

Thorgeirsson, Ó., *Historical earthquakes in North Iceland* (in Icelandic), Húsavík Academic Centre, 54pp, 2011.

Pakoksung, K., A. Suppasri, F. Imamura, C. Athanasius, A. Omang & A. Muhari, A., 2019. Simulation of the submarine landslide tsunami on 28 September 2018 in Palu Bay, Sulawesi Island, Indonesia, using a two-layer model. *Pure and Applied Geophys.*, 1-28, 2019.

NORTHQUAKE 2019 - The 3rd International Workshop on Earthquakes in North Iceland
Húsavík, North Iceland, 21-24 May 2019

ON THE SCALING OF EARTHQUAKE STRONG-MOTION IN NORTH ICELAND

Benedikt Halldórsson[1,2], Tim Sonnemann[1,2], Milad Kowsari[1], Sahar Rahpeyma[1], Birgir Hrafnkelsson[3], and Sigurjón Jónsson[4]

[1]*Faculty of Civil and Environmental Engineering, School of Engineering and Natural Sciences, and Earthquake Engineering Research Centre, University of Iceland (UI) (skykkur@hi.is, tsonne@hi.is, milad@hi.is, sahar@hi.is)*
[2]*Division of Processing and Research, Icelandic Meteorological Office (benedikt@vedur.is, tim@vedur.is)*
[3]*School of Engineering and Natural Sciences, University of Iceland (birgirhr@hi.is)*
[4]*King Abdullah University of Science and Technology (KAUST), Saudi Arabia (sigurjon.jonsson@kaust.edu.sa)*

Empirical ground motion models (GMM) are relatively simple equations that predict peak earthquake ground motion parameters that serve as a guide for the earthquake resistant design of structures. Therefore, they find their practical applications in probabilistic seismic hazard assessments (PSHA) where their simple form makes such calculations very cost effective and expedient. Previous seismic hazard studies for Iceland have relied on either a single theoretical GMM using (at the time, even more limited) local data from the SISZ (*Ólafsson and Sigbjörnsson*, 1999; *Ólafsson et al.*, 2001), a regional European empirical GMM (*Ambraseys et al.*, 2005), or several GMMs recommended for use in oceanic crustal regions (e.g., *Delavaud et al.*, 2012 in the harmonization of seismic hazard assessment in Europe, SHARE project). However, the incapability of GMMs from other regions in describing the attenuation of Icelandic earthquake peak ground motion or spectral response parameters has conclusively been confirmed, underpredicting in the near-fault region and overpredicting in the far-field (*Ólafsson and Sigbjörnsson*, 2004, 2006; *Ornthammarath et al.*, 2011; *Kowsari et al.*, 2019a, b; *Kowsari, 2019; Sonnemann*, 2019) (see Fig. 1).

Currently there exists a large collection of empirical GMMs for peak ground motions from earthquakes in shallow crustal interplate regions worldwide (*Abrahamson and Shedlock*, 1997; Douglas 2003, 2018; Abrahamson et al. 2008). A common trend is a deviation from self-similar scaling at larger magnitudes, in particular at near-fault distances. In part, this is caused by the recording sites being in proximity of the earthquake fault so that progressively smaller parts of the earthquake fault contribute to the peak motions of the ground motion recordings (e.g., *Halldorsson and Papageorgiou*, 2012). For that reason, the criteria for the inclusion of GMMs in PSHA for such regions is, among other things, that the functional forms must be able to account for the saturation of amplitudes with increasing magnitudes (non-self-similar scaling) and/or near-fault magnitude-dependent distance scaling (*Cotton et al.*, 2006; *Bommer et al.*, 2010). The strong earthquakes in the interplate transform zones of Iceland are indeed shallow, and any GMMs for use in PSHA for Iceland needs to account for such characteristics.

For the above reasons, new GMMs for Iceland are needed that (1) enable the non-self-similar scaling of ground motions, including magnitude-distance dependent saturation in the near-fault region, and (2) account for the uniquely rapid attenuation of peak parameters of ground motion or spectral response Iceland. In addition, (3) we need to avoid directly using large-magnitude data from other regions due to the abovementioned issues, and since the effects of regional attenuation and the desired deviation from self-similar scaling or magnitude-dependent saturation in the near-fault region have not

been decoupled. Therefore, we have addressed this issue in a novel way by considering several GMMs for peak ground acceleration (PGA) and 5%-damped pseudo-spectral acceleration (PSA) that have functional forms that satisfy the minimum requirements (*Kowsari et al.*, 2019b; *Kowsari*, 2019; *Sonnemann*, 2019). To remove their bias to Icelandic earthquake ground motions we recalibrated them to fit the Icelandic data in the context of the Bayesian statistical framework, where model inference was carried out using a Markov Chain Monte Carlo (MCMC) algorithm and random effects to partition the aleatory variability into inter-event and intra-event components (*Kowsari et al.*, 2019a). For the inference, we used both non-informative (i.e., traditional) and informative priors for selected model coefficients from the original GMMs. The new Bayesian GMMs inferred using non-informative prior density results in models having very poorly determined coefficients that control magnitude and/or magnitude-distance scaling. In other words, they cannot be trusted outside the magnitude range of the data (see Fig. 2, left). On the contrary, the Bayesian models inferred using informative priors for those coefficients from the original models now compensate for the lack of constraints from the local data by providing the desired and selective guidance from the ground motion behaviour from other regions (see Fig. 2, right).

Using informative priors for magnitude scaling and magnitude-distance scaling terms of the original models has resulted in models that not only capture the high near-fault amplitudes and rapid ground motion attenuation with distance in Iceland, but also introduce a controlled saturation of large magnitude ground motions, which is consistent with observations in other interplate regions where shallow crustal earthquakes occur. These Bayesian models using informative priors thus form a suite of new, essentially hybrid, empirical GMMs that can be used with confidence in predicting PGA and PSA for Icelandic earthquakes, in particular for the reassessment of the seismic hazard of Iceland.

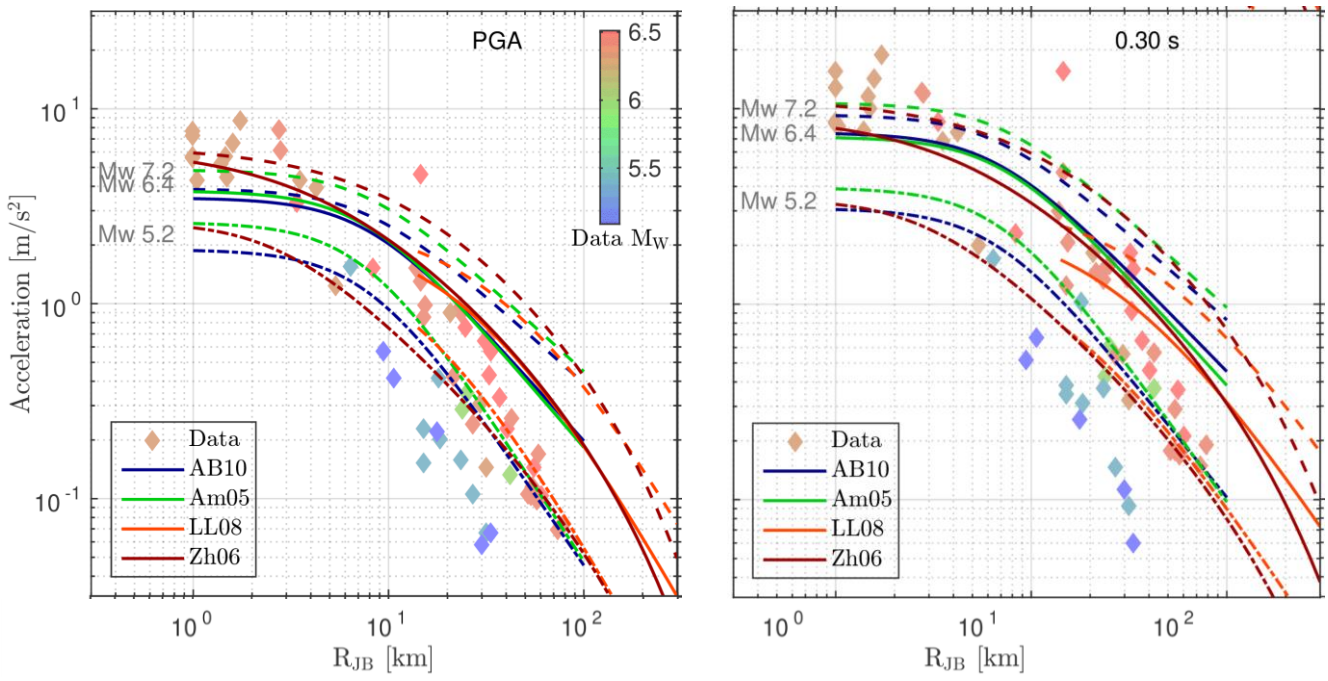

Figure 1. The attenuation of selected ground motion models for PGA and PSA at 0.3 s on rock, that have been recommended and used for PSHA in Iceland. The models are evaluated at M_w 5.2 (dash-dotted line), 6.4 (solid line) and 7.2 (dashed line). The M_w 6.4 is the weighted average magnitude of the last three large earthquakes in Iceland that account for the majority of the data. The rotation-invariant observed data are shown as color-coded diamonds by magnitude (from Kowsari et al., 2019b).

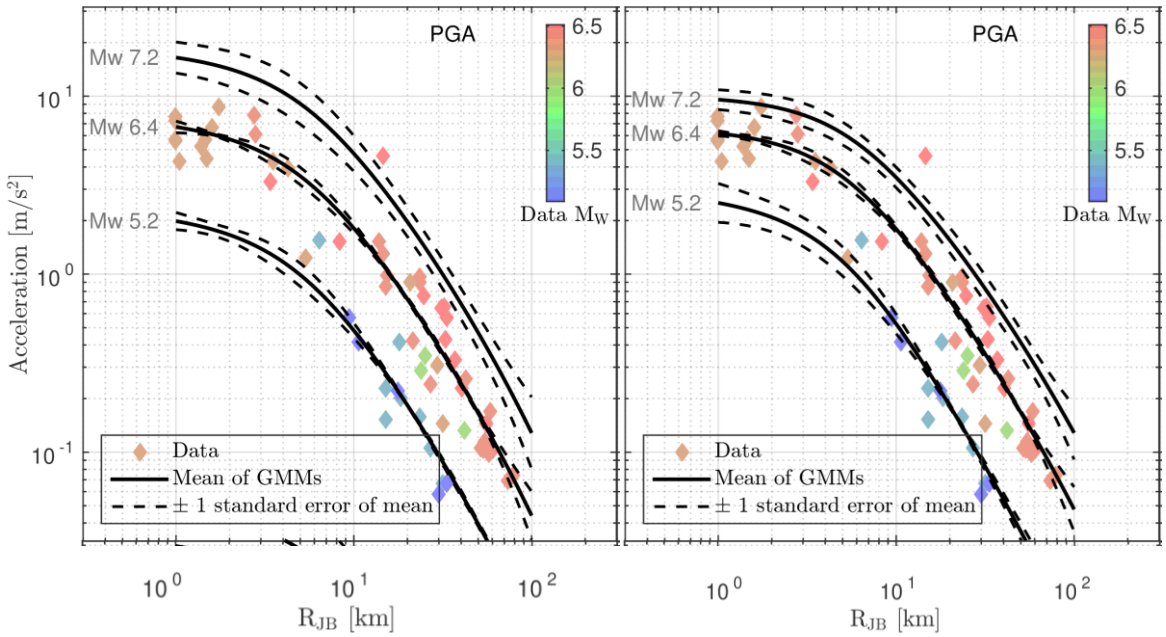

Figure 2. The mean of the non-informative Bayesian model predictions if PGA along with the ± 1 standard error of the mean vs. the observed data, shown as diamonds color-coded by magnitude. The mean of the Bayesian models using non-informative priors is shown on the left, while those using informative priors for selected parameters from other regions is shown on the right (from Sonnemann, 2019).

References

Ambraseys N.N., J. Douglas, S.K. Sarma & P.M. Smit, Equations for the estimation of strong ground motions from shallow crustal earthquakes using data from Europe and the Middle East: horizontal peak ground acceleration and spectral acceleration. *Bull. Earthquake Eng.* **3**, 1–53, 2005.

Bommer J.J., J. Douglas, F. Scherbaum et al., On the selection of ground-motion prediction equations for seismic hazard analysis. *Seismol. Res. Lett.* **81**, 783–793, 2010.

Cotton F, F. Scherbaum, J.J. Bommer & H. Bungum, Criteria for selecting and adjusting ground-motion models for specific target regions: Application to central Europe and rock sites. *J. Seismol.* **10**, 137–156, 2006.

Delavaud E, F. Cotton, S. Akkar et al., Toward a ground-motion logic tree for probabilistic seismic hazard assessment in Europe. *J. Seismol.* **16**, 451–473, 2012.

Kowsari M., *Bayesian Inference of Empirical Ground Motion Models to Icelandic Strong-motions and Implications for Seismic Hazard Assessment.* Ph.D. Dissertation, University of Iceland, 2019.

Kowsari M, B. Halldorsson, B. Hrafnkelsson et al., Calibration of ground motion models to Icelandic peak ground acceleration data using Bayesian Markov Chain Monte Carlo simulation. *Bull. Earthquake Eng.* **17,** 2841-2870, 2019a.

Kowsari M, T. Sonnemann, B. Halldorsson et al., Bayesian Inference of Empirical Ground Motion Models to Pseudo-Spectral Accelerations of South Iceland Seismic Zone Earthquakes based on Informative Priors. *Bull. Earthquake Eng.* (in review), 2019b.

Ólafsson S, S. Remseth & R. Sigbjörnsson, Stochastic models for simulation of strong ground motion in Iceland. *Earthquake Eng. Struct. Dyn.* **30**, 1305–1331, 2001.

Ólafsson S. & R. Sigbjörnsson, A theoretical attenuation model for earthquake-induced ground motion. J. Earthquake Eng., **3**, 287–315, 1999.

Ólafsson S. & R. Sigbjörnsson, Attenuation in Iceland compared with other regions. In: *First European Conference on Earthquake Engineering and Seismology (1ECEES)*. Geneva, Switzerland, paper no. 1157, 2006.

Ólafsson S. & R. Sigbjörnsson, Attenuation of strong ground motion in shallow earthquakes. In: *13th World Conference on Earthquake Engineering (13WCEE).* Vancouver, B.C., Canada, paper no. 1616, 2004.

Ornthammarath T, J. Douglas, R. Sigbjörnsson & C.G. Lai, Assessment of ground motion variability and its effects on seismic hazard analysis: A case study for Iceland. *Bull. Earthquake Eng.* **9**, 931–953, 2011.

Sonnemann T., *Earthquake Source Modelling and Broadband Ground Motion Simulation in South Iceland for Earthquake Engineering Applications*. Ph.D. Dissertation, University of Iceland, 2019.

NORTHQUAKE 2019 - The 3rd International Workshop on Earthquakes in North Iceland
Húsavík, North Iceland, 21-24 May 2019

SENSITIVITY ANALYSIS OF SEISMICITY PARAMETERS AND GROUND MOTION MODELS USED IN PSHA TO ITS INPUT ASSUMPTIONS: A CASE STUDY OF HÚSAVÍK, NORTH ICELAND

Milad Kowsari[1], Benedikt Halldórsson[1,2], Nasrollah Eftekhari[3], Jónas Þór Snæbjörnsson[4], and Sigurjón Jónsson[5]

[1]*Earthquake Engineering Research Centre & Faculty of Civil and Environmental Engineering, School of Engineering and Natural Sciences, University of Iceland, Selfoss, Iceland (milad@hi.is)*
[2]*Division of Processing and Research, Icelandic Meteorological Office, Reykjavik, Iceland (skykkur@hi.is)*
[3]*Faculty of Technology and Mining, Yasouj University, Choram, Iran (sn.eftekhari@gmail.com)*
[4]*School of Science and Engineering, Reykjavík University, Iceland (jonasthor@ru.is)*
[5]*King Abdullah University of Science and Technology (KAUST), Saudi Arabia (sigurjon.jonsson@kaust.edu.sa)*

Inputs to probabilistic seismic hazard analysis (PSHA) generally contain large uncertainties that significantly affect the hazard assessment results. These uncertainties can be identified and quantified for all the inputs of PSHA, including for the characteristics of seismic sources, the recurrence model described by seismicity parameters and the selection of ground motion models (GMMs). The input parameters should be analysed to evaluate the sensitivity of PSHA to their variability. This case-study deals with North Iceland, one of the most active seismic zones in north-western Europe, where earthquake data is affected by significant uncertainties in magnitude, location and occurrence time. Sensitivity analysis (SA) can be performed to study, either qualitatively or quantitatively, how changes in the model inputs affect the model response, thus revealing the sources of variability and help prioritizing efforts to reduce them. SA methods are generally categorized as either local or global. In local analysis, the change of the model output due to small perturbations of the inputs at a reference point is quantified by varying a certain input variable in a local area while keeping the other variables fixed. On the other hand, global SA methods aim to quantify the influence of uncertain inputs on the model response by apportioning the output variability to the variability of the inputs over their entire range of variations.

This study presents a global information-theoretic sensitivity analysis to investigate the influence of uncertainties in the seismicity parameters and GMMs on site-specific PSHA results for Húsavík, North Iceland. Fast computation time is considered as one of the major advantages of the information-theoretic approach compared to the common global SA methods. In this study, the parameters of the Gutenberg–Richter relationship (a- and b-values), the earthquake magnitude limits ($m_{\min}$ and $m_{\max}$), and GMMs for three segments of the Húsavík-Flatey Fault (HFF) were analysed in terms of the influence of their respective uncertainties on the variability of PSHA results. Two sets of GMMs were used in this study to demonstrate the effect of choice of model on the epistemic uncertainty. The first set includes GMMs proposed by *Akkar and Bommer* (2010), AB10; *Zhao et al.*, (2006), Zh06; *Lin and Lee* (2008), LL08 and *Ambraseys et al.*, (2005), Am05, all of which satisfy the criteria proposed by *Cotton et al.*, (2006) and *Bommer et al.*, (2010). The first two GMMs were proposed in the harmonization of seismic hazard assessment in Europe (SHARE) project as suitable GMMs for PSHA in tectonically-active regions on oceanic crust. The LL08 is another GMM that was used in the SHARE project and was also

chosen here due to the difference in its functional form. The Am05, which was obtained from European and Middle Eastern dataset, was also selected here because it has been applied in several seismic hazard studies in Iceland. The second set contains recalibrated versions of these GMMs to the Icelandic dataset of earthquake strong motion (*Kowsari et al.*, 2019).

Fig. 1 shows the results of a global SA of PSHA for Húsavík based on the three segments of the HFF, representing the relative contribution of each input parameter to the PSHA outputs. The hazard was assessed for PGA on a rock site with 2% and 10% probability of exceedance in 50 years.

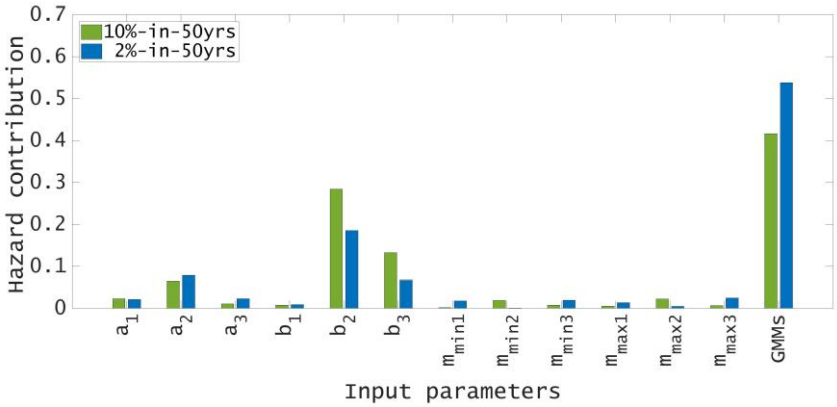

Figure 1. Relative contributions of the input parameters to the PSHA outputs of Húsavík at two hazard levels based on a three-segment representation of the Húsavík-Flatey Fault.

The SA clearly identifies the GMMs and the slope of the G–R relationship (i.e., the b-value) as the key controlling inputs that dominate the variability in the PSHA for the region under study. The a-value and the earthquake magnitude limits are less influential. In addition, we found that the degree of influence depends on the location of the site for which the hazard is assessed. We note that our study focuses only on the variability due to the seismicity parameters and GMMs. It is therefore important to extend this study to more advanced seismic source models and fault parameters, as well as incorporating near-fault effects on PSHA results. Furthermore, more emphasis needs to be put on spatial SA by presenting regional hazard maps for other ground motion parameters, such as spectral acceleration for a 5% damping ratio over the periods of engineering interest.

References

Akkar, S. & J.J. Bommer, Empirical equations for the prediction of PGA, PGV, and spectral accelerations in Europe, the Mediterranean region, and the Middle East, *Seismol. Res. Lett.* **81**,195–206, 2010.

Ambraseys, N.N., J. Douglas, K.K. Sarma & P.M. Smit, Equations for the estimation of strong ground motions from shallow crustal earthquakes using data from Europe and the Middle East: horizontal peak ground acceleration and spectral acceleration, *Bull. Earthquake Eng.* **3**, 1–53, 2005.

Bommer, J.J., J. Douglas, F. Scherbaum et al., On the selection of ground-motion prediction equations for seismic hazard analysis, *Seismol. Res. Lett.* **81**, 783–793, 2010.

Cotton, F., F. Scherbaum, J.J. Bommer & H. Bungum, Criteria for selecting and adjusting ground-motion models for specific target regions: Application to central Europe and rock sites, *J. Seismol.* **10**, 137–156, 2006.

Kowsari, M., B. Halldorsson, B. Hrafnkelsson, J. Snæbjörnsson & S. Jónsson, Calibration of ground motion models to Icelandic peak ground acceleration data using Bayesian Markov Chain Monte Carlo simulation, *Bull. Earthquake Eng.* **17**, 2841-2870, 2019.

Lin, P.S. & C.T. Lee, Ground-motion attenuation relationships for subduction-zone earthquakes in northeastern Taiwan, *Bull. Seismol. Soc. Am.* **98**, 220–240, 2008.

Zhao, J.X., J. Zhang, A. Asano et al., Attenuation relations of strong ground motion in Japan using site classification based on predominant period, *Bull. Seismol. Soc. Am.* **96**, 898–913, 2006.

NORTHQUAKE 2019 - The 3rd International Workshop on Earthquakes in North Iceland
Húsavík, North Iceland, 21-24 May 2019

SITE EFFECT ESTIMATION ON TWO ICELANDIC STRONG-MOTION ARRAYS USING A BAYESIAN MULTI-LEVEL MODEL FOR THE SPATIAL DISTRIBUTION OF EARTHQUAKE GROUND MOTION AMPLITUDES

Sahar Rahpeyma[1], Benedikt Halldórsson[2], Birgir Hrafnkelsson[3], and Sigurjón Jónsson[4]

[1]*Faculty of Civil and Environmental Engineering, University of Iceland (sahar@hi.is)*
[2]*Earthquake Engineering Research Centre, University of Iceland & Icelandic Meteorological Office (skykkur@hi.is)*
[3]*School of Engineering and Natural Sciences, University of Iceland (Birgirhr@hi.is)*
[4]*King Abdullah University of Science and Technology (KAUST), Saudi Arabia (sigurjon.jonsson@kaust.edu.sa)*

Better understanding of seismic ground motion characteristics literally leads to more accurate early-stage damage assessments and seismic risk mitigation. In Iceland, regardless of complex geological features that may exist at depth, the rock site characterization is typically used for earthquake engineering applications as recent volcanic lava-rock or older bedrock are exposed in many places. The corresponding site amplification is expected to be low and uniform in these regions; however, recent ground motion data collected on two small-aperture strong-motion arrays in south and north Iceland (ICEARRAY I and ICEARRAY II, respectively) exhibit considerable variations in the spatial distribution of ground-motion amplitudes. In this study, we implement the Bayesian Hierarchical Model (BHM) developed by *Rahpeyma et al.* (2018) to establish the regional geological influence on site responses for peak ground acceleration (PGA) as well as spectral acceleration (PSA) for periods of interest. A capable posterior inference scheme based on Markov chain Monte Carlo (MCMC) simulations is used to sample from the posterior density of the proposed model. BHM allows us to model the spatial distribution of ground motion amplitudes and also to quantify the associated uncertainties. The BHM shows quantitatively to what extent the respective source, path and site effects contribute to the overall variability of ground motion across the arrays (*Rahpeyma et al.*, 2018).

We implement the strong-motion data recorded on the dense urban strong-motion array in Hveragerði (ICEARRAY I) during the 29 May 2008, M_w6.3 Ölfus earthquake and its aftershocks in South Iceland, which showed considerable variation in ground-motion amplitudes recorded on multiple stations over a small area. This variation is of particular interest because ICEARRAY I is mainly located on lava-rock while the geological strata beneath the array is described as recurring piles of basaltic lavas with intermediate layers of sediments leading to strong “velocity reversals”. This is the case in Hveragerði and large parts of the South Iceland Fracture Zone where in addition the topography is roughly flat but covered by lava flows. Similarly, during the earthquake sequences in North Iceland in 2012-2013 significant variation of earthquake strong-motion amplitudes were observed on the dense urban strong-motion array in Húsavík (ICEARRAY II). Contrary to ICEARRAY I, the geologic profile and topography varies significantly across ICEARRAY II.

The multi-level BHM used in this study for the spatially distributed data consists of three levels i.e., data level, latent level and hyperparameter level. The observed log-scale PGA and PSA are modeled at the data level of the BHM as a function of model parameters. The latent level describes the distribution

of the latent parameter some of which are found in the distributional model of the observations. The joint distribution of the latent parameters is conditioned on the parameters in the hyperparameter level; these parameters are referred to as hyperparameters. A typical hyperparameter is a standard deviation of the distribution describing the corresponding latent parameter. The basic model for the prediction of a ground-motion parameter Y dependent on source, path and site parameters as Eq. (1):

$$Y_{es} = \mu_{es}(M_e, R_{es}, D_e) + \delta B_e + \delta S_s + \delta WS_{es} + \delta R_{es}, \quad e = 1, \dots, N, \qquad s = 1, \dots, Q \tag{1}$$

The subscripts e and s represent event and station, respectively. Y_{es} is the strong-motion parameter of interest for earthquake e recorded at station s. The predictive model, μ_{es}, is a function of independent variables for event e at station s. δB_e is the inter-event quantifying the systematic deviation of observed ground motions associated to an event e with respect to the ground motion model (GMM) prediction. δS_s is the site-term for station s, which can be used to scale the GMM prediction to a site-specific prediction. The spatially correlated event-station specific term, δWS_{es}, captures record-to-record variability (combination of e and s). δR_{es}, called as unexplained terms and accounts for effects that are not modeled by the other terms. We define the GMM as a linear predictive function of independent variables including the local magnitude of event e, M_e; hypocentral distance from event e to station s, R_{es}; and the hypocentral depth of event e, D_e. The GMM has the simple and common functional form as Eq. (2):

$$\mu_{es} = \beta_1 + \beta_2 M_e + \beta_3 \log R_{es} + \beta_4 D_e \tag{2}$$

Where $\boldsymbol{\beta}$ is the vector of the regression coefficients of the ground motion models (more details can be found in *Rahpeyma et al.*, 2018, 2019). Effectively, the total aleatory variability, σ^2_{total}, of the GMM presented in Eq. (1) can be quantified with the variance of the sum of the independent terms:

$$\sigma^2_{total} = \tau^2 + \phi^2_{S22} + \phi^2_{SS} + \phi^2_R \tag{3}$$

The inter-event variance (τ^2) quantifies the variation between events relative to the average ground motion level predicted by the GMM for each event. The inter-station variance (ϕ^2_{S2S}) quantifies the variability between stations, which then is primarily a manifestation of the localized variations such as the geological profiles beneath the stations. The event-station variance (ϕ^2_{SS}) can be defined as a measure of the spatial variability in the ground-motion amplitudes between stations within an event after taking into account the event and station terms. The purpose of this term is to quantify the remaining variations not already captured by the GMM or the event and station terms (i.e., a proxy for path effects). Finally, the unexplained term variance (ϕ^2_R) quantifies the variability in the measurement errors and other deviations that are not accounted for by other terms of the model. In this study, the BHM model is developed for the following ground-motion parameters of interest: PGA and PSA at nominated periods $T =$ 0.05, 0.10, 0.15, 0.20, 0.25, 0.30, 0.40, 0.50, 1.00, 2.00, 3.00 sec.

The results signify that site effects can dominate the spatial distribution of ground-motion parameters observed across both ICEARRAY I and ICEARRAY II. Although the site conditions across ICEARRAY I have been characterized as uniform "rock" with a relatively flat topography, station terms, ϕ_{S2S}, contribute $\sim 13\%$ to the total variability in the amplitudes of predicted ground motions across the array. In contrast to ICEARRAY I, the variation of the geologic profiles and topography is much greater across ICEARRAY II. As a result, the inter-station variability is shown to contribute up to $\sim 57\%$ of the total variability in the amplitudes of predicted ground motions across the array, with the contributions

being less constrained for ICEARRAY II than ICEARRAY I due to the relative sizes of the recorded ground motion databases. The station terms serve as indicators to what extent the ground motion amplitude can be expected to be either higher or lower than the mean over the array. Fig. 1 compares the posterior distributions of the station terms for ICEARRAY I & II.

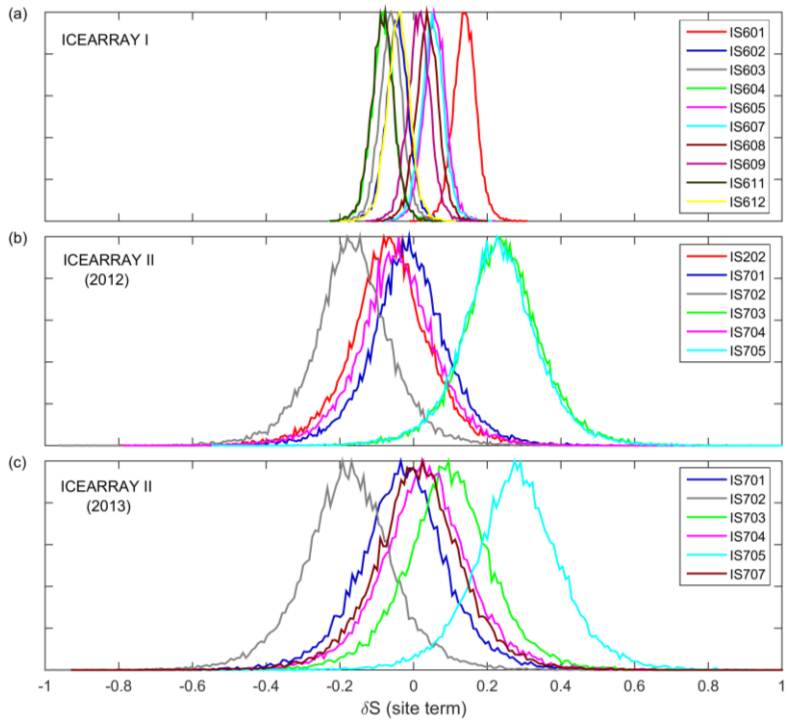

*Figure 1. Posterior distributions of station terms, **δS**, for ICEARRAY I (a) and ICEARRAY II 2012 and 2013 sequences (b and c, respectively) using MCMC simulations. (Adopted from Rahpeyma et al., 2019).*

For ICEARRAY I, the narrow posterior intervals all in the range of $0.0322 - 0.0325$ indicate that the station terms are well constrained. In contrast, the posterior distributions of ICEARRAY II have about three times larger posterior standard deviations in the range $0.1126 - 0.1298$. This is consistent with our expectation that for a relatively uniform rock site condition across Hveragerði the corresponding station terms should be relatively low with relatively narrow marginal posterior distributions. On the contrary, a larger range covered by station terms is expected where geologic profiles and topography vary considerably, along with relatively wider posterior distributions, determined from a relatively small dataset. It is worth mentioning that the different widths are likely due to a large dataset for ICEARRAY I.

On the other hand, a detailed site-effect investigation using the frequency dependent horizontal-to-vertical spectral ratio (HVSR) using ICEARRAY I recordings revealed that while the amplification levels remain relatively low, the predominant frequency varies systematically between stations and is found to correlate with geological units beneath the ICEARRAY I strong-motion stations (see *Rahpeyma et al.*, 2016, 2017 for more details). In particular, where the amplification curve is characterized by two clear predominant frequencies at (lower) 3-4 Hz and (higher) 8-9 Hz and relatively large amplitudes, clearly suggests the presence of two significant and sharp velocity contrasts underneath the station (e.g., station IS605 in Fig. 2).

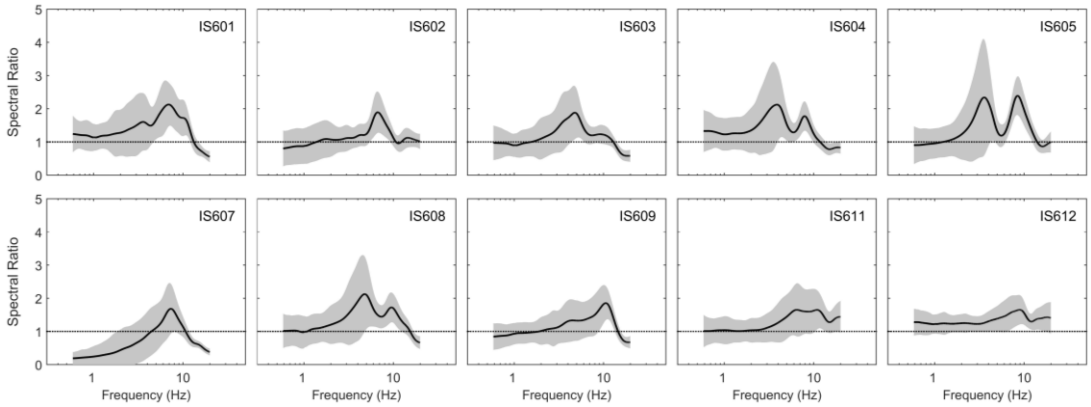

Figure 2. Mean HVSR$\pm\mathbf{1}\boldsymbol{\sigma}$ from earthquake data for ICEARRAY I stations located on lava-rock in Hveragerði, South Iceland. (Black solid and shaded area show mean HVSR and mean HVSR$\pm\mathbf{1}\boldsymbol{\sigma}$ from earthquake data).

As can be seen in Fig. 3, close to the resonance frequencies (i.e., 3-4 Hz and 8-9 Hz) the inter-station variabilities show larger mean values as well as larger associated uncertainties due to the resonance phenomenon that we observed in some stations such as IS604, IS605 and IS608.

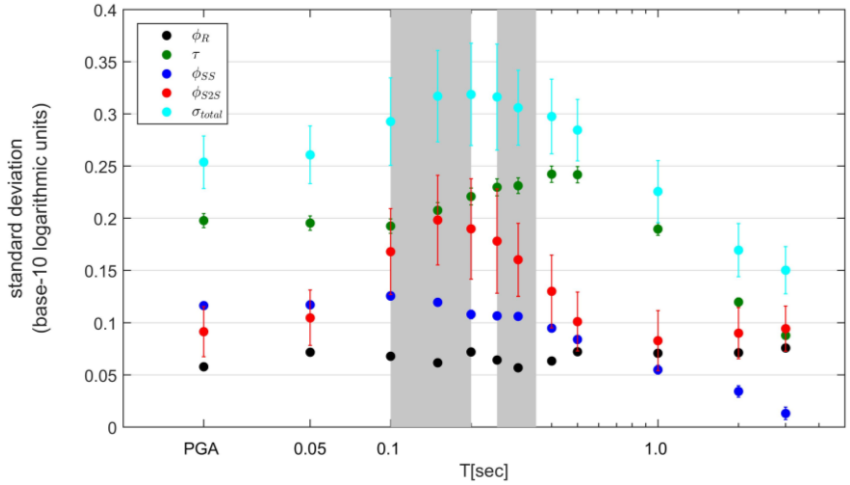

Figure 3. Comparing inter-event ($\boldsymbol{\tau}$), inter-station ($\boldsymbol{\phi_{S2S}}$), event-station ($\boldsymbol{\phi_{SS}}$), unexplained ($\boldsymbol{\phi_R}$) standard deviations and total standard deviation ($\boldsymbol{\sigma_{total}}$) for PGA and PSA. Error bars show the standard deviation of the posterior distribution. Gray areas indicate the resonance frequencies (3-4 Hz and 8-9 Hz) observed in some stations across ICEARRAY I.

The BHM used in this study provides quantitative information about the frequency dependence of site and geological effects. Hence, the results therefore have direct practical implications and importance for improved microzonation of earthquake hazard across the town. Consequently, this will enable a more optimal earthquake resistant design of structures as well as better urban planning.

References

Rahpeyma, S., B. Halldorsson & R.A. Green, On the distribution of earthquake strong-motion amplitudes and site effects across the Icelandic strong-motion arrays, In *Proc. to the 16th World Conference on Earthquake Engineering (16WCEE)*, Santiago, Chile, paper no. 2762, 2017.

Rahpeyma, S., B. Halldorsson, B. Hrafnkelsson, R.A. Green & S. Jónsson, Site effect estimation on two Icelandic strong-motion arrays using a Bayesian hierarchical model for the spatial distribution of earthquake peak ground acceleration, *Soil Dyn. Earthq. Eng.* **120**, 369–385, 2019.

Rahpeyma, S., B. Halldorsson, B. Hrafnkelsson & S. Jónsson, Bayesian hierarchical model for variations in earthquake peak ground acceleration within small-aperture arrays, *Environmetrics* **29**, e2497, 2018.

Rahpeyma, S., B. Halldorsson, C. Olivera, R.A. Green, S. Jónsson, Detailed site effect estimation in the presence of strong velocity reversals within a small-aperture strong-motion array in Iceland, *Soil Dyn. Earthq. Eng.* **89**, 136–151, 2016.

NORTHQUAKE 2019 - The 3rd International Workshop on Earthquakes in North Iceland
Húsavík, North Iceland, 21-24 May 2019

MICROSEISMIC RESPONSE CHARACTERISTICS OF TYPICAL GRAVEL FILLS IN ICELAND USING HVSR AND SSR TECHNIQUES

Thomas J. Kennedy[1], Benedikt Halldórsson[2,3], Russell A. Green[1], Jónas Þór Snæbjörnsson[4], and Sahar Rahpeyma[2]

[1]*Virginia Tech, United States (kennedyt@vt.edu; rugreen@vt.edu)*
[2]*University of Iceland, Iceland (skykkur@hi.is; sahar@hi.is)*
[3]*Icelandic Meteorological Office, Iceland (benedikt@vedur.is)*
[4]*Reykjavík University, Iceland (jonasthor@ru.is)*

Seismic design of buildings and other structures is required in seismically active regions. Unfavorable underlying soil conditions may result in a higher seismic hazard and larger seismic loading on infrastructure. Over the past few decades, the degree of building damage in earthquakes has been correlated to the local geological and geotechnical site conditions. The influence of local site conditions on ground motions are quantified by site response characteristics (e.g., the predominant site frequency, short- and long-period relative amplification factors, etc.) determined by site investigative analysis techniques, such as the horizontal-to-vertical spectral ratio (HVSR) and the standard spectral ratio (SSR). This paper highlights the typical site response characteristics of the most prevalent subgrades for building foundations in Iceland, namely the compacted gravel fill placed by the removal and replacement method. To achieve this objective, this paper first describes the removal and replacement method, then the tenets of the HVSR and SSR techniques used for microseismic/tremor data analysis, and finally, concluding remarks about site response characteristics of compacted gravel fill in Iceland.

The removal and replacement method is one of the most conceptually simple site improvement methods in geotechnical engineering. Instead of improving the in-situ soils at a site, the approach entails the complete removal and replacement of unfavorable soils with more competent, compacted coarse-grained fill (e.g., sand and gravel). The benefits of compacted gravel fill regarding static loading are well known (e.g., to increase bearing capacity and reduce settlement). However, the literature about the dynamic site response characteristics of gravel fill is sparse, despite its widespread use in earthquake-prone regions. It is worth mentioning that most of the fill used throughout the Reykjavík capital region originates from Vatnskarðsnáma, a quarry south of the capital region. A photograph illustrating the placement of compacted gravel fill is shown in Fig. 1.

To determine the dynamic site response characteristics at a site, microseismic/tremor measurements are taken at various times before and after gravel fill placement. At one site, the in-situ condition (i.e., pre-excavation) revealed the site response characteristics of the unfavorable soils, while measurements taken post-excavation atop the base layer provided a baseline from which relative amplification values may be determined. Finally, measurements taken at the final grade of compacted gravel fill show the site response characteristics before building construction.

All microseismic/tremor vibrations were measured by tridirectional Lennartz LE-3D/5s seismometers and recorded by REF TEK 130-01 high-resolution broadband seismic data acquisition systems from the LOKI instrument bank. The sensors were collecting data at a rate of 100 Hz with high gain. Each seismometer was buried with nearby soil to reduce the chance and extent of unwanted

perturbation from the weather.

Figure 4. Installation of compacted gravel fill from a profile view at Lundur Site 1 in Kópavogur. The vibro-roller compaction method is shown atop gravel fill underlain by a dense to very dense silty sand base layer.

The HVSR and SSR techniques were used to analyze the microseismic/tremor measurements taken at various stages of the removal and replacement process. The HVSR technique, initially proposed by *Nogoshi and Igarashi* (1971) and later popularized by *Nakamura* (1989, 2000), is based on the ratio the Fourier amplitude spectra (FAS) of the combined microseismic/tremor horizontal (H) components to the vertical (V) component over a bandwidth of engineering significance (e.g., 0.3 Hz to 25 Hz). The horizontal components were combined by the geometric mean and smoothed by the *Konno and Ohmachi* (1998) procedure using a *b*-value of 20. The SSR technique proposed by *Borcherdt* (1970) estimates the site effects of local soil by the ratio of the combined horizontal FAS of site ground motions to the combined horizontal FAS of ground motions recorded on a nearby rock outcrop or base layer (bedrock) condition.

The HVSR and SSR signatures for Lundur Site 1 in Kópavogur are shown in Fig. 2. The signatures represent the average of all ~60-minute individual time periods recorded throughout each night. The standard deviation is shown to illustrate the variability across frequencies. The in-situ soil condition was not available for measurements at this site. Therefore, a typical in-situ HVSR signature taken at a nearby site in Breidholt (~2 km away) is included in Fig. 2(a) for comparison. As may be seen from Fig. 2(b), the HVSR signature at the base layer is indicative of a competent stratum free of any site amplification tendencies. The placement of compacted gravel fill resulted in an HVSR signature with a clear predominant frequency at ~16 Hz with a relative amplification value of ~4.3 (cf. Fig. 2(c)). The SSR signature for Lundur Site 1 presented in Fig. 2(d) illustrates similar, but slightly higher values as the HVSR method.

Although only one site is presented herein, signatures from other sites with compacted gravel fill have shown similar trends. The removal of in-situ soils and replacement with compacted gravel fill generally shifts the predominant site frequency from the mid-band frequency range (4 – 8 Hz) to the high-band frequency range (12 – 16 Hz) and, at these frequencies, increases the relative site amplification as fill thickness increases. However, it is questionable whether this trend also applies to conditions where undulating lava rock comprises the base layer, as found in Hafnarfjörður. Additional investigations of sites underlain by lava rock are being carried out to draw stronger empirical observations.

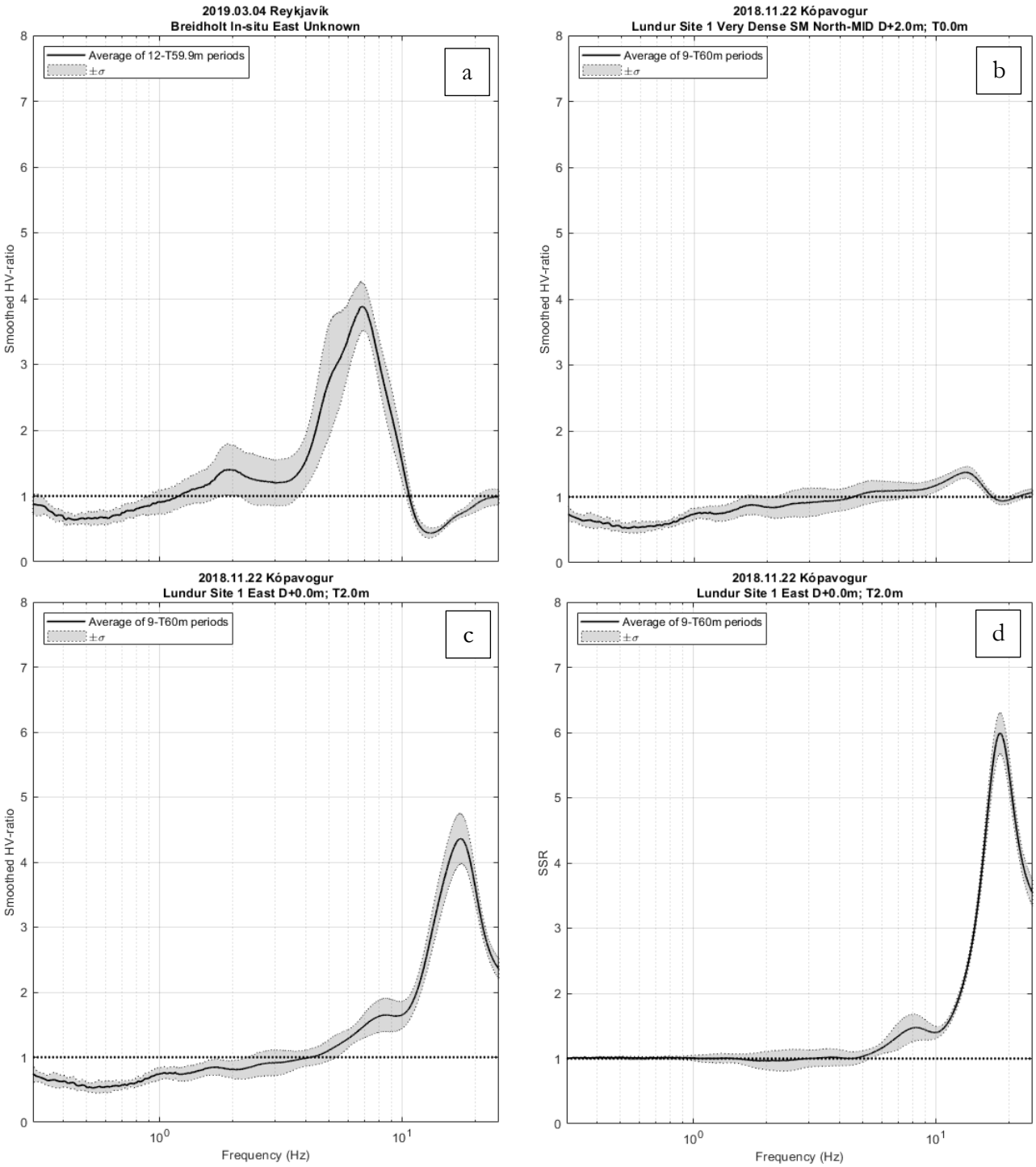

Figure 5. Results from Breiðholt in Reykjavík (a) and Lundur Site 1 in Kópavogur (b, c, and d). HVSR for the in-situ condition (a), the dense to very dense silty sand base layer condition (b), and compacted gravel fill of two-meter thickness (c) are shown. An SSR signature (d) is compared to an HVSR signature (c) for the same time and location.

References

Borcherdt, R.D., Effects of local geology on ground motion near San Francisco Bay, *Bull. Seismol. Soc. Am.*, **60**, 29–61, 1970.

Konno, K., and T. Ohmachi, Ground-motion characteristics estimated from spectral ratio between horizontal and vertical components of microtremor, *Bull. Seismol. Soc. Am.*, **88**, 228–41, 1998.

Nakamura, Y., A method for dynamic characteristics estimation of subsurface using microtremor on the ground surface, *Quarterly Report of Railway Technical Research Institute*, **30**(1), 25–30, 1989.

Nakamura, Y., Clear identification of fundamental idea of Nakamura's technique and its applications, In *Proceedings of the 12th World Conference on Earthquake Engineering*, Auckland, New Zealand, 2000.
Nogoshi, M., and T. Igarashi, On the amplitude characteristics of microtremor (Part 2)." *J. Seismol. Soc. of Japan*, **24**, 26–40, 1971.

NORTHQUAKE 2019 - The 3rd International Workshop on Earthquakes in North Iceland
Húsavík, North Iceland, 21-24 May 2019

CONCISE MAP-BASED REPRESENTATION OF THE TECTONICS, GEOLOGY, GEOMORPHOLOGY AND BUILDING STOCK OF HÚSAVÍK, NORTH ICELAND

Peter Waltl[1], Benedikt Halldórsson[2,3], Halldór G. Pétursson[4], and Markus Fiebig[5]

[1]*Technical University of Munich, Germany (peter.waltl@tum.de)*
[2]*Faculty of Civil and Environmental Engineering, School of Engineering and Natural Sciences, and Earthquake Engineering Research Centre, University of Iceland (UI) (skykkur@hi.is)*
[3]*Division of Processing and Research, Icelandic Meteorological Office (benedikt@vedur.is)*
[4]*Icelandic Institute on Natural History, Iceland (*hgp@ni.is*)*
[5]*BOKU University of Natural Resources and Life Sciences, Austria (markus.fiebig@boku.ac.at)*

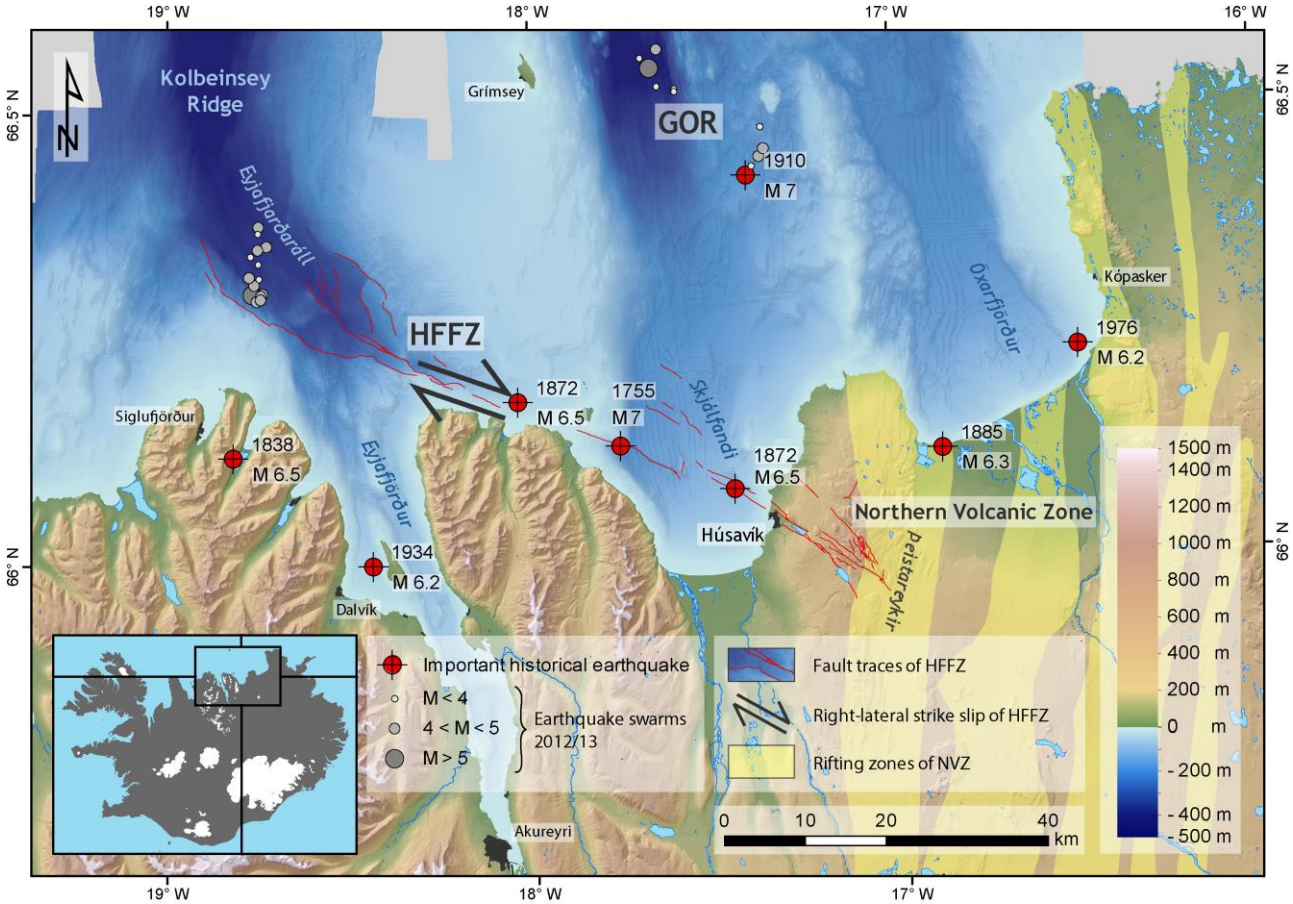

Figure 1. The town of Húsavík is situated on the Húsavík-Flatey Fault Zone (HFFZ) zone within the seismically active Tjörnes Fracture Zone (TFZ) of North Iceland. On land, the Northern Volcanic Zone (NVZ) is a part of the divergent plate boundary of that is the Mid-Atlantic Ridge. The yellow shaded areas in the NVZ represent the extent of the fissure swarms of separate volcanic systems on the extensional margin, and the solid red thin lines represent the main faults and fissure swarms of the transform zone (Hjartardóttir et al., 2015). Red crossed dots mark important historical earthquakes (with year and magnitude; Stefánsson et al., 2008), and gray-shaded dots indicate the locations of the most significant earthquakes during the 2012-2013 earthquake sequence on the western ends of the HFFZ and GOR, respectively.

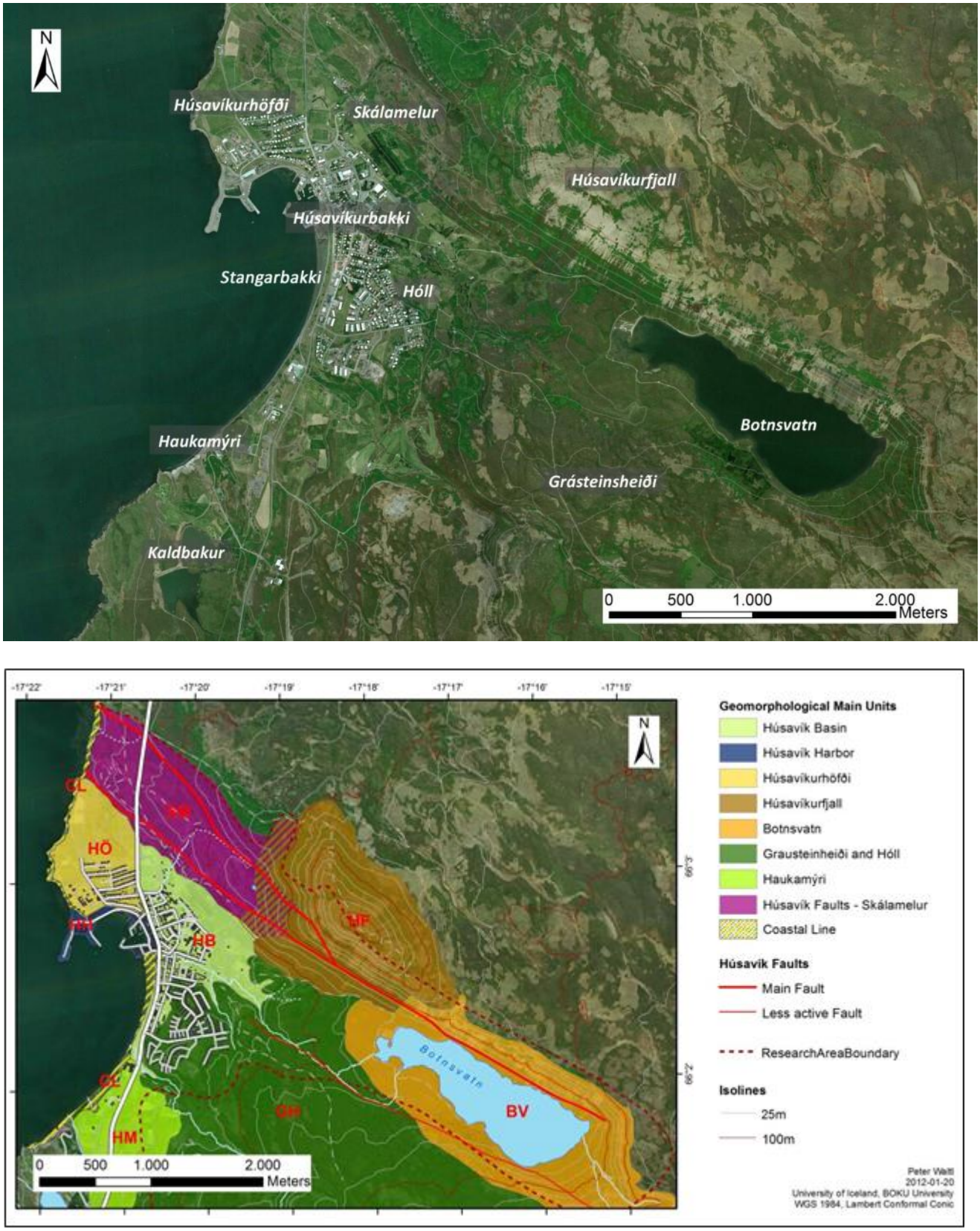

Figure 2. Main geological and geomorphological units in the greater Húsavík area, identified on the basis of mapped geology, elevation, slope inclinations (see Figures below) and field inspection.

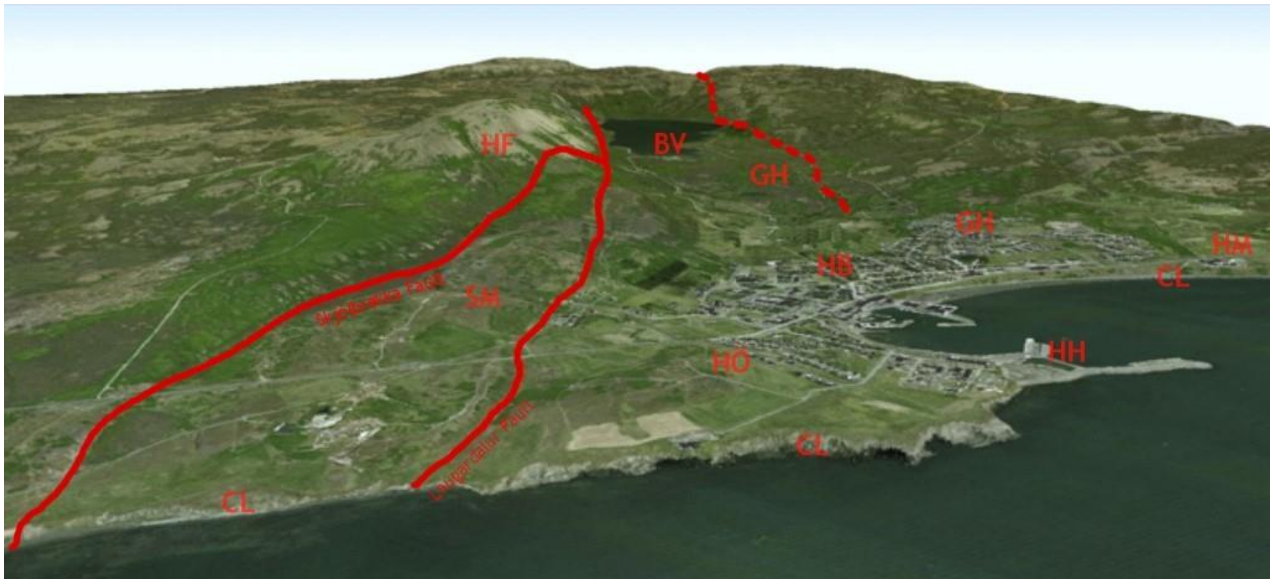

Figure 3. The view of a digital elevation model overlaid with an aerial photograph of Húsavík, seen from slight elevation towards the east-southeast. Húsavík sits in a tectonic pull-apart basin in which Lake Botnsvatn (BV) can be seen in the background. The surface traces of the Húsavík-Flatey Fault Zone (red thick lines) are identified as the Skjólbrekka- and Laugardalur Faults (from left to right) north of Húsavík and are the two main tectonic structures in the area. A third, less known fault east of Húsavík may be seen behind the settlements, further to the right (dashed line). The identified geomorphic units are marked by their letter combinations.

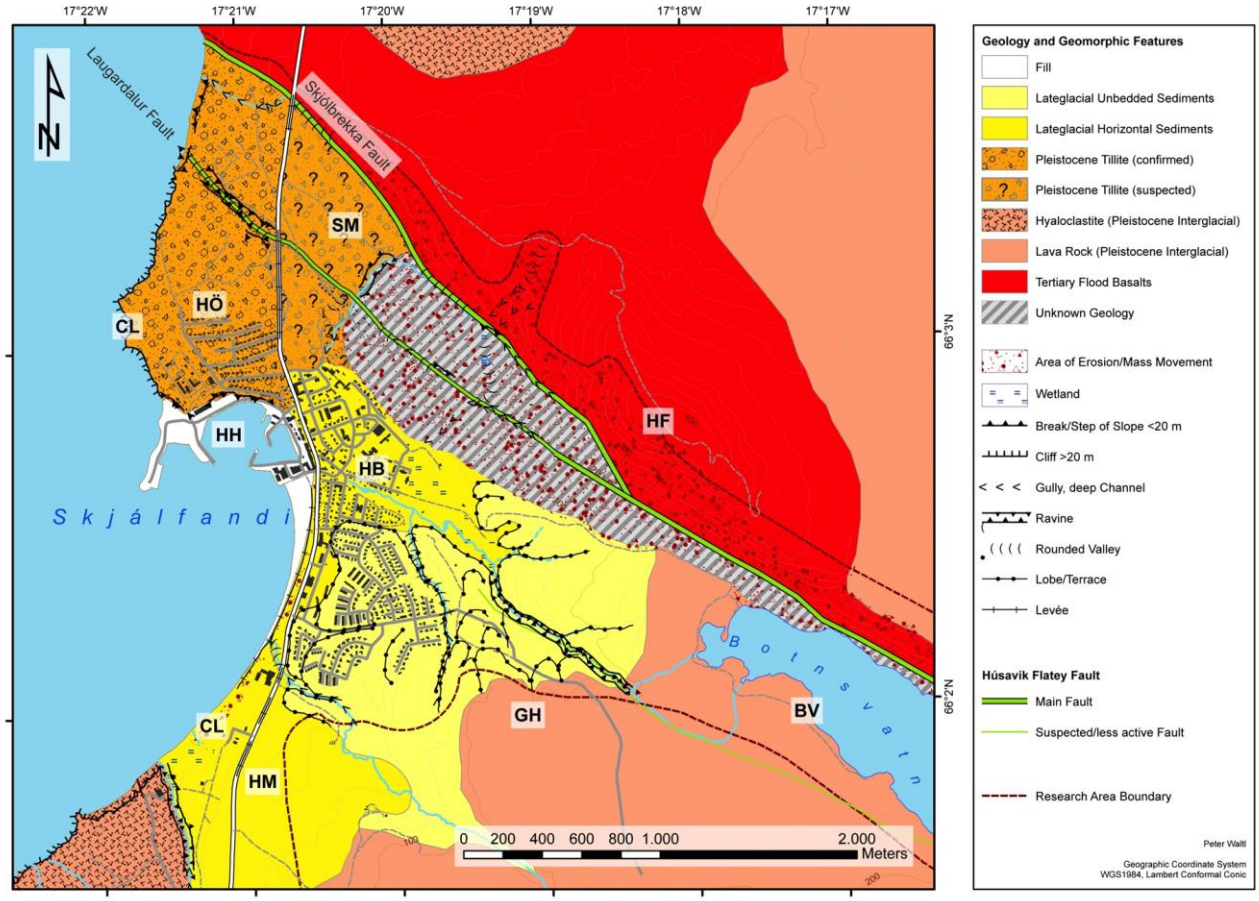

Figure 4. Geological units in the Húsavík region. The region is characterized by tillite in Höfði (HÖ), late glacial horizontal sediments in the Húsavík Basin (HB) and Haukamýri (HM), and unbedded sedimentary terraces at Hóll (in the westernmost part of the Grásteinsheiði unit, GH).

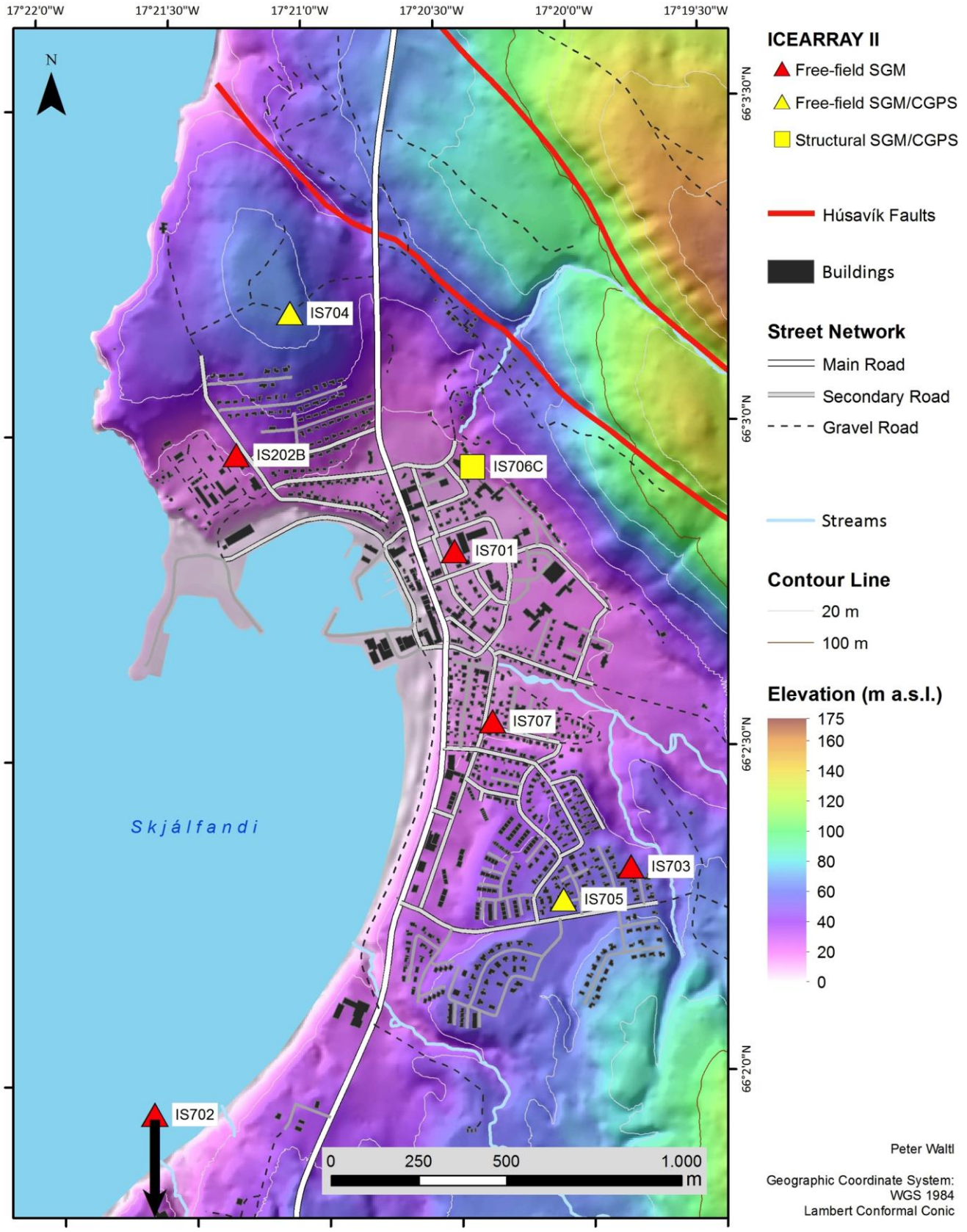

Figure 5. Topographical map of the town of Húsavík showing elevation differences relative to sea level. Also shown are the ICEARRAY II station locations in Húsavík: free-field strong ground motion (SGM) stations (red triangles), and collocated SGM and continuous GPS stations (CGPS) (yellow triangles). A single structural monitoring system in Húsavík Hospital building (yellow square) consists of a ground response SGM station on the ground floor, and two structural response sensors and a CGPS unit on the roof. The main tectonic features of the HFFZ are shown as red lines.

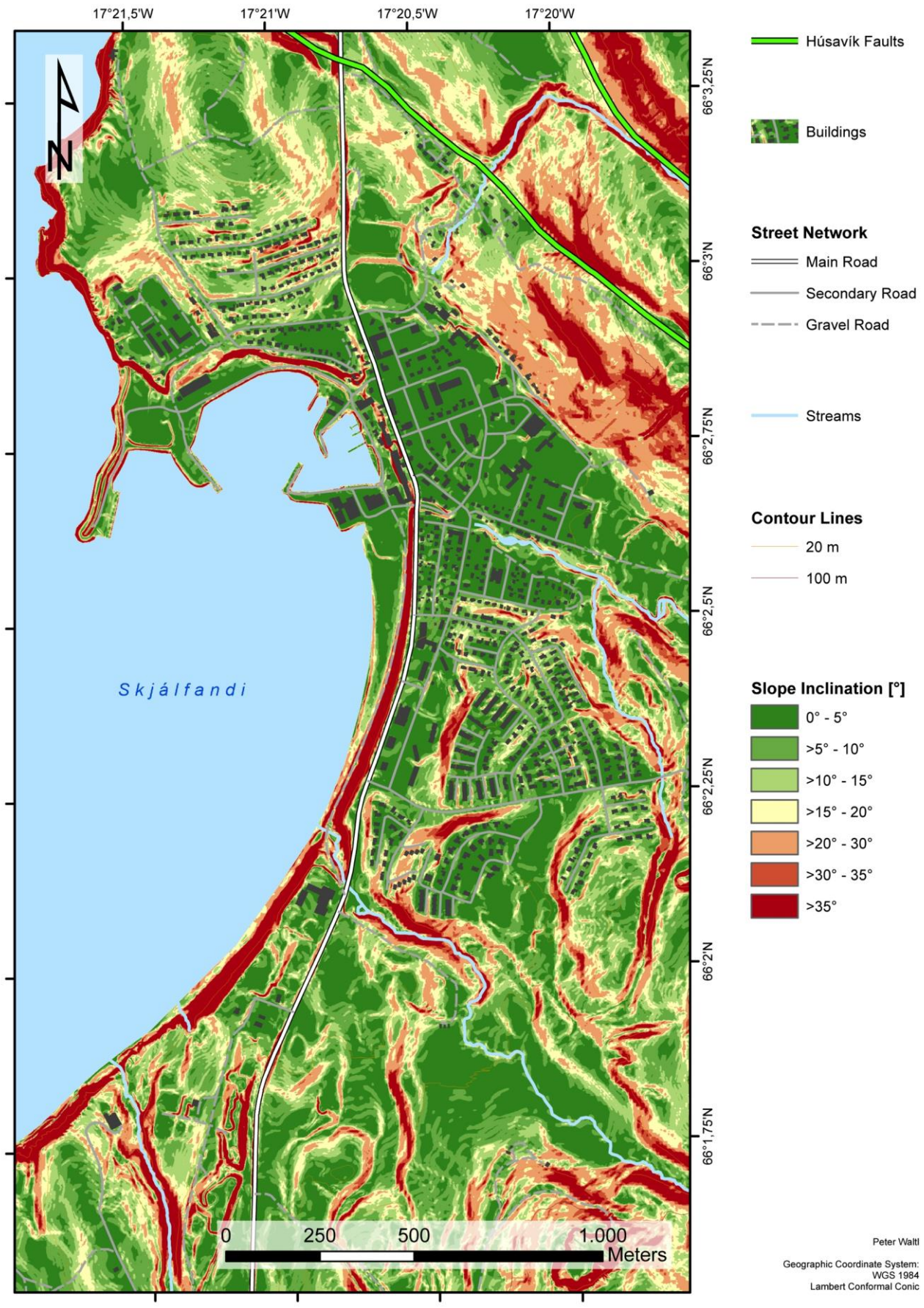

Figure 6. Slope inclinations (in degrees) within Húsavík. The steepest slopes are along the coast, the HFFZ surface traces, Húsavík mountain, and the terraces in southern part of town.

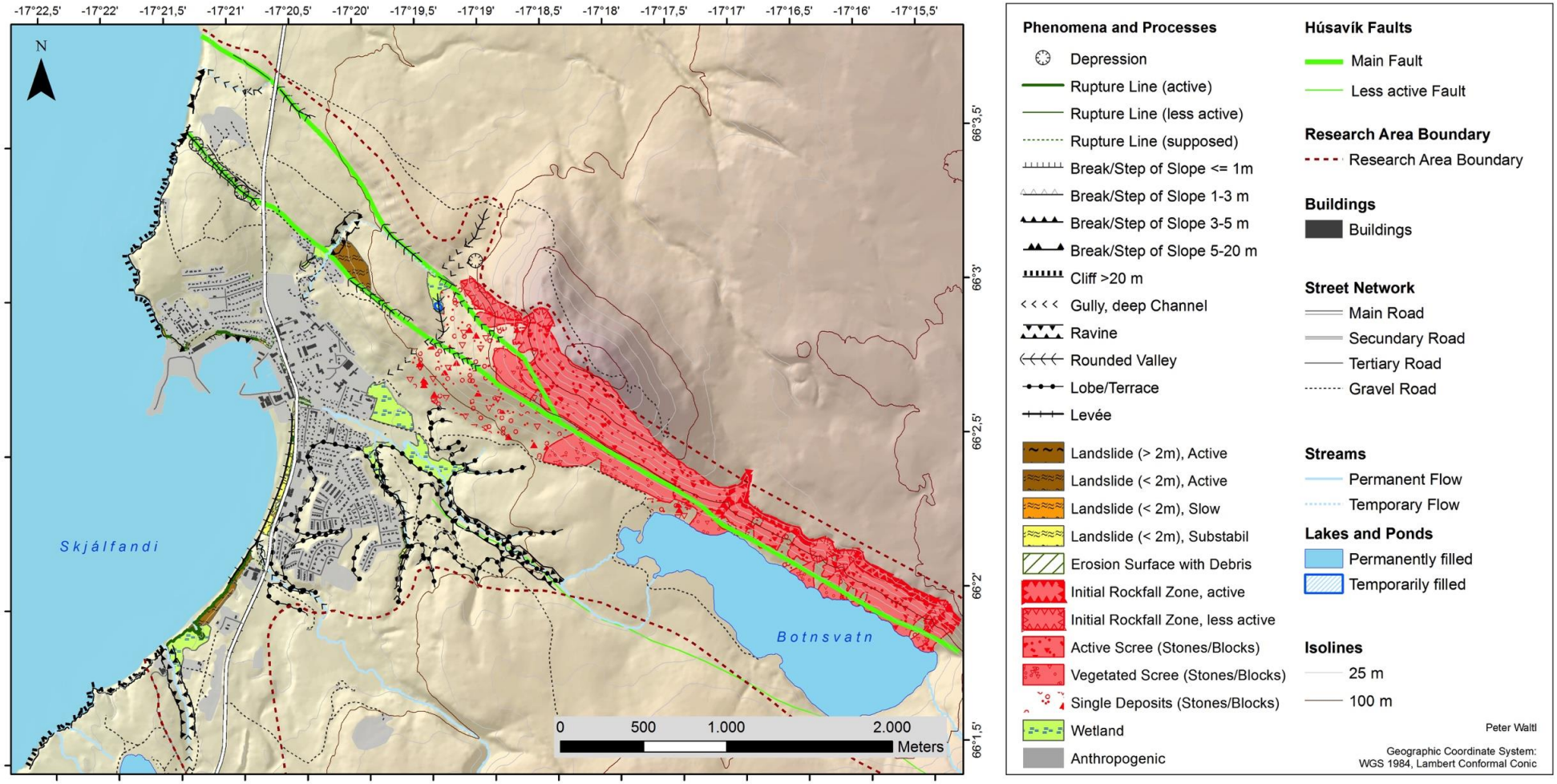

Figure 7. Geomorphic phenomena and processes in the Húsavík region. Most noticeable are areas along the coastline with vertical cliffs and steep slopes that are traversed by the Húsavík faults, especially the Botnsvatn incline and Húsavíkurfjall with their steep and relatively long slopes. Different forms of landslide activity as well as cliff collapses are most severe along the main fault.

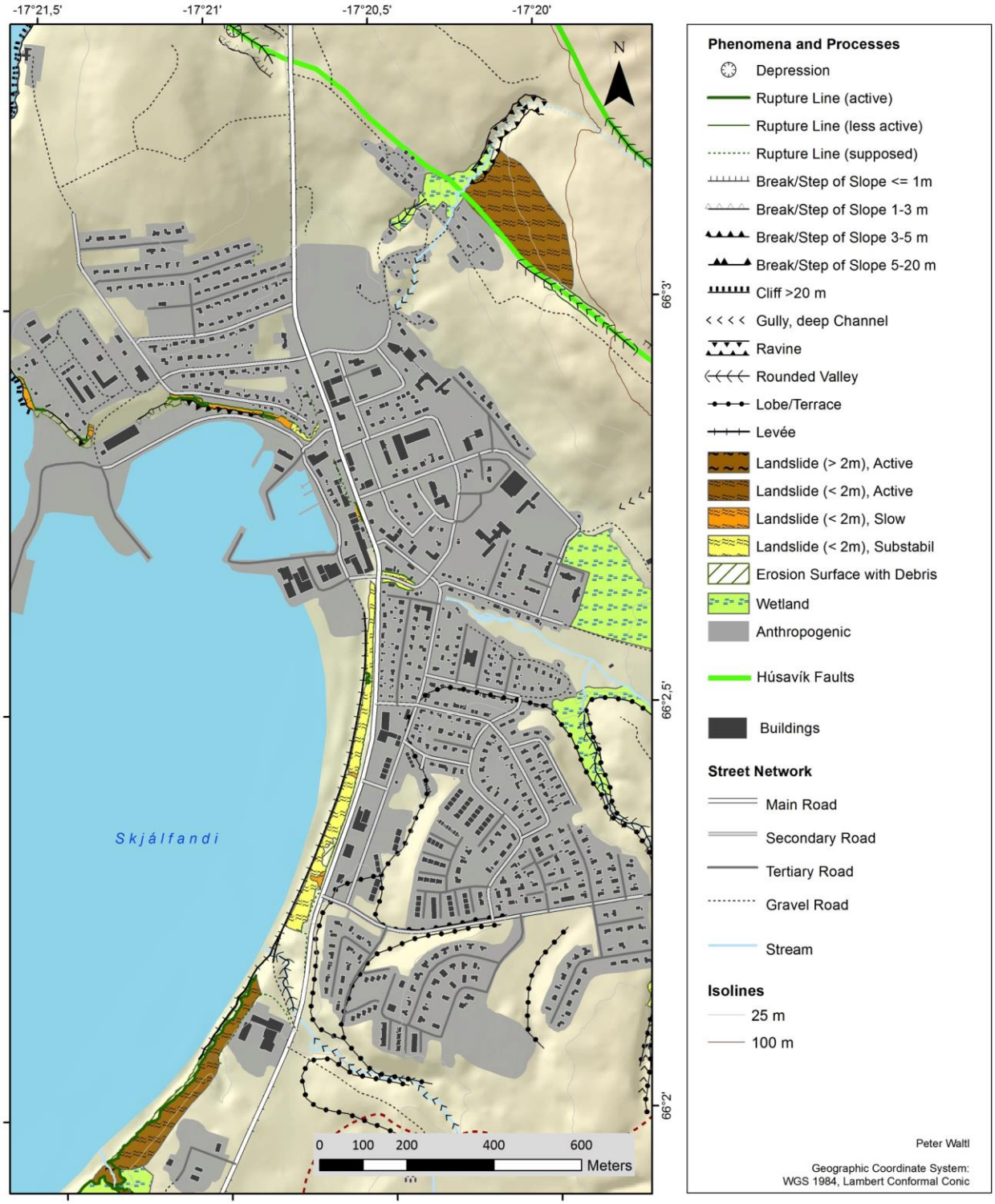

Figure 8. Geomorphic phenomena and processes within the town of Húsavík. Landslides are the most common process within the town itself. The steep slope along the coast of Haukamýri is particularly prone to deep seated, relatively extensive slides and has been very active in recent years.

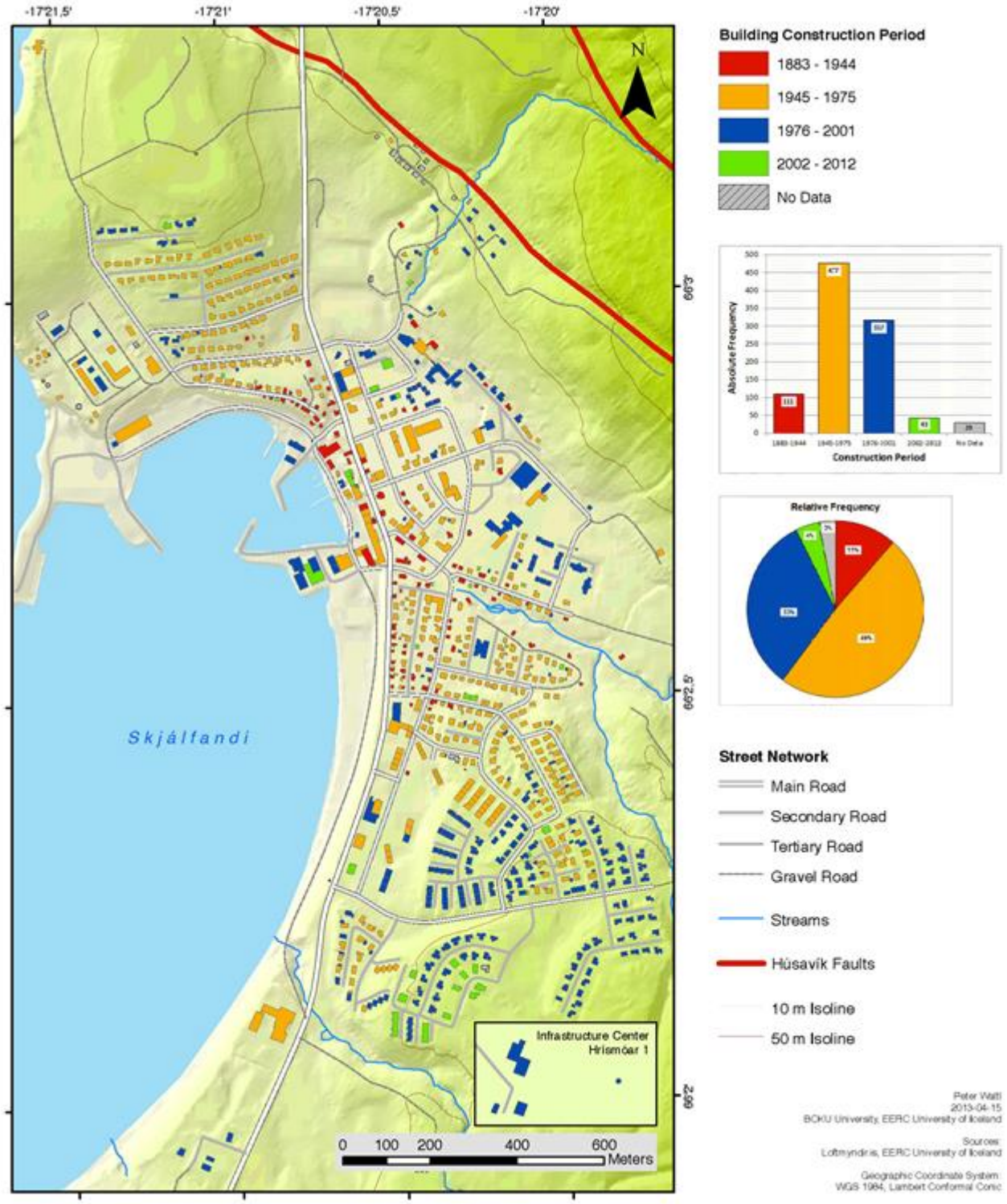

Figure 9. The spatial and temporal characteristics of the building stock in Húsavík, North Iceland, in terms of building construction period. The timelines of separation of the building stock into periods reflects the onset of validity of new building standards for the earthquake resistant design of structures in Iceland.

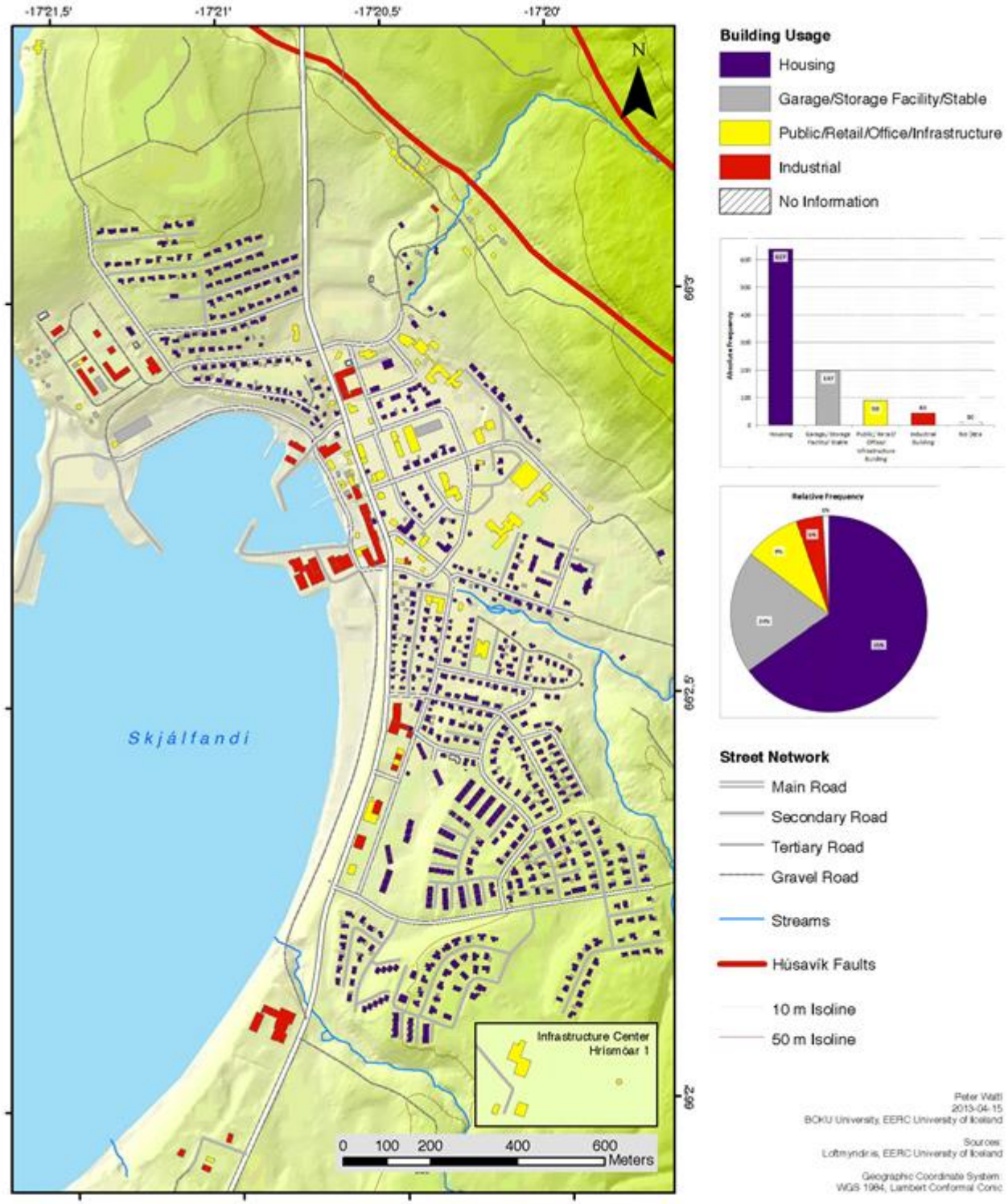

Figure 10. The spatial characteristics of the building stock in Húsavík, North Iceland, in terms of building usage.

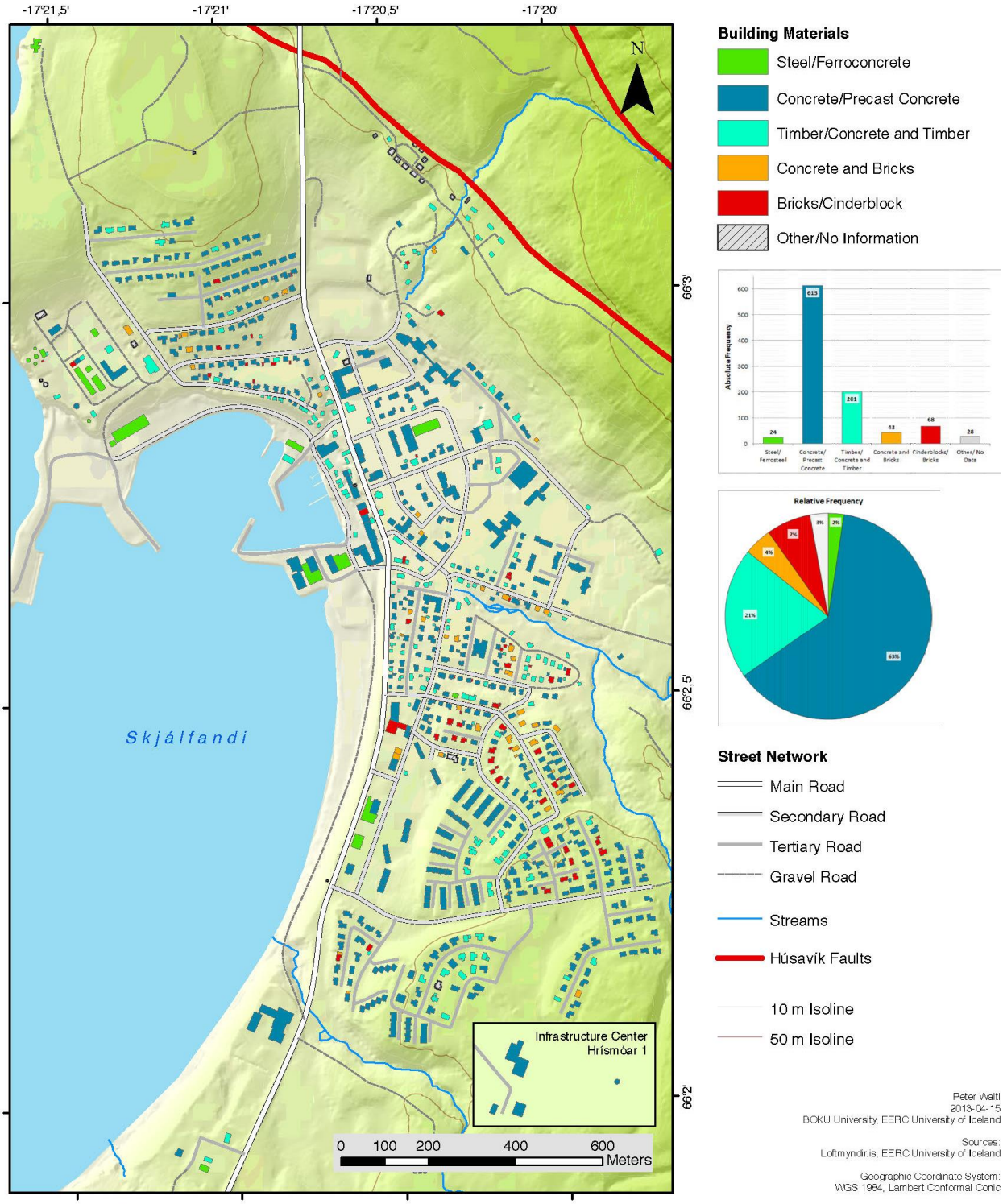

Figure 11. The spatial characteristics of the building stock in Húsavík, North Iceland, in terms of construction materials.

References

Hjartardóttir, Á.R., Einarsson, P., Magnúsdóttir, S., Björnsdóttir, Þ. and Brandsdóttir, B. Fracture systems of the Northern Volcanic Rift Zone, Iceland – An onshore part of the Mid-Atlantic plate boundary. In: Wright, T. J., Ayele, A., Ferguson, D. J., Kidane, T. & Vye-Brown, C. (eds) *Magmatic Rifting and Active Volcanism*. Geological Society, London, Special Publications, 420, http://dx.doi.org/10.1144/SP420.1, 2015

Stefánsson R., G.B. Gudmundsson and P. Halldorsson, Tjörnes fracture zone. New and old seismic evidences for the link between the North Iceland rift zone and the Mid-Atlantic ridge. *Tectonophysics*, **447**, 117–126, 2008.

Waltl, P., *Geomorphology and building stock of Húsavík, North Iceland: A uniform GIS database for application in hazard and risk modeling*. M.Sc. Thesis, BOKU University of Natural Resources and Life Sciences. Vienna, Austria, 2013.

Waltl, P., B. Halldorsson, H.G. Pétursson et al., The geological and urban setting of Húsavík, North Iceland, in the context of earthquake hazard and risk analysis. In: *Proceedings of the 2nd European Conference on Earthquake and Engineering Seismology (2ECEES)*. Istanbul, Turkey, 2014.

Waltl P., B. Halldorsson, H.G. Pétursson, M. Fiebig, Geomorphic assessment of the urban setting of Húsavík, North Iceland, in the context of earthquake hazard, *Jökull*, **68**, 27–46, 2018.

NORTHQUAKE 2019 - The 3rd International Workshop on Earthquakes in North Iceland
Húsavík, North Iceland, 21-24 May 2019

A FULL-WAVEFORM INVERSION MOMENT TENSOR CATALOG FOR ICELAND: PERSPECTIVES AND EXAMPLES FROM THE TJÖRNES FRACTURE ZONE

Félix Rodríguez Cardozo[1], Vala Hjörleifsdóttir[2,3], Kristín Jónsdóttir[4], Kristín Vogfjörð[4], Gunnar B. Guðmundsson[4], Arturo Iglesias[2], Sara Ivonne Franco[2], Halldór Geirsson[5], Nancy Trujillo Castrillon[1], and the IMO monitoring team

[1]*Earth Sciences Graduate Program, National Autonomous University of Mexico (UNAM), Mexico (felixrc@ciencias.unam.mx, canytas@gmail.com)*
[2]*Geophysics Institute, National Autonomous University of Mexico (UNAM), Mexico* (arturo@igeofisica.unam.mx, *ivonne@igeofisica.unam.mx)*
[3] *Reykjavík Energy, Iceland (vala.hjorleifsdotti@or.is)*
[4] *Icelandic Meteorological Office (*kristin.jonsdottir@vedur.is, *vogfjorð@vedur.is)*
[5] *Institute of Earth Sciences, University of Iceland (hgeirs@hi.is)*

An automatic routine for inverting seismic moment tensors for earthquakes larger than Mw 3.8, has been set up at the Icelandic Meteorological Office (IMO). It is based on the time-domain full-waveform inversion technique described by Dreger (*Dreger*, 2003). This routine is not only useful for monitoring purposes, but also for building up a moment tensor catalog for the larger earthquakes in Iceland (Mw > 3.8).

So far, this technique has been applied successfully for obtaining a catalog for events at Bárðarbunga during and after the caldera collapse in 2014 (*Rodriguez Cardozo et al.*, 2018), confirming the deflation-inflation cycle observed through the flipped polarities for body waves *(Jónsdóttir et al.*, 2017*)* (Fig.1).

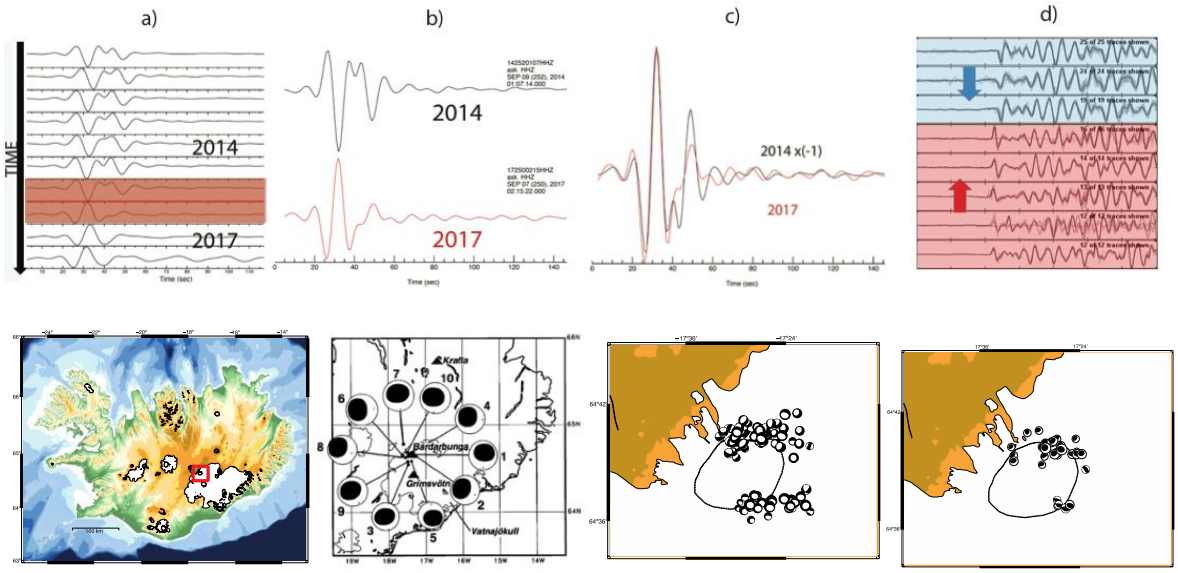

Figure 1. Above: flipped polarities (a, b, and c) of surface waves (20s-50s) for two events during (2014) and after (2017) the caldera collapse and flipped polarities (d) of body waves described in Jónsdóttir et al. (2017). Below: (a) Iceland and Bárðarbunga volcano (red square). (b) Reverse focal mechanisms reported by Nettles and Ekström (1998), between 1974

and 1996. (c) Normal focal mechanisms inverted during the caldera collapse (2014). (d) Reverse focal mechanisms after the caldera collapse (2017-2019), similar to the mechanisms for the 1974-1996 events.

With the aim of extending the moment tensor catalog to all Iceland, there is a milestone opportunity to apply this method to events in the Tjörnes Fracture Zone (TFZ), where IMO has reported 60 earthquakes with magnitudes larger than 3.8 since 2000.

In this work, we present preliminary results of waveform inversions for two episodes: (1) 10 events (3.8 < Mw < 4.6) in the TFZ between January and February 2018 and (2) 3 events in 2017 and 2019 (Fig. 2). In both cases, the fit between observed and synthetic seismograms is quite good (Fig. 3) and the focal mechanisms described by the moment tensors are consistent with the tectonics of the TFZ and historical reports of focal mechanisms in this zone (Fig. 4) (*Jónsdóttir et al.*, 2016).

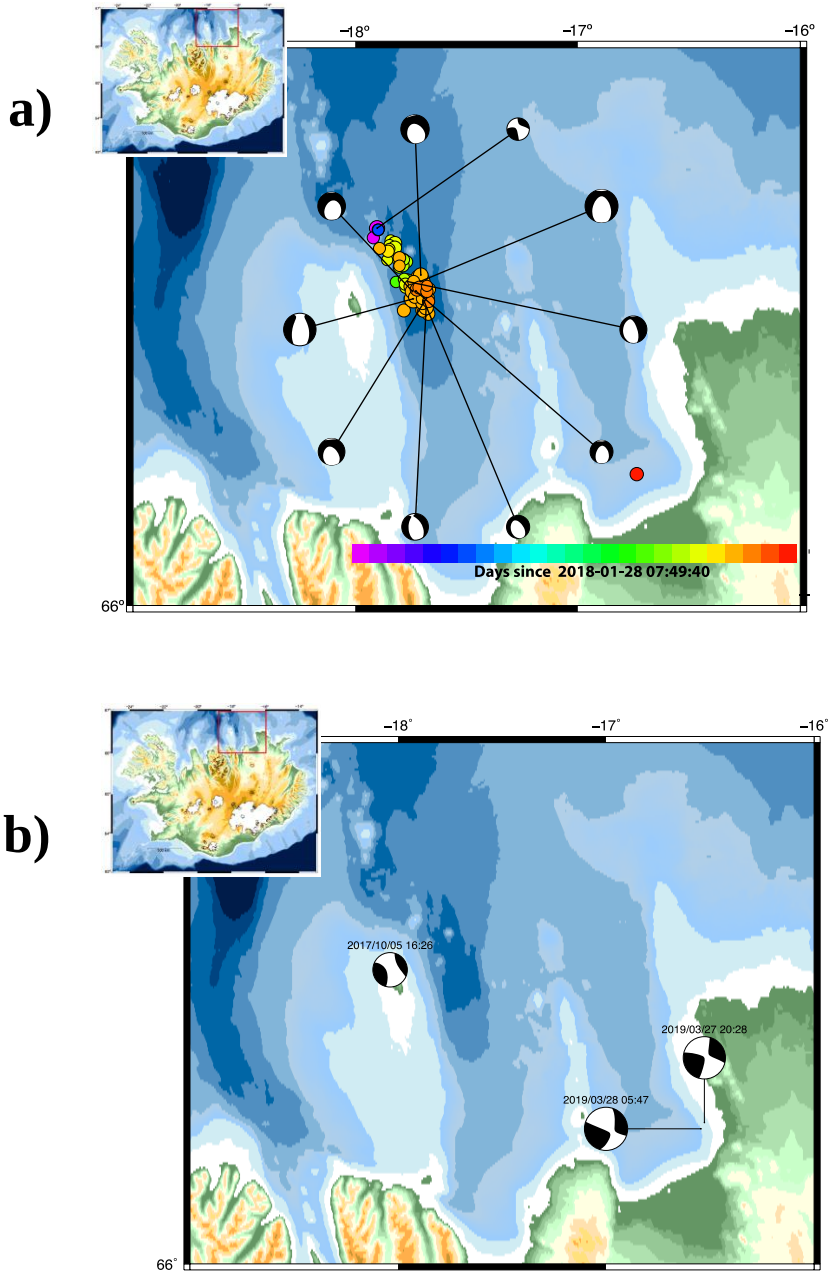

Figure 2. a) Focal mechanisms for events in October 2017 and March 2019 (3.6 < Mw. < 4.2) in the TFZ. b) Focal mechanisms for events between January and February 2018 (3.8 < Mw. < 4.6) in the TFZ.

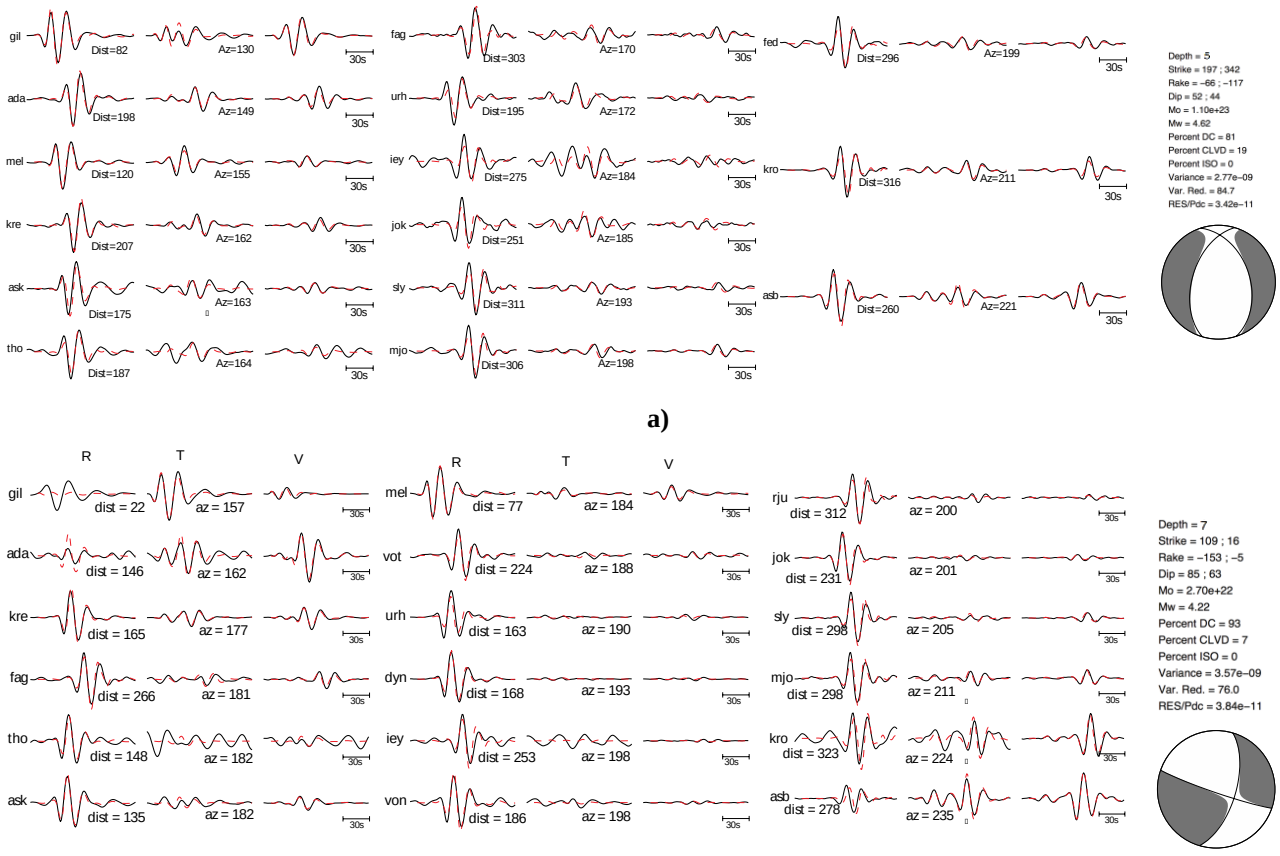

Figure 3. Observed (black) and synthetic seismograms (red) for earthquakes in the TFZ on a) 19 February 2018 at 05:32 (Mw 4.6), and on b) 28 March 2019 at 05:47 (Mw 4.2).

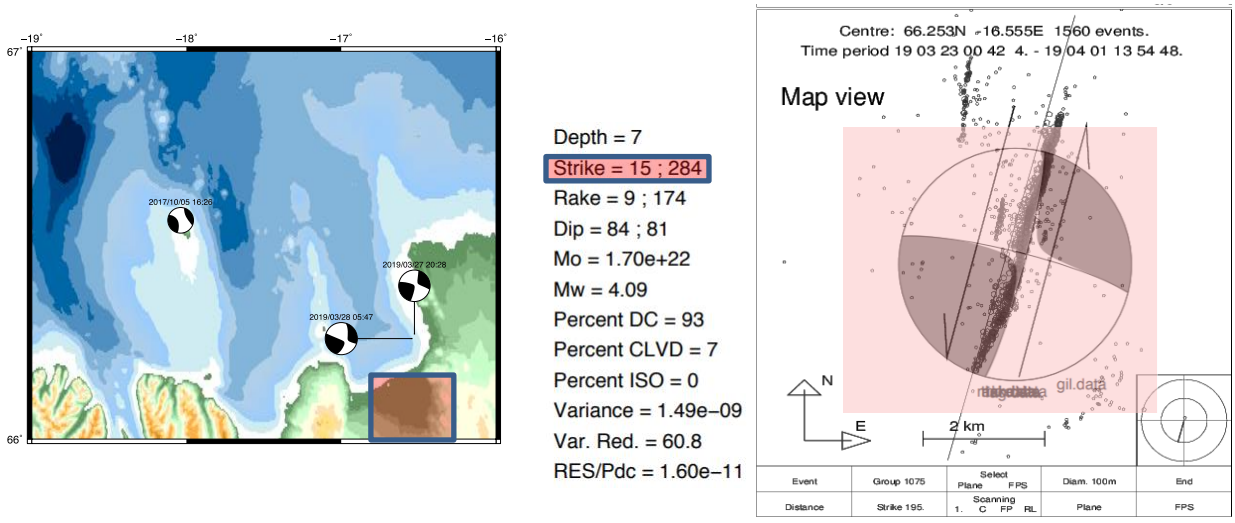

Figure 4. A moment tensor solution for the largest event of the 2019 Kópasker earthquake swarm, occurring on 27 March 2019 (Mw 4.09), see further information in Jónsdóttir et al. (2019). Observe how well the focal mechanism solution fits with the fault plane obtained by relocating many small events that occurred during the earthquake swarm.

References

Dreger, D.S., TDMT_INV: Time domain seismic moment tensor inversion, In: *International Geophysics*. Elsevier, p. 1627, 2003

Jónsdóttir, K., A. Hooper, K. Jónasson et al., Bárðarbunga volcano - post-eruption trends following the Holuhraun eruption in 2014-2015, *Geophys. Res. Abstracts*, **19**, EGU2017-12535-3, EGU General Assembly, 2017.

Jónsdóttir, K., G.B. Guðmundsson, M. Hensch and the SIL monitoring group, Earthquake swarms in the Tjörnes Fracture Zone in N-Iceland, 2012 and 2013. In *Proceedings of the 2nd workshop on Earthquakes in North Iceland*, Ed. R. Stefánsson et al., Húsavík Academic Centre, 55-56, 2016.

Jónsdóttir, K., G.B. Guðmundsson, L. Passarelli, S. Jónsson & monitoring team at IMO, The Kópasker seismic swarm in Spring 2019, In *Proceedings to the Northquake 2019 workshop* (this volume), 2019.

Nettles, M., and G. Ekström, Faulting mechanism of anomalous earthquakes near Bárdarbunga Volcano, Iceland. *J. Geophys. Res.*, **103**, 17973–17983, 1998.

Rodriguez Cardozo, F.R., V. Hjörleifsdóttir, K. Jónsdóttir, H. Geirsson and A. Iglesias, New insights about Bárðarbunga's seismic sources during and after the 2014-2015 caldera collapse events, Abstract S13A-07. AGU Fall Meet., 2018.

NORTHQUAKE 2019 - The 3rd International Workshop on Earthquakes in North Iceland
Húsavík, North Iceland, 21-24 May 2019

EARTHQUAKE SOURCE MODELING AND GROUND MOTION SIMULATION IN NORTH ICELAND

Tim Sonnemann[1,2], Benedikt Halldorsson[1,2], Birgir Hrafnkelsson[3], Sigurjón Jónsson[4], and Jónas Þ. Snæbjörnsson[5]

[1]*Earthquake Engineering Research Centre, University of Iceland (tsonne@hi.is, skykkur@hi.is)*
[2]*Icelandic Meteorological Office (tim@vedur.is, benedikt@vedur.is)*
[3]*Department of Mathematics, University of Iceland (birgirhr@ hi.is)*
[4]*King Abdullah University of Science and Technology (KAUST), Saudi Arabia (sigurjon.jonsson@kaust.edu.sa)*
[5]*School of Science and Engineering, Reykjavik University, Iceland (jonasthor@ru.is)*

Regarding strong ground motion due to earthquakes, there are two regions in Iceland that experience large earthquakes of magnitude M ~ 7 – the South Iceland Seismic Zone (SISZ) and the Tjörnes Fracture Zone (TFZ). Both being transform zones compensating for tectonic extension along the Mid-Atlantic Ridge, the SISZ is more populated than the TFZ and was shaken by a series of four medium-sized earthquakes of M6.0-6.5 from 1987 to 2008, all of which were recorded by nearby accelerometers. The TFZ, on the other hand, experienced its last seismic event of M>6 over 40 years ago in 1976 (M6.2) near Kópasker connected to the Krafla volcanic system rifting episode from 1975 to 1984 and no strong-motion records of M≥6 events are available for that area.

To estimate the potential intensity of ground motion during a larger earthquake in the TFZ, ground motion models (GMM) that were statistically constrained by records of other regions in the world would result in uncertain predictions as has been observed using records of the SISZ (*Kowsari et al.*, 2019). However, GMMs informed by the SISZ records are expected to fit TFZ motions better while still being an extrapolation, and physical simulations of earthquake rupture and the ensuing seismic wave-field might yield more realistic estimates according to the current scientific knowledge. Physics-based simulations mostly rely on geometric and geologic information instead of an already recorded ground motion dataset, thus allowing informed estimates in seismically active regions where no strong motions have been recorded yet.

A good summary of the tectonics and large earthquakes of the last 300 years of the TFZ is given by *Stefansson et al.* (2008). The TFZ can be characterized by two WNW-ESE trending fault zones, the Grímsey Oblique Rift (GOR) to the north and the Húsavík-Flatey Fault (HFF) to the south. The GOR is a completely offshore with north-south trending en-échelon series of segments, while the HFF is partly onshore touching the town of Húsavík and is mostly composed of WNW-oriented fault segments (*Einarsson*, 1991; *Metzger et al.*, 2011). Geodetic deformation studies have indicated that the HFF is locked to a depth of about 6 to 10 km and has accumulated strain equivalent to a single earthquake estimated at M 6.8-7.0 (*Metzger et al.*, 2013; *Metzger & Jónsson*, 2014), although it is unclear whether all segments of the HFF could rupture together. Depending on rupture nucleation location (hypocenter) and the final slip distribution on the fault, directivity effects could expose Húsavík to strong shaking, the level of which is to be estimated in future studies.

Given the absence of strong-motion records for the TFZ, the SISZ accelerometric dataset was selected to calibrate a seismological model. The SISZ consists of a completely onshore series of parallel

N-S trending bookshelf-type strike-slip faults, from where strong-motion records of four earthquakes of M 6.0-6.5 and various smaller events and aftershocks exist. The SISZ dataset has been used within the Bayesian statistical framework to constrain the parameters of a seismological model which uses the Specific Barrier Model (SBM) as its source representation (*Sonnemann et al.*, 2019). The SBM is a stochastic source model which provides representations of both a point-source and a finite source rupture (*Papageorgiou & Aki*, 1983a, b; *Papageorgiou*, 2003; *Halldorsson & Papageorgiou*, 2005).

The Bayesian inference on stress drop (local and global), path attenuation and site effects was executed with the point-source model, but in forward-simulations the parameter values can be used directly in the finite source model as well. This allows simulating near-fault effects as dependency of ground motion on the geometry of fault and receivers, rupture nucleation location and subevent distribution across the fault segments. The HFF and five surrounding locations were selected as source and receivers for five rupture scenarios (case 1 to 5, see Fig. 1a), while the input model parameter values were the inferred values from the SISZ dataset, and the resulting high-frequency (f > 1 Hz) ground motions were calculated. The HFF was parted into four segments of different lengths and widths, such that the rupture scenarios represent different states of activity on each segment. In case 1, all segments rupture unilaterally to the east from the hypocenter at the western edge; in case 2 the three western segments rupture from west to east, i.e. towards Húsavík; in case 3 the two segments west of Húsavík rupture unilaterally towards the town; in case 4 the same two segments experience bilateral rupture from the hypocenter being in the center of both segments combined; while in case 5 only the easternmost segment ruptures unilaterally from its eastern edge towards Húsavík. The five representative receiver locations are the towns Húsavík, Grenivík, Dalvík and Siglufjörður, and an unstable mountain slope at Skálavík bay (Fig. 1b). For each rupture scenario 25 randomized subevent location sets were produced to simulate part of the expected ground motion variability inherent in earthquakes due to randomly heterogeneous slip distributions. The used model parameter values and their meanings are given in Table 1.

The resulting peak ground acceleration (PGA) median estimates for Húsavík range from 20 to 33% g with an upper extreme case of 70% g. The median PGA estimates of most rupture cases are about 12% g for the Skálavík slope, while the median predictions for Siglufjörður, Grenivík and Dalvík all range from 0.8 to 7% g. The values indicate that hypothetical worst-case scenarios for the town of Húsavík might not only be an entire fault rupture like case 1 but also case 5, even though only one fault segment was set to rupture yielding a M6.1 earthquake (Fig. 1c). The reasons are that the eastern segment width was assumed to be larger than the width of the adjacent western segment, the rupture front moved unilaterally towards Húsavík and even though more segments rupture in the other cases, the resulting seismic waves are attenuated significantly due to their larger distances to the town. If the segment widths are reasonable, the relatively high aspect ratio of the fault means that the largest part of received seismic energy almost exclusively comes from the nearest fault segment. However, certain structures are vulnerable to shaking levels of about 10% g, such as unstable slopes which might come down as landslides. One such potential location has been identified at Skálavík (*Drouin and Sigmundsson, 2019*), implying that a fast-moving landslide of its size into Skjálfandi bay could cause a tsunami wave with its associated hazard for the surrounding coastal areas.

This preliminary study is limited by assuming fixed physical and geometric model parameter values with a 1D ground model and average rock site responses at all locations. Further, low-frequency wave-field synthetics would need to be added to obtain full broadband model simulations. No advanced simulations have been carried out for other locations and faults of the TFZ in this study, meaning that

the true variability and average behaviour including all uncertainties remain unexplored. The results are specific to the finite-fault SBM and the fixed assumptions explained above, which leads to underestimating the true range of possible ground shaking due to projected future earthquake scenarios. However, with increasing geophysical data availability about the TFZ and the local site conditions, more realistic calculations can be carried out, including seismic broadband simulations. This study is one of the first more advanced fault rupture simulations for the HFF and indicates a serious seismic threat level for Húsavík and surrounding areas, which might experience additional secondary effects such as landslides and even tsunamis. Future studies would be needed to increase the reliability of these predictions.

Table 1: Finite-fault SBM parameters and assumed values used in this studies' simulations.

Parameter	Value	Meaning
$\Delta\sigma_G$	30 bar	Global stress drop
$\Delta\sigma_L$	75 bar	Local stress drop
β	3.2 km/s	Shear wave velocity (near source, path)
ρ	2.8 g/cm^3	Rock density near source
ν	0.8	Ratio of rupture velocity to shear wave velocity
rtype	fract2	Type of pdf for SBM subevent sizes
a_1	0.4	Ratio of max. subevent size to total main event size
a_2	0.3	Ratio of min. subevent size to max. subevent size
sltype	uniform	Subevent location distribution type
Q_0	64	S-wave quality factor at 1.0 Hz
γ	0.91	S-wave quality factor frequency exponent
R_X	29 km	Crossover distance of geometric spreading type

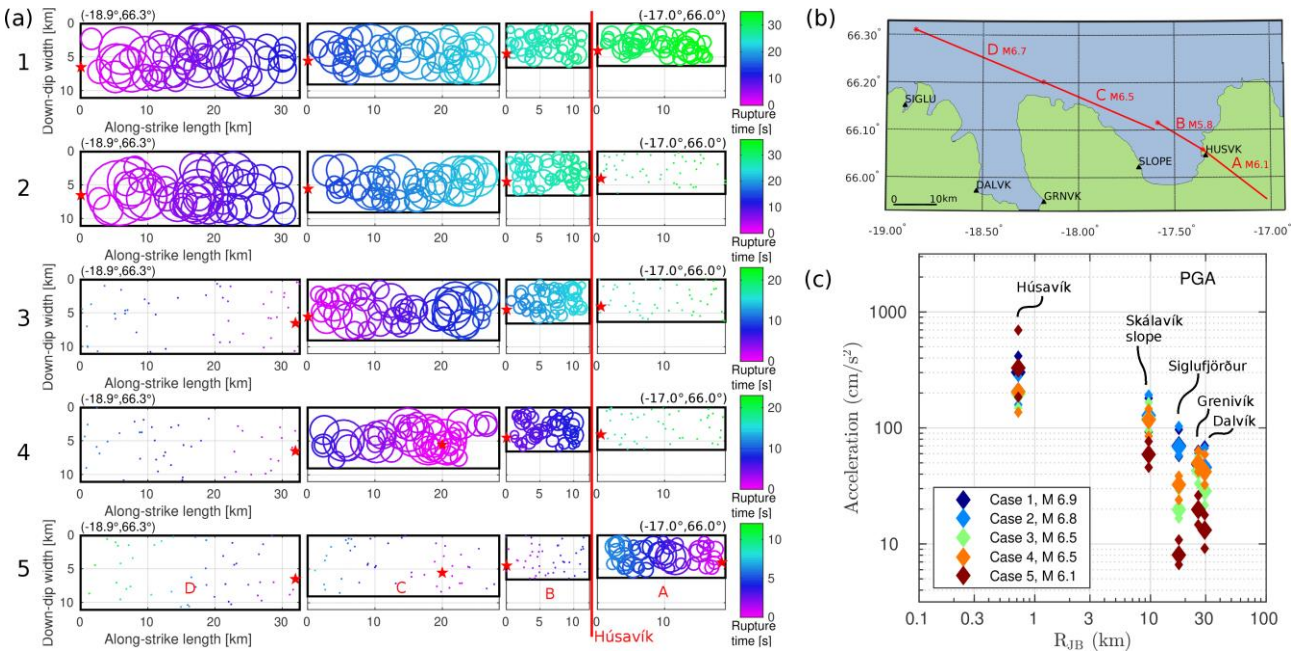

Figure 1: (a) Rupture scenarios with respective case number to the left. Each case is shown with all fault segments from west (left) to east (right) and the location of Húsavík is annotated with a red vertical line. Each segment's rupture front nucleation point is shown as red star, while the earthquake subevents are shown as circles colored by their respective rupture times. (b) Source – site geometry map indicating the simulation setup for the HFF and the five selected target locations in northern Iceland. The fault segments' locations and dimensions were derived from literature (see text), while their average maximum moment magnitude according to the relations of Wells & Coppersmith (1994) *are indicated next to their segment ID letter. (c) Simulated peak ground acceleration values versus distance for the five selected locations for all five rupture cases. The*

large symbols represent the median of the 25 randomized iterations per case, while the small symbols indicate 2.5 and 97.5 percentiles. The combined magnitudes of all segments per case are noted in the legend.

References

Drouin, V. & F. Sigmundsson, Monitoring slope instabilities with Sentinel-1 satellite interferometry, In *Proceedings to the Northquake 2019 workshop* (this volume), 2019.

Einarsson, P., Earthquakes and present-day tectonism in Iceland. *Tectonophysics*, **189**, 261–279, 1991.

Halldorsson, B. & Papageorgiou, A.S., Calibration of the Specific Barrier Model to Earthquakes of Different Tectonic Regions. *Bulletin of the Seismological Society of America*, **95**, 1276–1300, https://doi.org/10.1785/0120040157, 2005.

Kowsari, M., Halldorsson, B., Hrafnkelsson, B., Snaebjörnsson, J.Þ. & Jónsson, S., Calibration of ground motion models to Icelandic peak ground acceleration data using Bayesian Markov Chain Monte Carlo simulation. *Bulletin of Earthquake Engineering*, **17**, 2841–2870, https://doi.org/10.1007/s10518-019-00569-5, 2019.

Metzger, S. & Jónsson, S., Plate boundary deformation in North Iceland during 1992–2009 revealed by InSAR time-series analysis and GPS. *Tectonophysics*, **634**, 127–138, 2014.

Metzger, S., Jónsson, S. & Geirsson, H., Locking depth and slip-rate of the Húsavík Flatey fault, North Iceland, derived from continuous GPS data 2006-2010. *Geophysical Journal International*, **187**, 564–576, 2011.

Metzger, S., Jónsson, S., Danielsen, G., Hreinsdottir, S., Jouanne, F., Giardini, D. & Villemin, T., Present kinematics of the Tjörnes Fracture Zone, North Iceland, from campaign and continuous GPS measurements. *Geophysical Journal International*, **192**, 441–455, 2013.

Papageorgiou, A.S., The Barrier Model and Strong Ground Motion. *Pure and Applied Geophysics*, **160**, 603–634, https://doi.org/10.1007/PL00012552, 2003.

Papageorgiou, A.S. & Aki, K., A specific barrier model for the quantitative description of inhomogeneous faulting and the prediction of strong ground motion. I. Description of the model. *Bulletin of the Seismological Society of America*, **73**, 693–722, 1983a.

Papageorgiou, A.S. & Aki, K., A specific barrier model for the quantitative description of inhomogeneous faulting and the prediction of strong ground motion. Part II. Applications of the model. *Bulletin of the Seismological Society of America*, **73**, 953–978, 1983b.

Sonnemann, T., Halldorsson, B., Hrafnkelsson, B., Jónsson, S. & Jónsson, S., Bayesian Inference of a Physical Seismological Model to Earthquake Strong-motion in South Iceland. *Soil Dynamics and Earthquake Engineering*, **(in review)**, 2019.

Stefansson, R., Gudmundsson, G.B. & Halldorsson, P., Tjörnes fracture zone. New and old seismic evidences for the link between the North Iceland rift zone and the Mid-Atlantic ridge. *Tectonophysics*, **447**, 117–126, 2008.

Wells, D.L. & Coppersmith, K.J., New empirical relationships among magnitude, rupture length, rupture width, rupture area, and surface displacement. *Bulletin of the seismological Society of America*, **84**, 974–1002, 1994.

NORTHQUAKE 2019 - The 3rd International Workshop on Earthquakes in North Iceland
Húsavík, North Iceland, 21-24 May 2019

TOWARDS PHYSICS-BASED PROBABILISTIC SEISMIC HAZARD ASSESSMENT IN COMPLEX FAULT NETWORKS - THE CHEESE PROJECT

Bo Li[1], Sara A. Wirp[1], Alice-Agnes Gabriel[1], Michael Bader[2], Benedikt Halldórsson[3]

[1]*Ludwig-Maximilians Universität München (LMU), Germany*
(bo.li@geophysik.uni-muenchen.de, sara.wirp@geophysik.uni-muenchen.de, gabriel@geophysik.uni-muenchen.de)
[2] *Technical University of Munich (TUM), Germany (bader@in.tum.de)*
[3] *Icelandic Meteorological Office (benedikt@vedur.is)*

Iceland locates on the Mid-Atlantic Ridge due to the diverging movement of the North American and the Eurasian Plates. In the northern part, the extensional plate motion is accommodated by the Northern Volcanic Zone (NVZ), the Tjörnes Fracture Zone (TFZ) and the Kolbeinsey Ridge (KR). The TFZ is a seismically active transform zone consisting of two parallel fault systems- the southern ~100 km-long right lateral strike slip Húsavík–Flatey fault (HFF), and the northern Grímsey fault, 40 km north of the HFF and shows both normal and strike-slip motions. Previous study suggests the moment accumulated on the HFF fault since the last major earthquake in 1872 can result in an earthquake with magnitude 6.8 to 7 (*Metzger and Jónsson*, 2014) and leaves the Húsavík community under potential seismic risk.

Physics-based probabilistic seismic hazard assessment (PSHA) has been used to make official national hazard maps, develop building code requirements, determine earthquake insurance rates, and other safety decisions. However, current PHSA are generally based on empirical, time-independent assumptions that are simplified and conflict with earthquake physics. To improve the PHSA, we need to have a good knowledge of the tomography, a three-dimensional (3D) geological structures and velocity model of the study region, together with accurate fault network geometries and appropriate stress and frictional parameters, etc. And in order to better estimate the seismic hazard scenarios and for engineering applications, the frequency of the wave field needs to be resolved up to 10 Hz. As part of the Centre of Excellence for Exascale in Solid Earth (CHEESE) project, we plan to run numerous multi-physics simulations, and use Bayesian approaches to provide a more reliable probabilistic-based hazard estimation in North Iceland. To achieve this goal, two software packages- SeisSol and ExaHype will be applied.

SeisSol, a dynamic rupture software package, is capable to model earthquakes with a high degree of realism. Using an Arbitrary High Order Derivative Discontinuous Galerkin (ADER-DG) method it solves seismic wave propagation (elastic, visco elastic) and dynamic rupture problems on heterogeneous 3D models with high-order accuracy in space and time. Complex fault geometries and topography are efficiently combined with the aid of unstructured adaptive tetrahedral meshes and three-dimensional velocity structures, and visco elastic attenuation effects are handled successfully. These high model complexities make it possible to deploy the software for realistic earthquake rupture simulations like no other. It has been successfully applicated to model the dynamic ruptures of the 2016 Mw 7.8 Kaikōura earthquake (*Ulrich et al.*, 2019), the most complex rupture that has been observed so far (Fig. 1).

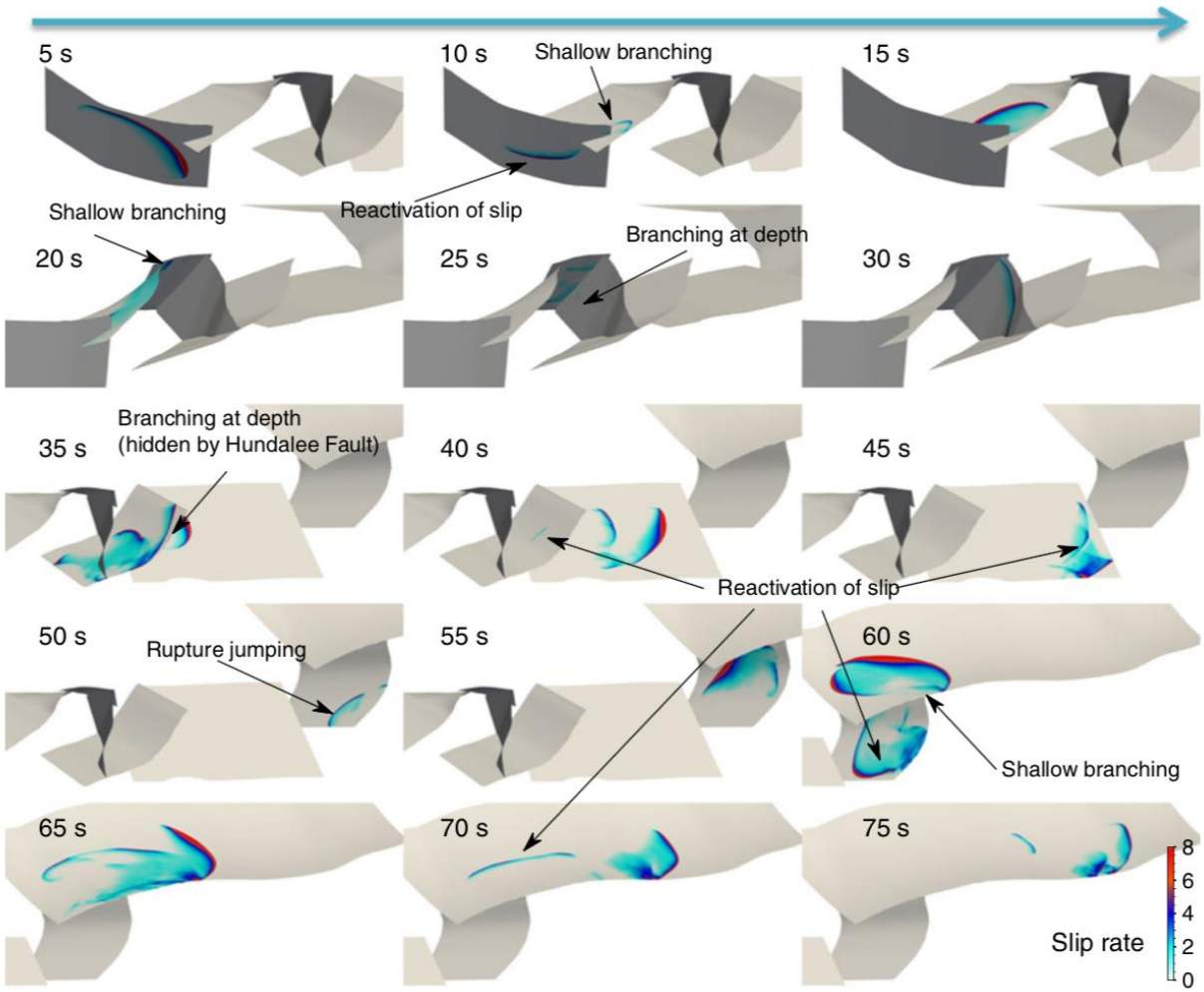

Figure 1. Overview of the simulated rupture propagation for the Kaikōura earthquake using SeisSol (Ulrich et al., 2019). Snapshots of the absolute slip rate are shown every 5 s.

ExaHyPE (Exascale High Performance Computing) focuses on the development of new mathematical and algorithmic approaches to exascale systems. Main objectives of the software are energy efficiency of supercomputer hardware and dynamically adaptive scalable algorithms. Within an adaptive mesh, the resolution of a simulation will be dynamically increased wherever it is necessary for the simulation. In this way, the greatest possible accuracy is achieved while the computer operations are kept to a minimum. Regional earthquake simulations promise to provide a fundamentally better understanding of what takes place during large-scale earthquakes and will help to quantify seismic hazards more accurately.

Our efforts will be integrated with on-going projects at LMU Munich. All developed software, workflow and analysis tools will be linked into on-going international research activities in computational seismology and earthquake source physics.

We will use the 3D dynamic rupture model for the HFF, with geometrically complex fault systems that Mirjam Weingärtner built in her master study as a start point. In this model, the depth of the fault segments is set to 6.3 km, while the locking depth of the HHF increasing from the east to the west has been observed (*Metzger et al.*, 2011), which may be the results of the lower thermal gradients in the west (*Flóvenz and Sœmundsson*, 1993). In the CHEESE project, we are going to use more local earthquake with less location uncertainties and recent tomography results (*Abril et al.*, 2016) to have

better constrain the fault geometries, the locking depth, and the 3D velocity models to implement in SeisSol. Stress distributions and variations, with their uncertainties can also be inferred from the local or regional earthquake focal mechanisms (*Townend et al.,* 2012). In addition, recent study shows clockwise declination deflections are largest near the HFF, and the deflections vary with distance from the fault, which imply the effect of off-fault deformation (*Titus et al.,* 2018). Thus, the off fault plasticity will be implemented in our dynamic modeling. Besides, the site effect, which shows strong spatial variations on the ground-motion amplitudes in Húsavík (*Rahpeyma et al.,* 2019), will also be incorporated in the PSHA. All those improvements can contribute to a more reliable seismic hazard estimation in the North Iceland.

References

Abril, C., A. Tryggvason, O. Gudmundsson, IMO-SIL Monitoring Group, NICE Gropu, Revisited local earthquake tomography in the Tjörnes Fracture Zone. In *Proceedings to the 2nd International Workshop on Earthquakes at North Iceland*, Húsavík Academic Centre, 32-34, 2016.

Flóvenz, Ó. and K. Sæmundsson, Heat flow and geothermal processes in Iceland, *Tectonophys.*, **255(1-2)**, 123-138, 1993.

Metzger S., S. Jónsson, and H. Geirsson, Locking depth and slip-rate of the Húsavík Flatey fault, North Iceland, derived from continuous GPS data 2006-2010. *Geophys. J. Int.*, **187**, 564-567, 2011.

Metzger, S., and S. Jónsson, Plate boundary deformation in North Iceland during 1992-2009 revealed by InSAR time-series analysis and GPS, *Tectonophysics*, **634**, 127-138, 2014.

Rahpeyma, S., B. Halldorsson, B. Hrafnkelsson, R.A. Green & S. Jónsson, Site effect estimation on two Icelandic strong-motion arrays using a Bayesian hierarchical model for the spatial distribution of earthquake peak ground acceleration. *Soil Dynamics and Earthquake Engineering*, **120**, 369-385, 2019.

Titus, SJ, W. Chapman, A.J. Horst, M. Brown M., & J.R. Davis, Distributed deformation in oceanic transform system: Applying statistical tools to structural and paleomagnetic data near the Húsavík-Flatey Fault, Northern Iceland, *Tectonics*, **37(10)**, 3986-4017, 2018.

Townend, J., S. Sherburn, R. Arnold, C. Boese & L. Woods, Three-dimensional variations in present-day tectonic stress along the Australia–Pacific plate boundary in New Zealand. *Earth Planet. Sci. Lett.*, **353–354**, 47–59, 2012.

Ulrich, T., A.A. Gabriel, J.P. Ampuero & W. Xu, Dynamic viability of the 2016 Mw 7.8 Kaikōura earthquake cascade on weak crustal faults. *Nature Communications*, **10(1)**, 1213, 2019.

NORTHQUAKE 2019 - The 3rd International Workshop on Earthquakes in North Iceland
Húsavík, North Iceland, 21-24 May 2019

AN OVERVIEW OF THE NORTH ANATOLIAN FAULT ZONE AND 3D CRUSTAL STRUCTURE OF WESTERN TURKEY BASED ON FULL-WAVEFORM TOMOGRAPHY

Yeşim Çubuk-Sabuncu[1], Tuncay Taymaz[2], and Andreas Fichtner[3]

[1]*Icelandic Meteorological Office, Iceland (yesim@vedur.is).*
[2]*Istanbul Technical University, Department of Geophysical Engineering, Turkey (taymaz@itu.edu.tr).*
[3]*ETH-Zurich, Department of Earth Sciences, Switzerland (andreas.fichtner@erdw.ethz.ch).*

Intense seismic activity and crustal deformation are observed in W-NW Turkey due to transition tectonics between the strike-slip North Anatolian Fault Zone (NAFZ) and the N-S directed extensional regime of the Aegean region. The NAFZ is a well-known 1600 km long continental right-lateral strike-slip fault that forms the northern tectonic boundary of the Anatolian Plate (Fig. 1). The fault zone originates from the Karlıova triple junction in the east and extends towards the Aegean Sea and mainland Greece. The NAFZ bifurcates into three fault branches (the Northern, the Middle and the Southern Branches) in the Marmara Region, where devastating earthquakes (e.g. 1999 Izmit M_w=7.4) cause significant seismic hazard in the region. The complex tectonic framework, including the extension of the NAFZ beneath the Marmara Sea, is still not well understood. Therefore, seismic imaging of the crust and upper mantle beneath western Turkey is crucial in order to obtain a better understanding of the regional seismotectonics. We investigate the 3-D seismic velocity structure in this rapidly deforming region using non-linear full-waveform tomography based on the adjoint method (*Çubuk-Sabuncu et al.*, 2017).

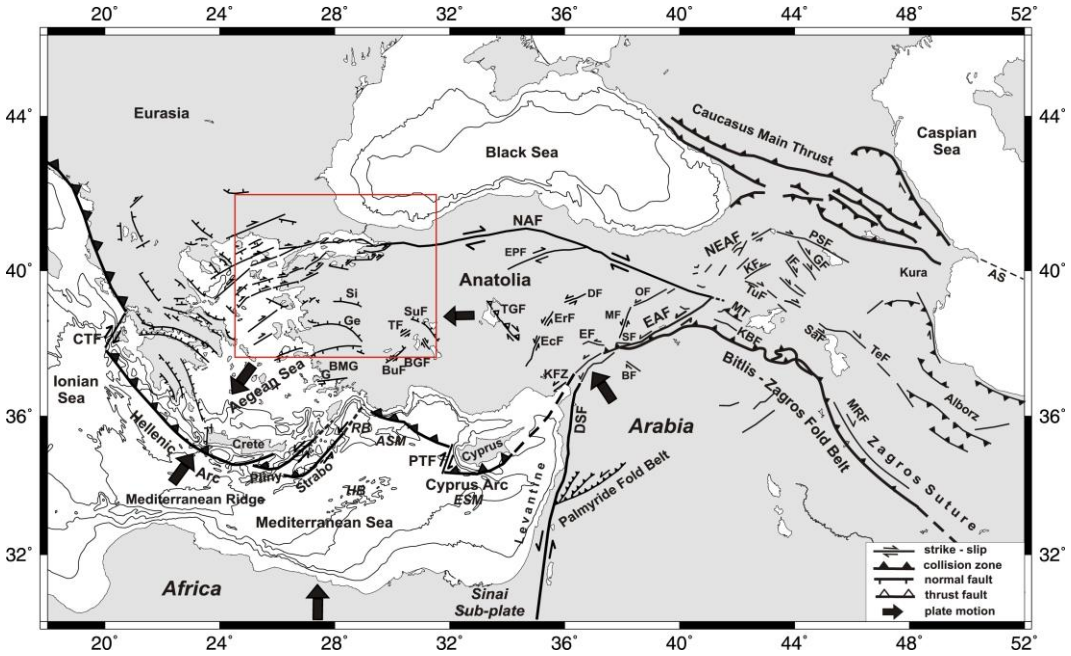

Figure 1. Active tectonic boundaries in the study area and surroundings, compiled from Mascle and Martin (1990), Taymaz et al. (1990, 1991), Saroğlu et al. (1992), Taymaz and Price (1992), Taymaz (1996), Aksu et al. (2008), Hall et al. (2008), Yolsal (2008), Yolsal-Çevikbilen and Taymaz (2012), Yolsal-Çevikbilen et al. (2014).

We select and simulate complete waveforms of 62 earthquakes ($M_w > 4.0$) that occurred from 2007-2015 at a maximum epicentral distance of 10°. Three-component data are obtained from broadband seismic stations of the Kandilli Observatory and Earthquake Research Center (KOERI, Turkey), the Hellenic Unified Seismic Network (HUSN, Greece) and the National Earthquake Research Center of Turkey (AFAD). To maximize tomographic resolution, we exploit all seismic phases, including body waves, surface waves and interfering phases on all three components. We filter observed and synthetic data between 0.01–0.125 Hz (8–100 s), which allows us to jointly resolve crustal and uppermost mantle structure. While body and surface waves at 8-50 s period are mostly sensitive to crustal heterogeneities, surface waves at 30-100 s period mostly constrain upper-mantle structure (*Fichtner et al.,* 2013a-b).

The spectral-element solver of the wave equation SES3D is used to simulate seismic wave propagation in 3-D spherical coordinates (*Fichtner et al.,* 2009). Our modeling domain is discretized by 69´888 degree-4 elements, corresponding to a total of around 9 million grid points. The Large Scale Seismic Inversion Framework (LASIF) workflow tool is also used to perform full seismic waveform inversion (*Krischer et al.,* 2015). The initial 3-D Earth model is implemented from the multi-scale seismic tomography study of *Fichtner et al.* (2013a-b). Discrepancies between observed and simulated synthetic waveforms are quantified using time- and frequency-dependent phase misfits, which enable a separation of phase and amplitude information (*Fichtner et al.,* 2008). The conjugate gradient optimization method is used to iteratively update the initial P velocity, SH velocity, SV velocity, and density models. The sensitivity kernels needed in the conjugate-gradient iteration were computed with the help of adjoint techniques (*Tarantola,* 1984; *Liu and Tromp,* 2006; *Fichtner et al.,* 2006a-b). We performed a resolution analysis for our 3-D radially anisotropic Earth model following the random probing method developed by *Fichtner and van Leeuwen* (2015). Resolution analysis by random probing yields position- and direction-dependent resolution lengths, thus being less subjective and more quantitative than synthetic recovery tests. We observe that beneath the most densely covered regions horizontal resolution reaches around 20 km. The comparison of crustal thickness obtained in our model, with crustal thicknesses reported by previous receiver function studies also indicates a good vertical resolution (0.3-2 km difference beneath stations). In order to confirm the model predictability and efficiency, the final 3-D Earth model is tested using forward wave simulations of earthquakes ($M \geq 3.7$) that were not used during the inversion process. Consequently, our 3-D Earth model is found to be successful in predicting waveforms at various source-receiver orientations with different source properties, and the misfit for both the actual (χ=1.04) and validation (χ=1.14) datasets are significantly smaller than for the initial model (χ_0=1.39).

The final Earth model reliably reveals the 3-D variations of SH and SV velocities in the crust and uppermost mantle beneath the Sea of Marmara and W Turkey. Our results provide new insight into the complex tectonic evolution of the region that evolved due to interactions of subduction roll-back, continental collision, extensional and strike-slip tectonics, block rotations, young and former magmatism (Oligocene-Neogene), high rate of fracturing and large-scale metamorphism. Low shear wave velocity anomalies (2.55–3.2 km/s) are observed at upper and mid crustal depths beneath fault zones (e.g. NAFZ), within the tectonically active deep sedimentary basins (5 km) of the Sea of Marmara and in the Gulf of Saros (<15 km) (Fig. 2). Low velocity zones also tend to mark the outline of young volcanic areas and partial melts within the crust (e.g., Kula Volcanic Province, Simav), in agreement with the high heat flow values (e.g. 220 mWm^{-2}) in the significant geothermal areas. Shear wave velocities are increased at mid-to-lower crustal depth and resolved low-velocity zones are within the reported seismogenic depths (15 km). Striking high-velocity features (>3.3 km/s) are found beneath the Menderes (Ge, BMG),

Kazdağ (BP) and Strandja (SM) massifs at all crustal depths, reflecting the high metamorphic composition beneath those regions. We also present vertical depth sections extracted from the 3-D absolute isotropic S-wave velocity model. Most vertical profiles display striking Moho undulations beneath W Turkey. Radial anisotropy is very strong (~20%) throughout the heavily fractured crust, further attesting to strong deformation and heterogeneity due to westward extrusion of the Anatolian Plate along the North Anatolian transform fault and extension in the Aegean. The regional-scale 3-D velocity model obtained in this study further refines the first-generation multi-scale Collaborative Seismic Earth Model of *Fichtner et al.* (2018).

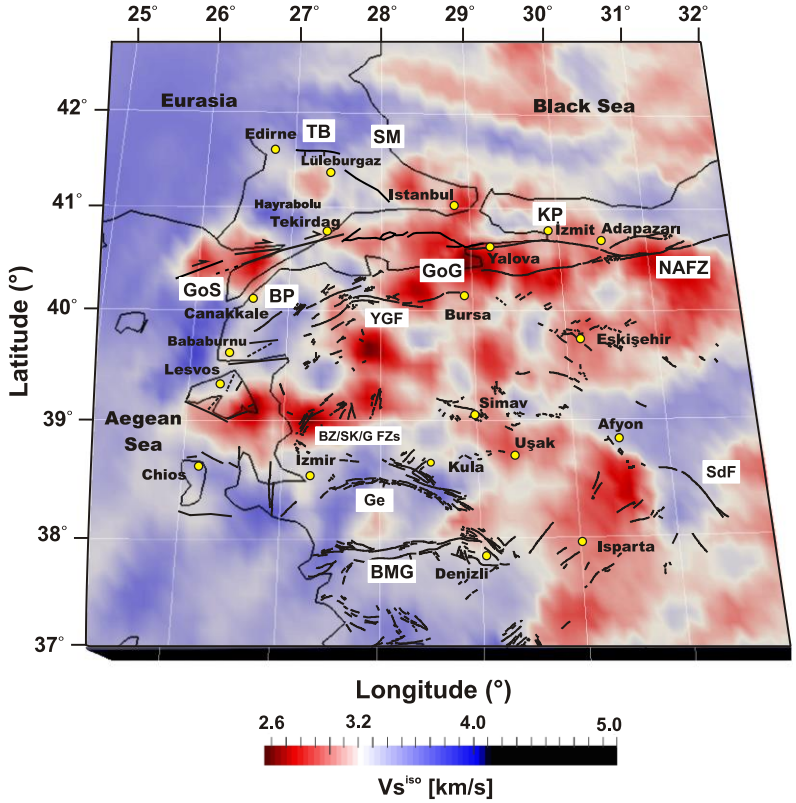

Figure 2. Isotropic S- wave velocity (V_S^{iso}) distributions (at 5 km depth) over major faults and geologic structures located in the study area. Thin black lines represent regional faults reported by Şaroğlu et al. (1992) and Le Pichon et al. (2001). Locations of several cities are marked with yellow circles. Abb: BMG: Büyük Menderes Graben, BP: Biga Peninsula, BZ: Bergama-Zeytindağ Fault Zone, Ge: Gediz Graben, GF: Gelenbe Fault Zone, GoG: Gulf of Gemlik, GoS: Gulf of Saros, KP: Kocaeli Peninsula, NAFZ: North Anatolian Fault Zone, SdF: Sultandağı Fault, SM: Strandja Massif, SK: Soma-Kırkağaç Fault Zone, TB: Thrace Basin, YGF: Yenice Gönen Fault Zone.

This study is supported by Istanbul Technical University Research Fund-ITU-BAP Project, the Scientific and Technological Research Council of Turkey (TUBITAK), EU–HORIZON-2020: COST Actions: Earth System Science and Environmental Management: ES1401-Time Dependent Seismology TIDES-STSMs (Short Term Scientific Missions), and the Alexander von Humboldt Foundation follow-up programme. We gratefully acknowledge support by the Swiss National Supercomputing Centre (CSCS) for allowing us to use the Piz Daint cluster.

References

Aksu, A.E., J. Hall, C. Yaltırak, Miocene-recent evolution of Anaximander mountain and Finike Basin at the junction of Hellenic and Cyprus Arcs, Eastern Mediterranean. *Marine Geol.*, **258**, doi:10.1016/j.margeo.2008.04.008, 2008.

Çubuk-Sabuncu Y., *3D Velocity structure for the sea of Marmara and surrounding region (NW Turkey) by using full waveform tomography*, Ph.D. Thesis, 342 pages, Istanbul Tech. Univ., Graduate School of Inst. of Sci. and Tech., Istanbul, Turkey (Supervisor: Prof. Dr. Tuncay Taymaz in collaboration with Prof. Dr. Andreas Fichtner), 2016.

Çubuk-Sabuncu, Y., T. Taymaz, and A. Fichtner, 3-D Crustal velocity structure of western Turkey: Constraints from full-waveform tomography. *Physics of the Earth and Planetary Interiors*, **270**, 90-112, 2017.

Fichtner, A., and T. van Leeuwen, Resolution analysis by random probing. *J. Geophys. Res., Solid. Earth*, **120**. http://dx.doi.org/10.1002/2015JB012106, 2015.

Fichtner, A., H.P. Bunge, and H. Igel, The adjoint method in seismology – I. Theory. *Phys. Earth Planet. Int.*, **157**, 86–104, 2006a.

Fichtner, A., H.P. Bunge, and H. Igel, The adjoint method in seismology – II. Applications: traveltimes and sensitivity functionals. *Phys. Earth Planet. Int.*, **157**, 105–123, 2006b.

Fichtner, A., B.L.N. Kennett, H. Igel, and H.P. Bunge, H.P., Theoretical background for continental- and global-scale full-waveform inversion in the time–frequency domain. *Geophys. J. Int.*, **175**, 665–685, 2008.

Fichtner, A., B.L.N. Kennett, H. Igel, and H.P. Bunge, H.P., Full seismic waveform tomography for upper-mantle structure in the Australasian region using adjoint methods. *Geophys. J. Int.*, **179**, 1703–1725, 2009.

Fichtner, A., J. Trampert, P. Cupillard, E. Saygin, T. Taymaz, Y. Capdeville, and A. Villaseñor, Multiscale full waveform inversion. *Geophys. J. Int.*, **194**, 534–556. http://dx.doi.org/10.1093/gji/ggt118, 2013a.

Fichtner, A., E. Saygin, T. Taymaz, P. Cupillard, Y. Capdeville, and J. Trampert, The deep structure of the North Anatolian Fault Zone. *Earth Planet. Sci. Lett.*, **373**, 109–117. http://dx.doi.org/10.1016/j.epsl.2013.04.027, 2013b.

Fichtner A., D.P. van Herwaarden, M. Afanasiev, S. Simuté, L. Krischer, Y. Çubuk-Sabuncu, T. Taymaz, L. Colli, E. Saygin, A. Villaseñor, J. Trampert, P. Cupillard, H.P. Bunge, and H. Igel, The collaborative seismic earth model: generation 1, *Geophys. Res. Lett.*, **45**, doi:10.1029/2018GL077338, 2018.

Hall, J., A.E. Aksu, C. Yaltırak, and J.D. Winsor, Structural architecture of Rhodes basin: A deep depocentre that evolved since the Pliocene at the junction of Hellenic and Cyprus Arcs, Eastern Mediterranean. *Marine Geol.* **258**, http://dx.doi.org/10.1016/ j.margeo.2008.02.007, 2008.

Krischer, L., A. Fichtner, S. Zukauskaite, and H. Igel, Large scale seismic inversion framework. *Seismol. Res. Lett.* **86(4),** 1198–1207. http://dx.doi.org/10.1785/0220140248, 2015.

Le Pichon, X., A.M.C. Şengör, E. Demirbağ, C. Rangin, C. İmren, R. Armijo et al., The active main Marmara fault, *Earth Planet. Sci. Lett.*, **192**, 595–616, 2001.

Liu, Q., and J. Tromp, Finite-frequency kernels based on adjoint methods. *Bull. Seis. Soc. Am.*, **96**, 2383–2397, 2006.

Mascle, J., and L. Martin, Shallow structure and recent evolution of the Aegean Sea: a synthesis based on continuous reflection profiles. *Marine Geol.*, **94**, 271–299, 1990.

Saroglu, F., Ö. Emre, and I. Kusçu, Active Fault Map of Turkey. 2 Sheets, General Directorate of Mineral Research and Exploration – GDMRAE, Ankara, Turkey, 1992.

Tarantola, A., Inversion of seismic reflection data in the acoustic approximation. *Geophysics*, **49**, 1259–1266, 1984.

Taymaz, T., S-P-wave travel-time residuals from earthquakes and lateral inhomogeneity in the upper mantle beneath the Aegean and the Aegean Trench near Crete. *Geophys. J. Int.*, **127**, 545–558, 1996.

Taymaz, T., and S. Price, The 1971 May 12 Burdur earthquake sequence, SW Turkey: a synthesis of seismological and geological observations. *Geophys. J. Int.* 108, 589–603, 1992.

Taymaz, T., J. Jackson, and D. McKenzie, Active tectonics of the north and central Aegean sea. *Geophys. J. Int.* **106**, 433–490, 1991.

Taymaz, T., J.A. Jackson, and R. Westaway, Earthquake mechanisms in the Hellenic Trench near Crete. *Geophys. J. Int.* **102**, 695–731, 1990.

Yolsal, S., *Source mechanism parameters and slip distributions of Crete-Cyprus arcs, Dead Sea Transform fault earthquakes and historical tsunami simulations.* Ph.D. Thesis, 523 pages, Graduate School of Institute of Science and Technology, Istanbul Technical University, Istanbul, Turkey (Supervisor: Prof. Dr. Tuncay Taymaz), 2008.

Yolsal-Çevikbilen, S., and T. Taymaz, Earthquake source parameters along the Hellenic subduction zone and numerical simulations of historical tsunamis in the Eastern Mediterranean. *Tectonophysics* **536–537**, 61–100, 2012.

Yolsal-Çevikbilen, S., T. Taymaz, and C. Helvacı, Earthquake mechanisms in the Gulfs of Gökova, Sıgacık, Kusadası, and the Simav Region (western Turkey): Neotectonics, seismotectonics and geodynamic implications, *Tectonophysics*, **635**, 100–124, 2014.
http://dx.doi.org/10.1016/j.tecto.2014.05.001.

NORTHQUAKE 2019 - The 3rd International Workshop on Earthquakes in North Iceland
Húsavík, North Iceland, 21-24 May 2019

GROUNDWATER MONITORING AT HÚSAVÍK AND HAFRALÆKUR, N ICELAND

Gabrielle Stockmann[1], Alasdair Skelton[2], Erik Sturkell[3], Ríkey Kjartansdóttir[1], Andri Stefánsson[1], Heike Siegmund[2], and Hreinn Hjartarson[4]

[1] *Institute of Earth Sciences, University of Iceland (gabrielle@hi.is, rikey@hi.is, as@hi.is)*
[2] *Department of Geological Sci., Stockholm Univ., Sweden (alasdair.skelton@geo.su.se, heike.siegmund@geo.su.se)*
[3] *Department of Earth Sciences, University of Gothenburg, Sweden (erik.sturkell@gvc.gu.se)*
[4] *Landsvirkjun, Iceland (Hreinn.Hjartarson@landsvirkjun.is)*

Two boreholes in North Iceland have been monitored for groundwater changes on a weekly basis since 2002 and 2008, respectively. One borehole, HU-01 is located close to the town of Húsavík, whereas the other borehole, HA-01 is located close to the school in Hafralækur (Fig. 1).

Figure 1. Map showing the Tjörnes peninsula in northern Iceland and the location of the two boreholes, HU-01 and HA-01. Source: Andrén et al. (2016).

The water is sampled by Hreinn Hjartarson from Landsvirkjun, who measures the temperature and pH shortly after sampling and takes care of the shipping of samples to the University of Iceland

where part of the water analysis is done. Once per month he brings samples to the Krafla power plant, where geochemist Júlía K. Björke measures the CO_2 and H_2S contents of the water samples. At the University of Iceland, the samples are analysed for major cations and anions. Other non-acidified samples are sent to Stockholm University in Sweden, where the stable isotope $\partial^{18}O$ and $\partial^{2}H$ are being analysed. The long time series thus obtained have provided a unique data set that has shown remarkable groundwater changes that coincide and even precede the two major earthquake swarms in September-October 2012 and April 2013, respectively. They also allow for statistical treatment of the data describing the likelihood of such groundwater changes coinciding with earthquakes as was recently presented by *Skelton et al.* (2019). Here we present the updated time series for the two boreholes together with the main conclusions of the results obtained so far.

Figure 2 illustrates two examples of the development of cation concentrations with time for the borehole HA-01 near Hafralækur. The figure depicts how the concentrations of sodium (Na) and silica (Si) increase around the time of the abovementioned earthquake swarms, with the largest earthquakes for each swarm marked with a line and magnitude. Especially the changes in sodium stand out, both in % change and because the increase in concentration began 6-8 weeks before each earthquake swarm (*Skelton et al.,* 2014) indicating precursor signals. This was accompanied by changes in $\partial^{2}H$, which began as early as six months prior to the earthquakes (*Skelton et al.,* 2014).

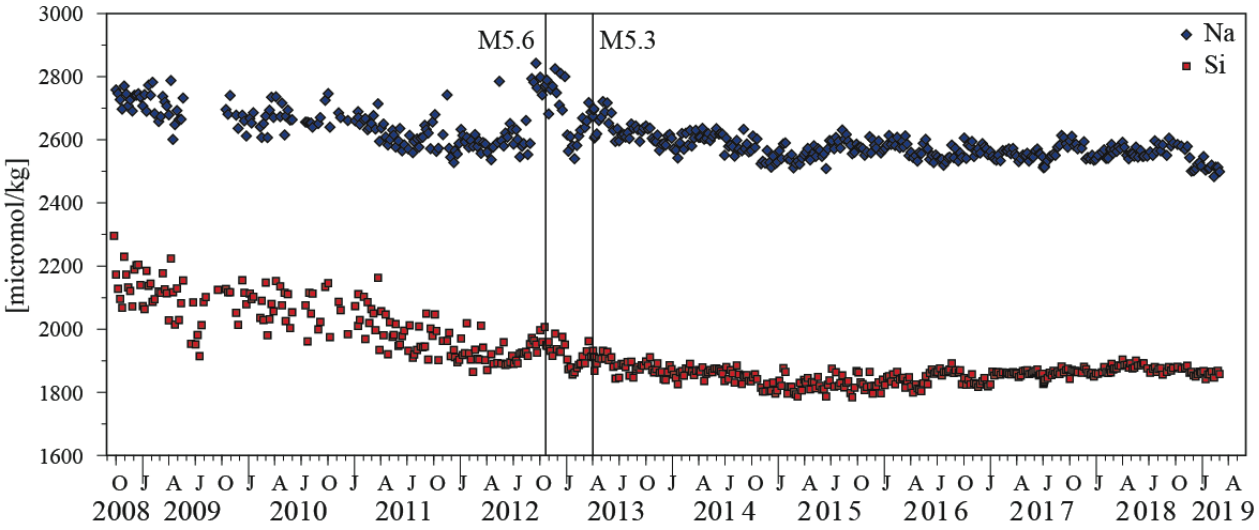

Figure 2. Changes in sodium (Na) and silica (Si) concentration with time for the borehole HA-01 at Hafralækur with the major earthquakes in 2012 and 2013 marked as M5.6 and M5.3, respectively.

Andrén et al. (2016) looked into the cause behind these (precursor) changes by combining the water chemistry data from borehole HA-01 with mineral data from drill cuttings obtained from nearby borehole HA-04 (Fig. 1). They proposed a model of incongruent dissolution of the zeolite mineral analcime ($NaAlSi_2O_6 \cdot H_2O$) preferentially releasing sodium into the groundwater prior to the earthquakes leading to the observed increase in concentration (Fig. 2). After the earthquakes, concentration falls back to a sort of normal state, which is interpreted as controlled by the replacement of labradorite by analcime. With the current data at hand, at least the cation data for HA-01 as shown on Figure 2 does not indicate that the current situation is similar to 2012-13. The data from 2013 onwards have been remarkably stable or shown a slight decrease in concentration. This again is interpreted as a long-term decrease of ion concentrations in response to secondary mineral precipitation along fractures and in vesicles in basalts (*Andrén et al., 2016).* The isotopic changes of $\partial^{18}O$ and $\partial^{2}H$ were assigned to a different

mechanism with mixing of aquifers leading to less negative isotope values. This implies that more modern groundwater seeps into the old Ice age groundwater normally found at the Hafralækur borehole.

The groundwater changes at Húsavík have been more difficult to monitor and interpret in recent years due to constructional changes at the borehole HU-01 site and due to pump failures. Whereas HA-01 is flowing artesian, the borehole HU-01 requires a pump to bring the water to the surface. Prior to the earthquakes in 2012-13, the pump broke and therefore no data is available around the critical time of the earthquakes from this borehole. What have previously been observed from this borehole are precursor signals in connection with the M5.8 earthquake on 16 September 2002. These were increased concentrations of certain metals (e.g. Cu, Zn, Mn, Cr) in the groundwater up to ten weeks prior to the earthquake (*Claesson et al.,* 2004, *Claesson et al.,* 2007). Isotope values of $\partial^{18}O$ and $\partial^{2}H$ were seen to be heavier before the earthquake and then return to lighter values equivalent to the isotope values we measure at the borehole today. The analytical procedure that is applied to the water samples nowadays does not include measurement of the trace elements described by *Claesson et al.* (2004), and it is therefore not currently possible to compare recent trace element data with the 2002 data. No further precursor changes have been observed from borehole HU-01 in Húsavík. However, post-earthquake changes have been observed on several occasions as described by *Wästeby et al.* (2014). They concluded it takes approximately eight years for earthquake-related fractures to 'heal', most likely as a consequence of secondary mineral precipitation sealing off fractures and freshly exposed rock surfaces.

In conclusion, unique time series of groundwater chemistry data from two boreholes in northern Iceland have allowed for a statistical assessment of coupling with earthquakes (*Skelton et al.,* 2019). An important conclusion of this study is that, even if we can state that a future earthquake will probably be preceded and/or followed by one or more hydrochemical shifts, we cannot necessarily state that future hydrochemical shifts will probably be followed and/or preceded by earthquakes.

References

Andrén, M., Stockmann, G., Skelton, A., Sturkell, E., Mörth, C-M., Guðrúnardóttir, H. R., N. S. Keller, N.S., Odling, N., Dahrén, B., Broman, C., Balic-Zunic, T., Hjartarson, H., Siegmund, H., Freund, F. and Kockum, I. Coupling between mineral reactions, chemical changes in groundwater and earthquakes in Iceland. *J. Geophys. Res.*, **121**, 2315–2337, 2016.

Claesson, L., Skelton, A.D.L., Graham, C.M., Dietl, C., Mörth, M., Torssander, P. and Kockum, I. Hydrogeochemical changes before and after a major earthquake. *Geology* **32**, 641–644, 2004.

Claesson, L., Skelton, A., Graham, C., and Mörth, C-M. The timescale and mechanisms of fault sealing and water-rock interaction after an earthquake. *Geofluids* **7**, 427–440, 2007.

Skelton, A., Andrén, M., Kristmannsdóttir, H., Stockmann, G., Mörth, C-M., Sveinbjörnsdóttir, Á, Jónsson, S., Sturkell, E., Guðrúnardóttir, H. R., Hjartarson, H., Siegmund, H. and Kockum, I. Changes in groundwater chemistry before two consecutive earthquakes in Iceland. *Nature Geoscience* **7**, 752–756, 2014.

Skelton, A., L. Liljedahl-Claesson, N. Wästeby, M. Andrén, G. Stockmann, E. Sturkell, C.-M. Mörth, A. Stefansson, E. Tollefsen, H. Siegmund, N. Keller, R. Kjartansdóttir, H. Hjartarson and I. Kockum. Hydrochemical changes before and after earthquakes based on long term measurements of multiple parameters at 2 sites in northern Iceland - a review. *J. Geophys. Res.,* **124**, 2702-2720, doi: 10.1029/2018JB016757, 2019.

Wästeby, N., Skelton, A., Tollefsen, E., Andrén, M., Stockmann, G., Claesson Liljedahl, L., Sturkell, E. and Mörth, M. Hydrochemical monitoring, petrological observation, and geochemical modeling of fault healing after an earthquake. *J. Geophys. Res.,* **119**, 5727–5740, 2014.

NORTHQUAKE 2019 - The 3rd International Workshop on Earthquakes in North Iceland
Húsavík, North Iceland, 21-24 May 2019

CREATING A MONITORING NETWORK FOR STUDYING HYDROLOGICAL CHANGES IN RELATION TO EARTHQUAKES. PROJECT STATUS.

Helga Rakel Guðrúnardóttir[1], Heiko Woith[2], Daniel Müller[2], and Remi Matrau[3]

[1] *Hobby Scientist (helga.rakel.gudrunardottir@gmail.com)*
[2] *GFZ German Research Center for Geosciences (heiko.woith@gfz-potsdam.de, dmueller@gfz-potsdam.de)*
[3] *King Abdullah University of Science and Technology (KAUST), Saudi Arabia (remi.matrau@kaust.edu.sa)*

A project to create a monitoring network for studying hydrological changes in relation to earthquakes in the Tjörnes Fracture Zone (TFZ) has been ongoing for a few years. A possible plan for an extensive network of monitoring stations covering the entire TFZ from Kópasker to Skagafjörður was put forward three years ago (*Guðrúnardóttir*, 2016). The aim was to significantly increase borehole monitoring efforts after promising chemical changes were detected in a couple of boreholes that could be correlated with significant earthquakes in the area (*Skelton et al.*, 2014).

While the network plans presented three years ago have not yet materialized, some steps have been taken to increase monitoring in boreholes in North Iceland. These include two field trips that were carried out to look more closely for possible boreholes to use for monitoring. In the August 2017 field trip, the focus was on the area around Húsavík, Tjörnes Peninsula and near Kópasker. We did some water-level measurements and looked at how suitable the boreholes were with respect to road access, security and access to electricity. A few interesting boreholes were identified while several other boreholes were deemed unsuitable.

In August 2018 we visited new boreholes that had been drilled on Tjörnes Peninsula a few months earlier. There we installed three new water-level loggers that collect measurements on water-level (pressure) and temperature, with one of the loggers also measuring conductivity. Two of the selected boreholes are new and one is an older borehole that we already looked at in 2017. All these boreholes are 3" wide, around 60 m deep and have around 3 m of casing. The measurement devices installed are Divers from vanEssen Instruments and are set up to collect measurements every 10 minutes that are stored in an internal memory. While these measurements are only thought of as temporary data collection and the Divers will only collect data for a few months, the preliminary results can show how the boreholes behave, before permanent equipment is installed that would send data continuously for real-time monitoring and analysis.

These field trips are quite important as the data from the borehole database cannot be used on its own to make decisions on which boreholes are suitable to be part of the monitoring network. Several boreholes listed in the database are in fact lost under roads or landslides and several boreholes are not listed in the database. Local knowledge has thus proved to be quite valuable.

Data from the three water-level loggers installed on Tjörnes Peninsula in August of 2018 were downloaded in May 2019 and the preliminary results are presented here. Given the limited time since the data were collected, it must be stressed that proper data analysis remains to be done, including comparing the data to other environmental variables, such as Earth tides, rainfall and air temperature.

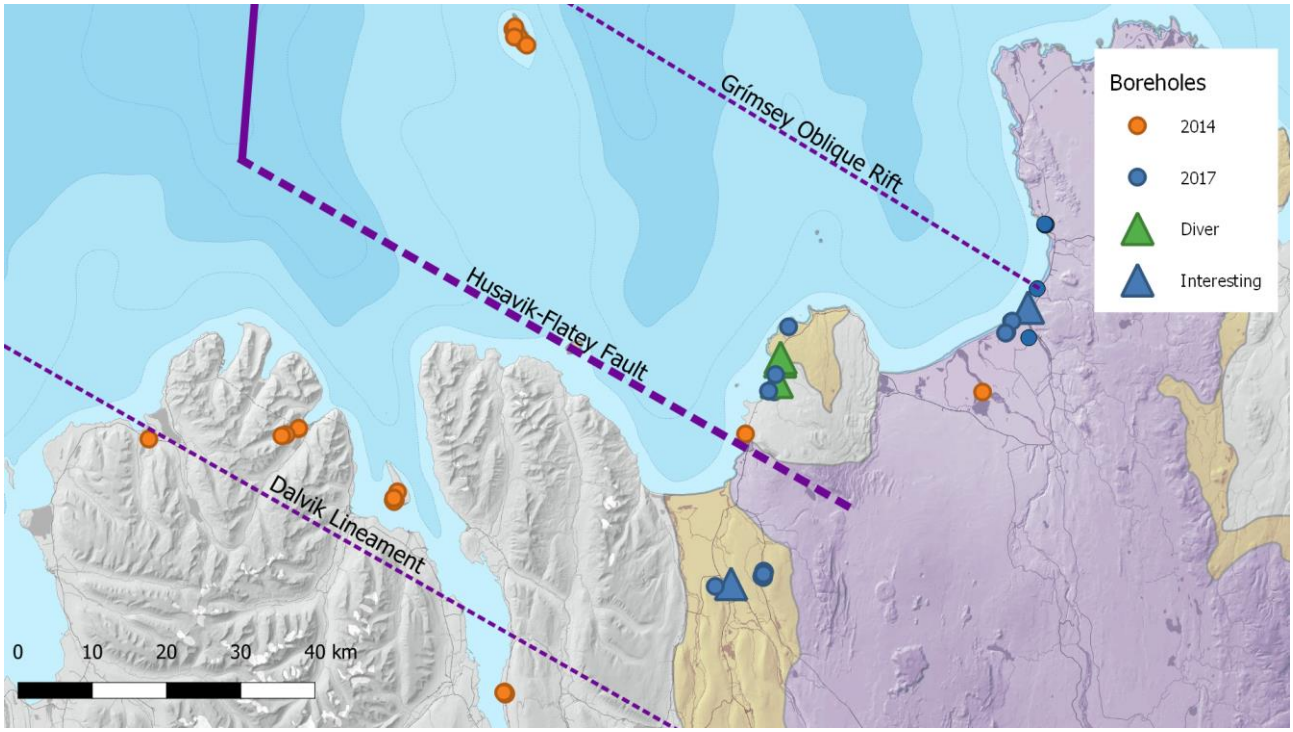

Figure 6 - Overview map of the Tjörnes Fracture Zone showing the boreholes visited in 2014 and 2017 and the location of the three water-level Divers installed in 2018. The yellow color show Plio-Pleistocene formations (3.3-0.3 My) and the purple color shows Upper Pleistocene formations (<0.7 My).

Figure 2 shows the water-level as the water column above the Diver measurement device in each borehole. The most dramatic changes were observed in borehole TJ-08, which is the northernmost borehole situated in a Plio-Pleistocene formation (3.3-0.3 My). Most noticeable are the two sharp increases in the water-level in borehole TJ-08 on 24 February 2019 at 00:40 and on 26 March 2019 at 12:50. These changes and other sharp increases in TJ-08 are marked with a yellow dotted line. Contemporary water-level increases are seen in the other two boreholes, TJ-04 and HV-01, although they appear less dramatic than in TJ-08. Also, the increases seem to show up a bit earlier in borehole TJ-04 and are not as sudden in HV-01.

To compare the water-level changes with earthquake occurrence during the same time period, we chose earthquakes of magnitude larger that 2 that occurred in the TFZ. The earthquake information was sourced from the IMO website weekly lists. At the first glance, there appears to be a clear correlation between the timing of some of the water-level increases and earthquake activity, indicated by the green dots in Figure 2. The three most active earthquake sequences, all seem to occur after water-level increase events. The earthquakes following the 8 November 2018 water-level event occurred near Grímsey at the distance of 40-60 km from TJ-08, while the earthquakes following the 24 February 2019 increase were in the Kolbeinsey area, at distances of over 93 km from the TJ-08 borehole. The earthquakes following the 26 March 2019 water-level event took place in the Kópasker area, about 30 km away from TJ-08.

The temperature data from borehole TJ-08 also shows two clear spikes (Fig. 3). These spikes have been marked with a red dotted line Figure 2-3. Both spikes happen as the water-level in borehole TJ-08 is rising rapidly. The first spike fits to the timing of the earthquakes near Kolbeinsey but the second spike does not seem to correspond to any earthquakes. However, at the same time as the second temperature spike is seen, the water-level in all the boreholes is rising (Fig. 2).

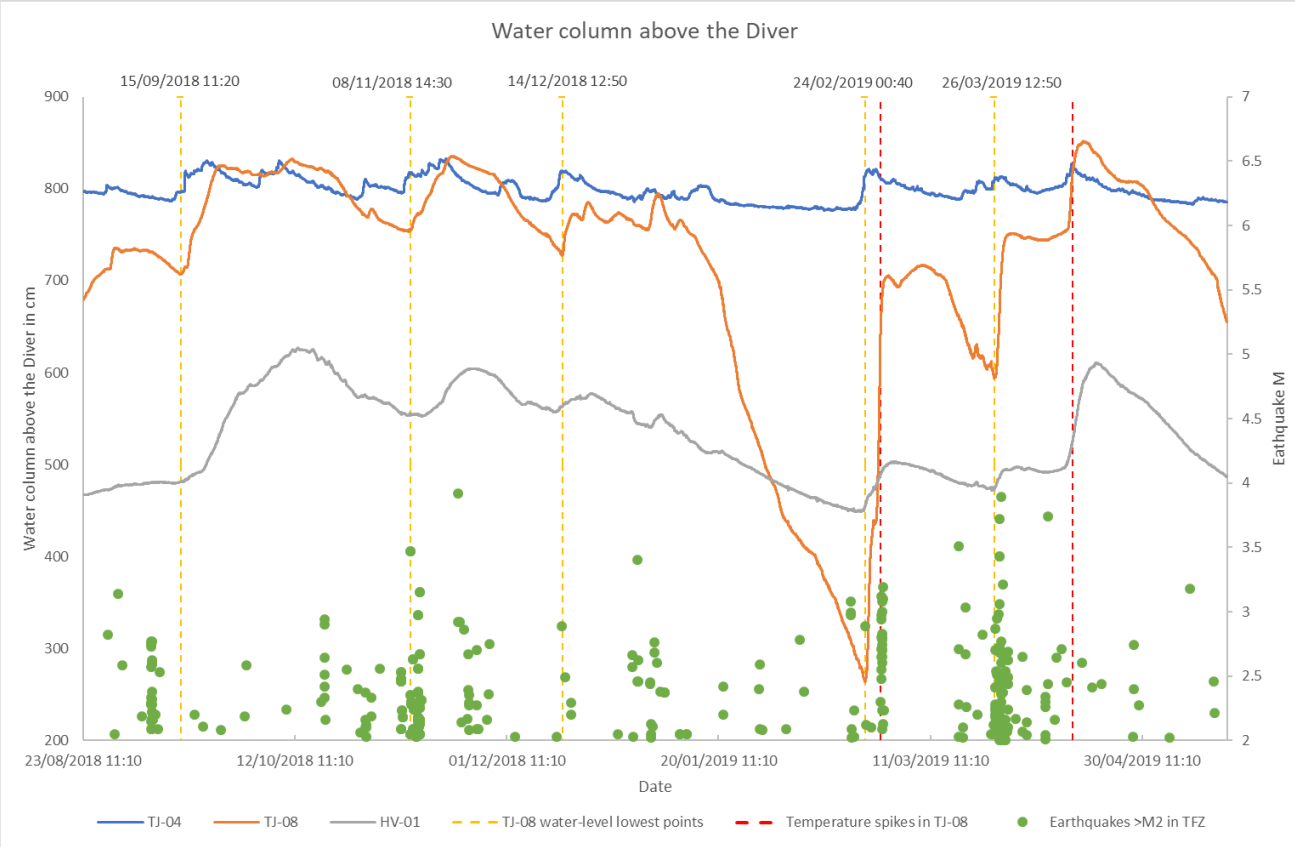

Figure 7 - Water-level in the three boreholes and earthquakes in the area. Yellow lines represent the lowest point in the water-level of TJ-08 before it starts to rise again. Exact time of this change is marked above the yellow lines. Red dotted line shows time of temperature spikes in TJ-08. Green dots represent earthquakes M>2 in the TFZ area.

In borehole TJ-04 the water temperature fluctuates more than in the other two boreholes. This borehole is located on the bank of a river stream in a small valley, near a small fracture showing signs of hydrothermal heat. However, even though the temperature in this borehole appears unstable, a clear drop in temperature can be seen on 24 February 2019, when a water-level rise event occurred.

While we can speculate about the borehole changes here and their correlation to earthquake activity, longer time-series and more data analysis are needed before drawing any solid conclusions about the possible correlation. In addition, further plans have been made to add more of these Divers in the Tjörnes Fracture Zone. Three more Divers are expected to be installed in the summer of 2019 and continued field work is also planned to identify the best boreholes for this project. The hope is that the Icelandic Met Office will in the future add data streamed from borehole Divers to their real-time multi-component monitoring. Therefore, one Diver-Link connection modem is planned to be installed in 2019 located at borehole TJ-08 to test real-time data transfer and analysis.

Acknowledgements

This project was started in cooperation between Stockholm University (SU), University of Akureyri (UNAK) and the Icelandic Meteorology Office (IMO), and was initially the basis for Helga Rakel Guðrúnardóttir's M.Sc. project in Geology at SU. However, Helga was not able to proceed with her studies at SU as planned due to an accident that resulted some physical disability. Despite this, she has kept the project alive and continued to work on it. Since 2016 the project has received support from KAUST and the GFZ German Research Centre for Geosciences.

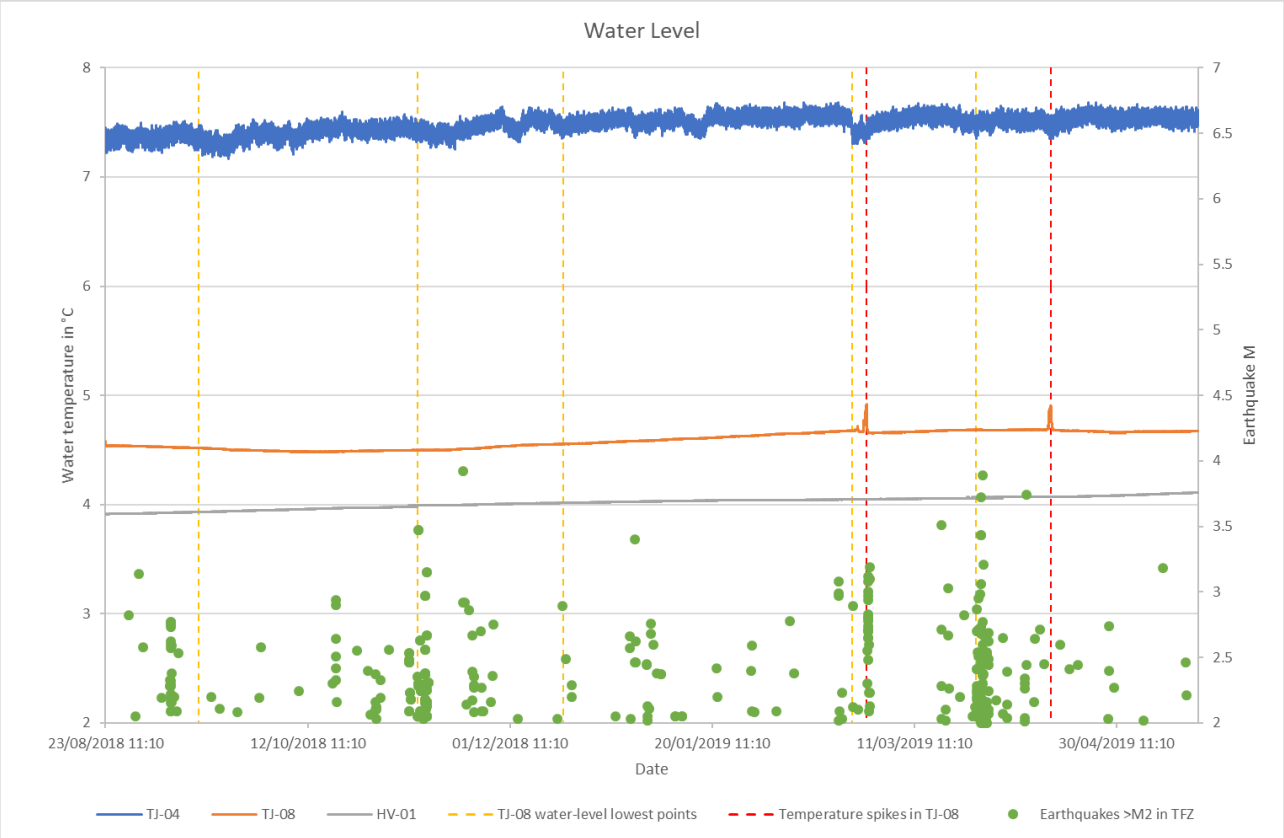

Figure 8 - Water temperature in °C in the three boreholes. Yellow lines represent the lowest point in the water-level of TJ-08 before it starts to rise again. Exact time of this change is marked above the yellow lines. Red dotted line shows time of temperature spikes in TJ-08. Green dots represent earthquakes M>2 in the TFZ area.

References

Guðrúnardóttir, H. R., Building a Monitoring Network for Studying Hydrological changes in Relation to Earthquakes, In *Proceedings to the 2nd International Workshop on Earthquakes in North Iceland*. Húsavík Academic Centre, 48-50, 2016.

Skelton, A., M. Andrén, H. Kristmannsdóttir et al., Changes in groundwater chemistry before two consecutive earthquakes in Iceland, Nature Geoscience, 7, 752-756, 2014.

NORTHQUAKE 2019 - The 3rd International Workshop on Earthquakes in North Iceland
Húsavík, North Iceland, 21-24 May 2019

AN UPDATE OF GPS MEASUREMENTS IN NORTH ICELAND

Sigurjón Jónsson[1], Rémi Matrau[1], Renier Viltres[1], Benedikt Ófeigsson[2]

[1]*King Abdullah University of Science and Technology (KAUST), Saudi Arabia (sigurjon.jonsson@kaust.edu.sa)*
[2]*The Icelandic Meteorological Office (IMO), Reykjavík, Iceland*

Observations of interseismic strain accumulation can put constraints on the average moment release rate of a fault zone and thus provide important information about seismic hazard. Past earthquakes also bring useful clues about expected level of activity, although locations and sizes of historical earthquakes are often uncertain. This is the case for the Tjörnes Fracture Zone (TFZ) in North Iceland where most large earthquakes occur offshore and historical accounts are limited. The earliest known earthquake in the TFZ took place near Flatey Island in 1262 and accounts contain about 30 significant events until 1900, as summarized in *Thorgeirsson (*2013). For the 20th century, the most complete information is in *Ambraseys and Sigbjörnsson* (2000). When the estimated moment of known large TFZ earthquakes during the past 300 years is added up (see Table 1 in *Jónsson* (2019) of this volume), it roughly corresponds to one magnitude 7 earthquake per century.

Earthquakes in North Iceland primarily occur on the Húsavík-Flatey Fault (HFF) and within the Grímsey Oblique Rift (*Einarsson*, 2008). These include the 1755 and 1872 earthquakes on the HFF and the 1910 and 1976 earthquakes in the GOR. In addition, several other large earthquakes have occurred in North Iceland outside of these two transform structures, e.g. the 1934 Dalvík and 1963 Skagafjörður earthquakes (*Stefánsson et al.,* 2008). This indicates that the transform motion in the TFZ, between the Northern Volcanic Zone in the southeast and the Kolbeinsey ridge in the northwest, is not all taken up by the HFF and the GOR, but that it is more distributed in the region.

To study interseismic strain accumulation in North Iceland and to assess how large portion of the relative motion appears to be focused on the two main lineaments (HFF and GOR), a campaign GPS network was installed in the area in 1995 (*Jouanne et al.,* 1999). This network has been remeasured and expanded several times during the past two decades (*Jouanne et al.,* 2006; *Metzger et al.* 2013). In particular, we improved the coverage of the network west of Akureyri in 2013 with a significant number of new stations on Tröllaskagi Peninsula (*Jónsson et al.,* 2016), to resolve possible strain southwest of the HFF and on the suggested Dalvík Lineament. The campaign GPS network has been occupied every three years during the last decade, i.e., in 2007, 2010, 2013, 2016, and 2019 and it now includes more than 80 survey sites (Fig. 1).

In addition to the campaign GPS network, ten continuous GPS stations (CGPS) were installed in North Iceland in 2006-7 (*Metzger et al.,* 2011) and added to the three CGPS stations that had been in operation since 2000-2002 (AKUR, ARHO, RHOF). Since then we have added stations SJUK and BAUG in Húsavík (in 2012), HELC in Eyjafjörður (in 2014), HRAC to the west and GJOG near Gjögurtá (in 2017, see Fig. 2), and most recently MANA in Mánáreyjar (in 2018, see Fig. 3). In addition, four stations near Mývatn, Krafla, and Theistareykir have been added by other parties, bringing the total number of CGPS stations in North Iceland to more than 20. The CGPS stations installed in 2006-7 were installed with Septentrio PolaRx2e GPS receivers and PolaNt antennas, while our later installations were equipped with Trimble NetR9 receivers and Zephyr Geodetic-2 antennas. Gradually, GPS receivers and

antennas of the older sites, including ARHO and RHOF, have been updated and now all our stations are operating with Trimble NetR9 receivers and Zephyr antennas (except GAKE and KOSK, which will be updated later in 2019). The stations collect data at both 1 s and 15 s intervals and data is transferred daily to the Icelandic Met Office, mostly via 3G modems. Together with the over 80 survey benchmarks, the North Iceland GPS network now contains over 100 GPS sites (Fig. 1).

Our previous results of GPS measurements (*Metzger et al.*, 2011; 2013) suggest that about 1/3 of the TFZ transfer motion is taken up by the HFF while the rest is likely mostly concentrated on the GOR. The results have also indicated that the locking depth of the HFF is roughly 6-10 km (*Metzger and Jónsson*, 2014), meaning that the moment accumulated on the HFF since the last large earthquakes of 1872, almost 150 years ago, likely corresponds to a magnitude 6.8-7.0 earthquake. Assuming similar parameters for the GOR, together the GOR and the HFF should produce earthquakes corresponding to a single magnitude 7.0-7.1 earthquake every 100 years, which is similar to what the historical earthquakes suggest. However, the earthquake occurrence can be highly non-uniform in time and influenced by major events, such as the Krafla rifting episode, which triggered the 1976 M_w6.3 Kópasker earthquake (*Passarelli et al.*, 2013), the last major earthquake in North Iceland, but put large part of the HFF into a stress shadow (*Maccaferri et al.*, 2013). Also, few events have been detected in fault trenches on the HFF, suggesting that the largest events on the HFF, possibly rupturing the entire fault, may be infrequent (*Harrington et al.*, 2016).

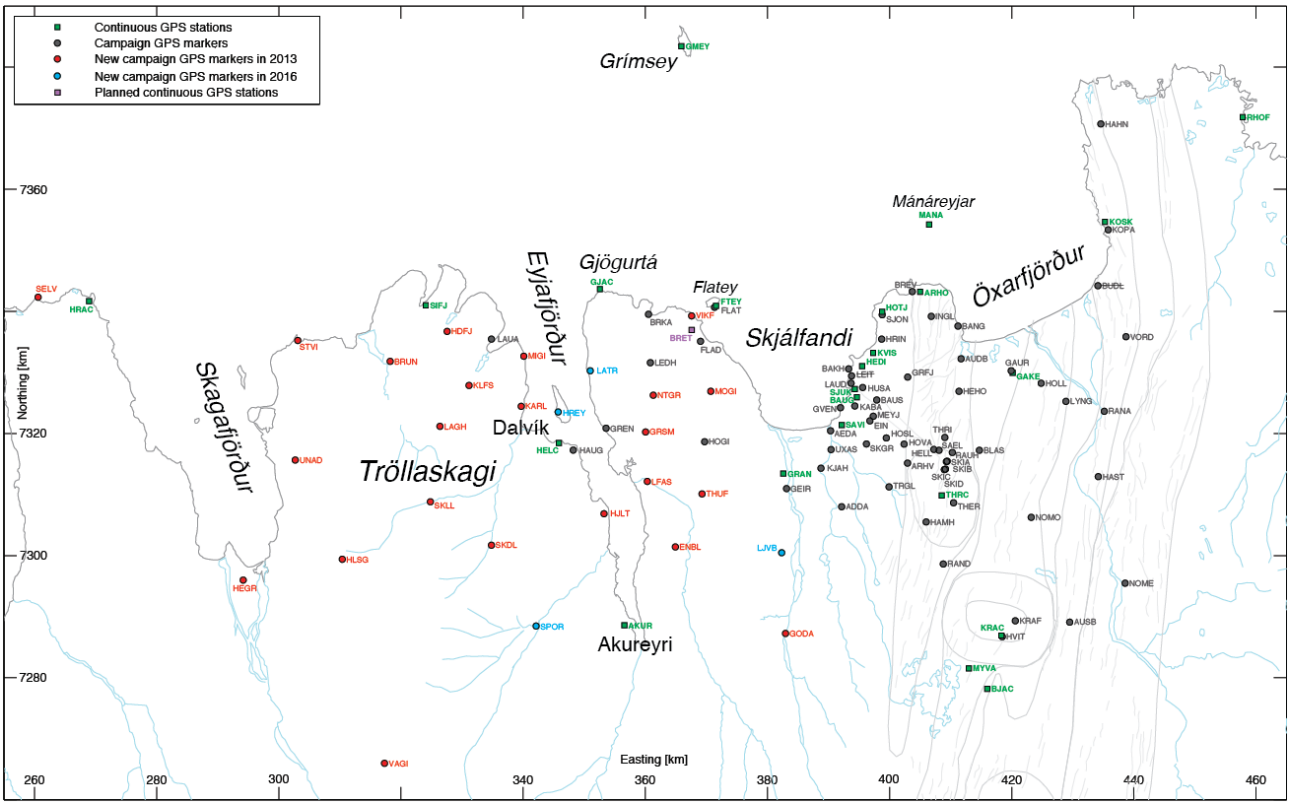

Figure 1. Map of campaign GPS survey sites (circles) and continuous GPS stations (green squares) in North Iceland. New survey sites added in 2013 and 2016 are labeled in red and light blue, respectively.

Figure 2. Photos of the CGPS station installation work at GJOC (left) near Gjögurtá. This isolated station is powered with a solar panel and a wind generator. On the right is the CGPS station HRAC located at the western edge of the network and close to an IMO seismic station.

Figure 3. The newest CGPS station in North Iceland is MANA on Lágey, one of the two islands in Mánáreyjar, installed in summer 2018. The photos were taken looking towards North (left) showing the antenna and the solar panel array used to power the station, and towards south (right) with Háey and the north coast in the background.

The CGPS station data is processed and used for monitoring at the IMO. As an example, we show the time series from the newest site MANA installed in 2018 (Fig. 3), which exhibits low noise level but a roughly 25-day long gap in January 2019 (Fig. 4), due to a power outage. As the station is located in a thriving puffin colony, we opted to install it without a wind generator and added more solar panels instead. However, the station still ran out of power in early January, due to the limited sun light at 66.298°N, which is only about 30 km south of the polar circle.

Another example of CGPS time series comes from station AKUR (Fig. 4). Here one can see a transient signal in late August 2014, which is during the large Bárðarbunga-Holuhraun intrusion (*Sigmundsson et al.*, 2015; *Ruch et al.*, 2016). The amplitude of the transient signal is about 5 mm to the north and 2-3 mm to west, indicating a northwesterly displacement of about 6 mm (Fig. 4). The opening of the emplaced dyke has been estimated to be ~5 m and the CGPS transients in north Iceland show that the intrusion had significant influence at distances of more than 200 km away from the intrusion, affecting all of North Iceland and beyond.

The next step in this project is to process the 2019 GPS survey data (survey in July-August, 2019), along with the data collected in 2016, 2013 and earlier surveys to produce an updated velocity field for North Iceland. These results will then be used to re-estimate the transfer-motion partition between the HFF and the GOR as well as the locking depth of the HFF. Our preliminary results show

that the velocity field is significantly improved with the addition of new surveys and that more complete picture of the strain on Tröllaskagi peninsula is emerging (*Matrau et al.*, 2018).

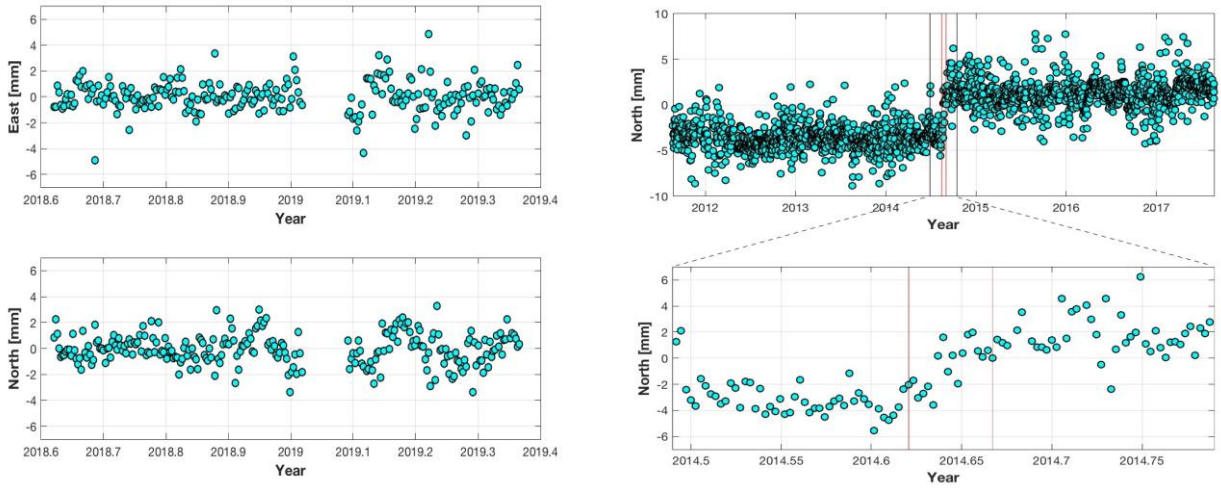

Figure 4. Time-series from the new MANA (left) CGPS site, East and North components, showing a gap in from 8 Jan. – 3 Feb., 2019, when it ran out of battery before the solar panels powered it back on in early February. Also shown is a detrended North component of station AKUR showing a ~5 mm transient signal due to the Bárðarbunga-Holuhraun intrusion. The red vertical lines mark 15 Aug. and 1 Sep., 2014, just before and after the main diking activity.

References

Ambraseys, N.N., and R. Sigbjörnsson. *Re-appraisal of the seismicity of Iceland*, Polytechnica – Engineering Seismology, 3, 183 pp, 2000.

Einarsson, P., Plate boundaries, rifts and transforms in Iceland, *Jökull* **58**, 35-58, 2008.

Harrington, J., U. Avsar, Y. Klinger, S. Jónsson & E.R. Gudmundsdottir, Fault trenching and geologic slip rates of the Húsavík-Flatey Fault, North Iceland, In: *Proc. to the 2rd workshop of earthquakes in North Iceland, 24-26*, 2016.

Jónsson, S., S. Metzger & B. Ófeigsson, Rate of moment accumulation on the Húsavík-Flatey Fault from GPS, In: *Proc. to the 2rd workshop of earthquakes in North Iceland, 17-19*, 2016.

Jónsson, S., Do large earthquakes in North Iceland usually occur in Winter? In: *Proceedings to the 3rd workshop of earthquakes in North Iceland* (this volume), 2019.

Jouanne, F., T. Villemin, V. Ferber, C. Maveyraud, J. Ammann, O. Henriot & J.L. Got, Seismic risk at the rift-transform junction in North Iceland, *Geophys. Res. Lett.*, **26**, 3689-3692, 1999.

Jouanne, F., T. Villemin, A. Berger & O. Henriot, Rift-transform junction in North Iceland: rigid blocks and narrow accommodation zones revealed by GPS 1997-1999-2002, *Geophys. J. Int.*, **167**, 1439-1446, 2006.

Maccaferri, F., E. Rivalta, L. Passarelli, and S. Jónsson. The stress shadow induced by the 1975-1984 Krafla rifting episode, *J. Geophys. Res.* **118**, doi:10.1002/jgrb.50134, 2013.

Matrau, R., S. Jónsson, S. Metzger, B. Ófeigsson & R. Viltres, Interseismic deformation of the Tjörnes Fracture Zone in North Iceland inferred from GPS, *Geophys. Res. Abstracts*, **20**, EGU2018-18872, 2018.

Metzger, S., S. Jónsson and H. Geirsson, Locking depth and slip-rate of the Húsavík Flatey fault, North Iceland, derived from continuous GPS data 2006-2010, *Geophys. J. Int.*, **187**, 564-576, 2011.

Metzger, S., S. Jónsson, G. Danielsen, S. Hreinsdóttir, F. Jouanne, G. Giardini, T. Villemin, Present kinematics of the Tjörnes Fracture Zone, North Iceland, from campaign and continuous GPS measurements, *Geophys. J. Int.* **192**, 441-455, 2013.

Metzger, S. and S. Jónsson, Plate boundary deformation in North Iceland during 1992-2009 revealed by InSAR time-series analysis and GPS, *Tectonophysics* **634**, 127-138, 2014.

Passarelli, L., F. Maccaferri, E. Rivalta, T. Dahm & E.A. Boku, A probabilistic approach for the classification of earthquakes as 'triggered' or 'not triggered'. *Journal of Seismology* **17**, 165-187, 2013.

Ruch, J., T. Wang, W. Xu, M. Hensch & S. Jónsson, Oblique rift opening revealed by reoccurring magma injection in central Iceland, *Nature Communications*, **7**:12352, DOI: 10.1038/ncomms12352, 2016.

Sigmundsson, F. et al., Segmented lateral dyke growth in a rifting event at Bárðarbunga volcanic system, Iceland, *Nature*, **517**, 191-195, 2015.

Stefánsson R., G.B. Gudmundsson and P. Halldórsson, Tjörnes fracture zone. New and old seismic evidences for the link between the North Iceland rift zone and the Mid-Atlantic ridge, *Tectonophysics* **447**, 117-126, 2008.

Thorgeirsson, Ó., *Historical earthquakes in North Iceland* (in Icelandic), Húsavík Academic Centre report, 54pp, 2011.

NORTHQUAKE 2019 - The 3rd International Workshop on Earthquakes in North Iceland
Húsavík, North Iceland, 21-24 May 2019

THE POTENTIAL USE OF SEAFLOOR GEODESY IN NORTH ICELAND

Halldór Geirsson[1], Vala Hjörleifsdóttir[2], Sigurjón Jónsson[3]

[1]*Institute of Earth Sciences, University of Iceland (hgeirs@hi.is)*
[2]*Reykjavík Energy, Iceland (vala.hjorleifsdottir@or.is)*
[3]*King Abdullah University of Science and Technology (KAUST), Saudi Arabia (sigurjon.jonsson@kaust.edu.sa)*

The plate divergence between the North-American and Eurasian plates in Iceland has been well recorded by continuous and campaign-style GPS observations, showing a full spreading rate of little less than 2 cm/year (*Geirsson et al.,* 2010; *Árnadóttir et al.,* 2009). The on-land part of the rift system links to the offshore Kolbeinsey Ridge north of Iceland through the mostly offshore Tjörnes Fracture Zone (TFZ), which consists of two main transform structures: the Húsavík-Flatey Fault (HFF) and the Grímsey Oblique Rift (GOR, *Einarsson et al.,* 2019). The mostly offshore location of the TFZ restricts GPS measurements to islands in the area (Flatey, Grímsey, and Mánáreyjar) and to on-land locations to the south of the TFZ (*Jónsson et al.,* 2019), providing only partial information about the plate-boundary deformation in this transform zone (*Metzger et al.,* 2011; 2013). To address this issue, we here discuss possible extensions of geodetic observations to the seafloor part of the TFZ.

In general, the same deformation processes that we observe on land are active offshore. These include: plate boundary processes, earthquake-related processes (co- and post-seismic deformation), magma-related processes (intrusions, reservoir pressure changes), loading and unloading of the crust (volcanic edifice changes, ocean loading, Glacio-Isostatic Adjustment), natural changes in hydrothermal systems, etc. To observe these processes, there exist several deformation measurement techniques that work offshore (Figure 1) and may hence be termed 'seafloor geodesy' (*Bürgmann & Chadwell*, 2014). Many of these techniques require long-term operation of instruments on the seafloor, which is challenging and expensive. Major issues for seafloor instrumentation include power, data transmission, and damage caused by bottom trawling for fishing.

Large-scale (dekameter-scale) topographical changes, such as due to new volcanic edifices, lava flows, landslide movements, or major faulting events, can be observed with multi-beam bathymetric mapping or side-scan sonar imaging (e.g., *Caress et al.,* 2012). *Maksymowicz* et al. (2017) obtained repeatability as low as approximately 2 m when using time-lapse multibeam to observe co-seismic offsets for the M8.8 Maule earthquake. However, quantification of topographical changes through DEM-differencing requires an adequate pre-existing DEM of the seafloor from before changes occur. Multi-beam bathymetric observations exist for the deeper parts of the TFZ (*Magnúsdóttir et al.*, 2015), but detailed mapping of the shallower parts is still lacking.

The simplest seafloor geodetic instrument is a pressure sensor, where changes in pressure are interpreted as vertical ground displacement after correcting for tidal motion and thermohaline effects on ocean density. The accuracy of pressure measurements depends somewhat on the timescale of the observations: for short-term changes (seconds to days), e.g., due to rapid inflation or faulting, the accuracy is high and the results useful (e.g., *Chadwick et al.,* 2012), but for longer-term observations (months to years) instrument drift and stability of the pressure sensor monument become an issue. Electronic tiltmeters can be deployed on the seafloor in a similar fashion as pressure sensors and can

provide useful information about vertical deformation, e.g., at volcanoes (*Nooner and Chadwick*, 2016). Typically, seafloor instruments are dropped to the bottom of the ocean, landing in soft

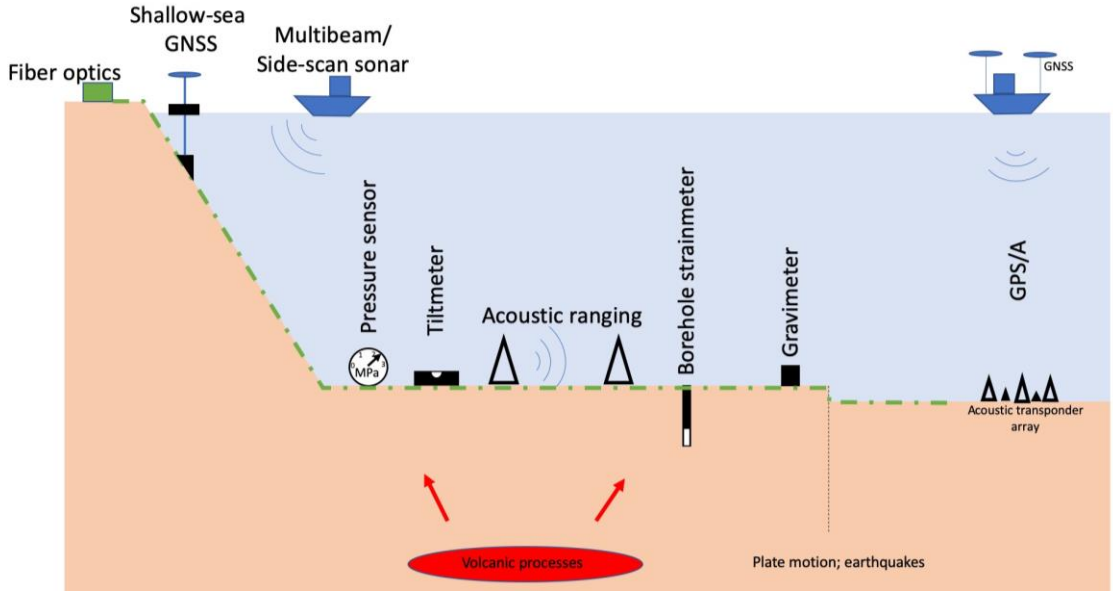

Figure 1. Summary of the different seafloor geodetic techniques.

sediments where it may take some time for the monument to settle in, however, it is also possible to bolt permanent monuments into fresh rock outcrops (*Nooner and Chadwick*, 2016). Furthermore, as the pressure sensors and tiltmeters only provide information about vertical deformation, they are more useful for detecting volcanic deformation than for measuring plate boundary deformation.

Another family of instruments is based on acoustic ranging, where the time delay between a submarine sound source and receiver is used as a measure of distance (e.g., *Petersen et al.*, 2019). Acoustic measurements need to be corrected for temporal variations in ocean temperature and salinity that both affect the speed of sound. In its most simple form, both the sound source and receiver are on the ocean floor and direct distance measurements (travel-time measurements) are made repeatedly. The measurement accuracy strongly depends on the length between the sound source and receiver, limiting practical baseline lengths within several km. Still, when installed across faults, this technique can be useful to detect fault creep or slip transients (*Urlaub et al.*, 2018). For another acoustic ranging technique called "GNSS-acoustic" (GPS/A or GNSS-A), which allows for 3-D displacement estimates, an array of 4-6 acoustic transponders are sunk to the ocean floor. A ship or an autonomous wave glider equipped with differential GNSS pings the acoustic transponder array to retrieve changes in position of the array with cm-scale precision. The Japanese coastguard has been performing GNSS-A measurements since the year 2000, revealing spectacular displacements of tens of meters for the 2011 M9.0 Tohoku earthquake (*Sato et al.*, 2011).

A recent addition to seafloor geodesy is the possible use of fibre optic cables to measure strain and seismic waves (*Jousset et al*, 2018; *Zumberge et al.*, 2018). Fibre optic cables, the same as typically used in communications, have randomly distributed impurities that reflect small amounts of light. A light source at the end of the cable is used to monitor the distances to all the different impurities, and hence the strain, or deformation, can be measured in the cable. Because of the possible high sampling rate for this technique, each impurity acts as a 1-D horizontal displacement seismometer. This technique has some advantages in terms of power and data transmission because the light injector is placed on land for a cable that can be laid out to the ocean floor. Some on-land experiments of fibre optic technique

have taken place on Reykjanes Peninsula, showing promising results (*Jousset et al.,* 2018) that provide information about what could be expected from offshore fiber optic cables. To measure long-distance strain with fibre optics requires correction for thermal expansion, which may be achieved by laying two parallel cables with different thermal expansion coefficients (*Zumberge et al.,* 2018).

In the Campi Flegrei caldera in Italy, experiments with continuous GNSS monuments anchored to the seafloor at shallow (dekameter) depths have proven useful, resulting in vertical precision similar to land-based continuous GNSS stations (*Iannaccone et al.,* 2018). Ongoing developments of anchored monuments aim to get accurate 3D positions by using heading and tilt measurements to correct for the wobble of the monument and to adapt the structure to as much as 200 m water depth (http://labs.cas.usf.edu/geodesy/).

In the Tjörnes Fracture Zone, we can expect plate-boundary deformation, earthquake-related deformation, as well as volcanic deformation. Based on the available GPS and InSAR measurements, *Metzger and Jónsson* (2014) found that the HFF takes up about 1/3 of the ~2 cm/year transform motion in the area, while the remaining 2/3 is probably focused on the GOR. This result is based solely on GPS measurements across the easternmost (on-land) part of the HFF. Seafloor geodetic techniques, such as GNSS-A, would help constraining better the transform partition between the HFF and GOR. In addition, little is known about what is going on within the volcanic systems offshore North Iceland, located along the GOR. Intensive seismic swarms have occurred near these systems but questions regarding possible associated magma movements remain unresolved.

If Iceland were to initiate research and monitoring using seafloor geodesy then obvious targets in addition to the TFZ would be the Reykjanes Ridge and Vestmannaeyjar islands. Because of the high costs involved it would pay off to co-locate as many types of instruments as possible, i.e. to make offshore observatories. Several geophysical offshore observatories exist today, for example near the subduction zones of Japan and Cascadia. However, the installation cost of such observatories is very high and the maintenance expensive and such an undertaking would thus require dedicated funding for long time.

References

Árnadóttir, et al., Glacial rebound and plate spreading: Results from the first countrywide GPS observations in Iceland. *Geophys. J. Int*., **177**(2), 691–716, 2009.

Bürgmann, R., & Chadwell, D., Seafloor geodesy, *Annual Review of Earth and Planetary Sciences* **42**, 509-534, 2014.

Caress, D.W. et al., Repeat bathymetric surveys at 1-metre resolution of lava flows erupted at Axial Seamount in April 2011, *Nature Geoscience*, **5**, 483-488, 2012.

Chadwick, W.W., S.L. Nooner, D.A. Butterfield & M.D. Lilley, Seafloor deformation and forecasts of the April 2011 eruption at Axial Seamount, *Nature Geoscience*, **5**, 474-477, 2012.

Einarsson, P., B. Brandsdóttir & Á.R. Hjartardóttir, Seismicity, faults, and bathymetry of the Tjörnes Fracture Zone, In: *Proceedings to the 3rd workshop of earthquakes in North Iceland* (this volume), 2019.

Geirsson et al., Overview of results from continuous GPS observations in Iceland from 1995 to 2010, *Jökull*, **60**, 3-22, 2010.

Iannaccone, et al., Measurement of Seafloor Deformation in the Marine Sector of the Campi Flegrei Caldera (Italy), *Journal of Geophysical Research: Solid Earth*, **123**(1), 66-83, 2018.

Jousset, P., Reinsch, T., Ryberg, T., Blanck, H., Clarke, A., Aghayev, R., ... & Krawczyk, C. M., Dynamic strain determination using fibre-optic cables allows imaging of seismological and structural features, *Nature Communications* **9**(1), 2509, 2018.

Jónsson, S., R. Matrau, R. Viltres & B. Ófeigsson, An update of GPS measurements in North Iceland, In: *Proceedings to the 3rd workshop of earthquakes in North Iceland* (this volume), 2019.

Magnúsdóttir, S., B. Brandsdóttir, N. Driscoll & R. Detrick, Postglacial tectonic activity within the Skjálfandadjúp basin, Tjörnes Fracture Zone, offshore Northern Iceland, based on high resolution seismic stratigraphy, *Marine Geology*, **367**, 159-170, 2015.

Maksymowicz, A., C. D. Chadwell, J. Ruiz, A. M. Tréhu, E. Contreras-Reyes, W. Weinrebe, et al., Coseismic seafloor deformation in the trench region during the Mw8.8 Maule megathrust earthquake, *Scientific reports*, **7**, 45918, 2017.

Metzger, S., S. Jónsson & H. Geirsson, Locking depth and slip-rate of the Húsavík Flatey fault, North Iceland, derived from continuous GPS data 2006-2010, *Geophys. J. Int.*, **187**, 564-576, 2011.

Metzger, S., S. Jónsson, G. Danielsen, S. Hreinsdóttir, F. Jouanne, G. Giardini & T. Villemin, Present kinematics of the Tjörnes Fracture Zone, North Iceland, from campaign and continuous GPS measurements, *Geophysical Journal International* **192**, 441-455, 2013.

Nooner, S.L. & W.W. Chadwick, Inflation-predictable behavior and co-eruption deformation at Axial Seamount, *Science*, **354**, 1399-1403, 2016.

Metzger, S. and S. Jónsson, Plate boundary deformation in North Iceland during 1992-2009 revealed by InSAR time-series analysis and GPS, *Tectonophysics* **634**, 127-138, 2014.

Petersen, F., Kopp, H., Lange, D., Hannemann, K., & Urlaub, M., Measuring tectonic seafloor deformation and strain-build up with acoustic direct-path ranging, *Journal of Geodynamics*, **124**, 14-24, 2019.

Sato, M., Ishikawa, T., Ujihara, N., Yoshida, S., Fujita, M., Mochizuki, M., & Asada, A., Displacement above the hypocenter of the 2011 Tohoku-Oki earthquake, *Science* **332**(6036), 1395-1395, 2011.

Urlaub, M. et al., Gravitational collapse of Mount Etna's southeastern flank, *Science Advances*, **4**, eaat9700, 2018.

Zumberge, M. A., Hatfield, W., & Wyatt, F. K., Measuring seafloor strain with an optical fiber interferometer, *Earth and Space Science*, **5**(8), 371-379, 2018.

NORTHQUAKE 2019 - The 3rd International Workshop on Earthquakes in North Iceland
Húsavík, North Iceland, 21-24 May 2019

PRE-EARTHQUAKE PROCESSES AND WARNINGS IN THE TJÖRNES FRACTURE ZONE

Ragnar Stefánsson[1] and Gunnar B. Guðmundsson[2]

[1] *University of Akureyri, Iceland (raha@simnet.is)*
[2] *Icelandic Meteorological Office (gg@vedur.is)*

Seismicity of the Tjörnes fracture zone (TFZ) expresses significant spatial perturbations of the stress field in the area (Fig. 1). Migration of the plate boundary with respect to the mantle plume, high-pressure pore fluids at depth that frequently propagate up into the brittle crust, and rifting episodes in the adjacent rift zones are among important factors that cause stress-field perturbations in the TFZ in both space and time. Such perturbations are reflected in fault-slip data at geological time scales as well as in present-day earthquake focal mechanisms (*Garcia et al.*, 2002, *Angelier et al.*, 2004). Even if future earthquakes will most likely take place on faults where past earthquakes, according to the thousand-year history, have most frequently occurred, we cannot rule out the possibility that strong stress perturbations lead to earthquakes on pre-existing faults with significantly different fault orientations. For example, during an earthquake sequence in Öxarfjörður in 1975-1976 we have seen how a normal-faulting stress regime changed to a strike-slip regime, and then back to a normal-faulting regime (*Stefánsson and Gudmundsson*, 2019).

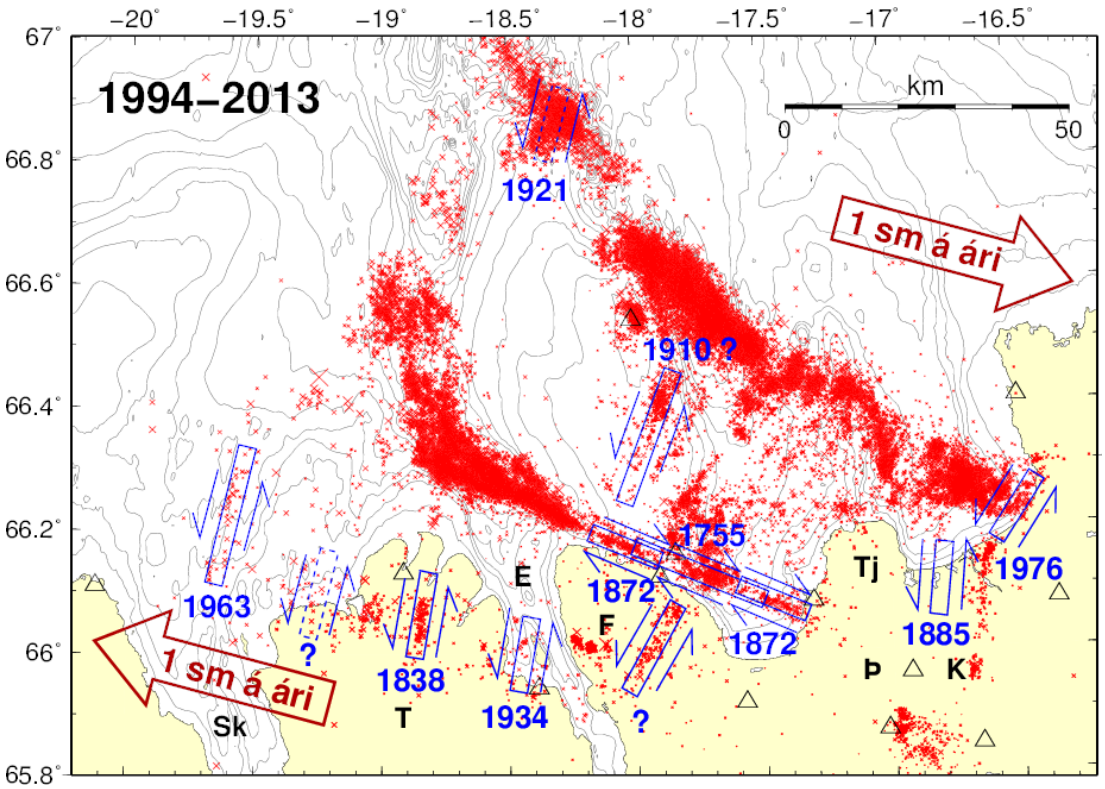

Figure 1. Earthquake locations (red dots), at the north coast of Iceland, outline the Tjörnes fracture zone. Boxes and arrows in blue show results of efforts to find fault planes and infer slip directions of past large (magnitude 6–7) earthquakes in the

area since 1755. The box length roughly corresponds to the magnitude, i.e., the longer boxes to magnitude around 7 the shorter to magnitudes around 6.5 events (from Stefánsson et al., 2008).

It is sometimes claimed that it is straight forward to predict earthquakes triggered by preceding rifting activity. Of course, rifting episodes cause strong perturbations in the stress field, which can serve as the first significant warning of a possible impending large earthquake. However, to predict a large earthquake that might follow such a perturbation, we need the same understanding as for predicting earthquakes occurring after a slow build-up in generic stress conditions, i.e., information about ongoing crustal processes in the local focal area of the impending earthquake. More specifically, information is needed about processes indicative of stress build-up in and around a hard core (asperity) as well as of micro-fracturing. These processes are best observed by a sensitive local micro-earthquake monitoring system and real time evaluation and modeling.

The goal of earthquake prediction research is to provide as detailed information as possible about an impending earthquake, i.e., its location, source fault, radiated energy distribution, time of occurrence and other information that might help mitigating the risk at the surface. It cannot be assumed that any two earthquakes are the same and, in particular, it cannot be assumed that the preparatory activity of any two earthquakes is identical. The experience in Iceland indicates that large earthquakes are preceded by observable processes. These processes may take place in strike-slip stress regimes, in areas of slow strike-slip displacement below the brittle crust and of upward migration of high-pressure fluids into it, observable by the most sensitive sensors (*Stefánsson*, 2011, *Stefánsson et al.*, 2011), or they may be a well-observable rift-opening process linked to upwelling of incompressible fluids, as shown in examples below, and they may be a mixture of all of this.

The method of earthquake prediction research for providing useful warnings to people and society is to continuously study ongoing processes, discover fault excitation at its early stage that may indicate preparation for a large earthquake, and by continuous multidisciplinary watching of ongoing crustal processes at these faults with data feeding into studies and models of these processes. On basis of constitutive relationships governing the processes, extrapolations in space and time can help forcasting the evolving activity. Gradual updating of parameters of the constitutive relationships, by a steady comparison of observed and predicted processes, is needed during the time span of the earthquake preparation activity to better constrain the processes and to improve predictions (*Stefánsson*, 2011).

Many argue that the main problem in earthquake prediction is to predict the time of a future large earthquake. Instead of focusing on the timing, the main objective of earthquake prediction should be to generate as realistic model as possible of the stress release process as long time as possible before it occurs. This can best be achieved by continuous research of the preceding crustal processes, which gradually brings new information that can help predicting the probable time of occurrence, the location of the fault plane and its orientation, the asperities, and the slip and distribution of the released energy.

Below we show examples of pre-earthquake activity before the earthquakes of M≥5.5 that have occurred in the TFZ since the start of the SIL micro-earthquake monitoring network in the region (Fig. 2). These examples have been taken from the routine catalogue of the Icelandic Meteorological Office.

The 1994 earthquake.

A magnitude 5.5 earthquake took place west of the Eyjafjarðaráll rift on 8 February 1994 (Fig. 3). No foreshocks were detected in the focal area. The SIL system in north Iceland had just started operating and was in a testing phase at the time of the earthquake, which may have reduced its detectability. However, that no foreshocks larger than magnitude 1 were observed indicates stability in the crust at

this location. The seismic activity observed in the nearby Eyjafjarðaráll before the earthquake (Fig. 3) cannot be considered as precursory activity as it is not untypical of the usual activity in that area.

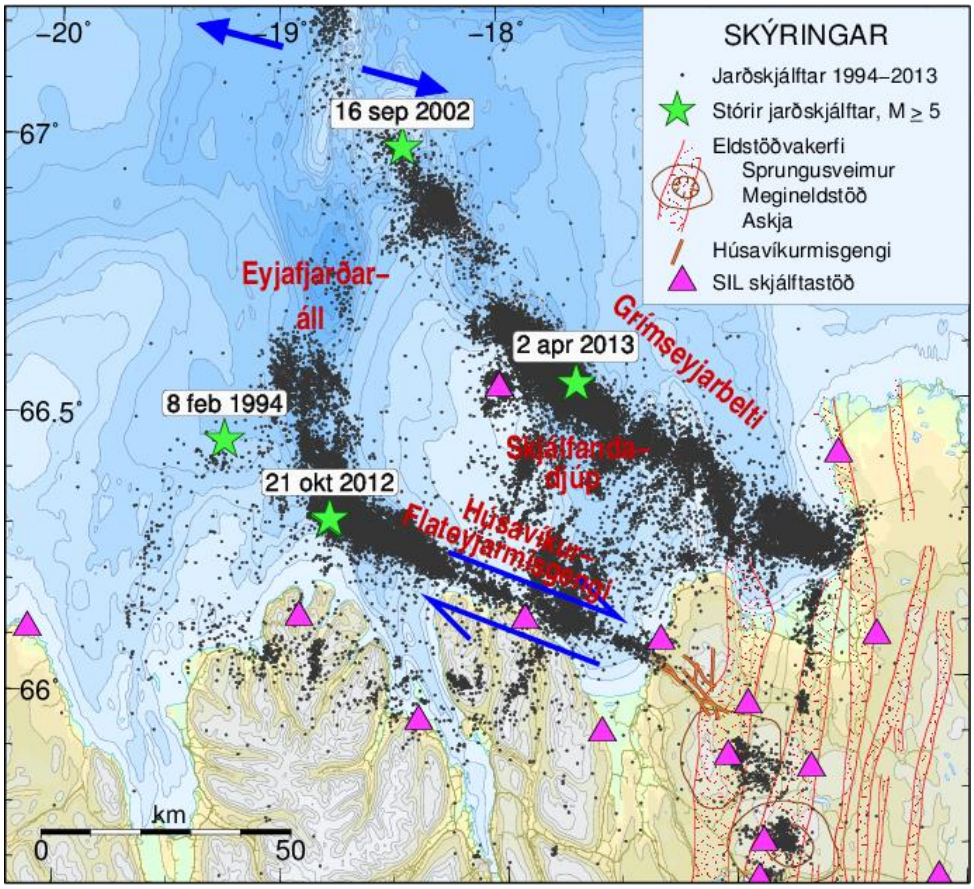

Figure 2. Map showing the dates and epicenters of the largest earthquakes (M>5) in the TFZ during 1994-2013 (green stars), small earthquakes (black dots), horizontal movement across the Húsavík-Flatey fault (blue arrows), seismic stations (pink triangles), and rift zones and central volcanoes as in Einarsson and Sæmundsson (1987).

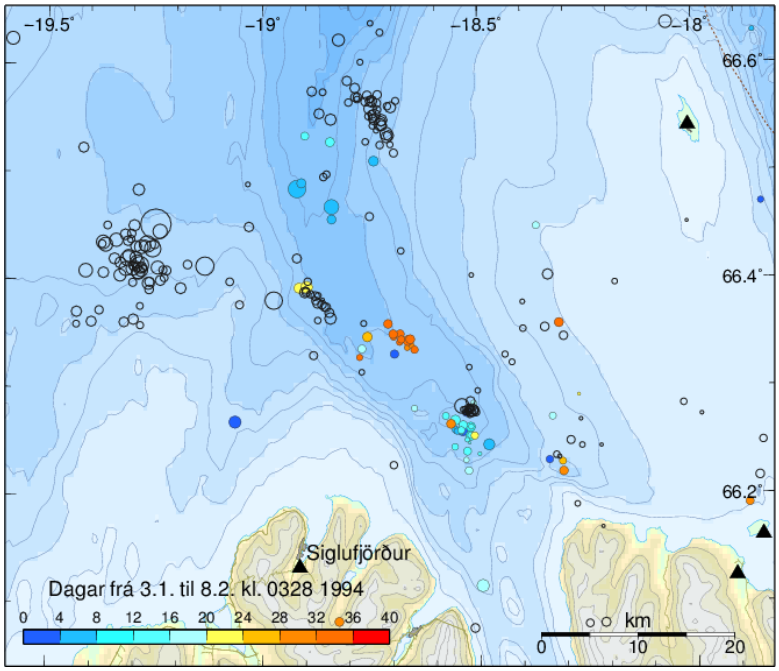

Figure 3. Map of the Eyjafjarðaráll rift and the western part of the Húsavík-Flatey fault, with the big black open circle showing the epicenter of the magnitude 5.5 earthquake on 8 Feb. 1994 at 03:28. Other open circles indicate 17 hours of aftershocks while colored circles show events during the 38 days before the mainshock, from 3 Jan. – 8 Feb., 1994.

The wide-spread post-activity, aftershocks, during only 17 hours (Fig. 3) are of great interest and although locations should be improved before drawing definite conclusions, they prompt some ideas that should be further looked into. The earthquake swarm to the south of the epicenter appears to suggest, albeit not strongly, a possible SSW-striking fault for the mainshock. There is also a vague indication of old fault weaknesses to the ESE of the epicenter, towards the Húsavík-Flatey fault, as well as to the NW of the epicenter, hinting at a possible westward continuation of HFF. Bear in mind that the mainshock epicenter is only 10 km east of the junction between the north end of the fault of the magnitude 7 Skagafjörður earthquake of 1963 and a possible westward prolongation of the HFF (Fig. 1). The strong aftershock activity in the Eyjafjarðaráll rift expresses its present-day crustal instability and near-lithostatic fluid pressure activity at seismogenic depths in the crust.

The 2012 earthquake

On 21 October 2012, a magnitude 5.6 earthquake occurred where the Eyjafjardaráll rift meets the HFF. In fact, two similar earthquakes occurred, close in time and space. A month before, an earthquake swarm had started 7 km further north in the rift. Both the foreshock activity and the mainshocks had normal faulting mechanisms (*Hensch et al.*, 2016). The seismicity that followed the mainshocks extended 25 km to ESE into the strike-slip stress regime of the HFF during the next two days (Fig. 4).

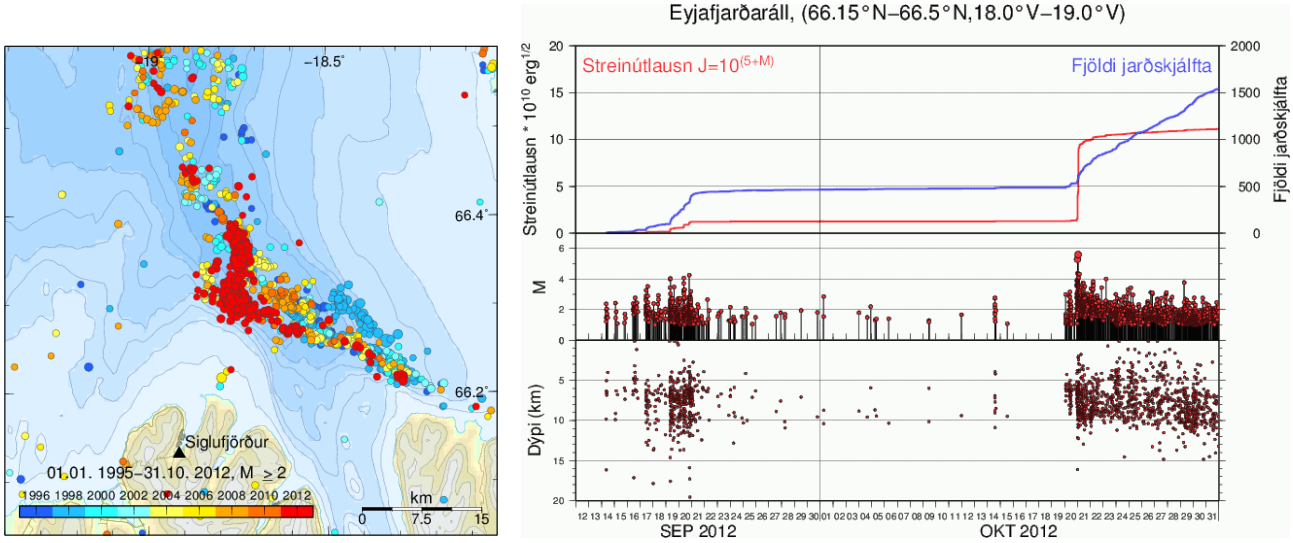

4 a) **4 b)**

Figure 4. a) The dense red circles show the seismic activity at the junction of the Eyjafjardaráll north-trending rift and the Húsavík-Flatey fault (HFF) from mid-Sept. to 31 Oct., 2012. The activity began in the northern part of the cluster in mid-Sept. and then moved 7 km to the south, a month later on 21 Oct. with the magnitude 5.6 earthquake at the junction to the HFF. In the following days earthquakes illuminated the HFF some 25 km to ESE. b) Time evolution of cumulative number (blue) of earthquakes (M>1) and strain release (red), as well as of event magnitude and depth.

Even if absolute depth estimates are not accurate, the relatively deep earthquakes in the premonitory cluster are of interest and point toward an upward fluid flow with subsequent induction of earthquakes at the bottom of the brittle crust, probably at 10 km depth (Fig. 4b). Earthquakes only occur in the ductile part of the crust during high strainrates or fast fluid flow. About a month of upward fluid migration appears to have created conditions for triggering the magnitude 5.6 earthquake, following one day of foreshock activity breaking the asperity of the mainshock.

The 2002 earthquake

On 16 September 2002 at 18:48, a magnitude 5.8 earthquake occurred in the Grímsey rift almost 100 km north of Iceland (Fig. 2). Its epicenter according to the Icelandic Met. Office was at 66.96°N, 18.45°W. Two months before, on 15 July, a 4-day swarm started after a 3-year period of relatively low seismic activity near the impending epicenter. The earthquakes in the swarm were relatively deep and most probably related to upward fluid flow (Fig. 5a). Another interesting feature is that foreshocks started simultaneously at two different locations, about 15-20 km apart (Fig. 5b), indicating slow displacement in the crust on a NNW-striking part of the rift, below a locked portion of a fault. The two ends of a slowly slipping fault are the places of the highest strain concentration of the crust and could thus potentially open up for high pressure fluids to ascend from below.

Seismic activity gradually increased during the last two weeks before the earthquake, presumably while a hard core was breaking up between the fluid-weakened places to the north and south. In Fig. 5b we see the foreshock activity and roughly one hour of aftershocks, mainly from inside the central hard core area.

A fault length of 10-15 km is rather long for a magnitude 5.8 earthquake, but can be explained by the fault being weakened by fluids from below, so the active brittle crust thickness would be only 5-7 km. The earthquake is a strike slip earthquake and according to NEIC the fault plane is near vertical and striking N55°W, if selected according to the early aftershocks.

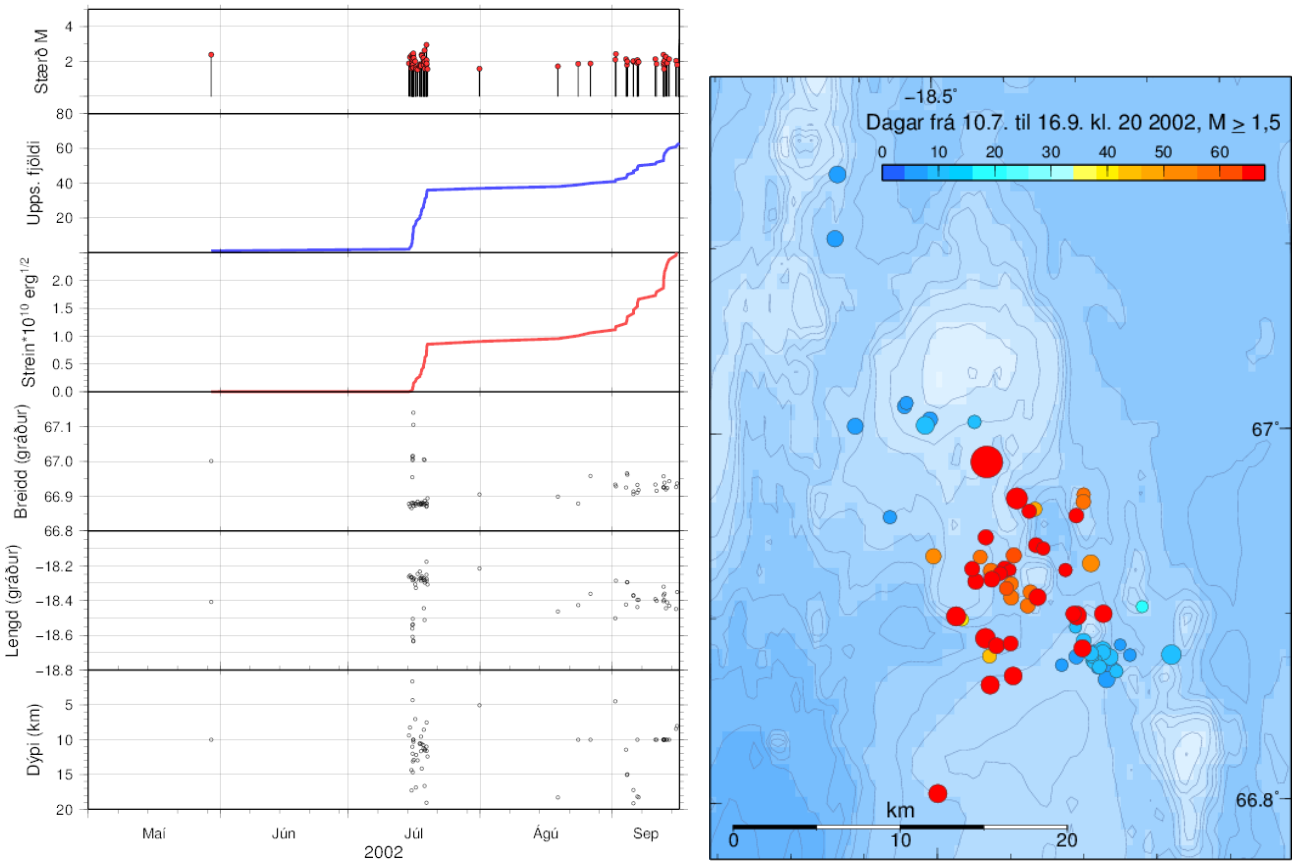

5a) **5b)**

Figure 5. Earthquake epicenters (M ≥ 1.5) in the region 66.8°N - 67.1°N and at ~18.5°W from May 2002 to 16 Sept., 2002, when a M 5.8 earthquake occurred at 18:48. a) Time evolution showing (from above) magnitude, cumulative number, strain, N° and E° location, and depth of the earthquakes until just before the mainshock. b) Map of the earthquakes with the color indicating event time from 10 July and until the mainshock (largest red circle). The map includes aftershocks for roughly an hour after the mainshock.

The 2013 earthquake

An earthquake of magnitude 5.5 occurred on the Grímsey belt, east of Grímsey Island on 2 April 2013 at 00:59. The epicenter was at 66.55°N, 17.66°W. Half a year before, a seismic swarm started at 15-20 km depth and 7-8 km NW of the eventual mainshock epicenter and also, at approximately the same time, at a similar distance to the SE of it. Dense activity at both locations lasted for half a month (Fig. 6). The two swarms were separated by a 6-7 km long earthquake-free area. Gradually, subsequent activity broke into that earthquake-free area, expressing that crustal fracturing progressed into a central unbroken hard core, i.e., an asperity of the impending mainshock. One and a half month before the M 5.5 earthquake struck, there was a sudden increase in activity (Fig. 6) and again 43 hours before the mainshock, when even more intense activity started. The earthquake, according to *Hensch et al*. (2016), was a strike-slip event on a vertical fault plane.

This is comparable to the preparation and nucleation of the earthquake in 2002. Fluid and stress-driven fracturing from the ends of an old fault, erode it towards its center, leaving in this case a 6-7 km core where stress and fracturing gradually enhances during the last part of the nucleation.

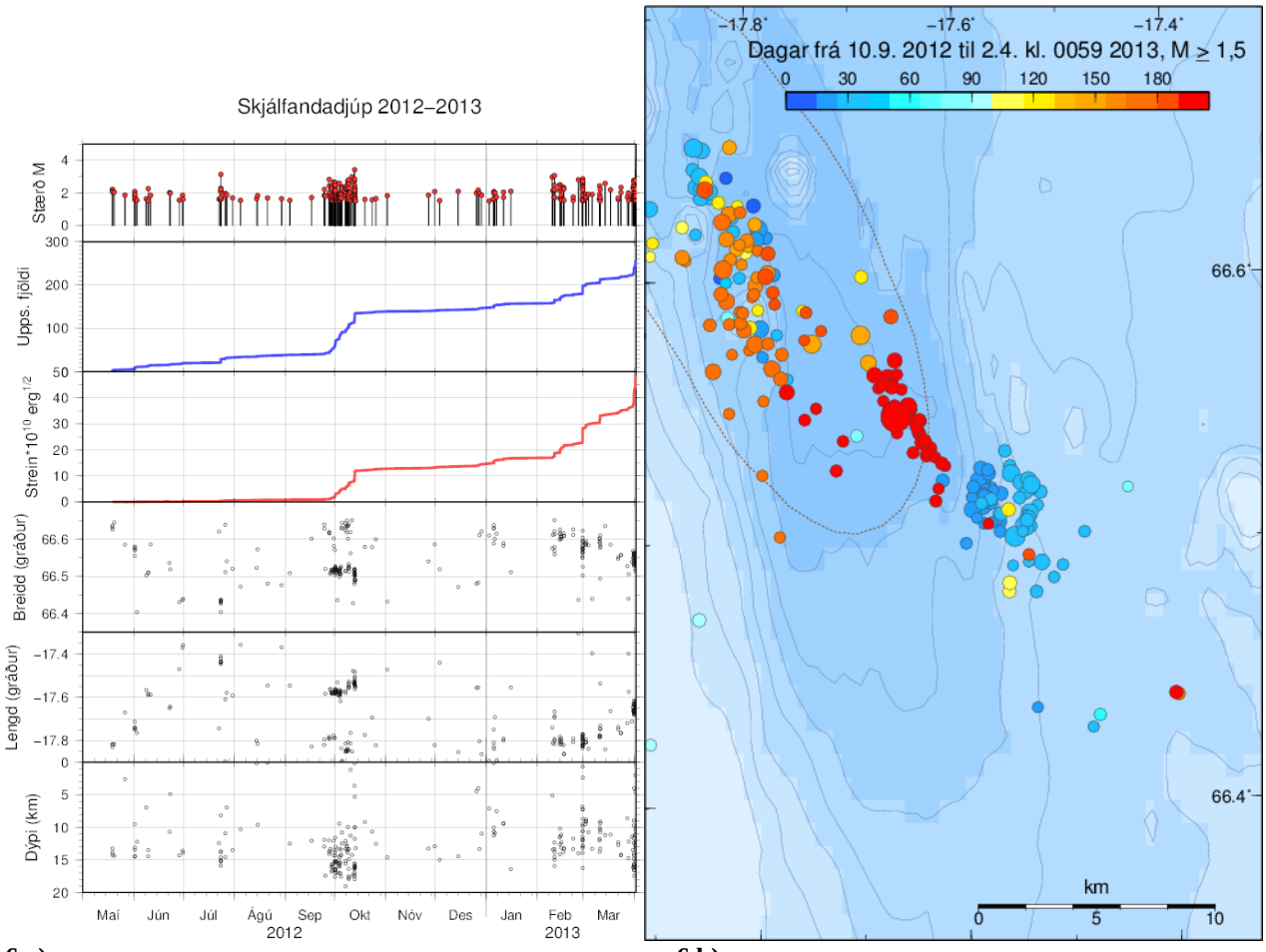

6 a) **6 b)**

Figure 6. Earthquakes M≥1.5 in the Grímsey rift, east of Grímsey Island, ahead of a M≥5.5 earthquake on 2 April, 2013 at 00:59. a) Time evolution of the seismicity showing (from above) magnitude, cumulative number, strain, N° and E° epicenter locations, and depth of the earthquakes, until just before the mainshock occurred. b) Map of the earthquakes with the color indicating time from 10 Sept. until the mainshock (largest circle). No aftershocks are shown.

Multidisciplinary monitoring and watching system

The above discussion and interpretations are mainly based on microearthquake seismicity observed ahead of the earthquakes. It is possible to extract much more physical information from the microearthquake activity for modeling pre-earthquake processes in the crust than has been done in this preliminary study. Other types of monitoring can certainly also provide real-time information significant for warnings and constraining the modeling. For example, *Skelton et al.* (2016) reported chemical changes in groundwater observed ahead of 3 of the mainshocks (in 2002, 2012, and 2013) discussed above.

The high fluid activity in the crust, especially in the eastern part of the TFZ, makes it feasible to install monitoring borehole strainmeters in available boreholes close to Húsavík. Borehole strainmeters have proven useful for monitoring crustal processes and for detecting eruption precursors in south Iceland. The strainmeter at Saurbær in Holt, SAU, (*Sacks et al.*, 1980) exhibited the strongest short-term signal before the first of the South Iceland earthquakes in 2000, Fig. 7, (*Stefánsson*, 2011). Two or three, or even only one borehole strainmeter close to Húsavík would be a significant addition to the existing monitoring network and possible warning service. Such data would also be useful to compare to other pre-earthquake signals, like groundwater chemical and water-level changes.

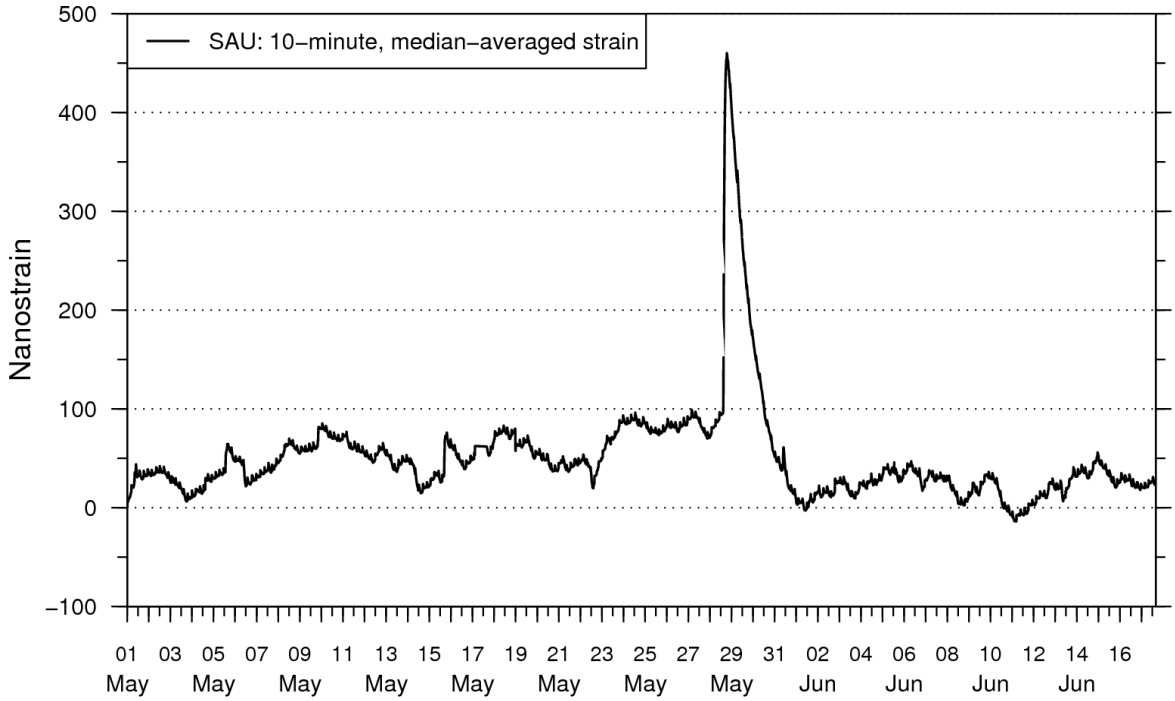

Figure 7. A large signal (termed the "big bump") measured by a Sacks-Evertsson borehole strainmeter at Saurbær (SAU) three weeks before and a few kilometers away from the epicenter of the 17 June 2000 earthquake in South Iceland. The data have been filtered and show 10-minute median values, with positive values showing compression. The data indicate a relatively calm situation at this frequency range, apart from this single peak, which is followed by slightly lower compression values until the time of the earthquake (at the right edge of the graph), than before it.

The "big bump" of Fig. 7 is an example of a strong shallow-origin pre-earthquake signal detected at only one borehole strain station and thus difficult to model as being a result of a deeper process, i.e., using these observations alone. However, such signals can be very useful as an alarm and process modeling if merged with other information like detailed microearthquake information and other shallow-origin information like groundwater chemical changes and pressure variations.

Although the TFZ would benefit from more types of monitoring, we already have enough monitoring infrastructure available in the area and geo-information for applying real time watching of crustal processes, which possibly could be useful for earthquake warnings in both the short and long term. Fig. 8 shows a block diagram of a partially automatic system for continuous watching of crustal processes, for information on crustal conditions and for warnings.

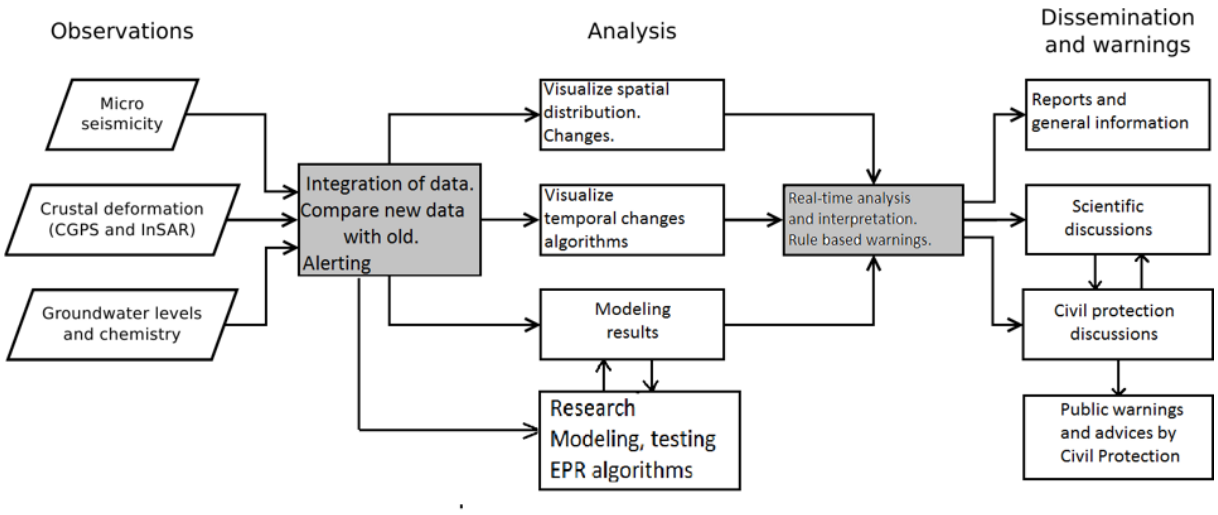

Figure 8. Block diagram showing the main components of an earthquake-watch system that could be applied to provide timely information and warnings ahead of earthquakes. All system components in the three left columns would be automatic, except "Research, modeling, testing of earthquake prediction research (EPR) algorithms" (middle-bottom).

How will the Grímsey-belt seismicity proceed towards SE?

Above I have described two earthquakes within the Grímsey belt that were parts of possible rifting events. The EW rifting across the 30-40 km NNW-striking belt east of Grímsey is still ongoing, see Fig. 9. The 18 March, 2019 intrusive seismic swarm started in this belt NE of Grímsey and almost and almost simultaneously, i.e., on 24 March, a relatively shallow but intensive swarm started near Kópasker (Fig. 9). The whole line GK 1 and GK 2 was strained by the intrusion and the straining was expressed in the intensive swarm activity of shallow earthquakes at the junction near Kópasker.

It is likely that stress loaded on the GK 1 line was released in the magnitude 7 earthquake in 1910, either by left-lateral slip on a NNE-striking fault, as suggested in Fig. 1, or by right-lateral slip on the WNW striking GK 1 line. The distribution of small earthquakes on the line during the intrusive event in March may indicate crustal instability and probably increasing seismic activity, but not necessarily a large earthquake. The 20-km-long GK 2 line, on the other hand, had no earthquakes larger than magnitude 1.5 during the March intrusive event. It seems no large earthquakes have occurred on this part of the Grímsey rift since beginning of worldwide seismology more than 100 years ago. It may be a zone of high stress build up, between the GK 1 that probably hosted the 1910 earthquake and the 1975-1984 Krafla rifting episode of the North Volcanic Zone.

The parts of the Grímsey belt, labelled here as GK 1 and GK 2, steadily accumulate stress as long as the HFF is locked, as it is now. The high level of distributed activity of small earthquakes between the HFF and the Grímsey belt may be indicative of high shearing stresses, which will be released sooner or later, possibly in a future large earthquake. Continuous earthquake-watching, by the methodology described in Fig. 8, is needed for the GK 1 and GK 2 zones of the Grímsey belt, in addition to the seismic zones of the HFF.

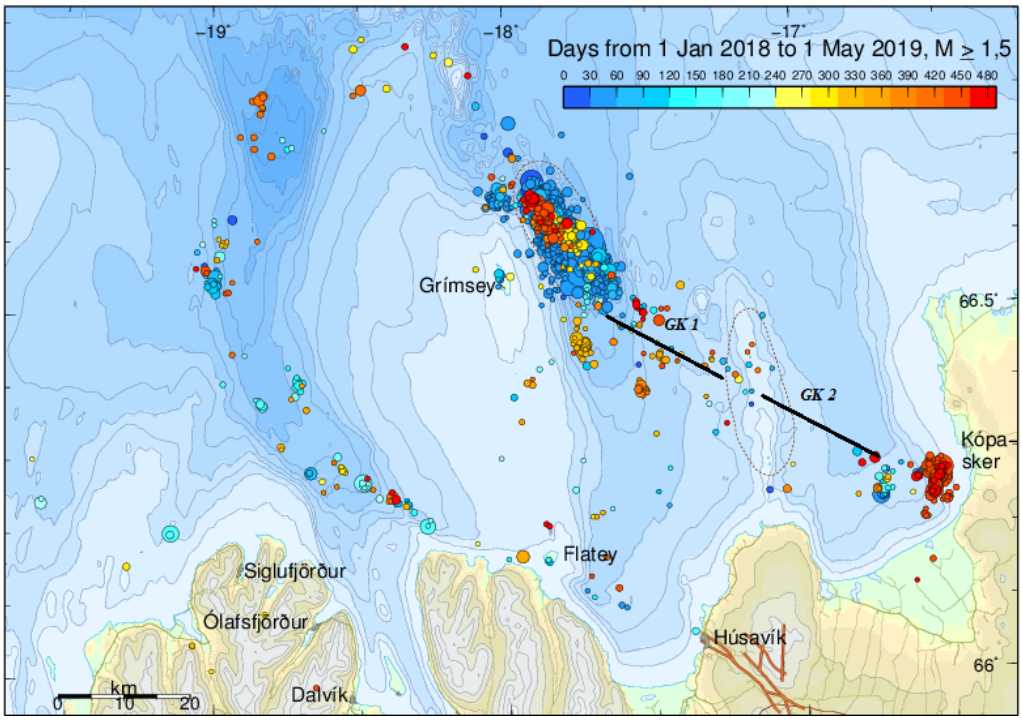

Figure 9. Earthquake epicenters (M ≥ 1.5) in the TFZ from 1 Jan. 2018 to 1 May 2019. Lines GK 1 and GK 2 are here suggested as possible fault segments of future large earthquakes.

References

Angelier, J., R. Slunga, F. Bergerat, R. Stefánsson, C. Homberg, Perturbation of stress and oceanic rift extension across transform faults shown by earthquake focal mechanisms in Iceland. *Earth Planet. Sci. Lett.*, **219**, 271–284, 2004.

Einarsson, P., and K. Sæmundsson, Earthquake epicenters 1982–1985 and volcanic systems in Iceland, map. In: T. Sigfússon (Ed.), *Í hlutarins eðli: Festschrift for Thorbjörn Sigurgeirsson.* Menningarsjódur, Reykjavík, 1987

Garcia, S., J. Angelier, F. Bergerat, C. Homberg, Tectonic analysis of an oceanic transform fault zone revealed by fault-slip data and earthquake focal mechanisms: the Husavik–Flatey Fault, Iceland. *Tectonophysics* **344**, 157–174, 2002.

Hensch, M., G.B. Guðmundsson, K. Jónsdóttir, and the SIL monitoring group, Seismic activity in North Iceland since 2011 with a special focus on the past three years In *Proceedings of the 2nd International Workshop on Earthquakes in North Iceland*, Húsavík Academic Centre, 2016.

Sacks, I.S., A.T. Linde, and R. Stefánsson, Installation of a borehole strainmeter array in Iceland, *DTM Yearbook* **79**, 495–498, Carnegie Institute of Washington, Washington, D.C., 1980.

Skelton, A., G. Stockmann, M. Andrén et al., Chemical changes in groundwater before and after earthquakes in Northern Iceland. In *Proceedings of the 2nd International Workshop on Earthquakes in North Iceland*, Húsavík Academic Centre, 2016.

Stefánsson, R., *Advances in earthquake prediction, research and risk mitigation*, Springer-Verlag in Berlin and Heidelberg in association with PRAXIS Publishing in UK, 271pp, 2011.

Stefánsson R., M. Bonafede, and G.B. Gudmundsson, Earthquake prediction research and the year 2000 earthquakes in the South Iceland Seismic Zone. *Bull. Seismol. Soc. Am.*, **101**, 1590-1617, 2011.

Stefánsson, R., and G.B. Guðmundsson, Kópasker earthquake in 1976, About pre-activity, location and post-activity. In *Proceedings of the Northquake 2019 workshop* (this volume), Húsavík Academic Centre, 2019.

NORTHQUAKE 2019 - The 3rd International Workshop on Earthquakes in North Iceland
Húsavík, North Iceland, 21-24 May 2019

TOWARDS IMPROVED SEISMIC MONITORING, EARTHQUAKE MODELING AND GROUND MOTION SIMULATION FOR EARLY WARNING AND HAZARD ESTIMATES IN NORTH ICELAND

Benedikt Halldórsson[1,2], the TURNkey team, and the ChEESE team[3]

[1]*Faculty of Civil and Environmental Engineering, School of Engineering and Natural Sciences, and Earthquake Engineering Research Centre, University of Iceland (UI) (skykkur@hi.is)*
[2]*Division of Processing and Research, Icelandic Meteorological Office (benedikt@vedur.is)*
[3]*www.cheese-coe.eu*

TURNkey

In 2017 the European Commission launched the Work Programme 2018-2020 of Horizon 2020, the European Union's Research and Innovation funding programme. Horizon 2020 is the World's largest multinational programme dedicated to research & innovation to which universities, research organizations, companies, governmental and non-governmental organizations can apply to participate. One of the pillars of the Work Programme is dedicated to "Societal Challenges" under which "SC5-17 Towards operational forecasting of earthquakes and early warning capacity for more resilient societies" was listed. The challenge is now being addressed by the project "*Towards more Earthquake-resilient Urban Societies through a Multi-sensor-based Information System enabling Earthquake Forecasting, Early Warning and Rapid Response actions*" (TURNkey) that formally started in June 2019 and is led by Norsar, the Norwegian seismic arrays institute in Norway. The TURNkey consortium consists of a strong multi-disciplinary team of experts of various backgrounds (geophysicists, seismologists, geologists, engineers, disaster risk managers, sociologists, instrument manufacturers, software developers, information technology experts, computer programmers and telecommunication experts) from 21 partner institutions, universities and companies in 10 European countries. University of Iceland is the Icelandic partner where the TURNkey efforts will be carried out by a multidisciplinary research group led by Dr. Benedikt Halldórsson.

TURNkey aims to make significant advances in the fields of Operational Earthquake Forecasting (OEF), Earthquake Early Warning (EEW) and the Rapid Response to Earthquakes (RRE), particularly when applying these systems in practice in Europe. This involves earthquake strong-motion research, development of infrastructure for monitoring of earthquake motions and their effects, investigating the character of ground motions in urban areas, along with hazard, vulnerability and risk analysis. The project will contribute to a more resilient society to the adverse effects of earthquakes by developing a flexible, extendable, robust and easy-to-use OEF/EEW/RRE system based on real-time data and a cloud-based computer platform. This system, the TURNkey FWCR platform will enable real-time ***F****orecasting* (of strong-motion) – *Early* ***W****arning* (of earthquake effects) – ***C****onsequence Prediction* (e.g., of damage potential) – ***R****esponse* (focused by effects). From the outset, the TURNkey project will be guided by the needs of major public and private stakeholders in six seismically active geographically-focused Testbeds (TB) in Europe, and will be advised and reviewed by a group of international experts.

TURNkey in Iceland will be based on dense urban infrastructure for earthquake monitoring and research in North and South Iceland. It will be based around the existing infrastructure of the Icelandic

strong-motion arrays in Hveragerði and Húsavík. The TURNkey system will consist of a user interface that allows the analysis of multi-system-measurements thus providing better insight and understanding of earthquake ground motions and their effects, in addition to allowing issuing alerts designed for the needs of each stakeholder. Along with improved mapping of different earthquake effects in urban areas, this will contribute to a rigorous evaluation of the operational and forecasting ability of such systems with respect to stakeholder needs. These developments will contribute to improved seismic resilience before, during and after a damaging earthquake and hence the reduction in losses.

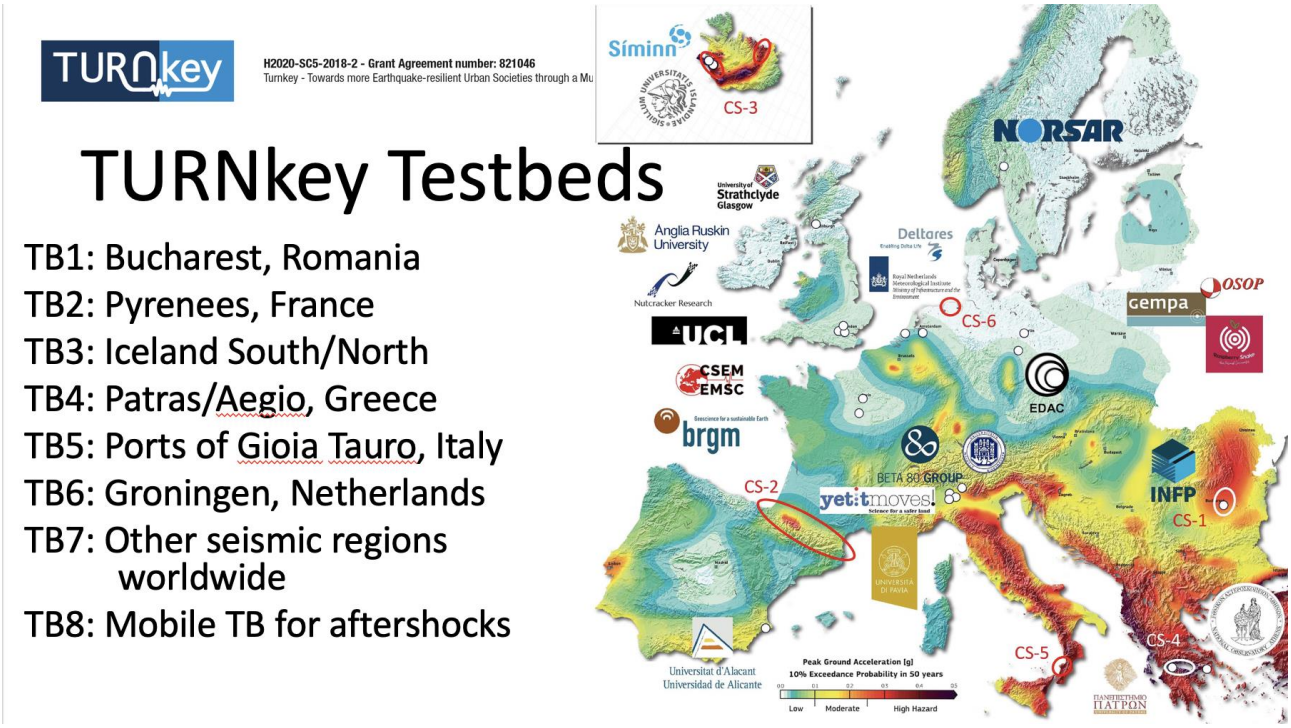

ChEESE

Another one of the pillars of the H2020 Work Programme is dedicated to "European Research Infrastructures" under which the Coordination and support action, and Research and Innovation action call "INFRAEDI-02-2018: HPC PPP - Centres of Excellence on High Performance Computing" was announced. The specific challenge was to create supporting Centres of Excellence (CoE) that promote the use of upcoming exascale computing capabilities for addressing scientific, industrial or societal challenges, and thus addressing the fragmentation of activities for excellence in HPC applications. This challenge is now being addressed by the new project "Centre of Excellence for Exascale in Solid Earth" (ChEESE), that started in November 2018.

ChEESE will establish a new Centre of Excellence in the domain of Solid Earth targeting the preparation of 10 European flagship codes for the upcoming pre-Exascale (2020) and Exascale (2022) supercomputer. The project will address 15 scientific, technical, and socio-economic Exascale Computational Challenges in the domain of Solid Earth, develop 12 Pilot Demonstrators and enable services oriented to society on critical aspects of geohazards like hazard assessment, urgent computing, and early warning. In this way, the project will bring together High-Performance Computing and High-end Data Analysis transversal European institutions in charge of operational geophysical monitoring

networks, and relevant stakeholders.

The project is led by the Barcelona Supercomputing Centre in Spain, and the consortium consists of 13 partners in 6 European countries. The Icelandic Meteorological Office is the Icelandic partner where the ChEESE efforts will be carried out by a multidisciplinary research group led by Dr. Benedikt Halldórsson and Dr. Sara Barsotti.

In Iceland, the project focuses on computational volcanology and computational earthquake and engineering seismology. High performance computing (HPC) will be used for real-time simulations of volcanic plume dynamics and high-resolution volcanic cloud dispersal forecast, including hazard assessment. HPC will also be used in real-time seismic simulations from large earthquake scenarios using kinematic and dynamic rupture models, and the systematic estimation of the seismic hazard sensitivity to such simulations, with focus on the Tjörnes Fracture Zone in North Iceland. In this way, IMO will take advantage of the Centre of Excellence to improve its internal research on seismic simulations, seismic hazard, volcanic ash modeling and volcanic hazard. The IMO will use the results of the project to produce new physics-based services for the scientific community and stakeholders.

A Center of Excellence for Exascale in Solid Earth

ChEESE

Centre of Excellence for Exascale in Solid Earth

10 new High Performance Computing Centres of Excellence (CoEs) have been created under H2020 e-Infrastructures. Among these, ChEESE is a 3-year project targeting at Solid Earth (SE) for the upcoming pre-Exascale (2020) and Exascale (2022) supercomputers.

15 Exascale Computational Challenges

ChEESE will address 15 scientific, technical and socio-economic Exascale Computational Challenges (ECC) in the domain of SE.

12 Pilot Demonstrators

ChEESE will develop 12 Pilot Demonstrators (PDs) and enable services oriented to society on critical aspects of geohazards like hazard assessment, urgent computing, and early warning forecast.

10 Flagship codes

10 different SE open source European codes have been selected in ChEESE

- 4 in computational seismology: EXAHYPE, SALVUS, SEISSOL, SPECFEM3D
- 2 in magneto hydrodynamics: PARODY_PDAF, XSHELLS
- 2 in physical volcanology: ASHEE, FALL3D
- 2 in tsunami modelling: T_HYSEA, L_HYSEA

Integrate

ChEESE will integrate around HPC and HAD European institutions in charge of operational geophysical monitoring networks, tier-0 supercomputing centers, academia, hardware developers, and third-parties from SMEs, Industry and public governance bodies (civil protection), and pan-European infrastructures, such as the European Plate Observing System (EPOS) and EUDAT.

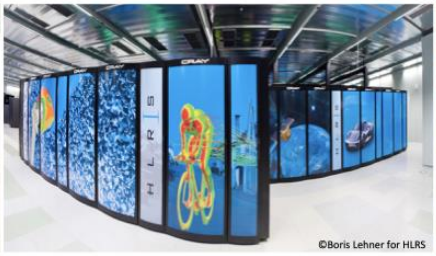

Partners:

Barcelona Supercomputing Center, Centro Nacional de Supercomputación; Bull atos technologies; CINECA; Icelandic Meteorological Office; IPGP; Istituto Nazionale di Geofisica e Vulcanologia; LMU Ludwig-Maximilians-Universität München; cnrs; NGI; ETH zürich; Technical University of Munich; Universidad de Málaga; HLRS

NORTHQUAKE 2019 - The 3rd International Workshop on Earthquakes in North Iceland
Húsavík, North Iceland, 21-24 May 2019

EARTHQUAKE MONITORING IN N-ICELAND AND THE HÚSAVÍK-FLATEY FAULT EARTHQUAKE EXERCISE HELD IN MAY 2019

Kristín Jónsdóttir[1], The IMO research and monitoring team[1], The National and Local Civil Protection response teams[2], The Road Authority response team[3], The Natural Catastrophe Insurance response team[4].

[1]*Icelandic Meteorological Office (kristinj@vedur.is)*
[2]*The Civil Protection Authority of Iceland*
[3]*The Road Authority of Iceland*
[4]*The Natural Catastrophe Insurance of Iceland*

The main goal of The Icelandic Meteorological Office (IMO) is to contribute towards increased safety and efficiency in society by monitoring, analysing, provide forecasts and, where possible, issue warnings and alerts about natural hazards. IMO has a long-term advisory role with the Civil Protection Authority of Iceland and issues public alerts about impending natural hazards. The seismic monitoring is the backbone of the real-time monitoring of seismic, volcanic and even flood hazards at IMO. Since the early 90's IMO has operated an automatic seismic acquisition system with a network of seismometers that initially were only located in South Iceland, but since 1994 also in the North Iceland (*Böðvarsson et a.*, 1999). All seismic stations of the network stream data to IMO's headquarters in Reykjavík where the data is automatically processed and later partly manually processed.

Since 2015, IMO has operated 24/7 natural hazard monitoring. This means that seismicity is monitored day and night. Various automatic warnings are in use, e.g., an earthquake early warning system has been in operation since 2016. It provides robust results on earthquake location and magnitude within 10-20 seconds from the earthquake occurrence time for events >M2.5 (*Behr et al.* 2016). In order to prepare the organization well to an emergency, contingency plans are in place for different hazards and in case of an impending natural hazard, the person on duty acts according to available contingency plans. These plans are reviewed at least annually, but they are also exercised.

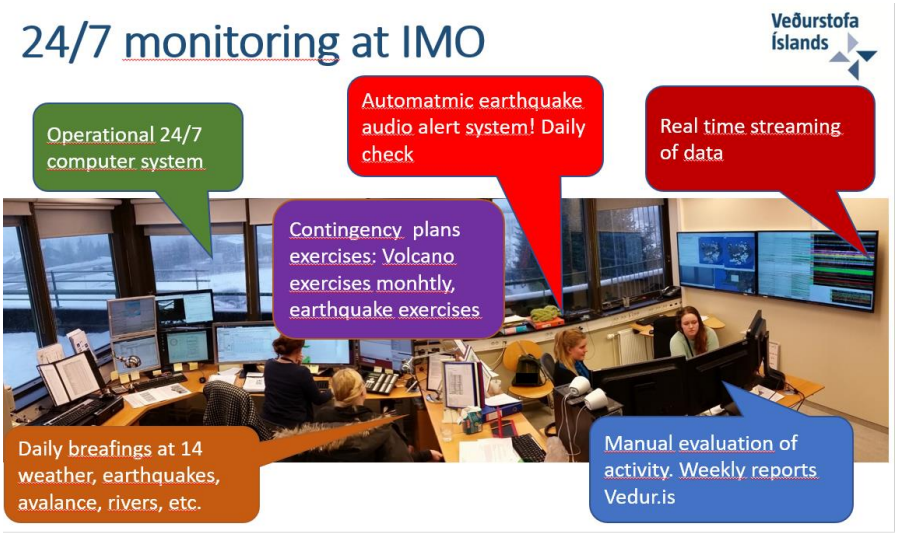

IMO organized a two-fold earthquake exercise on May 8th and 10th 2019, where scenarios of a significant earthquake and preceding seismic swarm on the Húsavík-Flatey Fault were played out. The exercise was co-organized by the National and Local Civil Protection response teams, the Natural Catastrophe Insurance response team and the Road Authority response team. The purpose of the exercise was to exercise contingency plans in place at each institute, to exercise communication within and between institutes and to increase the awareness of the earthquake hazard and even cascading hazards.

The main steps in preparing the exercise were to decide the main objectives of the exercise, design the scenarios and write up scripts for the relevant players of the exercise. A few meetings where held with the co-organizers some months before, where the main structure of the exercise was planned. The exercise was a "desk-exercise" meaning that the scenarios were not played out in the field. However, some telephone calls from the public were played and two crises meetings were played, at IMO and at the Coordination Centre of the Civil Protection.

Two main scenarios were thought to be realistic and important to exercise our response to. Firstly, the response to an intense swarm, i.e., to deal with the scenario of increased likelihood of a significant earthquake and for IMO to provide information and advice and warnings to its end-users. Secondly, to practise disaster response, i.e., the response to a significant earthquake that has cascading hazardous effects such as landslides and a tsunami, both of which have been reported in connection with significant historical earthquakes in Northern Iceland (*Thorgeirsson et al.,* 2011).

The exercises were held according to plan and were followed up by a web-survey (on SurveyMonkey) where all 35 participants that were involved in the exercise were asked to respond to and provide feedback. The survey showed that the main objectives of the exercise were successful as contingency plans were exercised, communication on various levels was practised. In addition, most players of the exercise thought that it had increased their knowledge of the earthquake hazard significantly.

Overall, the exercise showed that despite the uncertain nature of earthquakes, the response to a M6.5-M7 earthquake can be prepared, both by the monitoring teams as well as by the civil protection and other response teams. A priori knowledge of major earthquakes and their aftershocks as well as other possible cascading natural hazards are among the things that contingency plans can cover. An exercise of this kind is wildly important for the sake of efficient communication between the relevant institutions which is essential for an early response and can in turn safe lives in the case of a devastating earthquake.

References

Böðvarsson, R., S.Th. Rögnvaldsson, R. Slunga, and E. Kjartansson, The SIL data acquisition at present and beyond year 2000, *Phys. Earth Planet. Inter.*, **113**, 89–101, 1999.

Behr, Y., J.F. Clinton, C. Cauzzi, E. Hauksson, K. Jónsdóttir, C.G. Marius, A. Pinar, J. Salichon, and E. Sokos, The virtual seismologist in SeisComP3: A new implementation strategy for earthquake early warning algorithms, *Seismological Research Letters*, **87** (2A), 363–373. 2016.

Thorgeirsson, Ó., *Historical earthquakes in North Iceland* (in Icelandic), Húsavík Academic Centre report, 54pp, 2011.

NORTHQUAKE 2019 - The 3rd International Workshop on Earthquakes in North Iceland
Húsavík, North Iceland, 21-24 May 2019

MONITORING – PLANNING – ACTION
WHAT COMES AFTER RESEARCH AND MONITORING?

Rögnvaldur Ólafsson and Hjálmar Björgvinsson

National Commissioner of the Icelandic Police, Department of Civil Protection and Emergency Management, Reykjavík

All research and data are important for the civil protection authorities in Iceland. This information is used in planning and mitigation and is imperative during ongoing events. The civil protection science advisory board is an important forum for open dialogue about what is going on and what might happen in the future.

The civil protection authorities in Iceland are in close cooperation with the scientific community regarding natural hazards. Regular meetings are held with the civil protection science advisory board to go over the general status of natural hazards. Special meetings are also held to go over specific hazards that need further inspection.

The civil protection act covers all hazards that can cause damage to life, health, environment or property. The source of the threat can be from natural catastrophes or from human actions, epidemics, military action or other causes.

There is also an obligation to provide emergency relief and assistance due to any injury or damage that may occur or has occurred.

Information from research, hazard- and risk assessments is used to create coordinated civil protection plans describing everyone's role or responsibility.

The Icelandic Met Office is responsible for monitoring natural hazards and informing the civil protection authorities.

DISCUSSION SUMMARY AND RECOMMENDATIONS OF THE NORTHQUAKE 2019 WORKSHOP

Earthquake hazard and hazard research

The need of reassessing the seismic hazard for Iceland was pointed out, given all the new results and information presented at the Northquake 2019 workshop and published in recent years. This was not put forward as an idea for a research proposal, but rather as an important institutional task for some capable institution(s). The current seismic hazard map in use (for the entire country) is outdated and it is not exactly clear how it was produced, as seismic hazard assessments in Iceland up to this point have not been subject to peer review. The typical procedure is that the Civil Protection (CP) requests updated hazard information for a certain region (or the entire country) from the appropriate institution. In the case of seismic hazard, it seems appropriate that the CP and the Natural Catastrophe Insurance (NTI) of Iceland would request a full update of the seismic hazard assessment for Iceland from the Icelandic Met Office (IMO), after a dedicated funding source for the work has been identified.

A new two-year Rannís project was introduced during the discussion, a project that focuses on studying the sensitivity of seismic hazard analysis for North Iceland and other areas. This is important for identifying the most important longer-term research efforts to reduce uncertainties of hazard assessments. What key information needs to be collected? What efforts would be the most helpful? At the same time, researchers will, of course, continue to carry out their various earthquake hazard research efforts, producing results that will also help with future hazard assessments.

Cascading hazards (e.g., earthquake-triggered landslides and avalanches) are probably important to include in future seismic hazard assessments. They are certainly important to study further, but there is no funding for this type of research at the IMO. Therefore, research proposals to initiate new projects on cascading hazards are needed.

The IMO has been working on avalanche and landslide hazard maps for various parts of the country. They target areas that are in threat of possible landslide/avalanche activity. The hazard mapping focuses on where people live, i.e. focuses on houses at risk. The avalanche hazard and risk assessment work at the IMO could serve as examples of what could be done for other natural hazards. It was decided after the 1995 avalanche disasters in Súðavík and Flateyri that the avalanche situation in Iceland was unacceptable. In addition, it was agreed that it would not be enough to look at the avalanche hazard, but rather carry the calculations through to risk to individuals. The definition of risk was taken as the annual number of deaths of individuals in avalanches, which could be compared to traffic risks, for example. Furthermore, it was decided that it would be unacceptable to have avalanche risk in a given house that is significant in comparison to other risks (traffic, diseases, etc.). This approach might not be the best for other hazards, i.e., focusing on the economic risk might be more appropriate for seismic hazards. Maybe this could be a theme for the next workshop, i.e. to get together people who have been assessing hazard and risk for other types of natural hazards and other phenomena (e.g. traffic, diseases), and see what the earthquake hazard community could learn from these groups.

Estimated hazard and risk are dynamic, they change with new knowledge, new settlements, infrastructure, tourists, etc. While avalanches/landslides triggered by earthquakes would mostly occur in areas that are exposed to some avalanche/landslide hazard already, it is clear that we would have a high concentration of landslides/rockfall/avalanches near the earthquake sources, even in good weather when general landslide/avalanche risk would be deemed low.

It is important to distinguish between dynamic hazard mapping and real-time monitoring. The IMO monitoring team maybe needs to start thinking about how to address this, e.g. should we close skiing areas in North Iceland during intensive earthquake swarms when the probability of a larger event increases? Important to think about possible effects on roads, i.e. towns could become isolated in cases of many snow avalanches.

Risk reduction

When assessing seismic risk, it is not enough to focus only on the buildings themselves, but we also need to look at the interiors (false ceilings, light fixtures, etc.). Preventive measures are very important, as we learned from Hveragerði in the 2008 south Iceland earthquake. There are many simple and obvious things that can be done to make homes/buildings safer, and thus lower the seismic risk. Insurance companies in California request improvements and do inspections, and then people can lower their premiums. Here insurance companies do not cover earthquake damage and will thus not inspect for this. Maybe the NTI should request interior improvements and work with local authorities. Local interest groups (e.g., Lion's, Scouts, etc.) could be trained and then visit houses and offer to help people to make their homes safer. Some efforts in this direction were carried out in Húsavík in 2012. However, such efforts would be useful to undertake every few years and in more places than just in Húsavík.

In addition, vulnerable houses need to be improved. We know the building stock in Húsavík well and where vulnerable houses are. What should we do? Again here it would be important to involve the NTI and local authorities to help people/companies to improve these houses to make them safer or even purchase them such that nobody will need to live in them. A source of funding for such improvements is vital to identify.

Earthquake monitoring

The TurnKey project, in which IMO plays an important part, is about to start. It is funded to work towards operational earthquake forecasting (OEF) and operational earthquake early warning (EEW). The other related project IMO is involved in is RISE, which will advance earthquake prediction, especially in South Iceland, and study whether or not it could become operational.

In TurnKey, the IMO will discuss with stakeholders and focus on the needs of end users. One part is to look into the feasibility of EEW: Would EEW be useful for the stakeholders or not? The project will also focus on EEW of earthquake effects, i.e. the aim is to develop a system that will use real-time data to provide information, in near-real time, on the expected effects associated with major shaking. The project research will be based around densifying operational networks, in particular in urban areas. About 50 new accelerometers are coming (some added to SIL stations) and 6 continuous GPS stations. Within the project, the IMO will not focus much on operational earthquake forecasting, although the new instruments should help earthquake forecasting based on multiple sensors.

During the discussion, key outcomes of 20 years of multinational earthquake prediction research in Iceland, which included projects up to 2006, were reviewed. The work focused on the physics of earthquake prediction. The first part was the development of the SIL system, which was designed to record and locate all earthquakes down to magnitude zero. The system has been very useful for detecting micro-seismicity and patterns of these events, e.g. before major events. GPS instruments and strainmeters were also part of the system early on. The importance of monitoring multiple components (seismicity, strain, GPS, water chemistry) for detecting changes was strongly stressed, because signs of pre-activity can be different in different places, i.e. the initiation of the cracking before the major rupture.

The results of these research efforts strongly suggest that methods of prediction should be process oriented rather than based on individual precursors. The importance of observing multiple parameters was stressed.

A detailed schematic plan for the operation procedure for the monitoring and prediction was discussed. The earthquake monitoring at the IMO already does some of the tasks on that schematic plan, e.g., they stream a variety of data and visualize them together on monitors in the monitoring room. They do not, however, have any water level data, and only limited gas and chemistry data. Additional data streams can be added without too much effort. In the TurnKey project, further development of coherent multi-component visualization and analysis will be carried out.

The IMO monitoring team responds to crisis situations on case-by-case basis, with the unrest at Öræfajökull volcano as a recent example. In that case, they contacted and involved numerous people at several different institutions. This led to addition of many instruments for monitoring while the activity was the most intense. However, funding has not been secured for continuing operation and maintenance of these added instruments, despite the importance of continued monitoring of Öræfajökull volcano.

As the monitoring in the Tjörnes Fracture Zone is primarily limited to seismicity and GPS monitoring, there is a clear need to add more types of instruments for better multi-component monitoring in the area, e.g. by adding strainmeters, water-level measurements, buoys, etc. It is important to apply to the instrument fund of Rannís for more monitoring instruments in the area.

One point to note is the difference between the SISZ and the TFZ, as in the TFZ we already have a sort of operational earthquake forecast, because the IMO and the Civil Protection raise the alert level at the time of intense earthquake sequences. Large TFZ earthquakes in the past have often been a part of swarms, although there are important exceptions to this, e.g., the 1934 Dalvík, 1963 Skagafjörður, and likely the 1838 Siglufjördur earthquakes, which were not related to swarms. In addition, the 1885 Kelduhverfi event was not a part of a swarm, although one could possibly link it to a swarm that occurred quite a bit earlier and far away.

When it comes to possible short-term earthquake warnings, the monitoring limitations are basically the same as above, i.e. more data and more data of different type are needed. However, what is much more significant for short-term warnings is to perform analysis and research that makes rapid in-depth use of the enormous amount of data already available in the SIL system database, e.g., for inverting them and estimating properties of crustal processes at work in the seismogenic crust. This would be the most significant step forward for predicting the effects of and time of large earthquakes and some of these inversions have already been tested, now we needed to make them operational.

Recommendations:

- The seismic hazard in Iceland needs to be reassessed, given all the new information on ground motion models, earthquake activity, and related subjects presented at the Northquake 2019 workshop and published in recent years.
- For a new country-wide seismic hazard assessment effort, collaboration with key institutions, such as the Natural Catastrophe Insurance, the Civil Protection, and Landsvirkjun, is needed and a dedicated funding source for the task has to be identified.
- Once a new seismic hazard assessment has been completed and published, a new country-wide seismic risk assessment is also needed.
- New seismic hazard and risk products need to be presented and published such that they will be useful for a range of end users, not only to other researchers.

- Further research on cascading hazards (e.g. earthquake-triggered landslides, avalanches, and tsunamis) is needed and they should be included in future seismic hazard assessments.
- Enhancing multi-component real-time monitoring and analysis is important for better detection of pre-earthquake effects, as these effects may be different from one location to another.
- More components of possible change need to be added to the monitoring in North Iceland, e.g. borehole strain, water chemistry, temperature, and level measurements.
- Past decades have seen significant progress with regard to earthquake monitoring and research. A dedicated research effort focusing on earthquake prediction research in North Iceland, comparable to the research in the SISZ, is urgently needed. In addition, the knowledge and state of research is already ripe for building an automated, yet manually controlled, "geo-watching system" that makes in-depth use of collected data and has a rule-based warning schedule linking scientific evaluations to adequate actions for people and society.
- Immediate actions are needed to reduce seismic risk in North Iceland by improving interiors of homes and companies, e.g. by fixing heavy objects to walls and inspect false ceilings and light fixtures.
- It is also important to improve vulnerable buildings not built to the current building standards and bring them to an acceptable condition. A procedure of purchasing houses that are too vulnerable for improvements is needed.